

Dissertation zur Erlangung des Doktorgrades
der Fakultät für Biologie
der Ludwig-Maximilians-Universität München

**Functional characterisation
of microRNA-containing
Argonaute protein complexes**

vorgelegt von

Lasse Weinmann

2009

Ehrenwörtliche Versicherung

Ich versichere hiermit ehrenwörtlich, dass die vorgelegte Dissertation von mir selbstständig und ohne unerlaubte Hilfe angefertigt ist.

München, den 02.06.2009

Lara Weinmann

(Unterschrift)

Erklärung

Hiermit erkläre ich, *

- dass die Dissertation nicht ganz oder in wesentlichen Teilen einer anderen Prüfungskommission vorgelegt worden ist.
- dass ich mich anderweitig einer Doktorprüfung ohne Erfolg **nicht** unterzogen habe.

München, den 02.06.2009

Lara Weinmann

(Unterschrift)

Diese Dissertation wurde von Prof. Dr. Stefan Jentsch betreut. Die Dissertation wurde eingereicht am 04.06.2009.

1. Gutachter: Prof. Dr. Stefan Jentsch
2. Gutachter: Prof. Dr. Angelika Böttger

Mündliche Prüfung am: 13.07.2009

1. Table of Contents

1. Table of Contents	1
2. List of Publications	3
3. Abbreviations	5
4. Summary	7
5. Introduction	9
5.1. Classes of Small RNAs	10
5.2. Biogenesis of Small RNAs in Mammals	11
5.2.1. microRNA Biogenesis	11
5.2.2. piRNA Biogenesis	14
5.2.3. siRNAs from Exogenous Sources	17
5.2.4. endo-siRNA Biogenesis	19
5.3. Argonaute Proteins and the Functions of Mammalian Small RNAs	20
5.3.1. Ago Proteins and Small RNA Functions in Somatic Cells	22
5.3.1.1. Subcellular Localization of Ago Proteins – Insights and Open Questions	22
5.3.1.2. Ago Protein Complexes and Mechanisms of microRNA Function	27
5.3.1.2.1. Determinants of microRNA – Target Interactions	27
5.3.1.2.2. Mechanisms of microRNA-Guided Translational Repression	29
5.3.1.2.3. MicroRNA-Guided Destabilization of Target mRNAs	33
5.3.1.2.4. Other Mechanisms of microRNA Function	35
5.3.1.3. Ago2 and RNA Interference (RNAi)	36
5.3.2. Ago2 and endo-siRNAs	38
5.3.3. Piwi Proteins, piRNAs and Transposon Silencing in the Germline	39
5.4. Biological Roles of Animal miRNAs	40
5.5. Aims of the PhD Thesis	42
6. Discussion	44
6.1. Proteomic and Functional Analyses of Human Ago Protein Complexes	44
6.2. Identification and Functional Analyses of Ago-Associated Small RNAs	49

6.3. Identification and Functional Analyses of Ago-Associated Target RNAs	50
6.4. Reduction of siRNA Off-Target Effects by Blocking 5'-Phosphorylation of the Passenger Strand	52
7. References	53
8. Acknowledgements	63
9. Curriculum Vitae	64
10. Declaration of Individual Contributions to the Publications	66
11. Reprints of the Publications	75

2. List of Publications

Please note that my name has changed from Lasse Peters to Lasse Weinmann.

Publication 1:

Gunter Meister, Markus Landthaler, Lasse Peters, Po Yu Chen, Henning Urlaub, Reinhard Lührmann, and Thomas Tuschl: Identification of novel Argonaute-associated proteins. *Current Biology* 15, 2149-55 (2005)

Publication 2:

Michaela Beitzinger, Lasse Peters, Jia Yun Zhu, Elisabeth Kremmer and Gunter Meister: Identification of human microRNA targets from isolated argonaute protein complexes. *RNA Biology* 4, 76-84 (2007).

Publication 3:

Julia Höck, Lasse Weinmann, Christine Ender, Sabine Rüdell, Elisabeth Kremmer, Monika Raabe, Henning Urlaub and Gunter Meister: Proteomic and functional analysis of Argonaute-containing mRNA–protein complexes in human cells. *EMBO Reports* 8, 1052-60 (2007).

Publication 4:

Po Yu Chen*, Lasse Weinmann*, Dimos Gaidatzis, Yi Pei, Mihaela Zavolan, Thomas Tuschl and Gunter Meister: Strand-specific 5'-O-methylation of siRNA duplexes controls guide strand selection and targeting specificity. *RNA* 14, 263-74 (2008).

*** These authors contributed equally to this work**

Publication 5:

Sabine Rüdell, Andrew Flatley, Lasse Weinmann, Elisabeth Kremmer and Gunter Meister: A multifunctional human Argonaute2-specific monoclonal antibody. *RNA* 14, 1244-53 (2008).

Publication 6:

Thomas Ohrt, Jörg Mütze, Wolfgang Staroske, **Lasse Weinmann**, Julia Höck, Karin Crell, Gunter Meister and Petra Schwille: Fluorescence correlation spectroscopy and fluorescence cross-correlation spectroscopy reveal the cytoplasmic origination of loaded nuclear RISC *in vivo* in human cells. *Nucleic Acids Research* 36, 6439-49 (2008).

Publication 7:

Christine Ender, Azra Krek, Marc R. Friedländer, Michaela Beitzinger, **Lasse Weinmann**, Wei Chen, Sebastien Pfeffer, Nikolaus Rajewsky, and Gunter Meister: A Human snoRNA with MicroRNA-Like Functions. *Molecular Cell* 32, 519-28 (2008).

Publication 8:

Lasse Weinmann, Julia Höck, Tomi Ivacevic, Thomas Ohrt, Jörg Mütze, Petra Schwille, Elisabeth Kremmer, Vladimir Benes, Henning Urlaub, and Gunter Meister: Importin 8 Is a Gene Silencing Factor that Targets Argonaute Proteins to Distinct mRNAs. *Cell* 136, 496-507 (2009).

Publication 9:

Lasse Peters and Gunter Meister: Argonaute Proteins: Mediators of RNA Silencing. *Molecular Cell* 26, 611-23 (2007).

3. Abbreviations

3'-UTR	3'-untranslated region
5'-UTR	5'-untranslated region
<i>A. thaliana</i>	<i>Arabidopsis thaliana</i>
BCLL	B-cell chronic lymphocytic leukaemia
<i>C. elegans</i>	<i>Caenorhabditis elegans</i>
ChIP	chromatin immunoprecipitation
<i>D. melanogaster</i>	<i>Drosophila melanogaster</i>
Dnd1	Dead-end 1
dsRNA	double-stranded RNA
EGFP	enhanced green fluorescent protein
endo-siRNA	endogenous siRNA
Imp8	Importin 8
IRES	internal ribosome entry site
kDa	kilodalton
miRNA	microRNA
miRNA*	microRNA star
miRNP	miRNA-ribonucleoprotein complex
MOV10	Moloney leukemia virus 10
NMD	nonsense-mediated decay
orf	open reading frame
PABP	Poly(A)-binding protein
PAZ	piwi-argonaute-zwille
P-bodies	processing bodies
piRNA	Piwi-interacting RNA
PIWI	P-element induced wimpy testis
RBM4	RNA binding motif protein 4
RISC	RNA-induced silencing complex
RHA	RNA helicase A
RNAi	RNA interference
SG	Stress granule
siRNA	small interfering RNA
snoRNA	small nucleolar RNAs

SNP	single nucleotide polymorphism
<i>S. pombe</i>	<i>Schizosaccharomyces pombe</i>
SV40 NLS	<i>Simian virus 40</i> nuclear localization signal
TNRC6B	trinucleotide repeat-containing 6B

4. Summary

microRNAs (miRNAs) are small non-coding RNAs of 21-24 nt in size, which are endogenously expressed in higher eukaryotes and play important roles in processes such as tissue development and stress response and in several diseases including cancers. In mammals, miRNAs guide proteins of the Argonaute family (Ago proteins) to partially complementary sequences typically located in the 3'-untranslated regions (3'-UTRs) of specific target mRNAs, leading to translational repression or mRNA degradation. To gain further insight into the function of human miRNAs, we analyzed the protein as well as the RNA composition of miRNA-Ago protein complexes in molecular detail.

To identify novel Ago-interacting proteins, we isolated Ago complexes and investigated them by mass spectrometry and co-immunoprecipitation experiments. We found that trinucleotide repeat-containing 6B (TNRC6B), Moloney leukemia virus 10 (MOV10), RNA binding motif protein 4 (RBM4) and Importin 8 (Imp8) interact with human Ago proteins. Moreover, using RNA interference and EGFP and dual luciferase reporter assays, we demonstrated that these factors are required for miRNA function, indicating that we have identified new components of the miRNA pathway. Intriguingly, depletion of Imp8 does not affect the levels of mature miRNAs or the interaction of miRNAs with Ago proteins, but is required for efficient association of Ago-miRNA complexes with their target mRNAs. Thus, Imp8 is the first factor acting at the level of target mRNA binding, establishing a novel layer of regulation for the miRNA pathway. Imp8 is an Importin- β -like protein, which has previously been implicated in nuclear import of substrate proteins^{1, 2}. In line with these results, we demonstrated that a detectable fraction of Ago2 localizes to the nucleus of human cells. Moreover, knockdown of Imp8 by RNAi reduces the nuclear signal of Ago2, suggesting that Imp8 affects the nuclear localization of Ago2. Therefore, our data suggest that Imp8 has a dual function both in the cytoplasmic miRNA pathway and in nuclear transport of Ago proteins.

To identify small RNAs, which associate with human Ago proteins, we isolated, cloned and sequenced small RNAs bound to Ago1 and Ago2 complexes. In addition to known miRNAs, we found several small RNAs, which derive from small nucleolar RNAs (snoRNAs). We therefore investigated the function of one particular small RNA, which is derived from the snoRNA ACA45 and showed that it functions like a

miRNA. Interestingly, this small RNA is processed by the miRNA maturation factor Dicer, but does not require the microprocessor complex that is essential for processing of primary miRNA transcripts. Thus, we have identified a novel biogenesis pathway of a new class of small RNAs that can function like miRNAs.

To experimentally identify mRNAs that are stably associated with miRNA-Ago protein complexes, we isolated and analyzed Ago1 and Ago2-bound mRNAs by cloning and sequencing and by microarray hybridization techniques. Using dual luciferase reporter assays, we demonstrated that many Ago-associated mRNAs are indeed miRNA targets. Therefore, we have developed a method allowing for the identification of miRNA target mRNAs from cell lines or tissues of interest independently of computational predictions.

In a project that was independent of our studies on Ago protein complexes, we investigated structural and functional requirements for the activity of small interfering RNAs (siRNAs). siRNAs are small double-stranded RNAs of appr. 21 nt in size, which trigger the sequence-specific endonucleolytic degradation of perfectly complementary target transcripts upon binding to Ago2^{3, 4}. However, both single strands of a siRNA duplex can potentially have unwanted “off-target effects” by repressing partially complementary target mRNAs through binding to their 3'-UTRs⁵⁻⁸. We therefore developed a method to selectively inhibit the activity of the siRNA strand that is dispensable for target silencing (“passenger strand”) through chemical modification of its 5'-end. This method could be a useful tool for the design of highly specific siRNAs.

Taken together, we have analyzed the composition of Ago-miRNA protein complexes by a variety of methods and identified novel protein factors of the miRNA pathway, a novel class of small RNAs as well as a panel of previously unknown miRNA target mRNAs. The techniques for the purification and the analysis of Ago complexes that were developed in this study will provide useful tools for future analyses of miRNA pathway factors, small RNAs and miRNA target mRNAs from any tissue or cell line of interest.

5. Introduction

The biology of gene inactivation is a major focus of research since several decades. Specific gene inactivation can involve a variety of mechanisms including gene mutation or deletion, repression of transcription, translational repression, destabilization of mRNAs and degradation of protein products. In the laboratory, the inactivation of specific genes can be utilized to investigate their functions. However, methods to generate organisms with mutant genes or gene deletions are often time-consuming and more convenient techniques to silence gene expression were needed. One prominent method to achieve specific gene silencing is the transfection of oligonucleotides antisense to an mRNA of interest. Such antisense oligonucleotides bind to complementary mRNAs in a sequence-specific manner and lead to their destabilization⁹. However, antisense-mediated inhibition of mRNAs requires the presence of high (stoichiometric) amounts of antisense oligonucleotides. In contrast, small double-stranded RNAs can trigger highly efficient sequence-specific catalytic degradation of complementary target RNAs through endonucleolytic cleavage in a process termed RNA interference (RNAi). Because RNAi is based on a catalytic mechanism, it is effective at lower (sub-stoichiometric) concentrations compared to antisense-mediated gene silencing. RNAi was first shown in 1998, when Andrew Fire and Craig Mello made the surprising observation that double-stranded RNA (dsRNA) acts as a very potent trigger to silence complementary genes in *Caenorhabditis elegans* (*C. elegans*)¹⁰. Subsequent studies showed that the minimal triggers of RNAi are small interfering RNAs (siRNAs) of appr. 21 nucleotides (nt) in size that act as guides to silence complementary transcripts through endonucleolytic cleavage^{11, 12}. Since these reports, the field of small RNA-guided gene silencing has rapidly expanded. To date, a variety of different endogenously expressed small RNA species has been identified in the majority of eukaryotes, with *Saccharomyces cerevisiae* (*S. cerevisiae*) being a notable exception. Moreover, it is now apparent that small RNAs can also act through many mechanisms which are different from endonucleolytic cleavage^{13, 14}. Many studies have investigated the biological roles of small RNAs as well as their biogenesis pathways and their functions. The following introductory sections summarize known small RNA biogenesis pathways and their functions in mammals, together with the proteins that mediate their mechanisms of action.

5.1. Classes of Mammalian Small RNAs

Since the discovery of RNAi and the identification of siRNAs, numerous small RNA species have been identified, most of which derive from longer double-stranded RNA precursor molecules.

siRNAs are approx. 21 nt small double-stranded RNAs, which trigger silencing of perfectly complementary RNA molecules through endonucleolytic cleavage¹⁵. They carry characteristic phosphate groups on their 5' ends and 2 nt overhangs on their 3' ends¹⁶⁻¹⁸. Until recently, it was assumed that siRNAs in mammals can only derive from exogenous sources of double-stranded RNA such as viral replication intermediates. However, more recent studies reported that endogenous siRNAs (endo-siRNAs) are present in mouse oocytes and may act to suppress transposons¹⁹⁻²¹.

microRNAs (miRNAs) are 21-24 nt in size and can trigger translational inhibition or deadenylation of target mRNAs by binding to partially complementary sites in their 3'-untranslated regions (3'-UTRs)¹³. miRNAs are endogenously expressed in most eukaryotes and have diverse biological roles, e.g. in organ development, stress response and in various diseases including cancer²².

Piwi-interacting RNAs (piRNAs) are single-stranded germline-specific small RNAs of 24-30 nt in size which are thought to silence transposons, possibly through an RNAi-like mechanism²³. They carry characteristic methyl groups on the 2'-OH groups of their 3' terminal nucleotides^{24, 25}.

5.2. Biogenesis of Small RNAs in Mammals

5.2.1. microRNA Biogenesis

miRNAs are small RNAs of 21-24 nt in size which are endogenously expressed in most eukaryotes. Although the expression of particular miRNAs can be highly specific to a certain developmental stage or to a tissue, miRNA expression in general is thought to be ubiquitous throughout different tissues²⁶. Many miRNA genes are evolutionarily conserved, suggesting that miRNAs can have important biological functions²⁷.

miRNAs are typically transcribed as primary transcripts (pri-miRNAs) by RNA polymerases II or III in the nucleus (figure 1)^{28, 29}. In many cases, miRNA genes are genomically clustered such that pri-miRNA transcripts contain multiple mature miRNA sequences³⁰⁻³². Pri-miRNAs are further processed in the nucleus by a multiprotein complex termed microprocessor which contains the RNase III enzyme Drosha and the dsRNA binding protein DGCR8³³⁻³⁷. Microprocessor generates hairpin-structured pre-miRNAs, which are exported to the cytoplasm by the nuclear export receptor exportin 5³⁸⁻⁴⁰. In the cytoplasm, the RNase III-like enzyme Dicer cleaves off the precursor loop to generate double-stranded intermediates containing the mature miRNA and the corresponding duplex counterpart which is termed “miRNA star” (miRNA*)⁴¹. These intermediates typically contain 5' phosphate groups and 2 nt overhangs on the 3'-ends. One strand of the intermediate is incorporated into a miRNA-ribonucleoprotein complex (miRNP), which contains a member of the Ago subfamily of Argonaute proteins (Ago 1-4 in humans)⁴². Ago proteins directly bind to miRNAs and are the mediators of miRNA function. Small RNA loading to Ago proteins involves Dicer and the dsRNA binding proteins TRBP and/or PACT⁴³⁻⁴⁶. Additionally, helicases such as RNA helicase A (RHA) are likely to be required for efficient separation of the duplex strands⁴⁷. Interestingly, unwinding of the duplex could be facilitated by Ago2 itself. Ago2 cleaves the precursor hairpins of some miRNAs on the miRNA* side of the stem, yielding a nicked processing intermediate⁴⁸. miRNA/miRNA* duplexes from such processed hairpins are probably easier to unwind. Consistently, overexpression of Ago2 was reported to increase mature miRNA levels in some cell types⁴⁸. Loading of the single strands to miRNPs is mainly determined by the relative thermodynamic stability of the miRNA/miRNA* duplex

ends, such that the strand that is less stably paired at its 5' end becomes incorporated into a miRNP ("asymmetry rules")^{49, 50}. The mechanism underlying these asymmetry rules has not yet been completely resolved in mammalian cells. In *Drosophila melanogaster* (*D. melanogaster*) cells, the dsRNA binding protein R2D2 acts as an asymmetry sensor by binding to the more stable duplex end, thereby directing Ago2 to interact with the less stable duplex end⁵¹. PACT and TRBP are mammalian homologs of R2D2, and further studies will be required to investigate whether their function is similar to R2D2. Despite the evidence supporting the asymmetry rules, thermodynamic asymmetry does not reliably predict strand selection of all known duplexes, and it is likely that additional determinants of strand selection exist which have yet to be defined. In most cases, the mature miRNA is preferentially incorporated into a miRNP, whereas the miRNA* sequence is degraded. However, not all miRNA* species are unstable and a recent study suggested that some miRNA* sequences are functional, similar to mature miRNAs⁵². Upon binding to an Argonaute protein, miRNAs serve to guide the miRNP to partially complementary target sites on mRNAs. miRNPs can trigger target mRNA repression through translation inhibition or mRNA destabilization (section 5.3.1.2.)¹³. In addition, miRNAs can be generated from large introns of protein-coding genes. miRNA precursors are released from introns by the microprocessor complex before mRNA splicing is completed⁵³. Moreover, small introns which are released by the spliceosome can serve as pre-miRNAs⁵⁴⁻⁵⁶. Such miRNA precursors bypass Drosha/microprocessor processing and directly serve as substrates for nuclear export by exportin 5 and processing by Dicer. According to their biogenesis, such miRNAs have been termed mitrons. Furthermore, it was recently described that some snoRNAs serve as precursors of functional small RNAs that act like miRNAs^{57, 58}. miRNA target repression by such miRNAs is Drosha-independent, suggesting that snoRNA-derived miRNAs can bypass Drosha processing (publication 7, section 11).

Figure 1

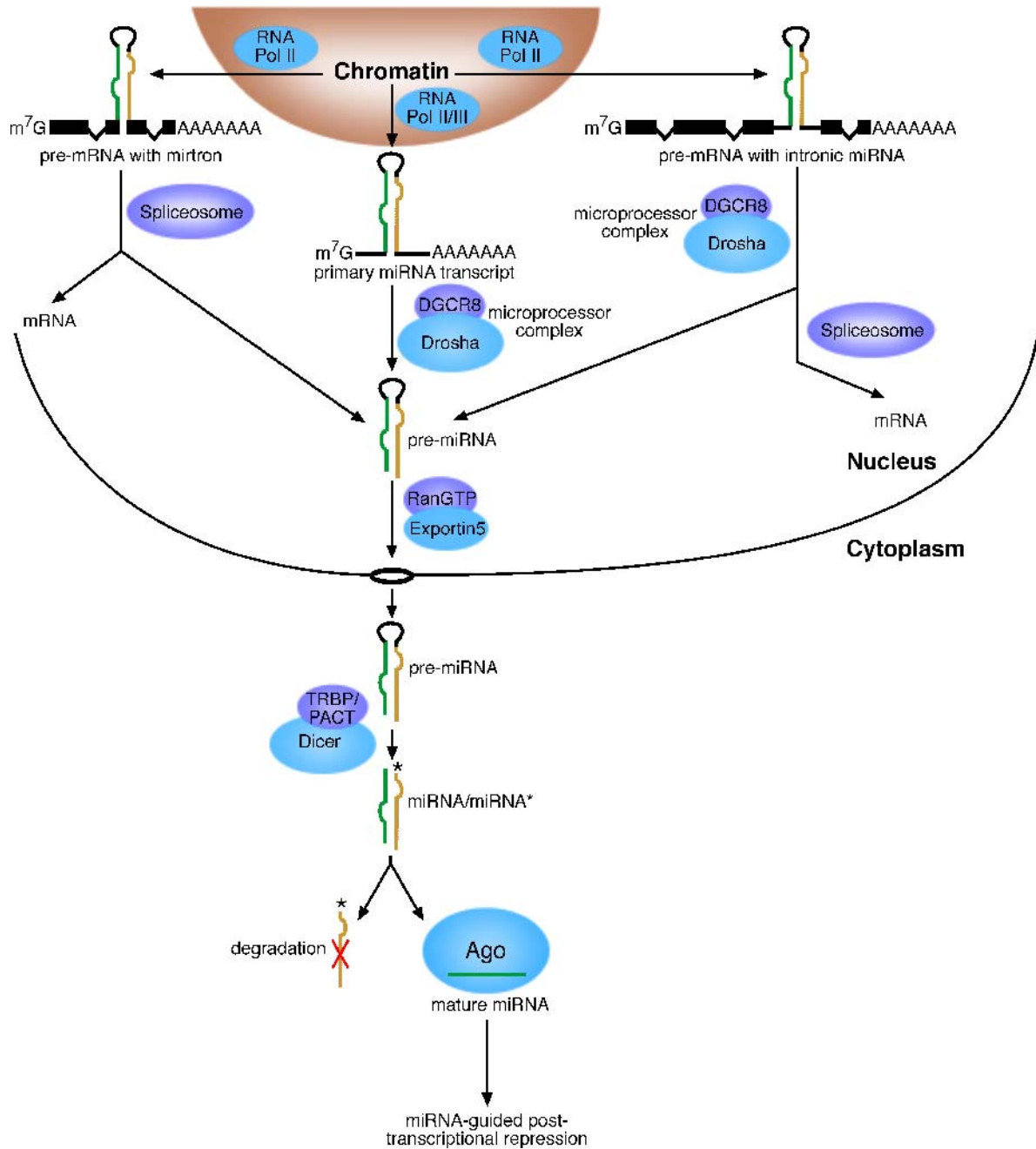


Figure 1: miRNA biogenesis pathways. MiRNA precursor transcripts are synthesized in the nucleus (upper panel). Pre-miRNAs are mostly processed from primary miRNA transcripts (upper middle panel) or from large introns of pre-mRNAs (upper right panel). Alternatively, they can be released from small hairpin-structured introns of pre-mRNAs by the spliceosome (upper left panel). Pre-miRNAs are exported into the cytoplasm by Exportin 5. They are further processed by Dicer to yield a miRNA/miRNA* processing intermediate (lower panel). Mature miRNAs are loaded to Ago protein complexes, whereas miRNA* sequences are mostly degraded. After loading, miRNAs guide Ago proteins to partially or perfectly complementary target sites on mRNAs, allowing for post-transcriptional gene silencing through different mechanisms.

5.2.2. piRNA Biogenesis

piRNA biogenesis is currently less well understood than miRNA biogenesis, and there are many questions that remain to be addressed. In contrast to miRNAs which are expressed throughout different tissues, piRNA expression has only been detected in germ cells and is most prominent in testes. piRNAs are single-stranded small RNAs of 24-30 nt in size which bind to Piwi proteins, a subclass of Argonaute proteins which is mainly expressed in germ cells⁵⁹⁻⁶¹. piRNA sequences are not conserved across species, but piRNAs are expressed from syntenic regions. Most piRNA sequence reads (>80%) that have been obtained from RNA cloning and deep sequencing approaches map to discrete genomic clusters^{59, 60}. In contrast to single miRNA sequences that can be highly abundant in small RNA libraries, most piRNA sequences are only present as single reads in libraries, with hundreds or thousands of different reads originating from each piRNA cluster. Interestingly, piRNA expression in testes changes during stages of sperm development. piRNAs which are expressed before the pachytene stage of meiosis arise from genomic clusters that frequently bear repetitive elements⁶². In contrast, piRNAs which are found from the pachytene stage until the round spermatid stage derive from a different set of genomic clusters with a lower repeat content^{59, 60}. Unlike miRNAs, the genomic context of piRNAs does not allow to calculate stable hairpin precursor structures, suggesting that piRNA biogenesis is different from miRNA processing. Loss-of-function studies in zebrafish and flies indicated that piRNA expression is independent of Dicer^{63, 64}. Since Dicer is capable of processing double-stranded RNA into small RNAs, these data suggest that piRNAs are processed from single-stranded precursor transcripts rather than from long double-stranded RNA. Nevertheless, studies in *D. melanogaster* showed that piRNAs can derive from corresponding sense and antisense transcripts of repetitive sequences^{65, 66}. piRNAs from antisense transcripts are mainly bound by the Piwi proteins Piwi and aubergine, whereas piRNAs from sense transcripts are incorporated into Ago3, a Piwi protein in *D. melanogaster*. Sense and antisense piRNAs are frequently found in pairs such that there is a 10 nt sequence complementarity of their 5' ends. This relation suggests an amplification mechanism in piRNA biogenesis that utilizes endonucleolytic activities of Piwi proteins to generate piRNAs^{65, 66}: Piwi or aubergine is loaded with a sense piRNA and cleaves the long antisense transcript to generate the 5' end of a piRNA which will

be incorporated into Ago3. Most likely, the 3' end of the antisense piRNA is generated by exonucleolytic processing. After 3' end trimming, piRNAs become methylated by a methylase which is a homolog of the plant protein Hen1 (mHen1 in mice and DmHen1 in *D. melanogaster*)^{24, 67-69}. Methylation occurs at the 2' OH groups of the piRNA 3' termini. DmHen1 mutants express shorter piRNAs, and piRNA levels are generally lower than in wild-type animals, suggesting that methylation may stabilize piRNAs, possibly by preventing aberrant exonucleolytic processing from the 3' end⁶⁷. Once the antisense piRNA is generated, the amplification cycle generates a new sense piRNA via the same "ping-pong" mechanism. In mice, this model is supported by deep sequencing studies of pre-pachytene piRNAs which are bound to the Piwi protein Mili (figure 2)⁶². However, it is unclear if all piRNAs are synthesized via the ping-pong mechanism. While this model may explain piRNA amplification, the initiating event for the amplification cycle remains to be determined. One possible mechanism that could initiate the ping-pong cycle is maternal transmission of piRNAs to the progeny which has been observed in *D. melanogaster*⁷⁰.

Figure 2

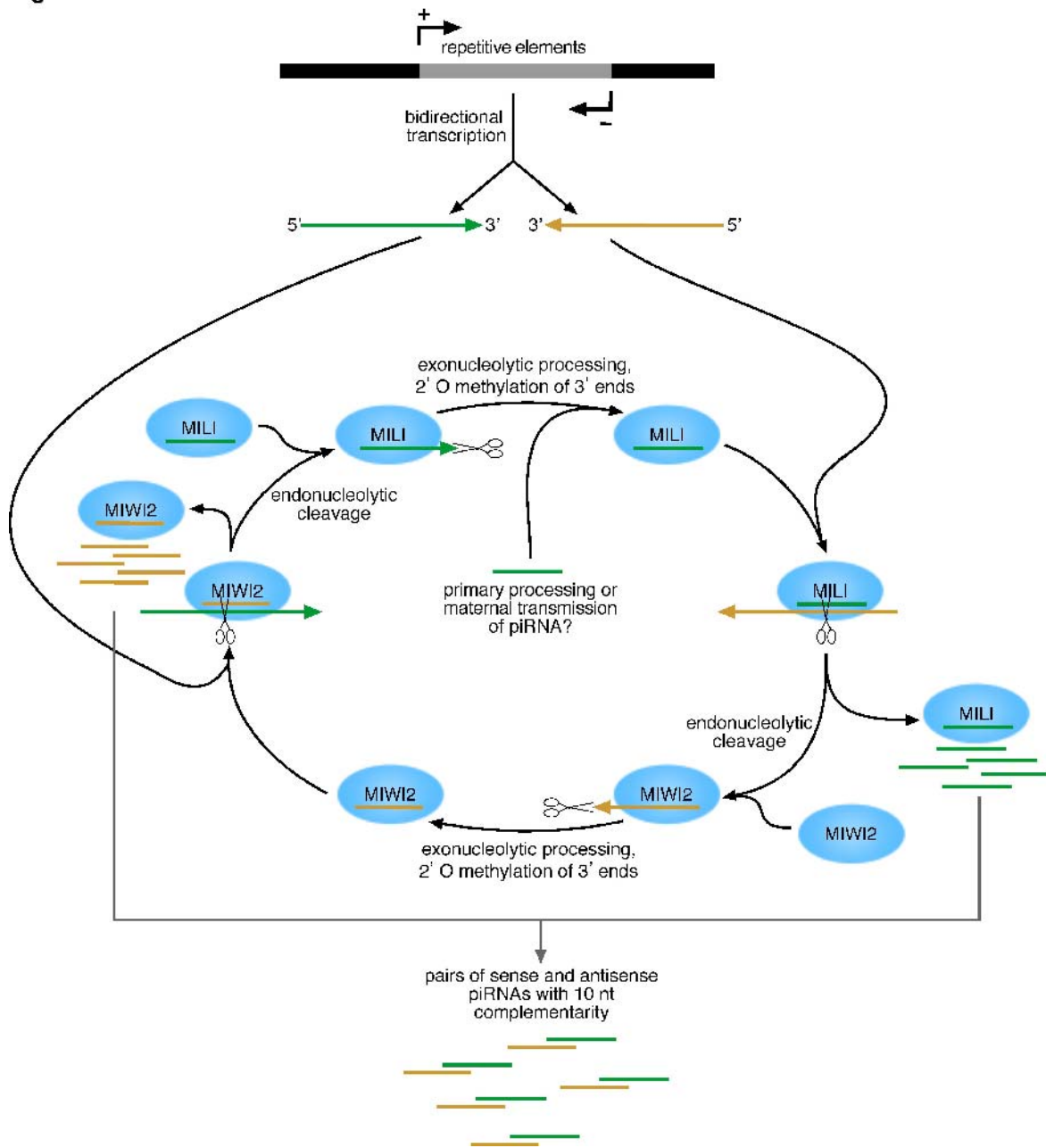


Figure 2: Ping-Pong model of piRNA biogenesis in mice. Bidirectional transcription from repetitive elements or piRNA clusters generates sense and antisense transcripts. MILI together with a piRNA cleaves one transcript strand to define the 5' end of a piRNA, which is subsequently incorporated into MIWI2. The 3' end of the MIWI2-associated piRNA is generated through exonucleolytic processing by an unknown nuclease, followed by 2' O methylation by mHen1. MIWI2 then binds and cleaves a transcript of the opposing transcript strand to define the 5' end of a piRNA, which is subsequently incorporated into MILI. Again, the 3' end of the new piRNA is generated and modified by exonucleolytic processing and 2' O methylation. The Ping-Pong model yields pairs of piRNAs with a 10 nt complementarity in their 5' regions. In mammals, the event that generates the first piRNA to initiate the cycle is unknown.

5.2.3. siRNAs from Exogenous Sources

siRNAs are small RNAs of appr. 21 nt in size which guide sequence-specific cleavage of highly complementary target RNA molecules by RNAi. Early reports showed that siRNAs are endogenously expressed in plants¹² and that they can also function in mammals when delivered by transfection¹¹, but evidence for the presence of endogenous siRNAs in mammals remained elusive for several years. However, mammalian cells express Dicer which can generate siRNAs from dsRNA^{16, 41}. An exogenous source of dsRNA are viral replication intermediates. Consistently, the RNAi pathway was demonstrated to be an important component of antiviral defence mechanisms in plants and in *Drosophila*^{71, 72}, and Dicer contributes to an antiviral response to influenza virus in mammalian cells⁷³.

siRNA biogenesis resembles the final steps of miRNA maturation (figure 3, left panel). Dicer processes long dsRNA to double-stranded siRNAs, which carry 5'-phosphate groups and 2 nt overhangs on their 3'-ends¹⁶⁻¹⁸. In contrast to miRNAs, which can repress translation in mammals through binding to human Ago1-4, siRNA-guided target cleavage only depends on Ago2, because only Ago2 has endonucleolytic activity^{3, 4}. The effector complex of RNAi which contains Ago2 is referred to as RNA-induced silencing complex (RISC)⁷⁴. It contains a single-stranded siRNA termed "guide strand" which guides target RNA cleavage. The opposing strand of the duplex (passenger strand) is mostly degraded. RISC loading is influenced by the same asymmetry rules that also determine miRNA loading^{49, 50}. Similar to miRNP loading, this process is facilitated by the double-stranded RNA binding proteins TRBP and/or PACT⁴³⁻⁴⁶. Moreover, it was recently demonstrated that Ago2 itself facilitates RISC maturation by cleaving the passenger strand⁷⁵⁻⁷⁷. The cleavage fragments of the passenger strand are less stably bound to the guide strand and are expected to rapidly dissociate, yielding cleavage-competent RISC loaded with a single-stranded siRNA.

Figure 3

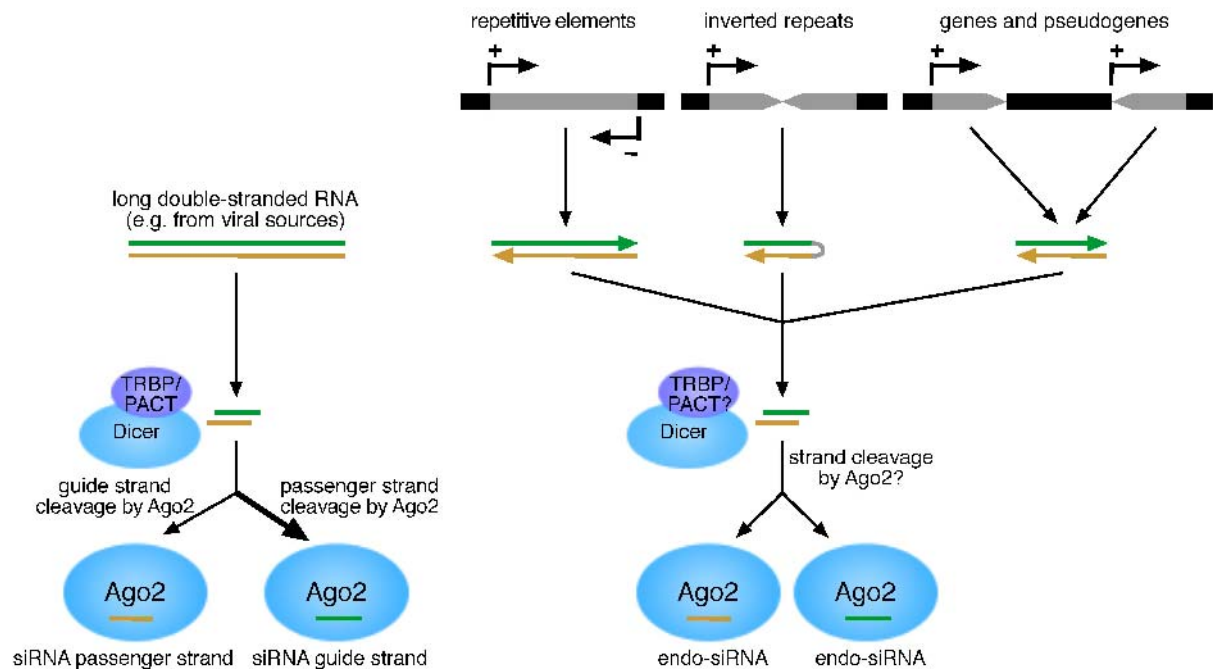


Figure 3: siRNA biogenesis pathways. siRNAs from exogenous sources of long double-stranded RNA are generated and loaded onto Ago2 by a complex containing Dicer and TRBP and/or PACT (left panel). RISC maturation is facilitated by the endonucleolytic activity of Ago2: Cleavage of the passenger strand by Ago2 facilitates the formation of active guide strand-RISC and vice versa. The formation of guide strand-RISC is preferred in most cases (bold arrow). Endo-siRNAs derive from endogenous sources of double-stranded RNA such as bidirectional transcription of repetitive elements, transcription of inverted repeats and pairs of genes and pseudogenes (right panel). Endo-siRNAs are processed by Dicer. However, it is currently unknown whether the endo-siRNA pathway requires TRBP, PACT and involves Ago2-guided siRNA passenger strand cleavage.

5.2.4. Endo-siRNA Biogenesis

Endogenous siRNAs (endo-siRNAs) were discovered early in plants and later also in several animal species^{12, 78}. However, small RNA cloning approaches from somatic mammalian cells have mainly identified miRNAs, and evidence for the presence of endo-siRNAs in mammals remained elusive for several years. Very recently, endo-siRNAs were found to be expressed in *Drosophila* cells and in mouse oocytes^{20, 21, 79, 80}. These siRNAs are appr. 21 nt in length and derive from various sources of long dsRNA, including antisense transcript pairs of genes and pseudogenes, bidirectional transcription of repetitive elements and inverted repeats (figure 3, right panel). It is currently unclear whether mammalian endo-siRNA are generated by the same pathway as siRNAs from exogenous sources. However, both pathways require Dicer^{21, 80}.

5.3. Argonaute Proteins and the Functions of Mammalian Small RNAs

Argonaute proteins were named after a mutation in *Arabidopsis thaliana* (*A. thaliana*) which causes a squid-like phenotype by affecting proper leaf development⁸¹. Although the number of Argonaute proteins strongly varies across different species, Argonaute proteins are present in all higher eukaryotes investigated. Mounting evidence indicates that these proteins are key factors of different small RNA-guided gene silencing pathways. Based on sequence homology, the Argonaute protein family can be subdivided into the Piwi and Ago protein families. Whereas humans express hsAgo1-4, mice have five different Ago proteins (mmAgo1-5)⁸². The Piwi protein family has been named after its founding member, the *D. melanogaster* protein P-element induced wimpy testis (PIWI)⁸³. It consists of four proteins in humans, HIWI1-3 and HILI, and three proteins in mice, MIWI1, MIWI2 and MILI. Whereas Ago proteins are ubiquitously expressed throughout different tissues, the expression of mammalian Piwi proteins is thought to be restricted to germ cells⁸⁴. Argonaute proteins are characterized by piwi-argonaute-zwille (PAZ) and PIWI domains⁸⁵ which have distinct roles in small RNA binding and function. The PAZ domain binds the 2 nt 3'-overhangs of small RNAs which are typical for Dicer processing products^{86, 87}. The PIWI domain is structurally similar to RNase H^{88, 89}. Indeed, the PIWI domain of some Argonaute proteins serves to cleave RNA substrates that are complementary to the bound small RNA. Such Ago proteins are termed "slicer". Similar to RNaseH, this endonucleolytic activity depends on a catalytic triad, which typically consists of a DDH motif. In case of human Ago2, the triad consists of D(597), D(669) and H(807)^{89, 90}. However, not all Argonaute proteins contain a DDH triad and are catalytically active. Moreover, some Argonaute proteins like human Ago3 contain a DDH triad but are catalytically inactive, indicating that the presence of the triad is not sufficient for cleavage activity. The region between the PAZ and PIWI domains contains a third functionally important module which is referred to as MID domain. It harbors a basic pocket that binds the characteristic 5'-phosphate groups of Dicer-processed small RNAs and anchors the small RNA on the protein surface^{91, 92}.

Despite the structural similarities among all Argonaute proteins, they are involved in different small RNA pathways with distinct functions such as translational regulation and transposon suppression.

5.3.1. Ago Proteins and Small RNA Functions in Somatic Cells

5.3.1.1. Subcellular Localization of Ago Proteins – Insights and Open Questions

Ago proteins localize to cytoplasmic RNA granules which are known as processing (P-) bodies or GW bodies⁹³⁻⁹⁵. P-bodies are enriched in proteins that act in various pathways of mRNA metabolism such as nonsense-mediated decay (NMD), deadenylation and decapping. Therefore, P-bodies are considered as cellular sites of mRNA surveillance and decay⁹⁶. The observation that Ago proteins localize to P-bodies suggested that these granules could also play a role in the miRNA pathway or even be essential for miRNA function. Indeed, there are several lines of evidence that support this hypothesis: First, several Ago-interacting proteins such as GW182/TNRC6A, TNRC6B, RCK/p54, Dcp1a and Dcp2 localize to P-bodies⁹⁷⁻¹⁰⁰. At least three of these proteins, RCK/p54, GW182/TNRC6A and TNRC6B, are essential for the miRNA pathway^{94, 97, 99}. Second, mRNAs can be targeted to P-bodies in a miRNA-dependent manner^{94, 101, 102}. Additionally, Ago proteins that carry mutations in the PAZ domain which abolish miRNA binding do not localize to P-bodies anymore¹⁰³. Taken together, these data put forward a model in which miRNAs together with Ago proteins bind to their target mRNAs and induce mRNP aggregation and sequestration into P-bodies (figure 4). These mRNAs may be subsequently degraded in P-bodies by the deadenylation and decapping machinery and the 5'->3' exonuclease Xrn1 or only translationally inhibited. Interestingly, it was shown that the CAT-1 mRNA can be translationally repressed by miR-122 and stored in P-bodies¹⁰¹. Upon cellular stress, CAT-1 mRNA is released from P-bodies by the AU-rich element binding protein HuR and efficiently translated. Thus, the recruitment of mRNAs to P-bodies is not a general commitment for decay but can be reversible at least in some cases.

Despite the evidence supporting a role of P-bodies in the miRNA pathway, recent studies proposed that P-bodies are formed as a consequence of mRNA silencing pathways but are not required for the functional integrity of the miRNA pathway^{97, 104}. P-bodies are thought to be highly dynamic structures, and it was demonstrated that the formation of visible P-bodies is sensitive to downregulation of several P-body

components^{94, 97, 104, 105}. Importantly, some P-body components such as LSm1 and LSm3 are required for visible P-body formation but not for miRNA function, indicating that macroscopic P-bodies are not essential for the miRNA pathway^{97, 104, 105}. Conversely, knockdown of miRNA pathway factors such as Dicer and Drosha depletes P-bodies. P-body formation can be rescued by expressing an artificial small RNA target together with the corresponding small RNA, suggesting that silencing pathways such as the miRNA pathway are upstream triggers of P-body formation^{104, 106}. However, although the knockdown of LSm proteins demonstrated that visible P-bodies are not essential for miRNA function, these experiments do not exclude the presence of sub-microscopic P-bodies, which could be required for the miRNA pathway. Clearly, high-resolution techniques such as electron microscopy will be needed to address this possibility.

P-bodies share several protein components with another class of cytoplasmic foci, so-called stress granules¹⁰⁷. Stress granules (SG's) are formed upon various forms of cellular stress such as heat shock or oxidative conditions. SG assembly is triggered by phosphorylation of the translation initiation factor eIF2 α , which reduces the availability of the eIF2 α -GTP-tRNA_i^{Met} complex for translation initiation and causes accumulation of stalled 48S pre-initiation complexes, which lack the initiation factors eIF2 and eIF5¹⁰⁷. A recent quantitative analysis of Ago protein localization revealed that only a minor portion of enhanced green fluorescent protein- (EGFP)-tagged Ago2 (1.3%) localizes to P-bodies and that the majority of Ago2 is diffusely distributed throughout the cytoplasm¹⁰⁸. Importantly, EGFP-Ago2 is also present in SG's. Photobleaching experiments showed that the pool of EGFP-Ago2 that localizes to SG's is more dynamic than the pool in P-bodies. Moreover, EGFP-Ago2 fails to localize to SG's but still localizes to P-bodies in Dicer knockout cells¹⁰⁸. These data would be consistent with the hypothesis that miRNAs repress their targets in SG's rather than in P-bodies. However, the fact that Ago2 localizes to P-bodies in Dicer-deficient cells could also be due to additional Dicer-independent pathways that target Ago2 to P-bodies such as Dicer-independent small RNA pools which have recently been reported¹⁰⁹.

One possible model to reconcile the data for P-bodies and stress granules is shown in figure 4: Upon cellular stress, 48S translation pre-initiation complexes which are inhibited by miRNAs (for details, see section 5.3.1.2.2.) could rapidly aggregate and be sequestered to stress granules. As stress granules frequently localize in the

vicinity of P-bodies, it is possible that repressed mRNAs are exchanged between these foci. Thus, miRNA targets could shuttle from stress granules to P-bodies after remodelling and removal of 40S subunits and some translation initiation factors which are not present in P-bodies such as eIF2 and eIF3. P-bodies could represent a more static storage site for some mRNAs and a site of decay for other mRNAs. However, miRNAs function in the absence of cellular stress and it is unknown whether SG's or related structures exist under such conditions. Thus, it is likely that a stress-granule-independent pathway exists which sorts repressed miRNA targets to P-bodies.

Although immunofluorescence experiments of mammalian Ago proteins typically show a mainly cytoplasmic staining pattern, several studies have focused on the localization and possible functions of Ago proteins in the nucleus. Nuclear functions of Ago proteins have been reported in many species such as *Schizosaccharomyces pombe* (*S. pombe*), *D. melanogaster*, *C. elegans* and in plants¹¹⁰, but nuclear Ago functions in mammalian cells are still a matter of debate. Sub-cellular fractionation experiments showed that Ago proteins are present in nuclear fractions, but these studies did not rule out the possibility that Ago signals could be due to an association with the outer nuclear envelope^{4, 111}. Similarly, nuclear transcripts such as U6 snRNA or 7SK RNA can be depleted by RNAi, suggesting that Ago2 may be present and active in the nucleus (figure 4, upper panel). It was, however, not excluded that these transcripts could transiently shuttle through the cytoplasm, allowing for degradation by Ago2¹¹¹.

In *S. pombe*, Ago guides transcriptional silencing by guiding heterochromatin formation¹⁴. Indeed, it was also shown in human cells that transfected siRNAs directed to promoter regions can either lead to transcriptional gene silencing or gene activation, depending on the target site within the promoter¹¹²⁻¹¹⁶. Chromatin immunoprecipitation (ChIP) experiments revealed that Ago proteins were recruited to the targeted promoters after siRNA transfection¹¹³⁻¹¹⁶. Moreover, transcriptional modulation was sensitive to the knockdown of Ago1 and/or Ago2, suggesting that these proteins can silence or activate gene expression when loaded with promoter-directed siRNAs (figure 4, upper panel). However, evidence that endo-siRNAs can guide transcriptional silencing in human cells remains elusive, and therefore it is currently unclear whether these silencing mechanisms are biologically relevant in humans. It will therefore be interesting to determine whether specific Ago-interacting

proteins are involved in this pathway and to investigate whether their roles are evolutionarily conserved. The present study describes the identification of Importin 8 (Imp8) as an Ago-interacting protein that can modulate nuclear localization of Ago proteins (publication 8).

Figure 4

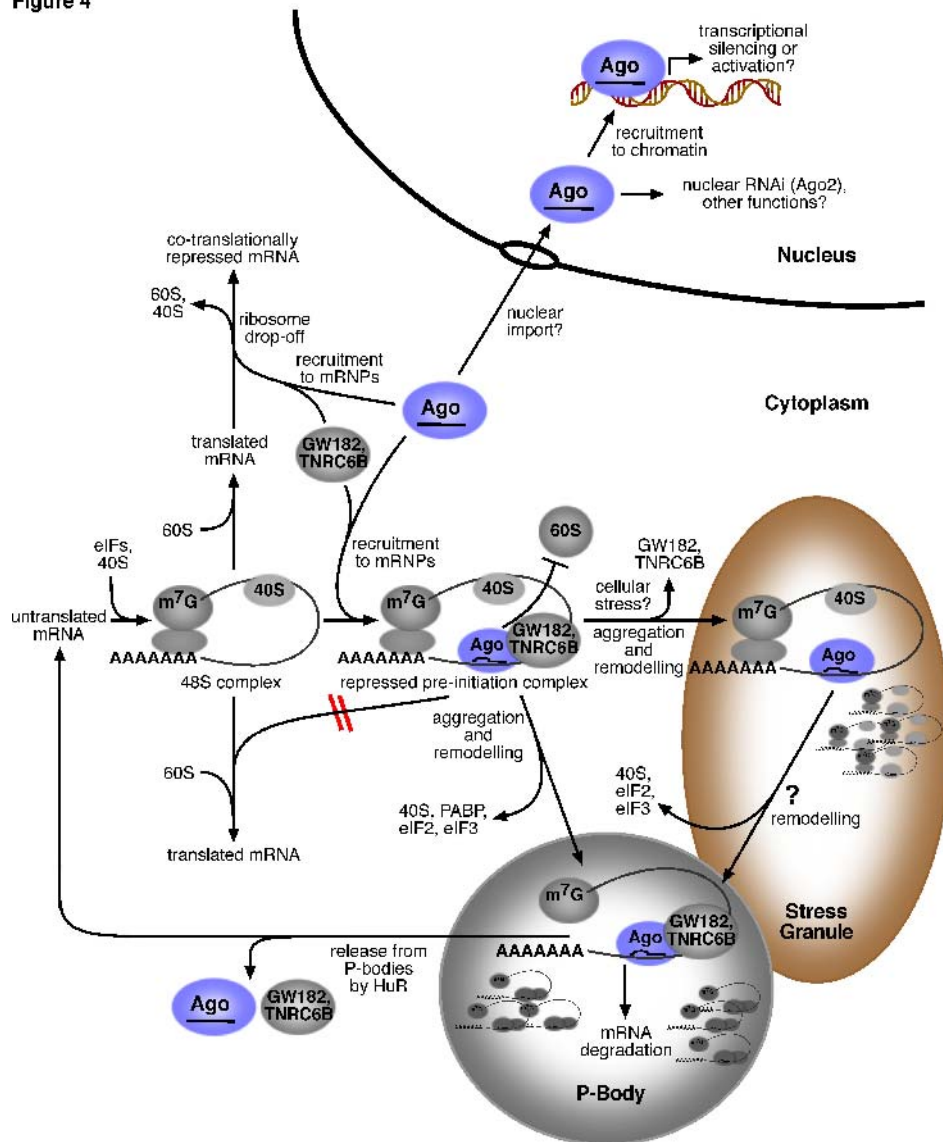


Figure 4: Subcellular localization of Ago proteins. In the cytoplasm, miRNAs and Ago protein complexes could be recruited to translating mRNAs and induce ribosome drop-off and co-translational repression (upper left panel). Alternatively, Ago protein complexes could bind to 48S pre-initiation complexes to repress translation initiation by preventing joining of the 60S ribosomal subunit (middle panel). Upon cellular stress, repressed pre-initiation complexes could be sequestered to Stress Granules (middle right panel). This requires remodelling of the complexes, as GW182 and TNRC6B are absent from Stress Granules. Alternatively, Repressed complexes could be sequestered to P-bodies (lower panel). Again, this requires remodelling, because 40S subunits, poly(A) binding protein (PABP), eIF2 and eIF3 are absent from P-bodies. It is also conceivable that repressed mRNPs are transferred from Stress Granules to P-bodies after remodelling, because both types of granules frequently localize close to each other. Repressed mRNAs can either be degraded in P-bodies or released by the RNA binding protein HuR to resume translation. In the nucleus, Ago proteins could bind to promoter elements to guide transcriptional gene activation or gene silencing. Additionally, Ago2 could cleave nuclear transcripts. Please note that several factors such as eIF6 have been omitted from the figure for simplicity.

5.3.1.2. Ago Protein Complexes and Mechanisms of microRNA Function

In somatic mammalian cells, Ago proteins bind to miRNAs^{57, 117} which serve as guides to recruit Ago proteins to partially complementary target sites on mRNAs. Upon binding to their target mRNAs, Ago proteins trigger posttranscriptional repression. Indeed, tethering of Ago proteins to mRNAs revealed that Ago binding is sufficient to repress a target mRNA, suggesting that Ago proteins are crucial mediators of miRNA function¹¹⁸. The following sections will focus on the mechanisms of posttranscriptional repression that are triggered by miRNAs and Ago proteins.

5.3.1.2.1. Determinants of microRNA – Target Interactions

MiRNAs can potentially regulate a high number of target mRNAs. Therefore many different experimental and computational approaches have tried to define principles of typical miRNA-miRNA target interactions to enable computational miRNA target predictions with high accuracy¹¹⁹.

An early study showed that the 5'-regions of metazoan miRNAs are more conserved than the 3'-parts, suggesting that they might be crucial for miRNA function¹²⁰. Such 5'-regions (nt 1-8 or nt 2-8) of miRNAs have been termed "seed sequences". Consistent with miRNA conservation data, miRNA-guided repression is relieved when pairing of the miRNA seed sequence to the miRNA target site is disrupted by mutations, indicating that seed pairing is important for target repression¹²¹⁻¹²³. Moreover, miRNA seed matches are highly conserved in human 3'-UTRs¹²⁴. Likewise, conserved miRNA seed matches display a significantly lower single nucleotide polymorphism (SNP) frequency than other conserved 3'-UTR elements, indicating that miRNA seed pairing is under negative selective pressure and that SNPs in many miRNA seed binding sites are likely to be deleterious¹²⁵. These experimental and computational data suggested that the miRNA seed pairing is the most crucial determinant of miRNA targeting. However, it was shown early that single mismatches in the seed region can be compensated by a high degree of complementarity in the 3' part of the miRNA sequence¹²¹. Thus, miRNA seed pairing is important but not always required for repression.

In addition to the properties of the miRNA target site itself, the surrounding context of the target 3'-UTR influences miRNA-guided repression. Statistically, miRNA target sites in long 3'-UTRs are more efficient when located at the beginning or at the end of the 3'-UTR¹²⁶. Moreover, an AU-rich 3'-UTR context statistically enhances the efficiency of miRNA target sites, most likely because those target sites are more accessible than others^{126, 127}.

Interestingly, a recent report showed that a miRNA which targets an mRNA in a particular cell type can fail to suppress the same target in a different cell type¹²⁸. These data suggested that miRNA-target interactions do not only depend on the properties of the miRNA and the target mRNA, but are also determined by other, cell-type specific factors. Such factors could be RNA binding proteins that either contribute to or prevent silencing of specific target mRNAs. Indeed, it was shown that miRNP access to 3'-UTRs can be blocked by the RNA binding protein Dead-end 1 (Dnd1), which binds to U-rich 3'-UTR elements¹²⁹.

The above-described paradigm that miRNPs can suppress mRNAs by binding to their 3'-UTRs is supported by many experimental and computational results. In contrast, miRNA binding to open reading frames (orf's) is thought to be unlikely, because translating ribosomes are expected to interfere with the binding of miRNPs. Indeed, a recent report showed that a mutation of a stop codon that generates a longer orf efficiently destroys miRNA binding sites that are located in the extended orf downstream of the mutated stop codon¹³⁰.

Interestingly, it was recently demonstrated that miRNPs can bind to the 5'-UTRs of ribosomal mRNAs and thereby suppress translation of the corresponding ribosomal proteins¹³¹. These results are consistent with earlier observations that fusion of miRNA binding sites to the 5'-UTRs of reporter constructs can trigger their repression¹²³. Clearly, more studies are required to investigate whether miRNA binding to 5'-UTRs is a frequent event or limited to a small set of target mRNAs.

5.3.1.2.2. Mechanisms of microRNA-Guided Translational Repression

Early studies in *Caenorhabditis elegans* (*C. elegans*) showed that the miRNA lin-4 acts to repress the expression of the lin-14 gene by binding to regulatory elements in the 3'-UTR of the lin-14 mRNA¹³²⁻¹³⁴. Interestingly, neither the levels of the lin-14 mRNA nor its poly(A)-tail length was affected by lin-4, arguing that lin-4 represses protein translation rather than mRNA stability¹³⁵. Notably, polysome association of the lin-14 mRNA was not altered by lin-4, suggesting that this miRNA inhibits translation at a step after initiation. Consistently, several studies showed that miRNAs as well as miRNA target mRNAs co-sediment with polysomes, arguing that miRNAs inhibit translation at the steps of elongation or termination¹³⁵⁻¹³⁷. Moreover, disassembly of polysomes by various agents co-ordinately shifts miRNAs, Argonaute proteins and miRNA targets to lighter polysome gradient fractions, suggesting that miRNPs may physically associate with polyribosomes^{136, 138, 139}. Consequently, it was postulated that miRNAs induce rapid “ribosome drop-off” from target mRNAs (figure 5)¹³⁶. Ribosome drop-off from translating mRNAs implies the production of immature polypeptide chains. Interestingly, it was shown that nascent polypeptide chains which are translated from miRNA target reporter constructs cannot be captured by antibodies directed to the N-terminus, suggesting that such nascent polypeptides may be rapidly degraded by a protease¹³⁹. However, direct evidence for this model remains elusive. Consistent with miRNA-guided repression of translation elongation, two studies reported that internal ribosome entry site (IRES)-mediated translation of reporter mRNAs can be inhibited by miRNAs, similar to cap-dependent translation^{136, 140}. Since mechanisms of IRES-mediated (cap-independent) and cap-dependent translation initiation are different, these data argue for miRNA-guided repression at post-initiation steps.

In spite of the evidence supporting miRNA-guided inhibition of translation elongation, other publications argue for miRNA-guided repression at the initiation step. Several lines of evidence suggest that miRNA function interferes with cap-dependent translation initiation: Reporter mRNAs which bear non-functional ApppN caps are resistant to miRNA-guided translation repression *in vitro* and in cell culture systems, whereas their m⁷G-capped counterparts are efficiently repressed, suggesting that the cap is involved in miRNA function¹⁴¹⁻¹⁴³. Moreover, IRES-mediated translation was

found to be resistant to miRNA-guided repression in some studies^{102, 141}. Consistently, addition of the cap-binding complex eIF4F relieves miRNA target repression *in vitro*, suggesting that miRNA function is related to the cap structure¹⁴². An attractive explanation for these observations is provided by a study which demonstrated that human Ago2 itself contains a motif that directly binds to the m⁷G cap structure¹⁴⁴. Mutational analysis showed that this motif is required for translational repression but is dispensable for endonucleolytic activity of Ago2. Thus, miRNA-loaded Ago2 may directly inhibit translation initiation by competing with the eIF4F complex for m⁷G cap binding, thereby preventing the assembly of a functional initiation complex. However, experiments in *Drosophila* cells suggested that the cap-binding motif of Ago2 is also required for the interaction with GW182¹⁴⁵. GW182 is a protein which interacts with Argonaute proteins and is required for translational repression downstream of miRNA binding¹⁴⁶. Therefore, the phenotype of Ago mutants in the cap-binding domain could partly be due to their inability to recruit GW182 to miRNA target mRNAs.

The model that miRNAs act on translation initiation is further supported by the finding that a high molecular weight complex containing TRBP, Ago2 and Dicer associates with the translation initiation factor eIF6¹⁴⁷. Depletion of eIF6 by RNAi abrogates miRNA silencing in *C. elegans* and in human cells. Interestingly, eIF6 is known to inhibit 80S ribosome assembly¹⁴⁸, raising the possibility that recruitment of eIF6 to mRNAs by the miRNA pathway could block translation initiation by preventing 60S subunit joining (figure 5). This model is also consistent with the observation that miRNA reporter constructs specifically associate with components of the 40S ribosomal subunit, but associate with fewer 60S subunits compared to reporters where miRNA binding sites were mutated¹⁴⁹. Moreover, primer extension experiments revealed that the AUG start codon of repressed reporter constructs is covered by a complex, suggesting that 40S subunits occupy the AUG codon of repressed mRNAs¹⁴⁹. Thus, it is likely that translation initiation of miRNA target mRNAs is blocked after scanning of the 5'-UTR for the start codon and before joining of the 60S subunit (figure 5).

Both models for miRNA function – initiation inhibition and elongation inhibition – are highly controversial. It is currently unclear whether opposing results are due to the different reporter systems or assays that have been used, or whether mechanisms of miRNA function could even be miRNA and/or miRNA target-specific. Most evidence

for an involvement of miRNAs in translation elongation is based on co-sedimentation studies of miRNAs, miRNA target mRNAs and Argonaute proteins with polyribosomes. Importantly, co-sedimentation does not necessarily imply physical interaction, and a recent study has challenged many interpretations of co-sedimentation data: In *Drosophila* cell extracts, miRNAs can induce the formation of heavy mRNP aggregates which are similar in size to polysomes and have therefore been termed “pseudo-polysomes”¹⁴³. It is therefore possible that such pseudo-polysomes were misinterpreted as polysomes in some of the studies which aimed to argue for the inhibition of translation elongation. However, pseudo-polysomes have only been observed in *Drosophila in vitro* systems so far and it is unclear whether pseudo-polysomes exist in other species and other experimental systems as well. In conclusion, miRNA mechanisms of translational repression are not completely resolved and further studies will be required to fully elucidate miRNA function.

Figure 5

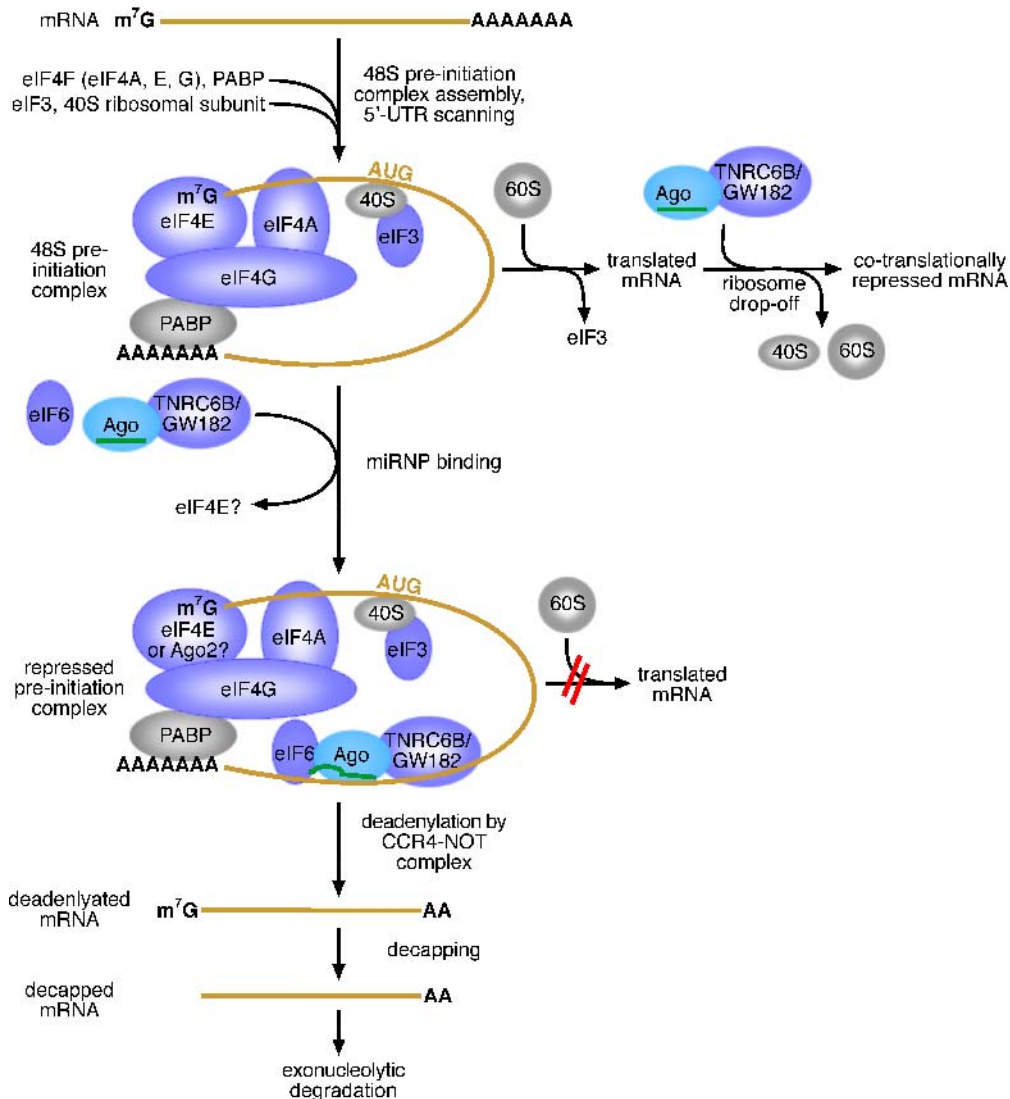


Figure 5: Possible mechanisms of miRNA and Ago protein function. Translation initiation involves the binding of the poly(A) binding protein (PABP) and the eIF4F complex to the mRNA, followed by joining of the 43S complex which contains the 40S ribosomal subunit and eIF3 (upper panels). Subsequently, the 43S complex scans the 5'-UTR for the AUG start codon. Translation elongation starts after joining of the 60S ribosomal subunit and dissociation of eIF3. It was proposed that Ago proteins and miRNAs inhibit translation during elongation by inducing ribosome drop-off (upper right panel). In contrast, it has been suggested by others that Ago proteins and miRNAs act on the 48S pre-initiation complex (middle panel) to prevent joining of the 60S ribosomal subunit, possibly in cooperation with eIF6. It is controversial whether Ago2 directly displaces eIF4E from the m^7G cap structure to inhibit translation initiation. GW182 and/or TNRC6B are thought to be generally required for miRNA function and are therefore expected to cooperate with Ago proteins in all known types of repression. Many repressed mRNAs are unstable, because GW proteins can trigger deadenylation and subsequent decapping and mRNA degradation (lower panels). Please note that several translation initiation factors have been omitted from the figure for simplification. Please also note that the exact composition of the repressed pre-initiation complex has not yet been determined and is therefore hypothetical.

5.3.1.2.3. MicroRNA-Guided Destabilization of Target mRNAs

Biochemical analyses of human Ago proteins revealed that Ago2 is an endonuclease that cleaves target RNAs which are highly complementary to the small RNA bound by Ago2^{3, 4}. Indeed, it was shown that miR-196 can trigger endonucleolytic cleavage of the HoxB8 mRNA in mice¹⁵⁰. However, miRNAs have only very few perfectly complementary targets in mammals and it is therefore unlikely that endonucleolytic cleavage is a widespread mechanism of miRNA function in these species. Nevertheless, mounting evidence indicates that miRNAs can not only trigger translational inhibition, but also destabilization of many target mRNAs¹⁵¹⁻¹⁵⁸. Such mRNA degradation processes involve recruitment of the deadenylation machinery rather than endonucleolytic cleavage by Ago2^{153, 158, 159}. The repressive effects of miRNAs and Ago proteins on target mRNAs depend on members of a conserved family of RNA binding proteins with Glycine-Tryptophan (GW) repeats that interact with Ago proteins^{94, 99, 146, 160} (see also publication 1, section 11). In humans, this family comprises TNRC6A (GW182), TNRC6B and TNRC6C, whereas *Drosophila* cells only express one family member, GW182. Experiments, which utilized tethering approaches of Ago1 and GW182 to mRNAs, revealed that *Drosophila* GW182 is required for target mRNA degradation and translational repression downstream of Ago1 mRNA binding¹⁵⁹. Inhibition of the interaction of GW and Ago proteins by using competing peptides relieves miRNA-guided silencing *in vitro* and in cell culture, suggesting that the interaction of GW182 and Ago proteins is required for miRNA-guided repression^{145, 161}.

GW182-triggered target mRNA degradation, but not translational repression requires the decapping DCP1:DCP2 complex as well as components of the deadenylation machinery, CAF1 and NOT1 (figure 5, lower panel)¹⁴⁵. Consistently, human Ago1 and Ago2 interact with Dcp1a and Dcp2¹⁰³. These data put forward a model in which miRNAs together with Ago proteins act to recruit proteins of the GW family to miRNA target mRNAs. GW proteins, in turn, trigger translational repression and often deadenylation and subsequent decapping of target mRNAs, which can eventually lead to mRNA degradation.

Recent proteome- and transcriptome-wide studies which utilized microarray and mass spectrometry approaches showed that the relative contribution of translational repression and mRNA destabilization to miRNA-guided repression varies depending

on the individual miRNA target^{151, 157}. Further studies will be required to find elements on 3'-UTR's and protein factors such as specific RNA binding proteins that determine the mechanisms of target repression.

5.3.1.2.4. Other Mechanisms of microRNA Function

Recent reports suggest that miRNAs are also capable of activating translation^{162, 163}. While miRNA-guided repression is predominant in proliferating cells, translation activation occurs during cell cycle arrest and can involve binding of miRNPs to AU-rich elements. Interestingly, miRNAs can repress and activate translation of the same targets, depending on the cell cycle stage¹⁶³. Notably, most studies on miRNA function have been performed in rapidly proliferating cell lines, raising the possibility that miRNA-guided translation activation might be a more general mechanism in resting cells. However, comprehensive analyses of miRNA targets during cell cycle arrest, which could provide more general support for such mechanisms, have not yet been performed.

5.3.1.3. Ago2 and RNA Interference (RNAi)

siRNAs trigger the cleavage of complementary target RNAs by binding to an Argonaute protein with endonucleolytic activity. Ago2 is the only human Ago protein with such “slicer” activity and it is therefore essential for RNAi^{3, 4}. Biochemical studies showed that the cleavage reaction requires Mg²⁺ ions, is ATP-independent and generates products with 5'-phosphates and 3'-OH groups^{164, 165}. Because siRNAs, which are generated by Dicer, carry 5'-phosphate groups, several groups have investigated a possible involvement of the 5'-phosphate in RNAi. To rule out phosphorylation of siRNAs by cellular kinases, these experiments employed chemically modified siRNAs with 5'-methoxy (CH₃O) groups, which cannot be phosphorylated. It is now widely accepted that the 5'-phosphate is required for RNAi, but it has been controversially discussed whether single-stranded siRNAs can form active RISC when lacking a 5'-phosphate^{3, 18, 90, 166-168}. Because chemically synthesized siRNAs are usually not phosphorylated, they have to be modified by cellular kinases in order to be active. Interestingly, it was recently shown that the kinase hClp1 phosphorylates siRNAs on their 5'-ends and is required for their activity¹⁶⁹.

While RISC loading likely involves the formation of larger complexes, mature siRNA-loaded active RISC can be as small as 100 kilodalton (kDa), and it was demonstrated that Ago2 together with a single-stranded siRNA can form a minimal RISC^{90, 170}. It therefore appears likely that Ago2-mediated endonucleolytic target RNA cleavage requires less factors than miRNA-guided repression, which targets translation initiation, elongation or mRNA stability through more complex mechanisms. However, depletion of the miRNA pathway factors GW182 and TNRC6B affects miRNA-guided mRNA cleavage, suggesting that these proteins enhance the efficiency of RNAi^{99, 146}.

RNAi was initially regarded as a highly specific process by which siRNAs can trigger the sequence-dependent degradation of perfectly complementary target RNAs. Therefore, RNAi is widely being used as a research tool to study loss-of-function phenotypes of particular genes of interest. However, mounting evidence suggests that siRNAs can downregulate a large number of partially complementary “off-target” transcripts in addition to their target. Similar to miRNA target mRNAs, siRNA off-

targets contain many sites in their 3'-UTRs which are complementary to nt 1-8 of the siRNA, i.e. the siRNA seed sequence⁵⁻⁸. Therefore, siRNA off-targeting resembles miRNA-guided repression and it is likely that siRNAs repress their off-targets by binding to all Ago proteins¹⁷¹. Indeed, siRNAs are efficiently loaded to human Ago1-4, similar to miRNAs³. Notably, thermodynamic asymmetry is often not sufficient to completely prevent incorporation of siRNA passenger strands into Ago protein complexes, indicating that both strands of siRNA duplexes can potentially have off-targets^{49, 50} (see also publication 4, section 11). siRNA off-target effects may cause false-positive results in loss-of-function experiments. Furthermore, off-target effects are an obstacle for therapeutic applications of siRNAs. Therefore, the reduction of siRNA off-target effects is a major goal of siRNA research. This thesis describes an efficient method to prevent the incorporation of the passenger strand into RISC to block its off-target effects (publication 4).

5.3.2. Ago2 and endo-siRNAs

Endo-siRNAs are present in mouse oocytes and derive from various sources of dsRNA including pairs of gene and complementary pseudogene transcripts and repetitive elements^{21, 80}. Transposon transcripts containing perfectly complementary binding sites for endo-siRNAs are upregulated in Dicer- or Ago2-deficient oocytes, suggesting that endo-siRNAs could target these repetitive elements, possibly through Ago2-mediated endonucleolytic cleavage^{21, 80}. However, a direct proof of endo-siRNA function is still missing.

In addition to transposon suppression, endo-siRNAs, which derive from gene-pseudogene pairs, are complementary to coding genes. Indeed, it was shown that Dicer and Ago2 mutants have elevated levels of endo-siRNA target mRNAs^{21, 80}. Importantly, those target mRNAs with a higher number of siRNA target sites are more strongly upregulated in Dicer-deficient mice than mRNAs with fewer matches²¹. Collectively, these data suggest that endo-siRNAs regulate several protein-coding genes.

Although mammalian endo-siRNAs have only been found in oocytes so far, loss of Ago2 causes severe developmental defects in somatic tissues such as failure to close the neural tube and swelling inside the pericardial membrane³. It remains to be investigated whether these somatic phenotypes are due to the function of Ago2 in miRNA-guided repression or its function in the endo-siRNA pathway, which might play a role in somatic development as well.

5.3.3. Piwi Proteins, piRNAs and Transposon Silencing in the Germline

Since their discovery, Piwi proteins have emerged as essential guardians of the genome in germ cells, and it becomes clear that they play key-roles in transposon suppression²³. In mammals, insight into the function of Piwi proteins is largely based on knockout studies of the three Piwi family members in mice, MIWI, MIWI2 and MILI. Loss of MILI or MIWI2 causes apoptosis of sperm cells around the pachytene stage of meiosis^{172, 173}, whereas defects in MIWI-deficient mice occur later at the haploid, round spermatid stage¹⁷⁴. Interestingly, both MILI- and MIWI2-deficient sperm cells display increased levels of DNA double-strand breaks, as assessed by staining of phosphorylated H2AX. Moreover, MILI- and MIWI2-deficient mice show higher levels of transposon transcripts^{172, 173}. These phenotypes could be explained by a model in which MILI and MIWI2 bind piRNAs from repetitive elements, which guide them to transposon transcripts. These transcripts could be repressed through RNAi-like degradation and/or transcriptional silencing. Loss of silencing in MILI- and MIWI2-deficient mice may lead to transposon “de-repression” and accumulation of DNA double-strand breaks. This model is supported by the observation that pre-pachytene piRNAs frequently derive from repetitive elements⁶². Notably, all Piwi proteins in mice carry the catalytic DDH triad that is required for endonucleolytic activity. Indeed, it has been observed that the rat Piwi protein Rivi co-fractionates with an endonucleolytic activity⁶¹. However, transposon cleavage activity of immunopurified Piwi proteins has not yet been observed in *in vitro* systems.

Because germline defects in MIWI-deficient mice manifest later than the meiotic phenotypes of MILI and MIWI2, it is possible that MIWI plays a different role in spermatogenesis. This hypothesis is supported by the finding that MIWI binds to mRNAs of proteins that are involved in spermatogenesis¹⁷⁴. Thus, MIWI might play a role that is similar to the function of Ago proteins in somatic cells.

5.4. Biological Roles of Animal miRNAs

Since their discovery, miRNAs are emerging as crucial regulators of diverse biological processes in higher eukaryotes. It was described early that *lin-4* and *let-7*, the founding members of the miRNA family, are involved in the development of *C. elegans* larvae, because mutants exhibit defects in developmental timing^{133, 175}. Other pioneering studies showed that miRNAs control asymmetric specification of certain *C. elegans* neurons¹⁷⁶⁻¹⁷⁸. Today, numerous studies indicate that miRNAs are important developmental regulators in many species including mice and humans¹⁷⁹. For example, mice deficient in the miR-17-92 cluster die shortly after birth with lung and heart defects¹⁸⁰. Moreover, this miRNA cluster is also essential for B-cell development¹⁸⁰. In contrast, miR-155 regulates cytokine production of T-cells and is required for proper T-cell development¹⁸¹.

Beside their role during development, it soon became apparent that the miRNA network is frequently de-regulated in cancer. The first evidence that miRNAs could function as tumor suppressors came from a study which reported that patients with B-cell chronic lymphocytic leukemia (BCLL) frequently carry deletions in the 13q14 locus which contains genes of miR-15a and miR-16-1¹⁸². More recent reports have shown that *let-7* functions as a tumor suppressor in lung cancer by suppressing the Ras oncogenes^{183, 184}. Today, several other tumor suppressor miRNAs have been characterized. In contrast to these miRNAs, other miRNAs can function as oncogenes when aberrantly expressed in certain cell types. For example, miR-21 is frequently upregulated in glioblastomas, and inhibition of miR-21 triggers apoptosis, indicating that miR-21 is important for glioblastoma cell survival^{185, 186}. Thus, miRNAs can act both as oncogenes and tumor suppressors, depending on the particular miRNA and the cell type. The importance of miRNAs in tumor biology is further corroborated by the finding that the expression of different miRNA pathway proteins is de-regulated in various cancer types. For instance, the genes for human Ago1, Ago3 and Ago4 are located in a region on chromosome 1 (1p34-35) which is frequently deleted in Wilms tumors of the kidney and in neuroblastomas¹⁸⁷. Moreover, reduced Dicer expression is significantly correlated with poor prognosis in lung cancer¹⁸⁸. Similarly, a recent study identified a mutation in TRBP which affects overall levels of mature miRNAs, destabilizes Dicer and frequently occurs in colon and endometrial tumors¹⁸⁹. Importantly, re-introduction of TRBP into cancer cells

inhibits tumor growth and restores mature miRNA levels, suggesting that the miRNA pathway has growth-suppressive functions in these tumors¹⁸⁹.

Taken together, miRNAs have diverse roles in development and in various diseases. To date, several miRNA targets have been characterized that may account for some of the phenotypes that are associated with the overexpression or the loss of certain miRNAs. However, it is widely assumed that each miRNA regulates many targets and it still remains a major challenge of the miRNA field to identify and to characterize these miRNA targets and their potential biological roles. This thesis describes a novel method to experimentally identify miRNA target mRNAs from their physical association with Ago protein complexes, providing a useful tool to find new miRNA targets (publications 2 and 8).

5.5. Aims of the PhD Thesis

Ago proteins are central components of siRNA- and miRNA-guided gene silencing complexes, because they are present in a complex together with small RNAs as well as their target RNAs. Moreover, Ago proteins likely bind to a variety of auxiliary protein factors that are important for small RNA-guided gene silencing. Therefore, the aim of this thesis is to purify Ago complexes and to identify and functionally characterize their protein, small RNA and mRNA components:

1) It is well established that Ago proteins associate with upstream factors of the miRNA biogenesis pathway such as Dicer and TRBP. However, very little is known about Ago-interacting proteins that function after the loading of miRNAs to Ago proteins: Firstly, it is unclear whether miRNPs find their target sites on 3'-UTRs by passive diffusion and base-pairing or whether additional factors exist which promote or antagonize binding of Ago proteins to their targets. Secondly, factors that are recruited by Ago proteins to achieve miRNA-guided translational repression and mRNA decay of miRNA targets are essentially unknown. Thirdly, it is unclear whether other 3'-UTR binding proteins could interact with Ago proteins to enhance or to relieve gene silencing. Thus, this thesis mainly focuses on novel Ago-associated proteins that function downstream of miRNA loading (publications 1, 3 and 8). We therefore aim to purify human Ago1-4 protein complexes by immunoprecipitating tagged and endogenous Ago proteins with appropriate antibodies, followed by the identification of interacting proteins by mass spectrometry. Next, we want to validate such interactions by different experimental approaches such as co-immunoprecipitation and *in vitro* binding assays. Finally, we aim to functionally investigate possible roles of Ago-interacting proteins in small RNA-guided gene silencing, using EGFP- or luciferase-based reporter systems for miRNA function.

2) Since Ago proteins are direct binding partners for different types of small RNAs, a second aim of this thesis is to identify novel types of small RNAs from immunopurified Ago protein complexes by RNA cloning and deep sequencing methods. After identifying these small RNAs, we will characterize them functionally, i.e. test whether they could act like known small RNAs such as miRNAs or siRNAs (publication 7). Importantly, the human transcriptome contains many small RNA sequences that are derived from various non-coding RNAs such as tRNAs, rRNAs

and scRNAs, and it is unclear which of these small RNAs are functionally incorporated into Ago protein complexes¹⁰⁹.

3) Bioinformatic miRNA target prediction algorithms are mostly based on assumptions such as perfect base-pairing of the miRNA seed sequence with the target site, which are true for many, but not all miRNA target sites^{119, 121}. Thus, it is likely that some of the predicted target sites are not functional. Conversely, some miRNA targets with non-canonical binding sites (e.g. sites with imperfect base-pairing of the seed sequence) are probably missed by most prediction algorithms. Therefore, an unbiased experimental method to identify miRNA target mRNAs is needed. Because Ago proteins physically associate with miRNA target mRNAs, we aim to establish a method to identify miRNA targets from immunoprecipitated Ago protein complexes by cloning and sequencing (publication 2) or microarray analyses (publication 8) of Ago-associated mRNAs.

In an independent project, we analyzed siRNA activities aiming at the improvement of RNAi specificity and efficiency. SiRNA off-target effects (sequence-specific downregulation of mRNAs that are unrelated to the siRNA target) are a major problem for siRNA applications in research and in medical therapies (section 5.3.1.3.). Depending on their incorporation into RISC, both strands of an siRNA duplex can potentially have off-target effects^{49, 50}. However, strands that are not incorporated into RISC will not have sequence-specific off-target effects, and only one strand (the guide strand) is required for silencing, while the opposing strand (passenger strand) is dispensable. Therefore, we chemically modified siRNA 5'-ends and analyzed incorporation into RISC (publication 4).

6. Discussion

6.1. Proteomic and Functional Analyses of Human Ago Protein Complexes

To identify new proteins that function in the miRNA pathway, we purified complexes of all four human Ago proteins and analyzed their composition by using mass spectrometry and co-immunoprecipitation experiments. (publications 1, 3, and 8). We identified the novel Ago-associated proteins TNRC6B and MOV10 and showed that they are required for miRNA-guided gene silencing (publication 1). TNRC6B belongs to a conserved family of proteins with glycine-tryptophan (GW) repeats which comprises three proteins in humans, TNRC6A/GW182, TNRC6B, and TNRC6C. Similar to TNRC6B, its human homologs TNRC6A/GW182⁹⁴ and TNRC6C¹⁹⁰ as well as GW proteins in other species are required for miRNA-guided gene silencing^{146, 160}. Studies in *Drosophila* revealed that GW proteins most likely function by recruiting the deadenylation machinery to mRNAs which are targeted by Ago proteins and miRNAs, thereby destabilizing the mRNAs¹⁵⁹. However, in cells where mRNA decay was inhibited by knockdown of decapping enzymes, GW proteins are still required for miRNA-guided translational repression, indicating that they play a role in translational repression as well¹⁵⁹. Today, the exact mechanisms by which GW proteins trigger silencing are still unclear. However, it was recently shown that the domain which triggers silencing maps to the C-terminal GW repeats (“silencing domain”)¹⁹⁰. Further studies will be required to fully elucidate the mechanisms of these central players of miRNA-guided gene silencing.

MOV10 is a putative RNA helicase and a homolog of the *Drosophila* protein armitage. Armitage is required for RISC assembly and siRNA function in *Drosophila* cell lysates, suggesting that the function of this putative helicase could be conserved^{191, 192}. It is conceivable that MOV10 might help to unwind miRNA/miRNA* intermediates, thereby enabling efficient loading of RISC and miRNPs with small RNAs. However, this has not been tested yet and the precise function of MOV10 is still unknown.

After this initial study, we characterized the proteomic composition of Ago protein complexes in more detail and found that Ago proteins reside in at least three different

complexes of different sizes (publication 3). The two larger complexes contain mRNAs and may therefore represent repressed mRNPs. We showed that in the large complexes, Ago proteins specifically associate with many RNA helicases in a RNA-dependent and independent manner. For instance, RHA and DDX36 associate with Ago proteins in an RNA-independent manner. Interestingly, it was later shown that RHA is required for RNAi, and it was proposed that it could be involved in RISC loading⁴⁷. Moreover, we identified several mRNA binding proteins that specifically co-immunoprecipitate with Ago1 and Ago2 in an RNA-dependent manner, suggesting that miRNPs may act in concert with these mRNA binding proteins to achieve repression of target mRNAs. Consistently, we demonstrated that RNA binding motif protein 4 (RBM4) is essential for repression of several miRNA targets, although its interaction with Ago proteins is RNA-dependent. This observation could be explained by a model, in which RBM4 binds to miRNA target mRNAs prior to miRNP binding. It may help to recruit Ago proteins to the target mRNAs or to stabilize the interaction of Ago proteins with miRNA target mRNAs. In this case, mRNAs would have to be marked by RBM4 or similar RNA binding proteins to become susceptible to Ago protein recruitment and miRNA-guided repression. The logical consequence of such a model would be that not all mRNAs with predicted miRNA binding sites are actually miRNA targets, but only those that contain binding sites for RBM4 or similar proteins. Consequently, it would be expected that RBM4 strongly associates with miRNA target mRNAs. Indeed, it has been observed that LARK, the *Drosophila* homolog of RBM4, associates with a pool of mRNAs that is strongly enriched in predicted miRNA binding sites¹⁹³. Nevertheless, it is also possible that RBM4 could be a more general 3'-UTR remodelling factor with additional roles in the miRNA pathway, because it was recently reported that RBM4 suppresses m⁷G-cap-dependent translation through CU-rich elements in the 3'-UTRs¹⁹⁴.

Next we extended our studies to include Ago3 and Ago4 in our proteomic and functional analyses. We found that Imp8 specifically interacts with Ago1-4 in an RNA-independent manner (publication 8). Imp8 belongs to a family of Importin β -like proteins that are involved in nuclear import of protein substrates^{1, 195}, raising the possibility that Imp8 could be a nuclear import receptor for Ago proteins. Nuclear functions of mammalian Ago proteins such as nuclear RNAi and Ago-dependent transcriptional silencing are controversially discussed in the small RNA research field (section 5.3.1.1.), because most studies on nuclear Ago functions rely on artificial

overexpression of small RNAs, and endogenous small RNAs that clearly function in the nucleus have not yet been identified. Moreover, the pathways that Ago proteins utilize for nuclear silencing are still unknown. Importantly, the subcellular localization of Ago proteins is also a matter of debate, because subcellular fractionation experiments suggest that a significant fraction of Ago proteins is in the nucleus, while most immunofluorescent approaches display a mainly cytoplasmic staining pattern. Therefore, we generated a monoclonal antibody to human Ago2 and re-investigated whether Ago2 localizes to the nucleus (publication 5). Interestingly, we found that Ago2 localizes to both the cytoplasm and the nucleus. The staining intensity from both compartments was strongly decreased when Ago2 was depleted by RNAi, suggesting that the nuclear signal was Ago2-specific. Strikingly, the localization of endogenous Ago2 was shifted towards the cytoplasm after knockdown of Imp8. Similar results were obtained with a cell line expressing EGFP-tagged Ago2 (publications 6 and 8). Thus, Imp8 affects nuclear localization of Ago2. Taken together, these data would be consistent with a model in which Imp8 imports Ago2 into the nucleus. However, the observation that Imp8 modulates the nuclear Ago2 pool could potentially also be due to indirect effects. For instance, a protein that strongly associates with Ago2 could be imported into the nucleus by Imp8, and its depletion from the nucleus after Imp8 knockdown might co-deplete Ago2 from the nucleus. In line with such a model, Ago2 lacks classical nuclear localization signals and it remains to be addressed which domains of Ago2 are responsible for nuclear targeting. Clearly, *in vitro* assays such as nuclear import assays of recombinant Ago proteins will be needed to resolve whether Imp8 directly imports Ago proteins into the nucleus. Notably, a significant portion of Ago2 remains in the nucleus after knockdown of Imp8, raising the possibility that other import receptors could contribute to nuclear Ago2 import as well. Alternatively, these results could be due to residual levels of Imp8 after siRNA transfection.

In conclusion, the finding that Imp8 modulates Ago protein localization is intriguing because Imp8 may be part of a pathway that facilitates nuclear functions of Argonaute proteins. Interestingly, the germline-specific Argonaute protein MIWI2 is mainly localized to the nucleus¹⁹⁶. Thus, further studies will be required to analyze whether Imp8 is a nuclear import receptor for MIWI2 with possible roles in germ cell maintenance.

In addition to its role for Ago protein localization, we noticed that Imp8 co-localizes with Ago proteins in cytoplasmic P-bodies (publication 8) which have been implicated in miRNA-guided gene silencing⁹⁶. This result and the fact that Imp8 interacts with Ago proteins suggested that Imp8 could play a role in the miRNA pathway. We demonstrated that Imp8 is indeed required for miRNA-guided gene silencing. In contrast to known miRNA pathway factors which function in miRNA maturation (e.g., Dicer and Drosha) or in steps downstream of target mRNA binding (e.g., TNRC6B and GW182), Imp8 is required for efficient binding of Ago proteins to their target mRNAs, as shown by microarray analysis of Ago2-associated miRNA targets. Thus, we identified Imp8 as the first factor that positively regulates miRNP binding to target mRNAs. Interestingly, we found that miRNA target mRNAs are not enriched in anti-Imp8 immunoprecipitates, suggesting that Imp8 does not stably interact with Ago2 on target mRNAs. Consistently, mass spectrometry analyses revealed that Imp8 co-immunoprecipitates with low molecular weight complexes of Ago2, but not with heavier complexes containing mRNAs (publication 3). Thus, Imp8 may preferentially interact with Ago proteins prior to target mRNA binding (see model in Figure 7, publication 8). It therefore remains to be investigated how Imp8 promotes the Ago-target mRNA interaction, although it interacts with mRNA-free miRNPs rather than with repressed mRNPs. Intriguingly, it was proposed that Importin β -like proteins could serve as chaperones for their substrate proteins by preventing unspecific aggregation with nucleic acids into insoluble complexes¹⁹⁵. We showed that knockdown of Imp8 does neither affect the levels of soluble Ago proteins nor their stability. However, it appears possible that Imp8 helps to maintain an active conformation of Ago proteins that is required for stable binding of target mRNAs. In such a model, Imp8 could bind to Ago proteins which are released from P-bodies and help to maintain the active conformation until the miRNP is recruited to a new miRNA target mRNA (Figure 7, publication 8). Notably, structural analysis of the *Thermus thermophilus* Argonaute protein revealed that the ternary complex of Argonaute together with a guide strand and a target RNA adopts a different conformation than the binary complex of Argonaute with the guide strand. The nucleic acid binding channel between the PAZ domain and the PIWI domain widens to accept the target RNA¹⁹⁷. Thus, target mRNA binding involves conformational changes, and it is tempting to speculate that Imp8 might be involved in maintaining a conformation that is capable of undergoing such rearrangements. However, we demonstrated that

while Imp8 is required for miRNA-guided repression of imperfectly complementary targets, it is dispensable for RNAi. RNAi also requires transient binding of Ago2 to the target mRNA. It therefore remains to be investigated whether RNAi and miRNA-guided repression requires different Ago protein conformations and whether one of them is specifically promoted by Imp8. Alternatively, Imp8 could promote a posttranslational modification of Ago proteins that is essential for stable target mRNA binding.

Considering that Imp8 is involved in nuclear targeting of Ago proteins as well as in Ago protein recruitment to target mRNAs, we wanted to investigate whether these two roles are linked or separable. We therefore targeted Ago2 to the nucleus in an Imp8-independent manner by fusing a *SV40* nuclear localization signal (*Simian virus 40* NLS) to its N-terminus (publication 8). Interestingly, we found that *SV40* NLS-Ago2 binds to miRNA target mRNAs in an Imp8-dependent manner, similar to wild-type Ago2. Thus, it appears that the role of Imp8 in the miRNA pathway is independent of its effects on the nuclear localization of Ago2. However, additional experiments could be performed to elucidate the relation between the two roles of Imp8 in more detail. For example, a search for Imp8 mutants that fail to target Ago2 to the nucleus but are still capable of targeting Ago2 to target mRNAs (or vice versa) may provide further insight into the two mechanisms of Imp8 function.

6.2. Identification and Functional Analyses of Ago-Associated Small RNAs

In addition to identifying Ago-associated proteins, we reasoned that purifying Ago1 and Ago2 complexes might help to find novel functional small RNAs, because small RNA pools from purified Ago proteins are expected contain less non-functional small RNA sequences (such as random degradation products of ribosomal RNAs or tRNAs) than total RNA pools. We therefore generated libraries of Ago1- and Ago2-associated small RNAs (publication 7). We were able to demonstrate for the first time that a snoRNA, ACA45, can serve as a precursor for a small RNA, which is incorporated into Ago complexes and functions as a miRNA. This small RNA represses its targets in a Drosha-independent manner but requires Dicer, suggesting that ACA45 directly serves as a Dicer substrate and bypasses Drosha processing. Moreover, we identified several other snoRNA-derived small RNA sequences in libraries from anti-Ago2 immunoprecipitates, indicating that snoRNA-derived small RNAs constitute a novel class of miRNA-like molecules. Thus, we have demonstrated that the purification of Ago proteins provides a useful tool to find novel functional small RNA molecules. Considering the numerous miRNA biogenesis pathways that have been described to date (e.g. processing from distinct genes, introns, snoRNAs and the mirtron pathway), it appears that the miRNA pathway can be fuelled by a variety of different substrates. It is therefore possible that in addition to snoRNAs, other non-coding RNA species can also serve as miRNA precursors, if they are structurally similar to pri-miRNAs or to processing intermediates of the miRNA pathway. The use of deep sequencing and cloning approaches from anti-Ago1-4 immunoprecipitates could help to identify such novel small RNA species.

6.3. Identification and Functional Analyses of Ago-Associated Target RNAs

Having specific antibodies to human Ago proteins in hand, we decided to extend our analyses to identify mRNAs that specifically associate with human Ago complexes. Because miRNAs guide Ago proteins to their target mRNAs, it was expected that immunoprecipitation of Ago proteins under appropriate conditions could be used to purify a transcript pool that is highly enriched in miRNA targets. Importantly, searches for miRNA target mRNAs were long hampered by the fact that it is difficult for target prediction algorithms to separate the noise of non-functional seed matches from functional miRNA target sites. Therefore, methods to identify miRNA targets in an unbiased manner were needed. Thus, we biochemically purified human Ago1 and Ago2 complexes by using monoclonal antibodies, isolated RNA from the immunoprecipitates and cloned long associated transcripts (publication 2). Using luciferase reporter assays for a panel of candidate mRNAs, we were able to demonstrate that many of the most abundant mRNAs in our libraries are repressed by miRNAs, demonstrating that our method is a useful tool to experimentally identify miRNA targets. This study demonstrated for the first time that it is possible to biochemically identify miRNA target mRNAs from mammalian cells. Similar results were obtained in an earlier study in *Drosophila* cells¹⁹⁸. Subsequent studies in mammalian cells (including publication 8) employed microarray analyses of Ago-associated mRNAs compared to total RNA pools, because this allows to normalize for the overall abundance of each transcript in total RNA pools and may reduce the number of false-positive miRNA targets¹⁹⁹⁻²⁰². These analyses showed that the Ago-associated mRNA pool is significantly enriched in miRNA seed matches, corroborating that this method is a valid tool for miRNA target identification. However, transcripts that associate with Ago proteins could potentially be targeted by any miRNA that is expressed in the cells used. Thus, it remains a challenge to identify the miRNA(s) and their target site(s) for each Ago-associated target mRNA. One possibility is to overexpress or to inhibit a particular miRNA and to identify the transcripts that join or disappear from the pool of Ago-associated mRNAs upon overexpression or inhibition. At least for miRNA overexpression, it has been demonstrated that the 3'-UTRs of those differentially associated transcripts are highly

enriched in seed matches for the overexpressed miRNA, suggesting that such methods can be used to assign Ago-associated target mRNAs to a miRNA of interest^{198, 200, 201}. However, miRNA overexpression could potentially create artifacts. Therefore, a method that inhibits endogenous miRNAs is expected to yield more reliable results compared to miRNA overexpression. Using qPCR experiments, we demonstrated that the let-7 target Hmga2 mRNA is efficiently depleted from Ago2 immunoprecipitates upon antisense inhibition of let-7, providing a proof of principle for such a technique (publication 8). However, in order to map miRNA binding sites to a narrow region of the target 3'-UTRs, different techniques would be required. For example, limited RNase digestion of the Ago2-miRNA-mRNA complex, followed by cloning and deep sequencing of target mRNA fragments that are protected by the Ago complexes may help to identify miRNA binding sites.

Interestingly, we found that in addition to target mRNAs, anti-Ago2 immunoprecipitates contain several highly enriched long non-coding transcripts such as H19 or MALAT-1. The interaction of these transcripts with Ago2 was validated by qPCR. Thus, it is likely that miRNAs target these transcripts, and it will be interesting to investigate the miRNA targeting mechanisms as well as the biological role of these interactions. Thus, our method has revealed unexpected interactions of Ago2 with non-coding transcripts, and application of this method to other cell lines and tissues will probably extend the knowledge about the functions and targeting mechanisms of Ago proteins and miRNAs.

6.4. Reduction of siRNA Off-Target Effects by Blocking 5'-Phosphorylation of the Passenger Strand

Finally, we wanted to re-investigate the role of the 5'-phosphate for the function of siRNAs (publication 4). Although it is known that siRNAs require a 5'-phosphate group to be functional, its precise role has been a matter of controversy in the past^{3, 18, 90, 166-168}. siRNAs which are transfected into cells or incubated with cell lysates become rapidly 5'-phosphorylated by the cellular kinase hClp1¹⁶⁹. We therefore used siRNA derivatives for our study that carried 5'-methoxy (CH₃O) groups to selectively block 5'-phosphorylation of one or both of the single strands. Interestingly, we found that single-stranded siRNAs are incorporated into RISC, irrespective of their 5'-phosphorylation status. However, when double-stranded siRNAs were loaded to Ago2, only those duplex strands were incorporated that carried a 5'-phosphate: Selective modification of one duplex strand with a 5'-methoxy group serves to exclude the modified strand from RISC, while the other strand is effectively incorporated and active. Considering these results, we asked whether it is possible to modulate the off-target activities of siRNAs with 5'-methoxy groups. In addition to their target mRNA, siRNAs can repress many off-target mRNAs by imperfectly base-pairing to their 3'-UTRs, similar to miRNAs (section 5.3.1.3.). Because these off-target effects substantially lower the specificity of siRNAs, they represent a major problem for the use of siRNAs in research and in clinical trials. Importantly, both siRNA strands can potentially have off-target effects, because the thermodynamic asymmetry of siRNA duplexes does not completely prevent RISC loading of passenger strands in many cases^{49, 50}. Using transcriptome-wide microarray analyses of siRNA off-target effects, we were able to demonstrate that 5'-methoxy groups on passenger strands can be used to selectively block their off-targeting activity. Thus, this modification may be a useful tool for the design of highly specific siRNAs.

7. References

1. Dean, K. A., von Ahsen, O., Görlich, D. & Fried, H. M. Signal recognition particle protein 19 is imported into the nucleus by importin 8 (RanBP8) and transportin. *J Cell Sci* 114, 3479-85 (2001).
2. Yao, X., Chen, X., Cottonham, C. & Xu, L. Preferential utilization of Imp7/8 in nuclear import of Smads. *J Biol Chem* 283, 22867-74 (2008).
3. Liu, J. et al. Argonaute2 is the catalytic engine of mammalian RNAi. *Science* 305, 1437-41 (2004).
4. Meister, G. et al. Human Argonaute2 Mediates RNA Cleavage Targeted by miRNAs and siRNAs. *Mol Cell* 15, 185-97 (2004).
5. Birmingham, A. et al. 3' UTR seed matches, but not overall identity, are associated with RNAi off-targets. *Nat Methods* 3, 199-204 (2006).
6. Jackson, A. L. et al. Expression profiling reveals off-target gene regulation by RNAi. *Nat Biotechnol* 21, 635-7. (2003).
7. Jackson, A. L. et al. Widespread siRNA "off-target" transcript silencing mediated by seed region sequence complementarity. *Rna* 12, 1179-87 (2006).
8. Lin, X. et al. siRNA-mediated off-target gene silencing triggered by a 7 nt complementation. *Nucleic Acids Res* 33, 4527-35 (2005).
9. Wagner, R. W. et al. Antisense gene inhibition by oligonucleotides containing C-5 propyne pyrimidines. *Science* 260, 1510-3 (1993).
10. Fire, A. et al. Potent and specific genetic interference by double-stranded RNA in *Caenorhabditis elegans*. *Nature* 391, 806-11 (1998).
11. Elbashir, S. M. et al. Duplexes of 21-nucleotide RNAs mediate RNA interference in mammalian cell culture. *Nature* 411, 494-498 (2001).
12. Hamilton, A. J. & Baulcombe, D. C. A species of small antisense RNA in posttranscriptional gene silencing in plants. *Science* 286, 950-2 (1999).
13. Filipowicz, W., Bhattacharyya, S. N. & Sonenberg, N. Mechanisms of post-transcriptional regulation by microRNAs: are the answers in sight? *Nat Rev Genet* 9, 102-14 (2008).
14. Lippman, Z. & Martienssen, R. The role of RNA interference in heterochromatic silencing. *Nature* 431, 364-70 (2004).
15. Zamore, P. D., Tuschl, T., Sharp, P. A. & Bartel, D. P. RNAi: Double-stranded RNA directs the ATP-dependent cleavage of mRNA at 21 to 23 nucleotide intervals. *Cell* 101, 25-33 (2000).
16. Elbashir, S. M., Lendeckel, W. & Tuschl, T. RNA interference is mediated by 21 and 22 nt RNAs. *Genes Dev* 15, 188-200 (2001).
17. Martinez, J., Patkaniowska, A., Urlaub, H., Lührmann, R. & Tuschl, T. Single-stranded antisense siRNAs guide target RNA cleavage in RNAi. *Cell* 110, 563-574 (2002).
18. Nykänen, A., Haley, B. & Zamore, P. D. ATP requirements and small interfering RNA structure in the RNA interference pathway. *Cell* 107, 309-21 (2001).
19. Ghildiyal, M. et al. Endogenous siRNAs derived from transposons and mRNAs in *Drosophila* somatic cells. *Science* 320, 1077-81 (2008).
20. Kawamura, Y. et al. *Drosophila* endogenous small RNAs bind to Argonaute 2 in somatic cells. *Nature* 453, 793-7 (2008).
21. Tam, O. H. et al. Pseudogene-derived small interfering RNAs regulate gene expression in mouse oocytes. *Nature* 453, 534-8 (2008).

22. He, L. & Hannon, G. J. MicroRNAs: small RNAs with a big role in gene regulation. *Nat Rev Genet* 5, 522-31 (2004).
23. Aravin, A. A., Hannon, G. J. & Brennecke, J. The Piwi-piRNA pathway provides an adaptive defense in the transposon arms race. *Science* 318, 761-4 (2007).
24. Kirino, Y. & Mourelatos, Z. Mouse Piwi-interacting RNAs are 2'-O-methylated at their 3' termini. *Nat Struct Mol Biol* 14, 347-8 (2007).
25. Ohara, T. et al. The 3' termini of mouse Piwi-interacting RNAs are 2'-O-methylated. *Nat Struct Mol Biol* 14, 349-50 (2007).
26. Bartel, D. P. MicroRNAs: genomics, biogenesis, mechanism, and function. *Cell* 116, 281-97 (2004).
27. Ibanez-Ventoso, C., Vora, M. & Driscoll, M. Sequence relationships among *C. elegans*, *D. melanogaster* and human microRNAs highlight the extensive conservation of microRNAs in biology. *PLoS ONE* 3, e2818 (2008).
28. Borchert, G. M., Lanier, W. & Davidson, B. L. RNA polymerase III transcribes human microRNAs. *Nat Struct Mol Biol* 13, 1097-101 (2006).
29. Lee, Y. et al. MicroRNA genes are transcribed by RNA polymerase II. *Embo J* 23, 4051-60 (2004).
30. Lagos-Quintana, M., Rauhut, R., Lendeckel, W. & Tuschl, T. Identification of novel genes coding for small expressed RNAs. *Science* 294, 853-858 (2001).
31. Lau, N. C., Lim, L. P., Weinstein, E. G. & Bartel, D. P. An abundant class of tiny RNAs with probable regulatory roles in *Caenorhabditis elegans*. *Science* 294, 858-62. (2001).
32. Lee, R. C. & Ambros, V. An extensive class of small RNAs in *Caenorhabditis elegans*. *Science* 294, 862-4. (2001).
33. Denli, A. M., Tops, B. B., Plasterk, R. H., Ketting, R. F. & Hannon, G. J. Processing of primary microRNAs by the Microprocessor complex. *Nature* 432, 231-5 (2004).
34. Gregory, R. I. et al. The Microprocessor complex mediates the genesis of microRNAs. *Nature* 432, 235-40 (2004).
35. Han, J. et al. The Drosha-DGCR8 complex in primary microRNA processing. *Genes Dev* 18, 3016-27 (2004).
36. Landthaler, M., Yalcin, A. & Tuschl, T. The human DiGeorge syndrome critical region gene 8 and its *D. melanogaster* homolog are required for miRNA biogenesis. *Curr Biol* 14, 2162-7 (2004).
37. Lee, Y. et al. The nuclear RNase III Drosha initiates microRNA processing. *Nature* 425, 415-9 (2003).
38. Bohnsack, M. T. et al. Exportin5 exports eEF1A via tRNA from nuclei and synergizes with other transport pathways to confine translation to the cytoplasm. *Embo J* 21, 6205-15 (2002).
39. Lund, E., Guttinger, S., Calado, A., Dahlberg, J. E. & Kutay, U. Nuclear export of microRNA precursors. *Science* 303, 95-8 (2004).
40. Yi, R., Qin, Y., Macara, I. G. & Cullen, B. R. Exportin-5 mediates the nuclear export of pre-microRNAs and short hairpin RNAs. *Genes Dev* 17, 3011-3016. (2003).
41. Bernstein, E., Caudy, A. A., Hammond, S. M. & Hannon, G. J. Role for a bidentate ribonuclease in the initiation step of RNA interference. *Nature* 409, 363-366 (2001).
42. Mourelatos, Z. et al. miRNPs: a novel class of ribonucleoproteins containing numerous microRNAs. *Genes Dev* 16, 720-8 (2002).

43. Chendrimada, T. P. et al. TRBP recruits the Dicer complex to Ago2 for microRNA processing and gene silencing. *Nature* 436, 740-4 (2005).
44. Gregory, R. I., Chendrimada, T. P., Cooch, N. & Shiekhattar, R. Human RISC couples microRNA biogenesis and posttranscriptional gene silencing. *Cell* 123, 631-40 (2005).
45. Haase, A. D. et al. TRBP, a regulator of cellular PKR and HIV-1 virus expression, interacts with Dicer and functions in RNA silencing. *EMBO Rep* 6, 961-7 (2005).
46. Lee, Y. et al. The role of PACT in the RNA silencing pathway. *Embo J* 25, 522-32 (2006).
47. Robb, G. B. & Rana, T. M. RNA helicase A interacts with RISC in human cells and functions in RISC loading. *Mol Cell* 26, 523-37 (2007).
48. Diederichs, S. & Haber, D. A. Dual role for argonautes in microRNA processing and posttranscriptional regulation of microRNA expression. *Cell* 131, 1097-108 (2007).
49. Khvorovova, A., Reynolds, A. & Jayasena, S. D. Functional siRNAs and miRNAs exhibit strand bias. *Cell* 115, 209-16. (2003).
50. Schwarz, D. S. et al. Asymmetry in the assembly of the RNAi enzyme complex. *Cell* 115, 199-208. (2003).
51. Tomari, Y., Matranga, C., Haley, B., Martinez, N. & Zamore, P. D. A protein sensor for siRNA asymmetry. *Science* 306, 1377-80 (2004).
52. Okamura, K. et al. The regulatory activity of microRNA* species has substantial influence on microRNA and 3' UTR evolution. *Nat Struct Mol Biol* 15, 354-63 (2008).
53. Kim, Y. K. & Kim, V. N. Processing of intronic microRNAs. *Embo J* 26, 775-83 (2007).
54. Berezikov, E., Chung, W. J., Willis, J., Cuppen, E. & Lai, E. C. Mammalian mirtron genes. *Mol Cell* 28, 328-36 (2007).
55. Okamura, K., Hagen, J. W., Duan, H., Tyler, D. M. & Lai, E. C. The mirtron pathway generates microRNA-class regulatory RNAs in *Drosophila*. *Cell* 130, 89-100 (2007).
56. Ruby, J. G., Jan, C. H. & Bartel, D. P. Intronic microRNA precursors that bypass Drosha processing. *Nature* 448, 83-6 (2007).
57. Ender, C. et al. A human snoRNA with microRNA-like functions. *Mol Cell* 32, 519-28 (2008).
58. Saraiya, A. A. & Wang, C. C. snoRNA, a novel precursor of microRNA in *Giardia lamblia*. *PLoS Pathog* 4, e1000224 (2008).
59. Aravin, A. et al. A novel class of small RNAs bind to MILI protein in mouse testes. *Nature* 442, 203-7 (2006).
60. Girard, A., Sachidanandam, R., Hannon, G. J. & Carmell, M. A. A germline-specific class of small RNAs binds mammalian Piwi proteins. *Nature* 442, 199-202 (2006).
61. Lau, N. C. et al. Characterization of the piRNA complex from rat testes. *Science* 313, 363-7 (2006).
62. Aravin, A. A., Sachidanandam, R., Girard, A., Fejes-Toth, K. & Hannon, G. J. Developmentally regulated piRNA clusters implicate MILI in transposon control. *Science* 316, 744-7 (2007).
63. Houwing, S. et al. A role for Piwi and piRNAs in germ cell maintenance and transposon silencing in Zebrafish. *Cell* 129, 69-82 (2007).
64. Vagin, V. V. et al. A distinct small RNA pathway silences selfish genetic elements in the germline. *Science* 313, 320-4 (2006).

65. Brennecke, J. et al. Discrete small RNA-generating loci as master regulators of transposon activity in *Drosophila*. *Cell* 128, 1089-103 (2007).
66. Gunawardane, L. S. et al. A slicer-mediated mechanism for repeat-associated siRNA 5' end formation in *Drosophila*. *Science* 315, 1587-90 (2007).
67. Horwich, M. D. et al. The *Drosophila* RNA methyltransferase, DmHen1, modifies germline piRNAs and single-stranded siRNAs in RISC. *Curr Biol* 17, 1265-72 (2007).
68. Kirino, Y. & Mourelatos, Z. The mouse homolog of HEN1 is a potential methylase for Piwi-interacting RNAs. *Rna* 13, 1397-401 (2007).
69. Saito, K. et al. Pimet, the *Drosophila* homolog of HEN1, mediates 2'-O-methylation of Piwi- interacting RNAs at their 3' ends. *Genes Dev* 21, 1603-8 (2007).
70. Brennecke, J. et al. An epigenetic role for maternally inherited piRNAs in transposon silencing. *Science* 322, 1387-92 (2008).
71. Ding, S. W. & Voinnet, O. Antiviral immunity directed by small RNAs. *Cell* 130, 413-26 (2007).
72. van Rij, R. P. et al. The RNA silencing endonuclease Argonaute 2 mediates specific antiviral immunity in *Drosophila melanogaster*. *Genes Dev* 20, 2985-95 (2006).
73. Matskevich, A. A. & Moelling, K. Dicer is involved in protection against influenza A virus infection. *J Gen Virol* 88, 2627-35 (2007).
74. Hammond, S. M., Bernstein, E., Beach, D. & Hannon, G. J. An RNA-directed nuclease mediates post-transcriptional gene silencing in *Drosophila* cells. *Nature* 404, 293-296 (2000).
75. Leuschner, P. J., Ameres, S. L., Kueng, S. & Martinez, J. Cleavage of the siRNA passenger strand during RISC assembly in human cells. *EMBO Rep* 7, 314-20 (2006).
76. Matranga, C., Tomari, Y., Shin, C., Bartel, D. P. & Zamore, P. D. Passenger-strand cleavage facilitates assembly of siRNA into Ago2-containing RNAi enzyme complexes. *Cell* 123, 607-20 (2005).
77. Miyoshi, K., Tsukumo, H., Nagami, T., Siomi, H. & Siomi, M. C. Slicer function of *Drosophila* Argonautes and its involvement in RISC formation. *Genes Dev* 19, 2837-48 (2005).
78. Okamura, K. & Lai, E. C. Endogenous small interfering RNAs in animals. *Nat Rev Mol Cell Biol* 9, 673-8 (2008).
79. Okamura, K. et al. The *Drosophila* hairpin RNA pathway generates endogenous short interfering RNAs. *Nature* 453, 803-6 (2008).
80. Watanabe, T. et al. Endogenous siRNAs from naturally formed dsRNAs regulate transcripts in mouse oocytes. *Nature* 453, 539-43 (2008).
81. Bohmert, K. et al. AGO1 defines a novel locus of *Arabidopsis* controlling leaf development. *EMBO J* 17, 170-180 (1998).
82. Peters, L. & Meister, G. Argonaute proteins: mediators of RNA silencing. *Mol Cell* 26, 611-23 (2007).
83. Lin, H. & Spradling, A. C. A novel group of pumilio mutations affects the asymmetric division of germline stem cells in the *Drosophila* ovary. *Development* 124, 2463-76 (1997).
84. Sasaki, T., Shiohama, A., Minoshima, S. & Shimizu, N. Identification of eight members of the Argonaute family in the human genome. *Genomics* 82, 323-30. (2003).

85. Cerutti, L., Mian, N. & Bateman, A. Domains in gene silencing and cell differentiation proteins: the novel PAZ domain and redefinition of the piwi domain. *Trends Biochem Sci* 25, 481-2 (2000).
86. Ma, J. B., Ye, K. & Patel, D. J. Structural basis for overhang-specific small interfering RNA recognition by the PAZ domain. *Nature* 429, 318-22 (2004).
87. Song, J. J. et al. The crystal structure of the Argonaute2 PAZ domain reveals an RNA binding motif in RNAi effector complexes. *Nat Struct Biol* 10, 1026-32. (2003).
88. Parker, J. S., Roe, S. M. & Barford, D. Crystal structure of a PIWI protein suggests mechanisms for siRNA recognition and slicer activity. *Embo J* 23, 4727-37 (2004).
89. Song, J. J., Smith, S. K., Hannon, G. J. & Joshua-Tor, L. Crystal structure of Argonaute and its implications for RISC slicer activity. *Science* 305, 1434-7 (2004).
90. Rivas, F. V. et al. Purified Argonaute2 and an siRNA form recombinant human RISC. *Nat Struct Mol Biol* 12, 340-9 (2005).
91. Ma, J. B. et al. Structural basis for 5'-end-specific recognition of guide RNA by the *A. fulgidus* Piwi protein. *Nature* 434, 666-70 (2005).
92. Parker, J. S., Roe, S. M. & Barford, D. Structural insights into mRNA recognition from a PIWI domain-siRNA guide complex. *Nature* 434, 663-6 (2005).
93. Jakymiw, A. et al. Disruption of GW bodies impairs mammalian RNA interference. *Nat Cell Biol* 7, 1267-74 (2005).
94. Liu, J. et al. A role for the P-body component GW182 in microRNA function. *Nat Cell Biol* 7, 1261-6 (2005).
95. Sen, G. L. & Blau, H. M. Argonaute 2/RISC resides in sites of mammalian mRNA decay known as cytoplasmic bodies. *Nat Cell Biol* 7, 633-6 (2005).
96. Eulalio, A., Behm-Ansmant, I. & Izaurralde, E. P bodies: at the crossroads of post-transcriptional pathways. *Nat Rev Mol Cell Biol* 8, 9-22 (2007).
97. Chu, C. Y. & Rana, T. M. Translation repression in human cells by microRNA-induced gene silencing requires RCK/p54. *PLoS Biol* 4, e210 (2006).
98. Eystathiou, T. et al. A phosphorylated cytoplasmic autoantigen, GW182, associates with a unique population of human mRNAs within novel cytoplasmic speckles. *Mol Biol Cell* 13, 1338-51 (2002).
99. Meister, G. et al. Identification of novel argonaute-associated proteins. *Curr Biol* 15, 2149-55 (2005).
100. van Dijk, E. et al. Human Dcp2: a catalytically active mRNA decapping enzyme located in specific cytoplasmic structures. *Embo J* 21, 6915-24 (2002).
101. Bhattacharyya, S. N., Habermacher, R., Martiny-Bar, C., Gutschalk, S., Closs, E. I. & Filipowicz, W. Relief of microRNA-mediated translational repression in human cells subjected to stress. *Cell* 125, 1111-24 (2006).
102. Pillai, R. S. et al. Inhibition of translational initiation by Let-7 MicroRNA in human cells. *Science* 309, 1573-6 (2005).
103. Liu, J., Valencia-Sanchez, M. A., Hannon, G. J. & Parker, R. MicroRNA-dependent localization of targeted mRNAs to mammalian P-bodies. *Nat Cell Biol* 7, 719-23 (2005).
104. Eulalio, A., Behm-Ansmant, I., Schweizer, D. & Izaurralde, E. P-body formation is a consequence, not the cause, of RNA-mediated gene silencing. *Mol Cell Biol* 27, 3970-81 (2007).

105. Andrei, M. A. et al. A role for eIF4E and eIF4E-transporter in targeting mRNPs to mammalian processing bodies. *Rna* 11, 717-27 (2005).
106. Pauley, K. M. et al. Formation of GW bodies is a consequence of microRNA genesis. *EMBO Rep* 7, 904-10 (2006).
107. Anderson, P. & Kedersha, N. RNA granules. *J Cell Biol* 172, 803-8 (2006).
108. Leung, A. K., Calabrese, J. M. & Sharp, P. A. Quantitative analysis of Argonaute protein reveals microRNA-dependent localization to stress granules. *Proc Natl Acad Sci U S A* 103, 18125-30 (2006).
109. Babiarz, J. E., Ruby, J. G., Wang, Y., Bartel, D. P. & Blelloch, R. Mouse ES cells express endogenous shRNAs, siRNAs, and other Microprocessor-independent, Dicer-dependent small RNAs. *Genes Dev* 22, 2773-85 (2008).
110. Matzke, M. A. & Birchler, J. A. RNAi-mediated pathways in the nucleus. *Nat Rev Genet* 6, 24-35 (2005).
111. Robb, G. B., Brown, K. M., Khurana, J. & Rana, T. M. Specific and potent RNAi in the nucleus of human cells. *Nat Struct Mol Biol* 12, 133-7 (2005).
112. Janowski, B. A. et al. Inhibiting gene expression at transcription start sites in chromosomal DNA with antigene RNAs. *Nat Chem Biol* 1, 216-22 (2005).
113. Janowski, B. A. et al. Involvement of AGO1 and AGO2 in mammalian transcriptional silencing. *Nat Struct Mol Biol* 13, 787-92 (2006).
114. Janowski, B. A. et al. Activating gene expression in mammalian cells with promoter-targeted duplex RNAs. *Nat Chem Biol* 3, 166-73 (2007).
115. Kim, D. H., Villeneuve, L. M., Morris, K. V. & Rossi, J. J. Argonaute-1 directs siRNA-mediated transcriptional gene silencing in human cells. *Nat Struct Mol Biol* 13, 793-7 (2006).
116. Li, L. C. et al. Small dsRNAs induce transcriptional activation in human cells. *Proc Natl Acad Sci U S A* 103, 17337-42 (2006).
117. Azuma-Mukai, A. et al. Characterization of endogenous human Argonautes and their miRNA partners in RNA silencing. *Proc Natl Acad Sci U S A* 105, 7964-9 (2008).
118. Pillai, R. S., Artus, C. G. & Filipowicz, W. Tethering of human Ago proteins to mRNA mimics the miRNA-mediated repression of protein synthesis. *Rna* 10, 1518-25 (2004).
119. Bartel, D. P. MicroRNAs: target recognition and regulatory functions. *Cell* 136, 215-33 (2009).
120. Lim, L. P. et al. The microRNAs of *Caenorhabditis elegans*. *Genes Dev* 17, 991-1008 (2003).
121. Brennecke, J., Stark, A., Russell, R. B. & Cohen, S. M. Principles of microRNA-target recognition. *PLoS Biol* 3, e85 (2005).
122. Doench, J. G. & Sharp, P. A. Specificity of microRNA target selection in translational repression. *Genes Dev* 18, 504-11 (2004).
123. Kloosterman, W. P., Wienholds, E., Ketting, R. F. & Plasterk, R. H. Substrate requirements for let-7 function in the developing zebrafish embryo. *Nucleic Acids Res* 32, 6284-91 (2004).
124. Lewis, B. P., Burge, C. B. & Bartel, D. P. Conserved seed pairing, often flanked by adenosines, indicates that thousands of human genes are microRNA targets. *Cell* 120, 15-20 (2005).
125. Chen, K. & Rajewsky, N. Natural selection on human microRNA binding sites inferred from SNP data. *Nat Genet* 38, 1452-6 (2006).
126. Grimson, A. et al. MicroRNA targeting specificity in mammals: determinants beyond seed pairing. *Mol Cell* 27, 91-105 (2007).

127. Kertesz, M., Iovino, N., Unnerstall, U., Gaul, U. & Segal, E. The role of site accessibility in microRNA target recognition. *Nat Genet* 39, 1278-84 (2007).
128. Didiano, D. & Hobert, O. Perfect seed pairing is not a generally reliable predictor for miRNA-target interactions. *Nat Struct Mol Biol* 13, 849-51 (2006).
129. Kedde, M. et al. RNA-binding protein Dnd1 inhibits microRNA access to target mRNA. *Cell* 131, 1273-86 (2007).
130. Gu, S., Jin, L., Zhang, F., Sarnow, P. & Kay, M. A. Biological basis for restriction of microRNA targets to the 3' untranslated region in mammalian mRNAs. *Nat Struct Mol Biol* 16, 144-50 (2009).
131. Orom, U. A., Nielsen, F. C. & Lund, A. H. MicroRNA-10a binds the 5'UTR of ribosomal protein mRNAs and enhances their translation. *Mol Cell* 30, 460-71 (2008).
132. Arasu, P., Wightman, B. & Ruvkun, G. Temporal regulation of *lin-14* by the antagonistic action of two other heterochronic genes, *lin-4* and *lin-28*. *Genes Dev* 5, 1825-33 (1991).
133. Lee, R. C., Feinbaum, R. L. & Ambros, V. The *C. elegans* heterochronic gene *lin-4* encodes small RNAs with antisense complementarity to *lin-14*. *Cell* 75, 843-54 (1993).
134. Wightman, B., Ha, I. & Ruvkun, G. Posttranscriptional regulation of the heterochronic gene *lin-14* by *lin-4* mediates temporal pattern formation in *C. elegans*. *Cell* 75, 855-62 (1993).
135. Olsen, P. H. & Ambros, V. The *lin-4* regulatory RNA controls developmental timing in *Caenorhabditis elegans* by blocking LIN-14 protein synthesis after the initiation of translation. *Dev Biol* 216, 671-80 (1999).
136. Petersen, C. P., Bordeleau, M. E., Pelletier, J. & Sharp, P. A. Short RNAs repress translation after initiation in mammalian cells. *Mol Cell* 21, 533-42 (2006).
137. Seggerson, K., Tang, L. & Moss, E. G. Two genetic circuits repress the *Caenorhabditis elegans* heterochronic gene *lin-28* after translation initiation. *Dev Biol* 243, 215-25 (2002).
138. Maroney, P. A., Yu, Y., Fisher, J. & Nilsen, T. W. Evidence that microRNAs are associated with translating messenger RNAs in human cells. *Nat Struct Mol Biol* 13, 1102-7 (2006).
139. Nottrott, S., Simard, M. J. & Richter, J. D. Human let-7a miRNA blocks protein production on actively translating polyribosomes. *Nat Struct Mol Biol* 13, 1108-14 (2006).
140. Lytle, J. R., Yario, T. A. & Steitz, J. A. Target mRNAs are repressed as efficiently by microRNA-binding sites in the 5' UTR as in the 3' UTR. *Proc Natl Acad Sci U S A* 104, 9667-72 (2007).
141. Humphreys, D. T., Westman, B. J., Martin, D. I. & Preiss, T. MicroRNAs control translation initiation by inhibiting eukaryotic initiation factor 4E/cap and poly(A) tail function. *Proc Natl Acad Sci U S A* 102, 16961-6 (2005).
142. Mathonnet, G. et al. MicroRNA inhibition of translation initiation in vitro by targeting the cap-binding complex eIF4F. *Science* 317, 1764-7 (2007).
143. Thermann, R. & Hentze, M. W. *Drosophila* miR2 induces pseudo-polysomes and inhibits translation initiation. *Nature* 447, 875-8 (2007).
144. Kiriakidou, M. et al. An mRNA m7G cap binding-like motif within human Ago2 represses translation. *Cell* 129, 1141-51 (2007).
145. Eulalio, A., Huntzinger, E. & Izaurralde, E. GW182 interaction with Argonaute is essential for miRNA-mediated translational repression and mRNA decay. *Nat Struct Mol Biol* 15, 346-53 (2008).

146. Rehwinkel, J., Behm-Ansmant, I., Gatfield, D. & Izaurralde, E. A crucial role for GW182 and the DCP1:DCP2 decapping complex in miRNA-mediated gene silencing. *Rna* 11, 1640-7 (2005).
147. Chendrimada, T. P. et al. MicroRNA silencing through RISC recruitment of eIF6. *Nature* 447, 823-8 (2007).
148. Ceci, M. et al. Release of eIF6 (p27BBP) from the 60S subunit allows 80S ribosome assembly. *Nature* 426, 579-84 (2003).
149. Wang, B., Yanez, A. & Novina, C. D. MicroRNA-repressed mRNAs contain 40S but not 60S components. *Proc Natl Acad Sci U S A* 105, 5343-8 (2008).
150. Yekta, S., Shih, I. H. & Bartel, D. P. MicroRNA-directed cleavage of HOXB8 mRNA. *Science* 304, 594-6 (2004).
151. Baek, D. et al. The impact of microRNAs on protein output. *Nature* 455, 64-71 (2008).
152. Bagga, S. et al. Regulation by let-7 and lin-4 miRNAs results in target mRNA degradation. *Cell* 122, 553-63 (2005).
153. Giraldez, A. J. et al. Zebrafish MiR-430 promotes deadenylation and clearance of maternal mRNAs. *Science* 312, 75-9 (2006).
154. Lim, L. P. et al. Microarray analysis shows that some microRNAs downregulate large numbers of target mRNAs. *Nature* 433, 769-73 (2005).
155. Rehwinkel, J. et al. Genome-wide analysis of mRNAs regulated by Drosha and Argonaute proteins in *Drosophila melanogaster*. *Mol Cell Biol* 26, 2965-75 (2006).
156. Schmitter, D. et al. Effects of Dicer and Argonaute down-regulation on mRNA levels in human HEK293 cells. *Nucleic Acids Res* 34, 4801-15 (2006).
157. Selbach, M. et al. Widespread changes in protein synthesis induced by microRNAs. *Nature* 455, 58-63 (2008).
158. Wu, L., Fan, J. & Belasco, J. G. MicroRNAs direct rapid deadenylation of mRNA. *Proc Natl Acad Sci U S A* 103, 4034-9 (2006).
159. Behm-Ansmant, I. et al. mRNA degradation by miRNAs and GW182 requires both CCR4:NOT deadenylase and DCP1:DCP2 decapping complexes. *Genes Dev* 20, 1885-98 (2006).
160. Ding, L., Spencer, A., Morita, K. & Han, M. The developmental timing regulator AIN-1 interacts with miRISCs and may target the argonaute protein ALG-1 to cytoplasmic P bodies in *C. elegans*. *Mol Cell* 19, 437-47 (2005).
161. Till, S. et al. A conserved motif in Argonaute-interacting proteins mediates functional interactions through the Argonaute PIWI domain. *Nat Struct Mol Biol* 14, 897-903 (2007).
162. Vasudevan, S. & Steitz, J. A. AU-rich-element-mediated upregulation of translation by FXR1 and Argonaute 2. *Cell* 128, 1105-18 (2007).
163. Vasudevan, S., Tong, Y. & Steitz, J. A. Switching from repression to activation: microRNAs can up-regulate translation. *Science* 318, 1931-4 (2007).
164. Martinez, J. & Tuschl, T. RISC is a 5' phosphomonoester-producing RNA endonuclease. *Genes Dev* 18 (2004).
165. Schwarz, D. S., Tomari, Y. & Zamore, P. D. The RNA-induced silencing complex is a Mg²⁺-dependent endonuclease. *Curr Biol* 14, 787-91 (2004).
166. Boutla, A., Delidakis, C., Livadaras, I., Tsagris, M. & Tabler, M. Short 5'-phosphorylated double-stranded RNAs induce RNA interference in *Drosophila*. *Curr Biol* 11, 1776-80 (2001).
167. Chiu, Y. L. & Rana, T. M. RNAi in human cells. Basic structural and functional features of small interfering RNA. *Mol Cell* 10, 549-561 (2002).

168. Schwarz, D. S., Hutvagner, G., Haley, B. & Zamore, P. D. Evidence that siRNAs function as guides, not primers, in the *Drosophila* and human RNAi pathways. *Mol Cell* 10, 537-548 (2002).
169. Weitzer, S. & Martinez, J. The human RNA kinase hCtp1 is active on 3' transfer RNA exons and short interfering RNAs. *Nature* 447, 222-6 (2007).
170. Rand, T. A., Ginalski, K., Grishin, N. V. & Wang, X. Biochemical identification of Argonaute 2 as the sole protein required for RNA-induced silencing complex activity. *Proc Natl Acad Sci U S A* 101, 14385-9 (2004).
171. Wu, L., Fan, J. & Belasco, J. G. Importance of translation and nonnucleolytic ago proteins for on-target RNA interference. *Curr Biol* 18, 1327-32 (2008).
172. Carmell, M. A. et al. MIWI2 is essential for spermatogenesis and repression of transposons in the mouse male germline. *Dev Cell* 12, 503-14 (2007).
173. Kuramochi-Miyagawa, S. et al. Mili, a mammalian member of piwi family gene, is essential for spermatogenesis. *Development* (2004).
174. Deng, W. & Lin, H. *miwi*, a murine homolog of *piwi*, encodes a cytoplasmic protein essential for spermatogenesis. *Dev Cell* 2, 819-830 (2002).
175. Reinhart, B. J. et al. The 21-nucleotide let-7 RNA regulates developmental timing in *Caenorhabditis elegans*. *Nature* 403, 901-6 (2000).
176. Chang, S., Johnston, R. J., Jr., Frokjaer-Jensen, C., Lockery, S. & Hobert, O. MicroRNAs act sequentially and asymmetrically to control chemosensory laterality in the nematode. *Nature* 430, 785-9 (2004).
177. Chang, S., Johnston, R. J., Jr. & Hobert, O. A transcriptional regulatory cascade that controls left/right asymmetry in chemosensory neurons of *C. elegans*. *Genes Dev* 17, 2123-37 (2003).
178. Johnston, R. J. & Hobert, O. A microRNA controlling left/right neuronal asymmetry in *Caenorhabditis elegans*. *Nature* 426, 845-9. (2003).
179. Ambros, V. The functions of animal microRNAs. *Nature* 431, 350-5 (2004).
180. Ventura, A. et al. Targeted deletion reveals essential and overlapping functions of the miR-17 through 92 family of miRNA clusters. *Cell* 132, 875-86 (2008).
181. Thai, T. H. et al. Regulation of the germinal center response by microRNA-155. *Science* 316, 604-8 (2007).
182. Calin, G. A. et al. Frequent deletions and down-regulation of microRNA genes miR-15 and miR-16 at 13q14 in chronic lymphocytic leukemia. *Proc Natl Acad Sci U S A* 99, 15524-9. (2002).
183. Johnson, S. M. et al. RAS is regulated by the let-7 microRNA family. *Cell* 120, 635-47 (2005).
184. Takamizawa, J. et al. Reduced expression of the let-7 microRNAs in human lung cancers in association with shortened postoperative survival. *Cancer Res* 64, 3753-6 (2004).
185. Chan, J. A., Krichevsky, A. M. & Kosik, K. S. MicroRNA-21 is an antiapoptotic factor in human glioblastoma cells. *Cancer Res* 65, 6029-33 (2005).
186. Ciafre, S. A. et al. Extensive modulation of a set of microRNAs in primary glioblastoma. *Biochem Biophys Res Commun* 334, 1351-8 (2005).
187. Koesters, R. et al. Human eukaryotic initiation factor EIF2C1 gene: cDNA sequence, genomic organization, localization to chromosomal bands 1p34-p35, and expression. *Genomics* 61, 210-8 (1999).
188. Karube, Y. et al. Reduced expression of Dicer associated with poor prognosis in lung cancer patients. *Cancer Sci* 96, 111-5 (2005).
189. Melo, S. A. et al. A TARBP2 mutation in human cancer impairs microRNA processing and DICER1 function. *Nat Genet* 41, 365-70 (2009).

190. Zipprich, J. T., Bhattacharyya, S., Mathys, H. & Filipowicz, W. Importance of the C-terminal domain of the human GW182 protein TNRC6C for translational repression. *Rna* 15, 781-93 (2009).
191. Cook, H. A., Koppetsch, B. S., Wu, J. & Theurkauf, W. E. The *Drosophila* SDE3 homolog armitage is required for oskar mRNA silencing and embryonic axis specification. *Cell* 116, 817-29 (2004).
192. Tomari, Y. et al. RISC assembly defects in the *Drosophila* RNAi mutant armitage. *Cell* 116, 831-41 (2004).
193. Huang, Y., Genova, G., Roberts, M. & Jackson, F. R. The LARK RNA-binding protein selectively regulates the circadian eclosion rhythm by controlling E74 protein expression. *PLoS ONE* 2, e1107 (2007).
194. Lin, J. C., Hsu, M. & Tarn, W. Y. Cell stress modulates the function of splicing regulatory protein RBM4 in translation control. *Proc Natl Acad Sci U S A* 104, 2235-40 (2007).
195. Jäkel, S., Mingot, J. M., Schwarzmaier, P., Hartmann, E. & Görlich, D. Importins fulfil a dual function as nuclear import receptors and cytoplasmic chaperones for exposed basic domains. *Embo J* 21, 377-86 (2002).
196. Aravin, A. A. et al. A piRNA pathway primed by individual transposons is linked to de novo DNA methylation in mice. *Mol Cell* 31, 785-99 (2008).
197. Wang, Y. et al. Structure of an argonaute silencing complex with a seed-containing guide DNA and target RNA duplex. *Nature* 456, 921-6 (2008).
198. Easow, G., Teleman, A. A. & Cohen, S. M. Isolation of microRNA targets by miRNP immunopurification. *Rna* 13, 1198-204 (2007).
199. Hendrickson, D. G., Hogan, D. J., Herschlag, D., Ferrell, J. E. & Brown, P. O. Systematic identification of mRNAs recruited to argonaute 2 by specific microRNAs and corresponding changes in transcript abundance. *PLoS ONE* 3, e2126 (2008).
200. Karginov, F. V. et al. A biochemical approach to identifying microRNA targets. *Proc Natl Acad Sci U S A* 104, 19291-6 (2007).
201. Landthaler, M. et al. Molecular characterization of human Argonaute-containing ribonucleoprotein complexes and their bound target mRNAs. *Rna* 14, 2580-96 (2008).
202. Weinmann, L. et al. Importin 8 is a gene silencing factor that targets Argonaute proteins to distinct mRNAs. *Cell* 136, 496-507 (2009).

8. Acknowledgements

I wish to thank Dr. Gunter Meister for excellent supervision of the projects, for tremendous support and encouragement and for many stimulating scientific discussions. I would also like to thank Prof. Dr. Stefan Jentsch for supervising this thesis and for the great support he gave to my projects and to our research group in general. Furthermore, I would like to thank Julia Höck, Sabine Rüdell, Christine Ender, Alexander Eichner, Jiayun Zhu, Dr. Michaela Beitzinger and Sabine Rottmüller for good collaboration within our group and all laboratory members for the friendly and cooperative atmosphere in the laboratory. I also wish to thank Prof. Dr. Olaf Stemmann for supporting the projects with excellent scientific and technical advice and for providing many useful tools and constructs. Moreover, I would like to thank the following external collaborators for good collaboration: Prof. Dr. Thomas Tuschl, Po Yu Chen, Dr. Vladimir Benes, Tomi Ivacevic, Prof. Dr. Petra Schwille, Dr. Thomas Ohrt, Jörg Mütze, Prof. Dr. Mihaela Zavolan, Dr. Dimosthenis Gaidatzis, Dr. Yi Pei, Prof. Dr. Dirk Görlich, Thomas Güttler, Prof. Dr. Witold Filipowicz and Dr. Michael Doyle. I am also indebted to Dr. Bernd Haas, Dr. Stephan Uebel, Ralf Zenke, Judith Scholz, Dr. Susanna Nagel and Dr. Simone Heubes from the Max-Planck-Institute of Biochemistry for technical advice and for providing tools for the projects. Finally, I wish to thank my wife Lisa Weinmann for invaluable personal support and encouragement.

9. Curriculum Vitae

Personal Data

Name: Lasse Weinmann
Birth name: Lasse Peters
Private address: Max Lebsche-Platz 34
D-81377 München
Germany
weinmann@biochem.mpg.de
Phone: private: 001149-89-52389290
work: 001149-89-85783423
mobile: 001149-179-1130986
Date of birth: 04/29/1978
Place of birth: Kiel, Germany
Marital status: married
Citizenship: german

Education

05/2005-06/2009 **PhD thesis** in the laboratory for RNA biology at the Max Planck-Institute of Biochemistry in Martinsried, Germany.
04/2005-05/2005 Journey across North America
12/2004-03/2005 Completion of Diploma research project
12/2004 **Diploma** in Biochemistry at the University of Tübingen, Germany. Grade: 1.0
04/2004-12/2004 **Diploma thesis** "Pharmacological reactivation of mutant p53 by small molecules and synergy with Apo2L/TRAIL" in the laboratory of Prof. Michael Weller at the Hertie Institute for Clinical Brain Research, Tübingen, Germany.
04/1999-12/2004 **Studies** in Biochemistry, Physical Chemistry and Pharmacology at the University of Tübingen, Germany
10/2002-09/2003 **Lab rotations** at the Max-Planck-Institute of Biochemistry in Martinsried, Germany
10/2001 **Intermediate examinations** at the University of Tübingen, Germany
10/1997-11/1998 Alternative Civilian Service
07/1997 **University entrance diploma** Grade: 1.0
08/1984-07/1997 **School education** at the "Freie Waldorfschule Kiel"

Teaching Activities

03/2008-09/2008	Supervisor for a Master student at the Max-Planck-Institute of Biochemistry
From 10/2005	Supervisor for several rotational students at the Max-Planck-Institute of Biochemistry
04/2002-07/2002	Supervisor for a practical course in Physical Chemistry at the University of Tübingen
10/2001-02/2002, 04/2001-07/2001	Supervisor for practical courses in Chemistry at the University of Tübingen

Awards and Fellowships

03/2009	Junior research award of the Max-Planck-Institute of Biochemistry for outstanding research in Biochemistry
05/2007	Prize for an excellent PhD student's talk at the "2nd Microsymposium on small RNAs" in Vienna, Austria
From 12/2005 to 05/2008	PhD fellowship of the Boehringer Ingelheim Fonds
10/2005	Prize for the best Diploma thesis of the year, awarded by the alumni organization of former Tübingen biochemists (MoBBEL)
07/1997	Book prize for best school performance in the subject Chemistry, awarded by the German chemical industry association

10. Declaration of Individual Contributions to the Publications

Publication 1:

Gunter Meister, Markus Landthaler, Lasse Peters, Po Yu Chen, Henning Urlaub, Reinhard Lührmann, and Thomas Tuschl: Identification of novel Argonaute-associated proteins.

Lasse Weinmann performed immunofluorescent analyses (Figure 2, supplemental Figure 1), GFP reporter assays (Figure 3) and analyzed siRNA knockdown efficiency (supplemental Figure 2). He contributed these figures as well as the corresponding figure legends and the methods section to the manuscript.

(Lasse Weinmann)



(Po Yu Chen)



Po Yu Chen 4/30/2009

(Gunter Meister)



(Thomas Tuschl)



(Stefan Jentsch)



Publication 2:

Michaela Beitzinger, Lasse Peters, Jia Yun Zhu, Elisabeth Kremmer and Gunter Meister: Identification of human microRNA targets from isolated argonaute protein complexes.

Lasse Weinmann established the dual luciferase reporter system for the miRNA target analyses that were performed in figure 2 and wrote the corresponding part of the methods section.

(Michaela Beitzinger)



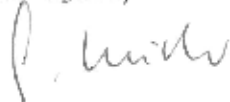
(Lasse Weinmann)



(Jia Yun Zhu)



(Gunter Meister)



(Stefan Jentsch)

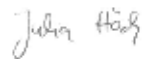


Publication 3:

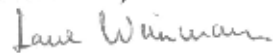
Julia Höck, Lasse Weinmann, Christine Ender, Sabine Rüdell, Elisabeth Kremmer, Monika Raabe, Henning Urlaub and Gunter Meister: Proteomic and functional analysis of Argonaute-containing mRNA–protein complexes in human cells.

Lasse Weinmann performed dual luciferase reporter assays to analyze the role of Ago-interacting proteins in the miRNA pathway (figure 4), validated siRNAs (suppl. Figure 5) and wrote the corresponding parts of the methods section.

(Julia Höck)



(Lasse Weinmann)



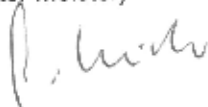
(Christine Ender)



(Sabine Rüdell)



(Gunter Meister)



(Stefan Jentsch)



Publication 4:

Po Yu Chen*, Lasse Weinmann*, Dimos Gaidatzis, Yi Pei, Mihaela Zavolan, Thomas Tuschl and Gunter Meister: Strand-specific 5'-O-methylation of siRNA duplexes controls guide strand selection and targeting specificity.

*These authors contributed equally to this work.

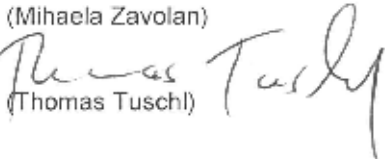
Lasse Weinmann performed functional analyses of modified siRNA duplexes by Northern Blotting (Figure 2b), luciferase assays (Figures 2e, 3c, and Figure 5) and GFP reporter assays (Figures 2d and 3b). Po Yu Chen performed *in vitro* RNA cleavage assays (Figure 2c), microarray experiments (Figure 4), and he analyzed siRNA off-target effects together with Dimos Gaidatzis (Figure 4). Other figures were contributed by Gunter Meister (Figure 1b, 1d) and Yi Pei (Figure 1c). Lasse Weinmann, Po Yu Chen, Dimos Gaidatzis, Mihaela Zavolan, Thomas Tuschl and Gunter Meister wrote the manuscript.

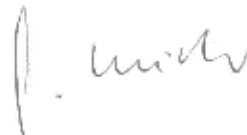
(Po Yu Chen)  Po Yu Chen 4/30/2009

(Lasse Weinmann) 

(Dimos Gaidatzis) 

(Yi Pei) 

(Mihaela Zavolan) 
(Thomas Tuschl) 

(Gunter Meister) 

(Stefan Jentsch) 

Publication 5:

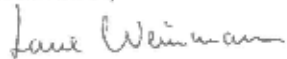
Sabine Rüdell, Andrew Flatley, Lasse Weinmann, Elisabeth Kremmer and Gunter Meister: A multifunctional human Argonaute2-specific monoclonal antibody.

Lasse Weinmann carried out immunofluorescent analyses (Figure 4b) and wrote the corresponding parts of the figure legends and the methods section.

(Sabine Rüdell)



(Lasse Weinmann)



(Gunter Meister)



(Stefan Jentsch)

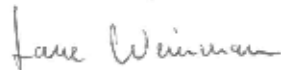


Publication 6:

Thomas Ohrt, Jörg Mütze, Wolfgang Staroske, Lasse Weinmann, Julia Höck, Karin Crell, Gunter Meister and Petra Schwille: Fluorescence correlation spectroscopy and fluorescence cross-correlation spectroscopy reveal the cytoplasmic origination of loaded nuclear RISC *in vivo* in human cells.

Lasse Weinmann analyzed EGFP-Ago2 expression levels of the cell line that was used in the publication and validated binding of EGFP-Ago2 to miRNAs by Northern Blotting (supplemental Figure 1b, 1c). He wrote the corresponding parts of the figure legends and the methods section.

(Lasse Weinmann)



(Julia Höck)



(Gunter Meister)



(Stefan Jentsch)



Publication 7:

Christine Ender, Azra Krek, Marc R. Friedländer, Michaela Beitzinger, Lasse Weinmann, Wei Chen, Sebastien Pfeffer, Nikolaus Rajewsky, and Gunter Meister: A Human snoRNA with MicroRNA-Like Functions

Lasse Weinmann validated the knockdown efficiency of siRNAs that were used in Figure 3b.

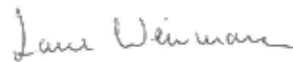
(Christine Ender)



(Michaela Beitzinger)



(Lasse Weinmann)



(Gunter Meister)



(Stefan Jentsch)



Publication 8:

Lasse Weinmann, Julia Höck, Tomi Ivacevic, Thomas Ohrt, Jörg Mütze, Petra Schwille, Elisabeth Kremmer, Vladimir Benes, Henning Urlaub, and Gunter Meister: Importin 8 Is a Gene Silencing Factor that Targets Argonaute Proteins to Distinct mRNAs.

Lasse Weinmann contributed all figures that are not mentioned below. He wrote the manuscript together with Gunter Meister. The microarray data of the manuscript (Figure 6b, 6d, 6e and supplemental Tables 3 and 4) were provided by Tomi Ivacevic and Vladimir Benes. The subcellular localization of EGFP-Ago was analyzed by Thomas Ohrt, Jörg Mütze and Petra Schwille (Figure 3c). Mass spectrometry was performed by Henning Urlaub (Figure 1a and supplemental Tables 1 and 2). *In vitro* binding of Ago proteins to Imp8 and migration of Imp8 on sucrose density gradients was analyzed by Julia Höck (Figure 1b, supplemental Figure 1). Monoclonal antibodies to human Ago3 and Ago4 were generated by Elisabeth Kremmer.

(Lasse Weinmann)



(Julia Höck)



(Tomi Ivacevic)



(Thomas Ohrt)



(Jörg Mütze)



(Petra Schwille)



(Elisabeth Kremmer)



(Vladimir Benes)

(Henning Urlaub)

Dr. H. Urlaub
Max-Planck-Institut
für biochemische Chemie
Karl-Friedrich-Höhler-Institut
Am Fassberg 11, D-37071 Göttingen
☒ D-37070 Göttingen

(Gunter Meister)



(Stefan Jentsch)

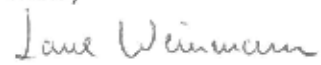


Publication 9:

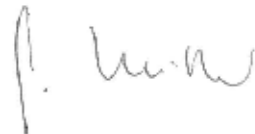
Lasse Peters and Gunter Meister: Argonaute Proteins: Mediators of RNA Silencing.

This review article was written by Lasse Weinmann and Gunter Meister.

(Lasse Weinmann)

Handwritten signature of Lasse Weinmann in cursive script.

(Gunter Meister)

Handwritten signature of Gunter Meister in cursive script.

(Stefan Jentsch)

Handwritten signature of Stefan Jentsch in cursive script.

11. Reprints of the Publications

All reprints were made with permission from the publishers.

Identification of Novel Argonaute-Associated Proteins

Gunter Meister,^{2,6,*} Markus Landthaler,² Lasse Peters,⁵ Po Yu Chen,⁵ Henning Urlaub,³ Reinhard Lührmann,⁴ and Thomas Tuschl^{1,2,*}

¹Howard Hughes Medical Institute

²Laboratory of RNA Molecular Biology
The Rockefeller University

1230 York Avenue, Box 186

New York, New York 10021

³Bioanalytical Mass Spectrometry Group

⁴Department of Cellular Biochemistry
Max-Planck-Institute of Biophysical Chemistry
Am Faßberg 11

D-37077 Göttingen

Germany

⁵Max Planck Institute for Biochemistry

Am Klopferspitz 18

D-82152 Martinsried

Germany

Summary

RNA silencing processes are guided by small RNAs known as siRNAs and microRNAs (miRNAs) [1–4]. They reside in ribonucleoprotein complexes, which guide the cleavage of complementary mRNAs [3, 4] or affect stability and translation of partial complementary mRNAs [1, 2, 5]. Argonaute (Ago) proteins are at the heart of silencing effector complexes and bind the single-stranded siRNA and miRNA [4, 6]. Our biochemical analysis revealed that Ago2 is present in a pre-miRNA processing complex that is able to transfer the miRNA into a target-mRNA cleaving complex. To gain insight into the function and composition of RNA silencing complexes, we purified Ago1- and Ago2-containing complexes from human cells. Several known Ago1- and/or Ago2-associated proteins including Dicer were identified, but also two novel factors, the putative RNA helicase MOV10, and the RNA recognition motif (RRM)-containing protein TNRC6B/KIAA1093. The new proteins localize, similar to Ago proteins, to mRNA-degrading cytoplasmic P bodies, and they are functionally required to mediate miRNA-guided mRNA cleavage.

Results and Discussion

Proteomic Analysis of Human Ago1 and Ago2 Complexes

We generated HeLa-cell lines stably expressing FLAG/HA-tagged Ago1 or Ago2 [7] and biochemically copurified Ago-associated proteins from HeLa-cell cytoplasmic extracts by double-affinity purification. Cytoplasmic extract was first passed over anti-FLAG-antibody-coated beads. Bound proteins were eluted under native

conditions with FLAG peptides, and the eluate was subsequently incubated with anti-HA-antibody-coated beads. The bound proteins were recovered and analyzed by SDS-PAGE and silver staining (Figure 1A, lanes 2 and 3). The visible bands were subjected to ESI tandem MS (LC-MS/MS) analysis. The most prominent proteins with molecular weights of about 100 kDa were identified as FLAG/HA-tagged Ago2 (lane 2) and Ago1 (lane 3). Additionally, Gemin3 and Gemin4, two proteins previously reported to be associated with human Ago2 [8], were also copurified with FLAG/HA-Ago2. The RNase III enzyme Dicer was also found to be stably associated with Ago1 and Ago2, consistent with very recent reports [9].

Among the silver-stained bands in both purifications, we identified four proteins that have not been previously linked to small-RNA-regulated gene silencing in human systems. The 175 kDa band was identified as TNRC6B isoform 1, also known as KIAA1093, a poorly characterized protein. The gene is annotated as trinucleotide repeat containing 6B, which encodes glycine-tryptophan (GW) repeats. The amino acid sequence of TNRC6B also contains an RNA recognition motif (RRM) at the C terminus, suggesting TNRC6B may function as a single-stranded-RNA binding protein. The 130 kDa band was identified as MOV10, a putative DExD-box helicase. MOV10 is a candidate ortholog of the plant protein SDE-3 and the *Drosophila melanogaster* protein Armitage [10–12], both of which are involved in RNAi. A third protein migrating at about 70 kDa was identified as the arginine methyltransferase PRMT5. The protein migrating at 50 kDa was found to be the translation factor eEF1 α .

The specific interactions of the affinity-purified components of the Ago complexes with Ago1 and Ago2 proteins were further examined by cotransfection and coimmunoprecipitation (co-IP) experiments. N-terminally tagged FLAG/HA-Ago1, FLAG/HA-Ago2, or FLAG/HA-GFP was cotransfected with N-terminally tagged myc-TNRC6B into HEK 293 cells (Figure 1B). Myc-TNRC6B coimmunoprecipitated with FLAG/HA-Ago1 and FLAG/HA-Ago2 (lanes 5 and 6), and myc-TNRC6B was absent in the FLAG/HA-GFP co-IP (lane 7). FLAG/HA-Ago1, FLAG/HA-Ago2, and FLAG/HA-GFP IPs were tested for association with PRMT5 via a specific polyclonal anti-PRMT5 antibody (Figure 1B, right panel). PRMT5 was detected only in the FLAG/HA-Ago1 and FLAG/HA-Ago2 IPs (lanes 9 and 10) and not in the FLAG/HA-GFP control IP (lane 11). To verify a specific interaction of MOV10 with the Ago proteins, N-terminally FLAG/HA-tagged MOV10 was cotransfected with N-terminally tagged myc-Ago1 or myc-Ago2 (Figure 1C). The FLAG/HA-tagged proteins were immunoprecipitated with anti-FLAG beads, and the bound proteins were analyzed by western blotting against the myc-tag (middle and right panel) and the FLAG/HA-tag (left panel). FLAG/HA-MOV10 coprecipitated with myc-Ago1 and myc-Ago2 (lanes 4 and 6), whereas no Ago proteins were detected in the FLAG/HA-GFP control IP (lanes 3 and 5). We were unable to confirm an association of eEF1 α with Ago1 or Ago2 via coimmunoprecipitation

*Correspondence: meister@biochem.mpg.de (G.M.); ttuschl@rockefeller.edu (T.T.)

⁶Present address: Max Planck Institute for Biochemistry, Am Klopferspitz 18, D-82152 Martinsried, Germany.

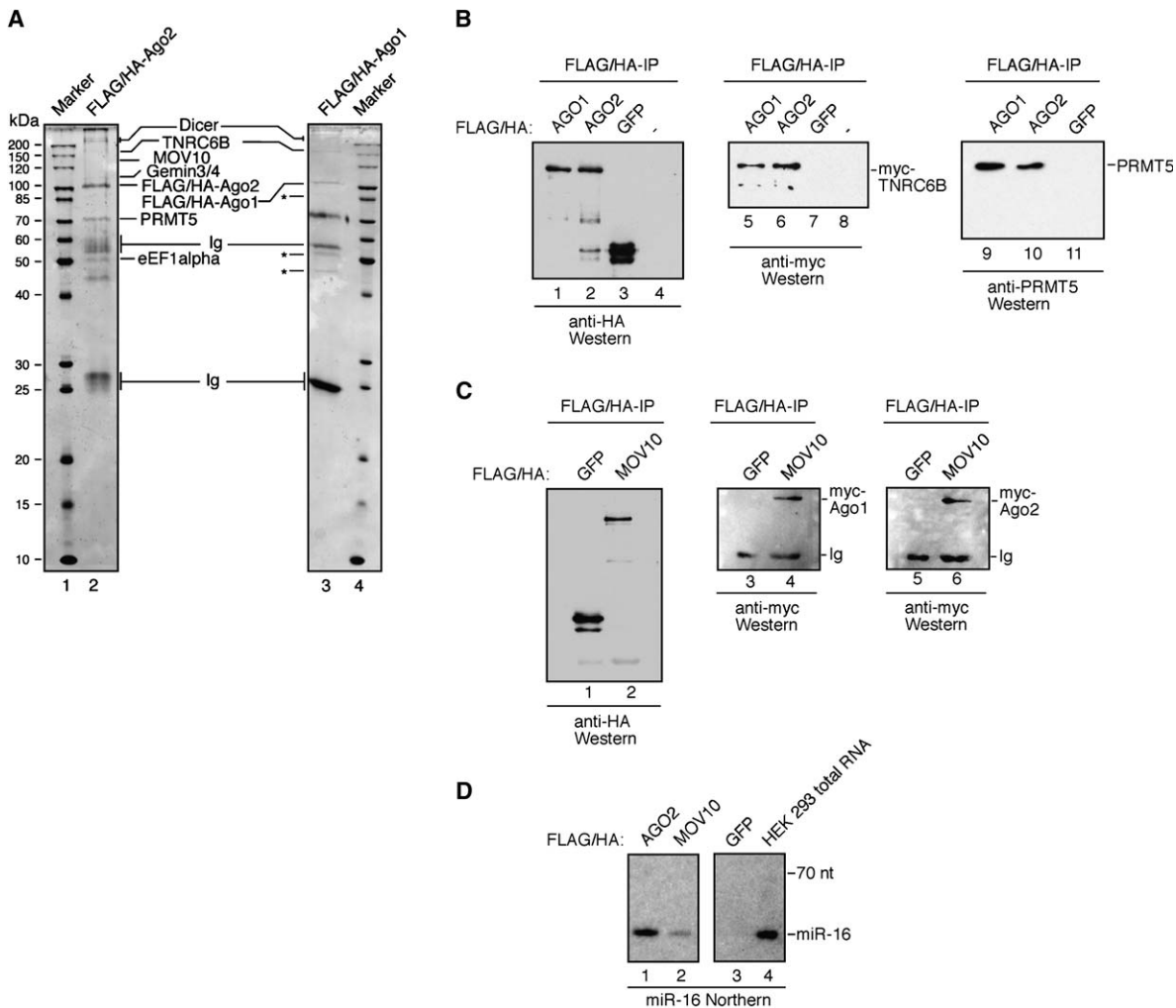


Figure 1. Biochemical Purification and Identification of Novel Ago-Associated Protein Factors

(A) Ago protein complexes were double-affinity-purified from HeLa cells stably transfected with FLAG/HA-tagged Ago1 (lane 3) and Ago2 (lane 2) plasmids. The proteins were separated by SDS-PAGE followed by silver staining and identification of the bands by ESI tandem MS (LC-MS/MS). The asterisks indicate so-far-unidentified proteins. Lanes 1 and 4 show molecular-weight markers.

(B) FLAG/HA-tagged Ago1 (lanes 1 and 5), FLAG/HA-tagged Ago2 (lanes 2 and 6), and FLAG/HA-tagged GFP (lanes 3 and 7) were cotransfected with myc-TNRC6B. In lanes 4 and 8, no FLAG/HA plasmid was cotransfected. Anti-FLAG immunoprecipitates were analyzed by western blotting with anti-HA (lanes 1–4) or anti-myc antibodies (lanes 5–8). FLAG/HA-tagged Ago1 (lane 9), FLAG/HA-tagged Ago2 (lane 10), and FLAG/HA-tagged GFP (lane 11) were transfected into 293 HEK cells. Anti-FLAG immunoprecipitates were analyzed by western blotting with specific polyclonal anti-PRMT5 antibodies.

(C) FLAG/HA-tagged MOV10 (lanes 2, 4, 6) and FLAG/HA-tagged GFP (lanes 1, 3, 5) were cotransfected with myc-tagged Ago1 (lanes 3 and 4) or with myc-tagged Ago2 (lanes 5 and 6). Anti-FLAG immunoprecipitates were analyzed by western blotting with anti-HA (lanes 1 and 2) or anti-myc antibodies (lanes 3–6).

(D) FLAG/HA-tagged Ago2 (lane 1), FLAG/HA-tagged MOV10 (lane 2), and FLAG/HA-tagged GFP were transfected into HEK 293 cells. RNA was extracted from anti-FLAG immunoprecipitates and analyzed by northern blotting with a probe specific to miR-16. Total RNA extracted from HEK 293 cells is shown in lane 4.

approaches. Therefore, it is unclear whether the binding of eEF1 α to the Ago2 complex is specific.

Ago proteins specifically associate with mature miRNAs [7]. We therefore investigated whether MOV10 interacts with miRNA-loaded Ago protein complexes. We transiently transfected FLAG/HA-tagged Ago2, FLAG/HA-tagged MOV10, and FLAG/HA-tagged GFP into HEK 293 cells (Figure 1D). FLAG/HA-tagged proteins were immunoprecipitated with anti-FLAG antibodies. Coprecipitated RNAs were extracted from the beads and analyzed by northern blotting with a probe specific

to miR-16, a highly abundant miRNA in HEK 293 cells. miR-16 was specifically detected in the FLAG/HA-Ago2 as well as the FLAG/HA-MOV10 immunoprecipitate (lanes 1 and 2), and this detection is indicative of an interaction of MOV10 with mature-miRNA-containing Ago protein complexes. No signal was observed in the control-IP (lane 3).

Taken together, our results indicate that MOV10, TNRC6B, and PRMT5 specifically associate with Ago proteins. We were unable to detect MOV10 and PRMT5 in the FLAG/HA-Ago1 purification, presumably

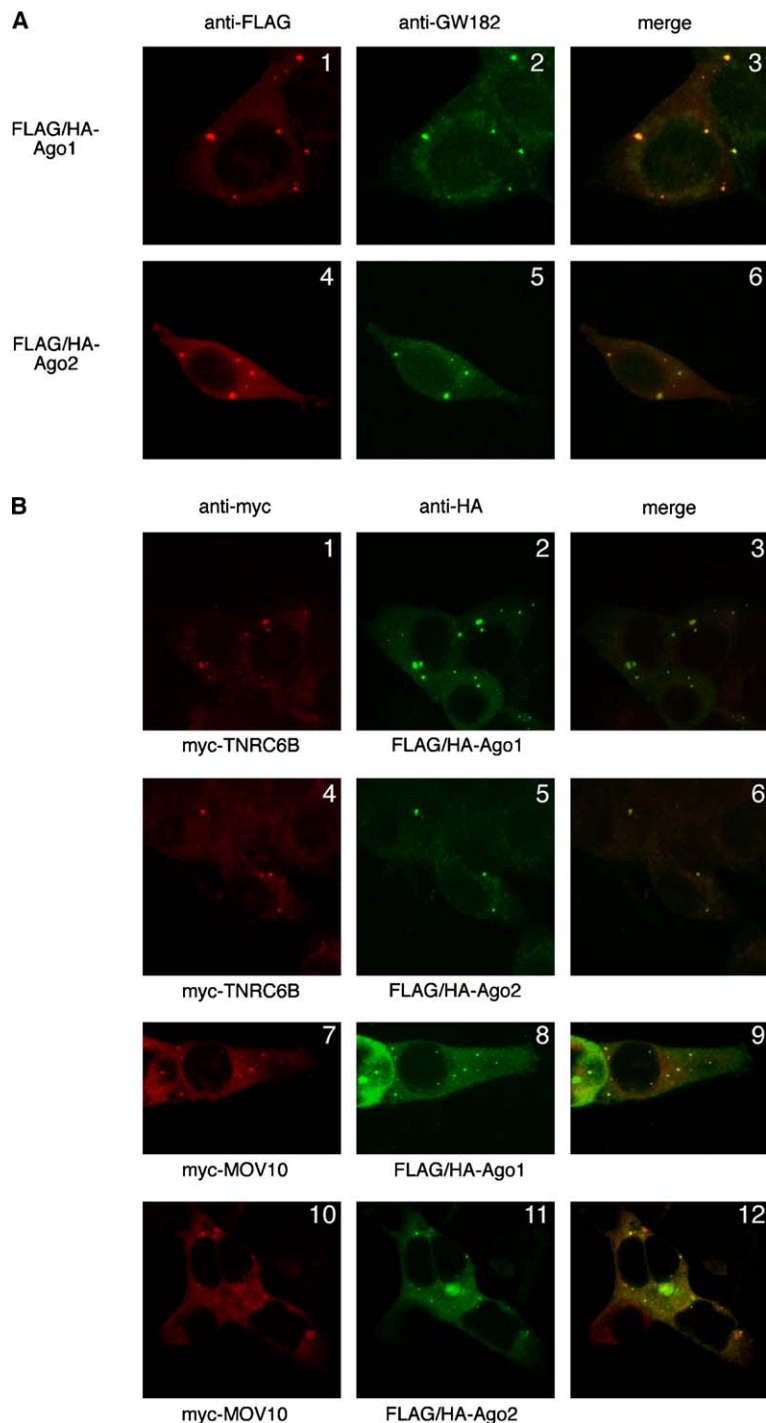


Figure 2. Human Ago1 and Ago2 Colocalize with TNRC6B and MOV10 in Cytoplasmic P Bodies

(A) FLAG/HA-Ago1 was transiently expressed in HEK 293 cells, and the fixed cells were probed with rabbit anti-FLAG and monoclonal mouse anti-GW182 antibodies. The cells were stained with secondary fluorescein-conjugated anti-mouse and Texas Red-conjugated anti-rabbit antibodies. The cells were analyzed with a TCS SP2 confocal laser microscope (Leica). (A₁) shows FLAG/HA-Ago1, (A₄) shows FLAG/HA-Ago2, and (A₂) and (A₅) show GW182 localization. (A₃) and (A₆) show the merged images. (B) FLAG/HA-Ago1 (B₁₋₃ and B₇₋₉), FLAG/HA-Ago2 (B₄₋₆ and B₁₀₋₁₂), and myc-TNRC6B (B₁₋₆) as well as myc-MOV10 (B₇₋₁₂) were coexpressed in HEK 293 cells. The fixed cells were probed with mouse anti-HA and rabbit anti-myc antibodies. Protein localization was analyzed as described in (A).

because the amounts available for purified FLAG/HA-Ago1 complexes were less compared to FLAG/HA-Ago2 complexes (Figure 1A, compare lane 2 and 3).

MOV10 and TNRC6B Colocalize with Ago Proteins in Cytoplasmic P Bodies

Recently, it has been demonstrated that Ago proteins as well as miRNAs localize to specific cytoplasmic loci termed processing bodies, or P bodies [13–15]. Furthermore, TNRC6B is a protein homologous to the P body component GW182 [16], which is also known as

TNRC6A. Therefore, we tested whether the novel biochemically identified Ago-complex components localize to P bodies as well. We transiently expressed FLAG/HA-tagged Ago1 and Ago2 in HEK 293 cells. After 48 hr, the cells were fixed and immunofluorescence studies were performed with anti-FLAG antibodies. Both Ago1 and Ago2 were concentrated in cytoplasmic P bodies (Figure 2A, left panel) as shown by costaining with antibodies directed against the P body marker protein GW182 (Figure 2A, middle and right panel). For colocalization studies of Ago1 and Ago2 with the biochemically

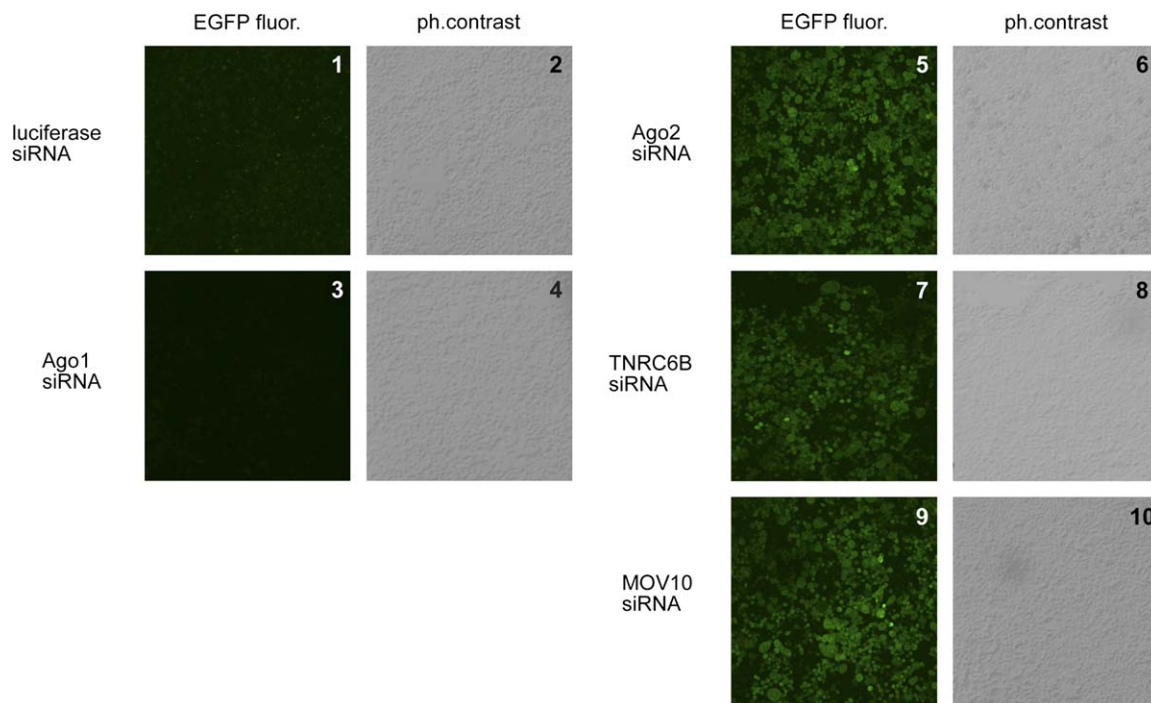


Figure 3. MOV10 and TNRC6B Are Required for miR-21-Guided Cleavage Activity in HeLa-Cell Culture

A stable HeLa-cell line that expresses EGFP carrying a sequence with perfect complementarity to miR-21 in its 3' UTR was transfected with control siRNAs complementary to the luciferase mRNA (1 and 2) or Ago1 (3 and 4), Ago2 (5 and 6), TNRC6B (7 and 8) and MOV10-specific siRNA duplexes (9 and 10). Fluorescence and phase-contrast images were recorded 5 days after transfection with a TCS SP2 confocal laser microscope (Leica Microsystems, Germany).

identified complex components TNRC6B and MOV10, we transiently expressed FLAG/HA-Ago1 and FLAG/HA-Ago2 together with myc-TNRC6B or myc-MOV10 in HEK 293 cells (Figure 2B). Immunostaining with anti-myc antibodies demonstrated that both TNRC6B and MOV10 localized to cytoplasmic granules (Figures 2B₁, 2B₄, 2B₇, and 2B₁₀). Moreover, these granules also contained FLAG/HA-Ago1 or FLAG/HA-Ago2 as shown by probing the same cells with anti-HA antibodies (Figures 2B₂, 2B₅, 2B₈, and 2B₁₁). An overlay of the respective images shows that both Ago1 and Ago2 colocalize with TNRC6B and MOV10 in cytoplasmic P bodies (Figures 2B₃, 2B₆, 2B₉, and 2B₁₂). No specific signal has been observed when the primary anti-FLAG, anti-HA, or anti-myc antibodies were omitted from the staining procedure (Figure S1 in the Supplemental Data available with this article online).

MOV10 and TNRC6B Are Required for miRNA-Guided mRNA Cleavage In Vivo

To learn about the function of Ago2 and its complex components TNRC6B and MOV10 in cultured cells, we used a previously developed GFP-based positive-readout reporter cell line [7, 17]. In this cell line, the expression of GFP is repressed by miR-21. Transfection of 2'-O-methyl oligonucleotides antisense to miR-21 blocked endogenous miR-21 and derepressed GFP expression [7, 17]. In this reporter system, we depleted Ago1, Ago2, TNRC6B, and MOV10 mRNAs by using siRNAs (Figure 3). The knockdown of the specific mRNA was monitored by quantitative RT-PCR (qRT-PCR, Figure

S2). Similar to previous findings, depletion of Ago1 (Figure 3₃), as well as transfection of control siRNAs, (Figure 3₁) has no influence on GFP expression, whereas knockdown of Ago2 resulted in strong upregulation of GFP (Figure 3₅) [7]. Knockdown of MOV10 (Figure 3₉) as well as TNRC6B mRNA (Figure 3₇) resulted in GFP-signal upregulation comparable to targeting of Ago2, indicating that MOV10 and TNRC6B were required for miR-21-guided mRNA cleavage in cultured cells.

Very recently, it has been shown that also *Caenorhabditis elegans* and *D. melanogaster* homologs of the TNRC6 family are required for miRNA-guided gene silencing and are present in P bodies [18, 19]. Because members of the human Ago subfamily as well as miRNAs and their target mRNAs were reported to localize to cytoplasmic P bodies [13–15], it is tempting to speculate that some of the newly identified factors, including TNRC6B, mediate targeting of Ago complexes to P bodies, while at the same time they might act in assembly of the silencing complexes and/or in guiding target recognition.

In Vitro Reconstitution of Target-RNA Cleaving RISC/miRNPs Supplying dsRNA Precursors

Because Dicer copurified with FLAG/HA-Ago1 and FLAG/HA-Ago2, we tested whether Dicer also associated with other Ago proteins and whether Dicer-containing Ago complexes showed biochemical Dicer activity. We transiently expressed FLAG/HA-tagged Ago1 through Ago4 and MOV10 in HEK 293 cells. After 48 hr, cells were harvested and the FLAG/HA-tagged proteins were immunoprecipitated. The IP was incubated with internally

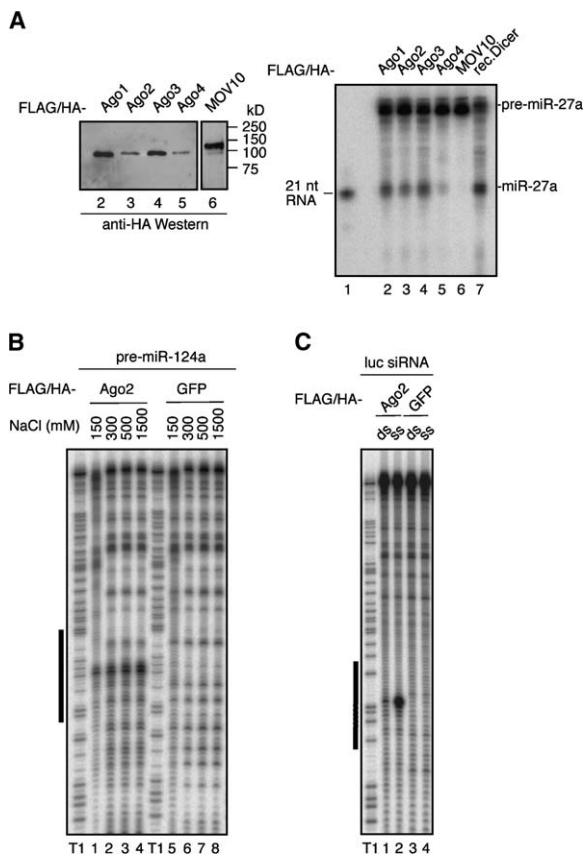


Figure 4. Human Ago2 Is Associated with Dicer, Allowing Cleavage of miRNA Precursors, Incorporation of the miRNA into Ago2 Complexes, and Cleavage of Complementary Target RNA

(A) HEK 293 cells were transiently transfected with FLAG/HA-tagged Ago1, 2, 3, 4, and FLAG/HA-tagged MOV10 (lanes 2–6). Immunoprecipitates were incubated with a Dicer substrate RNA derived from the miR-27a precursor that has been internally ³²P labeled. The processed RNA products were analyzed by 15% denaturing RNA PAGE followed by phosphoimaging. In lane 7, recombinant Dicer was used, and lane 1 shows a 21-nt-long RNA as size marker. An anti-HA western blot indicating the amounts of FLAG/HA-tagged Ago proteins used for the Dicer reaction is shown to the left.

(B) Immunoprecipitations of FLAG/HA-tagged Ago2 (lanes 1–4) or FLAG/HA-tagged GFP (lanes 5–8) were washed with 150 mM, 300 mM, 500 mM, or 1500 mM NaCl and subsequently preincubated with an in vitro-transcribed miR-124a-1 precursor followed by incubation with a ³²P-cap-labeled target RNA that carried a sequence element perfectly complementary to the mature miR-124.

The reactions shown in (C) were preincubated with single-stranded or double-stranded siRNAs directed against a luciferase target RNA. Cleaved RNA products shown in (B) and (C) were separated by 8% denaturing RNA PAGE and visualized by phosphoimaging. Partial nuclease T1 digestions of the miR-124 and the luciferase target RNAs are indicated as T1. The target-RNA sequence element that is covered by miR-124 and the siRNA against the luciferase mRNA is shown as black lines to the left of the gels.

radioactively labeled pre-miR-27a, and the processing products were subsequently analyzed by denaturing PAGE (Figure 4, right panel). As a positive control, we incubated pre-miR-27a with commercially available recombinant human Dicer (Stratagene). All of the FLAG/HA-Ago IPs (lanes 2–5) as well as the positive control (lane 7) supported pre-miRNA processing to 21-nt RNA products, indicating co-IP of Dicer cleavage activity. The FLAG/HA-MOV10 IP, however, did not contain Dicer

activity, suggesting that MOV10 functions downstream of the Dicer cleavage step (lane 6) or that it is only transiently associated with the RISC loading or assembly complex.

The coexistence of Dicer and Ago proteins in Ago-purified complexes and the presence of Dicer activity prompted us to examine whether RISC can be reconstituted in vitro by using pre-miRNAs as input. Previously, it was shown that single-stranded 21-nt RNAs but not duplex siRNAs reconstitute cleavage activity by using partly purified or recombinant Ago2 [20, 21]. To avoid contamination of endogenously expressed miRNAs from HeLa or HEK 293 cells in such an assay, we chose the neuron-specific pre-miR-124a-1. Pre-miR-124a-1 was transcribed in vitro and mimicked the Drosha processing products carrying a 2 nt 3' overhang at the base of the stem loop. FLAG/HA-Ago2 or FLAG/HA-GFP IPs from HEK 293 cells were preincubated with pre-miR-124a-1 and followed by the addition of a ³²P-cap-labeled substrate RNA perfectly complementary to miR-124a. The cleaved RNA products were analyzed by denaturing PAGE (Figure 4B). Only the incubation with FLAG/HA-Ago2 IP (lane 1) but not the FLAG/HA-GFP control IP (lane 5) resulted in a specific miR-124a-guided cleavage product, which indicated that Dicer, RISC-loading, and RISC activity coprecipitated with FLAG/HA-Ago2. The activity of the complexes is increased after a high-salt wash up to 1.5 M NaCl (lanes 1–4), possibly suggesting that endogenously associated dsRNA may have been removed and the proteins were free to incorporate the exogenously added pre-miR-124a. We also examined whether RISC can be reconstituted by using duplex siRNA (Figure 4C). FLAG/HA-Ago2 or FLAG/HA-GFP IPs were preincubated with the duplex siRNA directed against firefly luciferase mRNA. A ³²P-labeled substrate RNA was subsequently added, and the cleaved RNA products were analyzed as described above. The FLAG/HA-Ago2 IP, but not the FLAG/HA-GFP IP, supported target-RNA cleavage. The cleavage activity reconstituted on FLAG/HA-Ago2 beads when input duplex siRNA was used was about 10–20-fold weaker than when single-stranded siRNA was used at the same concentrations (lane 2), presumably as a result of very low amounts of coprecipitated protein complex(es) that are required for unwinding and/or RISC loading. In summary, we demonstrated that human Ago2 coprecipitated with components required for miRNA processing, unwinding of the small RNA duplex, RISC loading, and cleavage of a substrate RNA.

Integration of the Factors in an Interaction Network

Crystallographic studies of Ago proteins revealed unique structural and enzymatic features required for binding small RNAs processed by RNase III enzymes and for guiding target-mRNA recognition as well as cleavage [21–28]. To define the protein network of individual members of the human Ago subfamily, we applied biochemical methods to identify such interactors. Among the identified proteins, we found Dicer stably associated with Ago1- and Ago2-containing complexes; Dicer was previously shown to bind to the PIWI-box of Ago proteins through one of its RNase III domains [29]. Human Dicer was also shown to be present in a complex together with the dsRNA binding domain (dsRBD) protein TRBP,

and that this complex interacted with Ago proteins [9, 30]. However, it is only here where functional biochemical studies support the existence of such a small-RNA processing and targeting “holo-RISC” complex.

MOV10 is a human homolog of the *D. melanogaster* DExD-box protein Armitage. In *D. melanogaster* lysates, Armitage is required for early RISC assembly as demonstrated in gel-shift experiments [12]. Armitage is also essential for miRNA-guided translational regulation in *D. melanogaster* and suggests a general role for Armitage in all RNA silencing processes [10, 12]. MOV10 might have a similar function in assembling miRNA-containing silencing complexes and/or acts in subsequent steps.

The arginine-methyltransferase PRMT5 specifically generates symmetric dimethyl-arginines in its target proteins [31]. Among other RNA binding proteins, such targets are “like-Sm” proteins (LSm proteins), which are involved in pre-mRNA splicing and mRNA turnover [32]. Interestingly, LSm-proteins also localize to cytoplasmic P bodies [33], and it will be very interesting to examine whether PRMT5 and/or LSm-proteins are required for the localization of Ago proteins to cytoplasmic P bodies. Though we assume that PRMT5 is part of human “holo-RISC” and mediates methylation of arginine residues on some yet-to-be-identified “holo-RISC” component(s), we did not identify classic target motifs composed of arginines usually flanked by two glycines in known components of silencing complexes. Further biochemically studies are needed to address the role of these new enzymatic activities present in RNA-silencing-mediating complexes.

Supplemental Data

Supplemental Data include Supplemental Experimental Procedures and two Supplemental Figures and are available with this article online at: <http://www.current-biology.com/cgi/content/full/15/23/2149/DC1/>.

Acknowledgments

We thank J. Meyer, L. Dinic, and A. Rice for excellent technical support; S. Malik and R. Roeder for the FLAG/HA expression vector and help with generating stable cell lines; and Y. Pei, Y. Dorsett, S. Pfeffer, P. Landgraf, and A. Patkaniowska for discussion. We also thank the Kazusa DNA Research Institute (Japan) for the TNRC6B cDNA. G.M. was supported by Emmy Noether fellowship 2064/1 of the Deutsche Forschungsgemeinschaft and the Max Planck Society, and M.L. was supported by a postdoctoral fellowship of the Irma T. Hirsch trust. This work was also supported by National Institutes of Health Grant R01 GM068476-01 to T.T. and by BMBF grant 0311856 to T.T. and R.L.

Received: August 18, 2005

Revised: October 6, 2005

Accepted: October 18, 2005

Published online: November 10, 2005

References

1. Ambros, V. (2004). The functions of animal microRNAs. *Nature* 431, 350–355.
2. Bartel, D.P. (2004). MicroRNAs: Genomics, biogenesis, mechanism, and function. *Cell* 116, 281–297.
3. Dykxhoorn, D.M., Novina, C.D., and Sharp, P.A. (2003). Killing the messenger: Short RNAs that silence gene expression. *Nat. Rev. Mol. Cell Biol.* 4, 457–467.
4. Meister, G., and Tuschl, T. (2004). Mechanisms of gene silencing by double-stranded RNA. *Nature* 431, 343–349.
5. Jackson, A.L., and Linsley, P.S. (2004). Noise amidst the silence: Off-target effects of siRNAs? *Trends Genet.* 20, 521–524.
6. Carmell, M.A., Xuan, Z., Zhang, M.Q., and Hannon, G.J. (2002). The Argonaute family: Tentacles that reach into RNAi, developmental control, stem cell maintenance, and tumorigenesis. *Genes Dev.* 16, 2733–2742.
7. Meister, G., Landthaler, M., Patkaniowska, A., Dorsett, Y., Teng, G., and Tuschl, T. (2004). Human Argonaute2 mediates RNA cleavage targeted by miRNAs and siRNAs. *Mol. Cell* 15, 185–197.
8. Mourelatos, Z., Dostie, J., Paushkin, S., Sharma, A., Charroux, B., Abel, L., Rappsilber, J., Mann, M., and Dreyfuss, G. (2002). miRNPs: A novel class of ribonucleoproteins containing numerous microRNAs. *Genes Dev.* 16, 720–728.
9. Chendrimada, T.P., Gregory, R.I., Kumaraswamy, E., Norman, J., Cooch, N., Nishikura, K., and Shiekhattar, R. (2005). TRBP recruits the Dicer complex to Ago2 for microRNA processing and gene silencing. *Nature* 436, 740–744. Published online June 22, 2005. 10.1038/nature03868.
10. Cook, H.A., Koppetsch, B.S., Wu, J., and Theurkauf, W.E. (2004). The *Drosophila* SDE3 homolog armitage is required for oskar mRNA silencing and embryonic axis specification. *Cell* 116, 817–829.
11. Dalmay, T., Horsefield, R., Braunstein, T.H., and Baulcombe, D.C. (2001). SDE3 encodes an RNA helicase required for post-transcriptional gene silencing in *Arabidopsis*. *EMBO J.* 20, 2069–2078.
12. Tomari, Y., Du, T., Haley, B., Schwarz, D.S., Bennett, R., Cook, H.A., Koppetsch, B.S., Theurkauf, W.E., and Zamore, P.D. (2004). RISC assembly defects in the *Drosophila* RNAi mutant armitage. *Cell* 116, 831–841.
13. Liu, J., Valencia-Sanchez, M.A., Hannon, G.J., and Parker, R. (2005). MicroRNA-dependent localization of targeted mRNAs to mammalian P-bodies. *Nat. Cell Biol.* 7, 719–723.
14. Pillai, R.S., Bhattacharyya, S.N., Artus, C.G., Zoller, T., Cougot, N., Basyuk, E., Bertrand, E., and Filipowicz, W. (2005). Inhibition of translational initiation by Let-7 MicroRNA in human cells. *Science* 309, 1573–1576. Published online August 4, 2005. 10.1126/science.1115079.
15. Sen, G.L., and Blau, H.M. (2005). Argonaute 2/RISC resides in sites of mammalian mRNA decay known as cytoplasmic bodies. *Nat. Cell Biol.* 7, 633–636.
16. Eystathiou, T., Chan, E.K., Tenenbaum, S.A., Keene, J.D., Griffith, K., and Fritzler, M.J. (2002). A phosphorylated cytoplasmic autoantigen, GW182, associates with a unique population of human mRNAs within novel cytoplasmic speckles. *Mol. Biol. Cell* 13, 1338–1351.
17. Landthaler, M., Yalcin, A., and Tuschl, T. (2004). The human DiGeorge syndrome critical region gene 8 and its *D. melanogaster* homolog are required for miRNA biogenesis. *Curr. Biol.* 14, 2162–2167.
18. Ding, L., Spencer, A., Morita, K., and Han, M. (2005). The developmental timing regulator AIN-1 interacts with miRISCs and may target the argonaute protein ALG-1 to cytoplasmic P bodies in *C. elegans*. *Mol. Cell* 19, 437–447.
19. Rehwinkel, J., Behm-Ansmant, I., Gatfield, D., and Izaurralde, E. (2005). A crucial role for GW182 and the DCP1:DCP2 decapping complex in miRNA-mediated gene silencing. *RNA* 11, 1640–1647. Published online September 21, 2005. 10.1261/rna.2191905.
20. Liu, J., Carmell, M.A., Rivas, F.V., Marsden, C.G., Thomson, J.M., Song, J.J., Hammond, S.M., Joshua-Tor, L., and Hannon, G.J. (2004). Argonaute2 is the catalytic engine of mammalian RNAi. *Science* 305, 1437–1441.
21. Rivas, F.V., Tolia, N.H., Song, J.J., Aragon, J.P., Liu, J., Hannon, G.J., and Joshua-Tor, L. (2005). Purified Argonaute2 and an siRNA form recombinant human RISC. *Nat. Struct. Mol. Biol.* 12, 340–349.
22. Ma, J.B., Yuan, Y.R., Meister, G., Pei, Y., Tuschl, T., and Patel, D.J. (2005). Structural basis for 5'-end-specific recognition of guide RNA by the *A. fulgidus* Piwi protein. *Nature* 434, 666–670.

23. Parker, J.S., Roe, S.M., and Barford, D. (2005). Structural insights into mRNA recognition from a PIWI domain-siRNA guide complex. *Nature* 434, 663–666.
24. Song, J.J., Smith, S.K., Hannon, G.J., and Joshua-Tor, L. (2004). Crystal structure of Argonaute and its implications for RISC slicer activity. *Science* 305, 1434–1437.
25. Ma, J.B., Ye, K., and Patel, D.J. (2004). Structural basis for overhang-specific small interfering RNA recognition by the PAZ domain. *Nature* 429, 318–322.
26. Song, J.J., Liu, J., Tolia, N.H., Schneiderman, J., Smith, S.K., Martienssen, R.A., Hannon, G.J., and Joshua-Tor, L. (2003). The crystal structure of the Argonaute2 PAZ domain reveals an RNA binding motif in RNAi effector complexes. *Nat. Struct. Biol.* 10, 1026–1032.
27. Yan, K.S., Yan, S., Farooq, A., Han, A., Zeng, L., and Zhou, M.M. (2003). Structure and conserved RNA binding of the PAZ domain. *Nature* 426, 468–474.
28. Yuan, Y.R., Pei, Y., Ma, J.B., Kuryavyi, V., Zhadina, M., Meister, G., Chen, H.Y., Dauter, Z., Tuschl, T., and Patel, D.J. (2005). Crystal structure of *A. aeolicus* Argonaute, a site-specific DNA-guided endoribonuclease, provides insights into RISC-mediated mRNA cleavage. *Mol. Cell* 19, 405–419.
29. Tahbaz, N., Kolb, F.A., Zhang, H., Jaronczyk, K., Filipowicz, W., and Hobman, T.C. (2004). Characterization of the interactions between mammalian PAZ PIWI domain proteins and Dicer. *EMBO Rep.* 5, 189–194.
30. Haase, A.D., Jaskiewicz, L., Zhang, H., Laine, S., Sack, R., Gagnon, A., and Filipowicz, W. (2005). TRBP, a regulator of cellular PKR and HIV-1 virus expression, interacts with Dicer and functions in RNA silencing. *EMBO Rep.* 6, 961–967.
31. Meister, G., Eggert, C., and Fischer, U. (2002). SMN-mediated assembly of RNPs: A complex story. *Trends Cell Biol.* 12, 472–478.
32. He, W., and Parker, R. (2000). Functions of Lsm proteins in mRNA degradation and splicing. *Curr. Opin. Cell Biol.* 12, 346–350.
33. Ingelfinger, D., Arndt-Jovin, D.J., Luhrmann, R., and Achsel, T. (2002). The human LSm1–7 proteins colocalize with the mRNA-degrading enzymes Dcp1/2 and Xrnl in distinct cytoplasmic foci. *RNA* 8, 1489–1501.

Note Added in Proof

This text differs slightly from the version previously published online, in which MOV10 was incorrectly identified as a DEAD-box helicase; MOV10 actually belongs to the DExD superfamily. In addition, the authors wish to cite the following paper as evidence that Gemin3 and Gemin4 functionally interact with Ago2: Hutvagner, G., and Zamore, P.D. (2002). A microRNA in a multiple-turnover RNAi enzyme complex. *Science* 297, 2056–2060.

Research Paper

Identification of Human microRNA Targets From Isolated Argonaute Protein Complexes

Michaela Beitzinger¹

Lasse Peters¹

Jia Yun Zhu¹

Elisabeth Kremmer²

Gunter Meister^{1,*}

¹Laboratory of RNA Biology; Max Planck Institute of Biochemistry; Martinsried, Germany

²GSF - Institute of Molecular Immunology; Munich, Germany

*Correspondence to: Laboratory of RNA Biology; Max Planck Institute of Biochemistry; Am Klopferspitz 18; Martinsried 82152 Germany; Tel.: +49.89.8578.3420; Fax: +49.89.8578.3430; Email: meister@biochem.mpg.de

Original manuscript submitted: 05/28/07

Manuscript accepted: 06/28/07

This manuscript has been published online, prior to printing for RNA Biology, Volume 4, Issue 2. Definitive page numbers have not been assigned. The current citation is: RNA Biology 2007; 4(2):

<http://www.landesbioscience.com/journals/rnabiology/abstract.php?id=4640>

Once the issue is complete and page numbers have been assigned, the citation will change accordingly.

KEY WORDS

RNAi, RNA interference, microRNAs, Argonaute, gene silencing, non-coding RNAs, translation, gene regulation

ABBREVIATIONS

ds	double stranded
nt	nucleotide
Ago	Argonaute proteins
miRNAs	microRNAs
UTR	untranslated region
IRES	internal ribosome entry site

ACKNOWLEDGEMENTS

We thank Sabine Rottmüller for technical assistance. Our research is supported by the Max-Planck-Society, the Deutsche Forschungsgemeinschaft (Me 2064/2-1 to G.M.) and the European Union (LSHG-CT-2005-037900 to G.M.). L.P. receives a fellowship of the Boehringer Ingelheim Fonds.

ABSTRACT

MicroRNAs (miRNAs) constitute a class of small non-coding RNAs that regulate gene expression on the level of translation and/or mRNA stability. Mammalian miRNAs associate with members of the Argonaute (Ago) protein family and bind to partially complementary sequences in the 3' untranslated region (UTR) of specific target mRNAs. Computer algorithms based on factors such as free binding energy or sequence conservation have been used to predict miRNA target mRNAs. Based on such predictions, up to one third of all mammalian mRNAs seem to be under miRNA regulation. However, due to the low degree of complementarity between the miRNA and its target, such computer programs are often imprecise and therefore not very reliable. Here we report the first biochemical identification approach of miRNA targets from human cells. Using highly specific monoclonal antibodies against members of the Ago protein family, we co-immunoprecipitate Ago-bound mRNAs and identify them by cloning. Interestingly, most of the identified targets are also predicted by different computer programs. Moreover, we randomly analyzed six different target candidates and were able to experimentally validate five as miRNA targets. Our data clearly indicate that miRNA targets can be experimentally identified from Ago complexes and therefore provide a new tool to directly analyze miRNA function.

INTRODUCTION

MiRNAs form a highly conserved class of small non-coding RNAs with regulatory functions in processes as diverse as development, cell differentiation or apoptosis.¹⁻³ MiRNA genes are often organized in genomic clusters, which give rise to one primary transcript containing multiple miRNAs. MiRNAs, however, also derive from one individual transcript or frequently originate from intronic sequences.¹⁻³ MiRNA genes are transcribed by RNA polymerases II or III to generate primary miRNA transcripts that are poly-adenylated and capped.^{4,5} Primary miRNA transcripts are processed by the nuclear microprocessor complex, which contains the RNase III enzyme Drosha and its co-factor DGCR8.⁶⁻⁸ Drosha produces stem-loop structured miRNA precursors (pre-miRNAs) with characteristic two nucleotide (nt) 3' overhangs.⁹ The pre-miRNA hairpin is further transported to the cytoplasm by the export receptor Exportin 5 where it is further processed by the RNase III enzyme Dicer.^{3,10,11} Dicer most likely recognizes the two nt overhangs and cleaves 21 nt from the ends to produce a short-lived double stranded (ds) miRNA/miRNA* RNA which is subsequently unwound and only one strand is incorporated into miRNA-protein complexes (miRNPs) and gives rise to the mature miRNA.^{3,10,11}

MiRNAs guide members of the Argonaute protein family to partially complementary sequences within the 3' UTR of target mRNAs to either regulate their translation into protein or their stability.^{12,13} Argonaute proteins are highly conserved and contain PAZ (PIWI-Argonaute-zwille) and PIWI domains. Structural studies have demonstrated that the PAZ domain forms a highly specific binding module for 2 nt 3' overhangs generated by RNase III enzymes. In contrast, PIWI domains fold similar to RNase H and may therefore function as endonucleases.¹⁴⁻¹⁶ Indeed, it has been demonstrated for some Ago proteins that they are endonucleolytically active and such proteins have therefore been termed "Slicer". Interestingly, in mammalian cells Ago2 is the only member of the Ago protein family, which has endonuclease activity, although the critical amino acids are conserved in some other Ago proteins as well.^{17,18}

MiRNAs recognize partially complementary binding sites located in the 3' UTR of target mRNAs and function as guides for protein effectors such as Ago proteins.¹³ It has been shown that miRNP-binding to specific target mRNAs can regulate gene expression in different ways. On target sites with a high degree of complementarity, miRNAs function alike siRNAs and guide sequence-specific cleavage of the target mRNA.¹⁹ Targets with low degree of complementarity can either be destabilized by recruiting de-capping and de-polymerization enzymes or their translation is repressed without altering mRNA levels.¹² While sequence-specific cleavage of target RNAs is well understood, the mechanism of how miRNAs guide translational repression or destabilization is only poorly understood.

The mode of miRNA-guided translational repression is still a matter of debate. Initial studies in *Caenorhabditis elegans* (*C.elegans*) have shown that miRNAs as well as target mRNAs associate with polysomes in sucrose gradients and it has been suggested that miRNAs function after initiation and presumably at the elongation steps of translation.^{20,21} Later on, it has been reported that also mammalian miRNAs can be found on polysomes and a ribosome drop-off model has been suggested, which describes the rapid ribosome drop-off from mRNAs that are targeted by miRNAs.²²⁻²⁴ Controversially, it has been demonstrated that miRNAs interfere with translation initiation steps. Moreover, cap-independent translation mediated by internal ribosome entry sites (IRES) is not sensitive to miRNA-guided regulation, indicating that miRNAs inhibit translation initiation.^{25,26} Very recently, two reports supported this model. First, miRNPs associate with the 60S ribosomal subunit and eIF6, a protein known to prevent assembly of 80S ribosomes.²⁷ Second, in a *Drosophila* in vitro translation system, miRNAs induce the formation of dense miRNPs that co-migrate with polysomes.²⁸ These structures have been termed pseudo-polysomes and may reflect the structures that have been interpreted as polysomes in other studies.

Novel mechanistic insights into miRNA function came from recent studies on Ago proteins. Mourelatos and co-workers identified a motif within Ago proteins, which specifically recognizes and binds the m7G cap of mRNAs, thus preventing binding of eIF4E binding. This Ago-m7G cap interaction therefore leads to the inhibition of translational initiation.²⁹

Due to the low degree of complementarity between miRNAs and target mRNAs, only a few mammalian target mRNAs have been discovered and validated thus far. Computer algorithms have been developed to predict putative miRNA targets and it has been found that seven to eight nt at the 5' end of the miRNA is the most important determinant for target specificity. Such sequences are also called "seed sequence".³⁰⁻³³ Based on seed sequence conservation and free binding energy, miRNA targets have been predicted in a variety of different organisms. The different prediction programs find about 100 to 150 different targets for one miRNA. Some algorithms even predict one third of all human mRNAs as miRNA targets. Computer programs usually predict targets on a genome wide scale irrespective of tissue-specific mRNA and miRNA expression patterns. Therefore, it is very difficult to find miRNA targets that are specific to tissues or cell lines. Interestingly, it has been proposed earlier, that miRNA-mRNA interactions are restricted to specific tissues in *C. elegans*.³⁴ It is becoming more and more apparent that it is very important to develop biochemical tools to identify only subsets of miRNA targets from specific tissue material.

Here we report the first biochemical miRNA target identification approach. Using specific monoclonal antibodies against human Ago1 and Ago2, we succeeded to co-immunoprecipitate Ago-bound

mRNAs. We generated a cDNA library from the Ago-associated mRNAs and identified a significant number by sequencing. We further validated six Ago-bound mRNAs either by inhibiting or over-expressing miRNAs that have been predicted to regulate the respective mRNAs.

MATERIALS AND METHODS

Reporter constructs. To generate miRNA reporter plasmids which express the firefly luciferase mRNA with a 3'UTR sequence of interest and renilla luciferase as a transfection control, pMIR-REPORT (Ambion) was modified as follows: The renilla luciferase gene with a SV40 promoter and a poly(A) site was PCR-amplified from the pRL-SV40 plasmid (Promega) and inserted into the SspI site of pMIR-REPORT. Additionally, an HSV-TK promoter was PCR-cloned from pRL-TK (Promega) and inserted into pMIR-REPORT to replace the CMV promoter of the firefly luciferase gene.

Luciferase expression constructs were generated by cloning of the 3'UTRs of STMN1, HMGB1, Raver2, SERBP1, DNAJB11 and SFPQ into the modified pMIR vector (pMIR-RL) described above. The 3'UTRs were cloned via PCR amplification from cDNA libraries and ligated into the corresponding SacI and NaeI sites of pMIR-RL. The primer sequences are:

SERBP1, 5'-CGCTGAGCTCCTGGATGCCATAAGACAACCCT, 5'-CGCTGCCGGCTTAACTGGTACACACTGTTTCAC;
Raver2, 5'-CGCTGAGCTCGTTAAGCTCTCTCCTAATAAACC, 5'-CGCTGCCGGCTCCCAATAAAAAGTTTATTTATG;
SFPQ, 5'-CGCTGAGCTCATGTGATATTTAGGCTTTCATT, 5'-CGCTGCCGGCTCATGTTTAAACATCTTTAATTC;
DNAJB11, 5'-CGCTGAGCTCGAGTGAATAAAAATTGGACTTTG, 5'-CGCTGCCGGCTTCATGAAAAAATAACAACAA;
HMGB1, 5'-CGCTGAGCTCGTTGGTTCTAGCGCAGTTTTTT, 5'-CGCTGCCGGCTTACTGCAATTATTAGTTTTATT;
STMN1, 5'-CGCTGAGCTCTTTGTTCTGAGAACTGACTTTC, 5'-CGCTGCCGGCCTACAGCAGTACATAAAGTTTT.

The sequences of miR-let7a, miR-26a, miR-26b, miR-29b, miR-99a, miR-100 and miR-141 were cloned as oligonucleotides into pSuper (oligoengine) according to the manufacturer's protocol. miR-let7a, 5'-GATCCCTGGGATGAGGTAGTAGGTTGTATAG TTTTAGGGTACACCCACCCTGGGAGATAACTATACAAT CTACTGTCTTTCTATTTTTTA;

miR-26a, 5'-GATCCCGTGGCCTCGTTCAAGTAATCCAGGAT AGGCTGTGCAGGTCCCAATGGGCTATTTCTTGGTTACTT GCACGGGGACGCTTTTTTA;

miR-26b; 5'-GATCCCCCGGGACCCAGTTCAAGTAATTCAG GATAGGTTGTGTGCTGTCCAGCCTGTTCTCCATFACTTG GCTCGGGGACCGTTTTTA;

miR-29b, 5'-GATCCCCTTCAGGAAGCTGGTTTCATATGGT GGTTTAGATTTAAATAGTGATTGTCTAGCACCATTGAAA TCAGTGTCTTGGGGTTTTTA;

miR-99a, 5'-GATCCCCCATTTGGCATAAACCCTAGATCCG ATCTTGTGGTGAAGTGGACCGCACAAAGCTCGCTTCTATG GGCTGTGTCAGTGTGTTTTTA;

miR-100, 5'-GATCCCCCTGTTGCCACAAACCCTAGATCC GAACTTGTGGTATTAGTCCGCACAAGCTTGTATCTATAGG TATGTGCTGTTAGGTTTTTA;

miR-141, 5'-GATCCCCGGCCGGCCCTGGGTCCATCTTCC AGTACAGTGTGGATGGTCTAATTGTGAAGCTCCTAACA CTGTCTGGTAAAGATGGCTCCCGGGTGGTTCTTTTTTA.

2'-O-methylated miRNA inhibitors were designed as antisense oligos

to the mature miRNAs according to the miRNA registry (microrna.sanger.ac.uk/sequences/index.shtml).

Transfections and luciferase assays. Plasmid transfections for luciferase assays were performed with 50 ng pMIR-RL 3'UTR and 200 ng pSuper-miRNA vector or 40 pmol 2'OMe-miRNA-inhibitor per 2×10^4 cells in a 48-well plate using EscortV transfection reagent (Sigma) as described by the manufacturer. For Co-transfection of DNA and 2'OMe-miRNA-inhibitors, pMIR-RL 3'UTR were transfected 6 h after transfection with the 2'OMe-miRNA-inhibitors. Luciferase activity was measured 48 h after transfection using a dual luciferase reporter system as described by the manufacturer (Promega).

Cell lysates and immunoprecipitations. HEK 293 cells were lysed in buffer containing 25 mM Tris HCl pH 7.4, 150 mM KCl, 0.5% NP-40, 2 mM EDTA, 1 mM NaF, 0.5 mM DTT and protease inhibitors (Roche) and centrifuged at 10000 g for 10 min at 4°C. For immunoprecipitations 5 ml of hybridoma supernatant from monoclonal anti-Ago1-4B8 and anti-Ago2-5D4 antibodies were coupled to approx. 80 μ l Protein-G-Sepharose (GE Healthcare). Beads were subsequently incubated with 10 ml of HEK 293 lysate (approx. 10 μ g/ μ l) for 5 h under constant rotation at 4°C. After incubation, the beads were washed three times with washing buffer (300 mM KCl, 50 mM Tris-HCl pH 7.4, 1 mM MgCl₂, 0.1 % NP-40). Finally, the beads were washed once with PBS. Co-precipitated RNA was extracted using one volume of phenol and subsequently precipitated from the aqueous phase using three volumes of Ethanol. The RNA pellet was used for oligo-dT purification and library generation.

cDNA synthesis and library generation. The cDNA library was generated by Vertis Biotechnology (Weihenstephan, Germany). Briefly, immunoprecipitated mRNAs were subjected to oligo-dT purification. The purified mRNAs were reverse transcribed using reverse transcriptase and oligo-dT as primer. The single stranded cDNA was used for second-strand synthesis using random hexamers as primers. The resulting cDNA was cloned into a TOPO vector (Invitrogen) according to the manufacturer's instructions. The plasmids were subsequently transformed into E.coli to generate cDNA libraries. In order to identify individual cDNAs from the libraries, bacteria were separated on agar plates and individual colonies were picked for plasmid DNA preparation. Plasmids were sequenced in a 96 well format by LARK (UK).

Monoclonal antibodies. For monoclonal antibody production Lou/C rats were immunized subcutaneously and intraperitoneally with a mixture of Ago1-GST or Ago2-GST fusion protein (50 μ g), 5 nmol CPG oligonucleotide (ODN 2006, TIB Molbiol, Berlin, Germany), 500 μ l PBS and 500 μ l IFA. After a six-week interval a final boost without adjuvant was given three days before fusion of the rat spleen cells with the murine myeloma cell line P3X63-Ag8.653 (ZIT). Hybridoma supernatants were tested in an ELISA using bacterially expressed Ago1 or Ago2 fusion protein or an

irrelevant GST fusion protein. mAbs reacting only with Ago1-GST or Ago2-GST fusion proteins were analyzed in western blotting and immunoprecipitation. Only Ago1-4B8 (rat IgG2a) recognized the protein specifically in western blotting. However, both Ago1-4B8 and Ago2-5D4 recognized only Ago1 or Ago2 specifically and were used in this study.

RESULTS

Isolation of Ago-bound mRNAs. Based on structural studies on archaeal Ago proteins, it is very likely that Ago proteins do not only bind to small RNAs but also directly contact the regulated target RNAs.^{35,36} We therefore hypothesized that Ago proteins may form stable Ago mRNPs that can be biochemically analyzed. We generated highly specific monoclonal antibodies against human Ago1 and Ago2. Clone Ago1-4B8 recognized specifically tagged Ago1 and a 100 kDa band in human cell extracts (data not shown). Moreover, Ago1-4B8 immunoprecipitated only tagged Ago1 but not Ago2 (Fig. 1A). Clone Ago2-5D4 did not show any signal in western blots but specifically immunoprecipitated tagged Ago2 but not Ago1

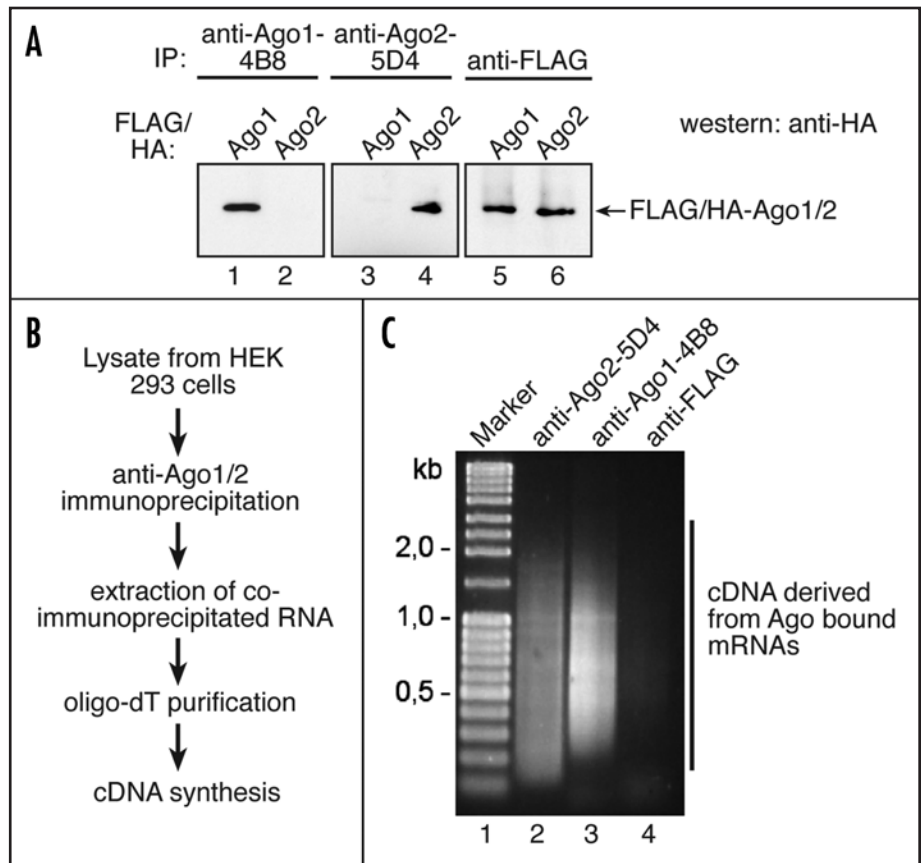


Figure 1: Biochemical isolation of mRNAs that are associated with human Ago1 or Ago2. (A) Monoclonal antibodies against Ago1 (4B8, lanes 1 and 2), against Ago2 (5D4, lanes 3 and 4) and the FLAG tag (lanes 5 and 6) were bound to Protein-G Sepharose beads and used for immunoprecipitations of FLAG/HA-tagged Ago1 (lanes 1, 3 and 5) and FLAG/HA-tagged Ago2 (lanes 2, 4 and 6). Immunoprecipitated proteins were analyzed by western blotting using anti-HA antibodies. (B) Schematic presentation of the Ago1- and Ago2-associated mRNA purification protocol. (C) Monoclonal antibodies Ago1-4B8 (lane 3), Ago2-5D4 (lane 2) or a monoclonal antibody against the FLAG-tag (lane 4) were coupled to Protein-Sepharose beads and incubated with HEK 293 lysates. Co-immunoprecipitated mRNAs were reverse transcribed and second-strand cDNA synthesis was performed using random hexamers. Lane 1 shows a DNA size marker.

Table 1 **Ago1-associated mRNAs**

mRNA			# of clones	miRanda	TargetScan	picTAR
Nuclear-encoded						
ANKRD47	ankyrin repeat domain 47	NM_198471.1	2	-	-	-
APPBP1	amyloid beta precursor protein binding protein 1	NM_003905.3	2	-	+	-
ATF4	activating transcription factor 4	NM_001675.2	3	-	-	-
ATIC	5-aminoimidazole-4-carboxamide ribonucleotide formyl transferase/ IMP cyclohydrolase	NM_004044.4	2	-	-	-
ATP5F1	ATP synthase, H ⁺ transporting, mitochondrial F0 complex, subunit B1, nuclear gene, mitochondrial protein	NM_001688.4	3	-	-	-
BTF3L4	basic transcription factor 3-like 4	NM_152265.1	2	-	+	-
C10orf84	Chromosome 10 open reading frame 84	NM_022063.1	2	-	-	-
C19orf2	Chromosome 19 open reading frame 2	NM_003796.2	2	+	+	+
C21orf51	Chromosome 21 open reading frame 51	NM_058182.2	2	-	-	-
C2orf25	Chromosome 2 open reading frame 25	NM_015702.1	3	-	+	-
C6orf48	Chromosome 6 open reading frame 48	NM_001040438.1	2	-	-	-
CALM2	calmodulin 2	NM_001743.3	2	-	+	+
CCDC28A	Coiled-coil domain cont. 28a	NM_015439.2	3	+	-	+
CCNB1IP1	Cyclin B1 interac. Protein	NM_021178.3	2	-	-	-
CDC26	cell division cycle 26 homolog	NM_139286.3	3	-	-	-
CPVL	carboxypeptidase, vitellogenic-like	NM_019029.2	2	-	-	-
CTNNA1	catenin (cadherin-associated protein)	NM_003798.1	2	-	+	+
CUL1	Cullin 1	NM_003592.2	2	+	+	+
DEX1	dexamethasone-induced transcript	NM_014015.3	2	-	+	+
DHFR	Dihydrofolate reductase	NM_000791.3	2	+	-	-
DNAJB11	Hsp40/ DNAJ	NM_016306.4	3	+	+	+
EEF1A1	eucaryotic translation elongation factor 1 alpha	NM_001402.5	4	+	+	+
EEF1G	eukaryotic translation elongation factor 1 gamma	NM_001404.4	2	+	-	-
EIF4A2	eukaryotic translation initiation factor 4A, isoform 2	NM_001967.3	2	+	+	+
Fam18B	family with sequence similarity 18, member B	NM_016078.3	2	+	-	-
FBLN1	fibulin 1 variant c	NM_001996.2	2	+	-	-
FHL1	four and a half LIM domains 1	NM_001449.3	2	+	+	-
GNAS	GNAS complex locus variant 1	NM_000516.3	2	+	+	+
GNL2	Guanine nucleotide binding protein like 2	NM_013285.1	2	-	-	-
HEBP2	heme binding protein 2	NM_014320.2	2	-	-	-
HMGB1	High mobility group box 1	NM_002128.3	6	+	+	+
HNRPA2B1	heterogenous nuclear ribonucleoprotein A2/ B1	NM_002137.2	4	+	+	+
HNRPD	heterogenous nuclear ribonucleoprotein D AU rich element RNA-binding protein 1	NM_031370.2	2	+	+	-
HNRPH1	heterogenous nuclear ribonucleoprotein H1	NM_005520.1	2	+	+	+
IARS	isoleucin-tRNA synthetase	NM_002161.3	2	-	-	-
IMPDH2	IMP (inosine monophosphate) dehydrogenase 2	NM_000884.2	2	-	-	-
KIF22	kinesin family member 22	NM_007317.1	2	-	-	-
LDLR	low density lipoprotein receptor (familial hypercholesterolemia)	NM_000527.2	2	+	+	-
LOC388181	hypothetical protein LOC388181	XR_019273.1	2	-	-	-
LTK	leukocyte tyrosine kinase	NM_002344.3	2	+	-	-
Myc	v myc myelocytomatosis viral oncogene homolog	NM_002467.3	2	+	+	+
NDUFV3	NADH dehydrogenase (ubiquinone) flavoprotein 3, nuclear protein encoding mitochondrial protein	NM_021075.3	2	-	-	-
NM23B	non metastatic cells 2 protein	NM_001018139.1	2	-	-	-
NOLA2	Nucleolar protein	NM_001034833.1	3	+	-	-
NOP5/ NOP8	nuclear protein NOP5/ NOP8	NM_015934.3	3	-	-	-
NPM1	Nucleophosmin	NM_002520.5	6	+	+	+
NRD1	nardilysin	NM_002525.1	2	-	-	-
NT5C3L	5'-nucleotidase, cytosolic III-like	NM_052935.2	2	-	-	-
PABPC1	poly A binding protein, cytoplasm	NM_002568.3	4	+	+	+
PAIBP1	Pai mRNA binding protein	NM_015640.3	2	+	-	+
POMP	proteasome maturation protein	NM_015932.2	2	+	-	-
POUF2F	POU domain TF	NM_002698.1	6	+	+	+
PSAT1	phosphoserine aminotransferase 1	NM_021154.3	3	-	-	-
PSMA4	proteasome (prosome, macropain) subunit, alpha type, 4	NM_002789.3	2	-	-	-
PTMA	prothymosin alpha(gene sequence 28)	NM_002823.2	2	-	+	-
PTP4A2	predicted protein tyrosine phosphatase type IVA	XM_001132357.1	2	+	+	+
RAB13	Ras oncogene family	NM_002870.2	2	-	-	-
RasL10B	ras like family 10 member B	NM_033315.2	2	+	+	+
RAVER2	PTB binding 2	NM_018211.2	2	+	+	-
RPL11	ribosomal protein L11	NM_000975.2	2	-	-	-
RPL15	ribosomal protein L15	NM_002948.2	3	+	+	-
RPL24	ribosomal protein L24	NM_000986.3	2	-	-	-

Table 1 continued

RPL29	ribosomal protein L29	NM_000992.2	3	-	-	-
RPL3	ribosomal protein L3	NM_00967.3	3	-	-	-
RPL41	ribosomal protein L41	NM_021104.1	4	-	-	+
RPL6	ribosomal protein L6	NM_000970.3	5	+	-	-
RPL7	ribosomal protein L7	NM_000971.3	3	+	-	-
RPL9	ribosomal protein L9	NM_000661.4	2	+	-	-
RPS11	ribosomal protein S11	NM_001015.3	2	+	-	-
RPS14	ribosomal protein S14	NM_005617.3	2	+	-	-
RPS16	ribosomal protein S16	NM_001020.4	2	+	-	-
RPS24	ribosomal protein S24	NM_033022.2	3	-	-	-
RPS27A	ribosomal protein S27A	NM_002954.3	2	-	-	-
RPS27L	ribosomal protein S27L	NM_015920.3	2	-	-	-
RPS3A	Ribosomal protein S3A	NM_001006.3	2	-	-	-
RPS6	ribosomal protein S6	NM_001010.2	6	-	-	-
RUVBL1	RuvB-like1	NM_003707.1	2	-	-	-
SCD	stearoyl-CoA desaturase	NM_005063.4	2	+	+	+
SFPQ	PTB associated	NM_005066.1	2	+	+	+
SNAPC5	Small nuclear RNA activating complex	NM_006049.2	2	+	-	-
SSB	Sjorgen syndrome antigen B	NM_003142.2	2	-	-	-
STMN1	Stathmin1/ oncoprotein 18	NM_005563.3	4	+	+	+
TCEAL4	transcription elongation factor A (SII) like 4	NM_024863.4	2	-	-	-
TCEB1	transcription elongation factor B SIII	NM_005648.2	2	-	+	-
TNFRSF12A	tumor necrosis factor receptor superfamily, member 12A	NM_016639.1	2	+	-	-
TPT1	tumor protein translationally-controlled 1	NM_003295.1	2	+	+	-
VDAC2	Voltage-dependent anion channel	NM_003375.2	3	+	+	+
WDSOF1	WD repeats and SOF1 domain containing	NM_015420.4	2	-	-	-
WIBG	within bgcn homolog	NM_032345.1	2	-	+	-
YBX-1	YB	NM_004559.3	5	+	+	+
YIPF5	YIP1 domain family	NM_030799.6	2	-	+	-
Mitochondrion-encoded						
ATP6	ATP-synthase F0 subunit 2	NC_001807.4	3	-	-	-
Cox1	cytochrome c oxidase subunit I	NC_001807.4	2	-	-	-
Cox3	cytochrome c oxidase subunit III	NC_001807.4	5	-	-	-
ND1	NADH dehydrogenase subunit2	NC_001807.4	3	-	-	-

(Fig. 1A). Therefore, we used the antibodies for affinity purification of Ago complexes (Fig. 1). Monoclonal antibodies Ago1-4B8 or Ago2-5D4 were immobilized on Protein-G-Sepharose beads and incubated with HEK 293 cell lysates. After stringent washing, the co-immunoprecipitated Ago-bound RNAs were extracted and subjected to oligo-dT purification to purify mRNAs from other Ago-associated RNA species (Fig. 1B). The isolated mRNAs were reverse transcribed, cloned and subjected to second-strand synthesis using random hexamer oligos (Fig. 1C). Interestingly, both the Ago1 and the Ago2-specific monoclonal antibodies pull-down mRNAs indicated by a RNA smear over a broad range of the agarose gel (lanes 2 and 3). A monoclonal antibody directed against the FLAG-tag was used as a control and did not immunoprecipitate visible amounts of mRNAs (lane 4), indicating that the Ago1 and Ago2 mRNA signal is specific. Taken together, we have demonstrated that Ago1 and Ago2 form stable mRNPs in human cells that can be biochemically isolated.

Cloning and identification of Ago bound mRNAs. In order to identify and further analyze the mRNA pools that were isolated from Ago1 and Ago2 mRNPs, the cDNAs described above were cloned and transformed into *E. coli* to produce Ago-associated mRNA libraries. About 600 colonies from each of the libraries were picked and the corresponding plasmids were sequenced (Table 1 and Table 2). Since it cannot be excluded that the libraries contain a limited number of mRNAs that are unspecifically bound to the beads, we removed all the single hits from the list and considered only enriched mRNAs as miRNA target candidates (all cloned mRNAs are shown in supplementary tables 1 and 2). To further analyze the list of Ago-bound mRNAs that we have obtained, we employed three target

prediction algorithms that are widely used (Miranda, targetScan, pictar). Surprisingly, only about 60% of the Ago1-bound mRNAs and about 50% of the Ago2-bound mRNAs are predicted as miRNA targets. Moreover, we also find high numbers of messages that are encoded by the mitochondrion indicating that pools of cellular mRNAs that have not been analyzed by target prediction programs so far are subject to miRNA regulation as well. In order to gain insight into Ago1 and Ago2 function, we compared the Ago1-bound mRNAs with the Ago2-bound mRNAs (supplementary table 3). We find that only a limited number of mRNA overlap between Ago1 and Ago2 suggesting that many miRNA targets might be specific to one Ago protein.

Taken together, we have demonstrated that mRNAs specifically co-purify with human Ago1 and Ago2 complexes. Interestingly, prediction algorithms have not identified many of the identified Ago-bound mRNAs. Therefore, our data suggest that larger numbers of mRNAs as previously anticipated might be under the control of the miRNA pathway.

Validation of identified mRNAs. For detailed analysis of the specificity of the Ago-bound mRNAs, we validated a number of mRNAs by different experimental approaches. We chose six mRNAs from the Ago1-bound cDNA library that are also predicted as miRNA targets by different algorithms and cloned the 3' UTRs behind a firefly luciferase reporter gene (for predictions see supplementary figure 1). Notably, all miRNAs that have been tested are also associated with Ago1 in HEK 293 cells (data not shown, submitted elsewhere). The reporter plasmids were co-transfected with 2'O-methylated antisense inhibitors against endogenous miRNAs that are predicted to bind to the respective 3'UTRs (Figure 2, left

Table 2 **Ago2-associated mRNAs**

mRNA			# of clones	miRanda	Target scan	pictar
Nuclear-encoded						
ASNS	asparagine synthetase (ASNS), transcript variant 3	NM_183356.1	4	-	-	-
CCDC72	coiled-coil domain containing 72	NM_015933.2	2	-	-	-
CNBP	CCHC-type zinc finger, nucleic acid binding protein (CNBP)	NM_003418.1	2	+	-	-
CTPS	CTP synthase	NM_001905.1	2	-	-	-
DDX48	DEAD (Asp-Glu-Ala-Asp) box polypeptide 48 (DDX48)	NM_014740.2	3	-	-	-
DPM1	dolichyl-phosphate mannosyltransferase polypeptide 1, catalytic subunit (DPM1)	NM_003859.1	2	-	-	-
EBNA1BP2	EBNA1 binding protein 2 (EBNA1BP2)	NM_006824.1	2	-	-	-
EEF1A1	eukaryotic translation elongation factor 1 alpha 1 (EEF1A1)	NM_001402.5	2	+	+	+
EEFIG	eukaryotic translation elongation factor 1 gamma	NM_001404.4	2	+	-	-
EIF1	eukaryotic translation initiation factor 1	NM_005801.3	2	+	-	-
EIF3S3	eukaryotic translation initiation factor 3, subunit 3 gamma, 40kDa	NM_003756.2	2	-	-	-
ENY2	enhancer of yellow 2 homolog (Drosophila) (ENY2)	NM_020189.4	2	-	+	+
FABP5	fatty acid binding protein 5 (psoriasis-associated) (FABP5)	NM_001444.1	2	-	-	-
GJA1	gap junction protein, alpha 1, 43kDa (connexin 43) (GJA1)	NM_000165.2	2	+	+	+
GLUL	glutamate-ammonia ligase (glutamine synthetase), transcript variant 1	NM_002065.4	2	+	-	-
GMNN	geminin, DNA replication inhibitor	BC005185.1	2	-	-	-
HADH2	hydroxyacyl-Coenzyme A dehydrogenase, type II (HADH2), nuclear gene encoding mitochondrial protein, transcript variant 1	NM_004493.2	2	-	-	-
HAX1	HCLS1 associated protein X-1 (HAX1), transcript variant 1	NM_006118.3	2	-	-	-
HMGB1	high-mobility group box 1 (HMGB1)	NM_002128.3	2	+	+	+
HNRPA2B1	heterogeneous nuclear ribonucleoprotein A2/B1 (HNRPA2B1), transcript variant B1	NM_031243.1	2	+	+	+
IARS	isoleucine-tRNA synthetase, transcript variant 1	NM_013417.2	5	-	-	-
NAP1L1	nucleosome assembly protein 1-like 1, transcript variant 1	NM_139207.1	4	+	+	-
NP	nucleoside phosphorylase (NP)	NM_000270.1	2	-	-	-
NPM1	nucleophosmin (nucleolar phosphoprotein B23, numatrin) (NPM1), transcript variant 1	NM_002520.5	2	+	+	+
OAZ1	ornithine decarboxylase antizyme 1 (OAZ1)	NM_004152.2	2	-	-	-
PABPC1	poly(A) binding protein, cytoplasmic 1	NM_002568.3	4	+	+	+
PABPN1	poly(A) binding protein, nuclear 1 (PABPN1)	NM_004643.1	3	+	+	+
PDCD10	programmed cell death 10 (PDCD10), transcript variant 2	NM_145859.1	2	+	+	+
PRDX3	peroxiredoxin 3 (PRDX3), nuclear gene encoding mitochondrial protein, transcript variant 1	NM_006793.2	2	+	-	-
PSMB6	proteasome (prosome, macropain) subunit, beta type, 6	NM_002798.1	2	-	-	-
RNF166	ring finger protein 166 (RNF166)	NM_178841.2	2	-	-	-
RPL3	ribosomal protein L3 (RPL3), transcript variant 1	NM_000967.3	2	-	-	+
RPL36A	ribosomal protein L36a (RPL36A)	NM_021029.4	2	-	-	-
RPL39	ribosomal protein L39 (RPL39)	NM_001000.2	2	-	-	-
RPL4	ribosomal protein L4	NM_000968.2	3	-	-	-
RPL41	ribosomal protein L41 (RPL41), transcript variant 1	NM_021104.1	4	-	-	+
RPL7	ribosomal protein L7 (RPL7)	NM_000971.3	3	+	-	-
RPS27A	ribosomal protein S27a (RPS27A)	NM_002954.3	3	-	-	-
RPS3A	ribosomal protein S3A (RPS3A)	NM_001006.3	5	-	-	-
RPS4x	ribosomal protein S4, X-linked (RPS4X)	NM_001007.3	2	-	-	-
SET	SET translocation (myeloid leukemia-associated) (SET)	NM_003011.1	4	+	+	-
STMN1	stathmin 1/oncoprotein 18 (STMN1), transcript variant 3	NM_005563.3	2	+	+	+
TOMM20	translocase of outer mitochondrial membrane 20 homolog	NM_014765.1	3	+	+	+
TPI1	triosephosphate isomerase 1	NM_000365.4	2	+	+	+
TPT1	tumor protein, translationally-controlled 1 (TPT1)	NM_003295.1	2	+	-	-
TUBB	tubulin, beta (TUBB)	NM_178014.2	2	+	+	+
VDAC2	voltage-dependent anion channel 2 (VDAC2)	NM_003375.2	2	+	+	+
Mitochondrion-encoded						
COX3	cytochrome c oxidase subunit III	NC_001807.4	3	-	-	-
TNRK	mitochondrionally encoded tRNA lysine	NC_001807.4	2	-	-	-

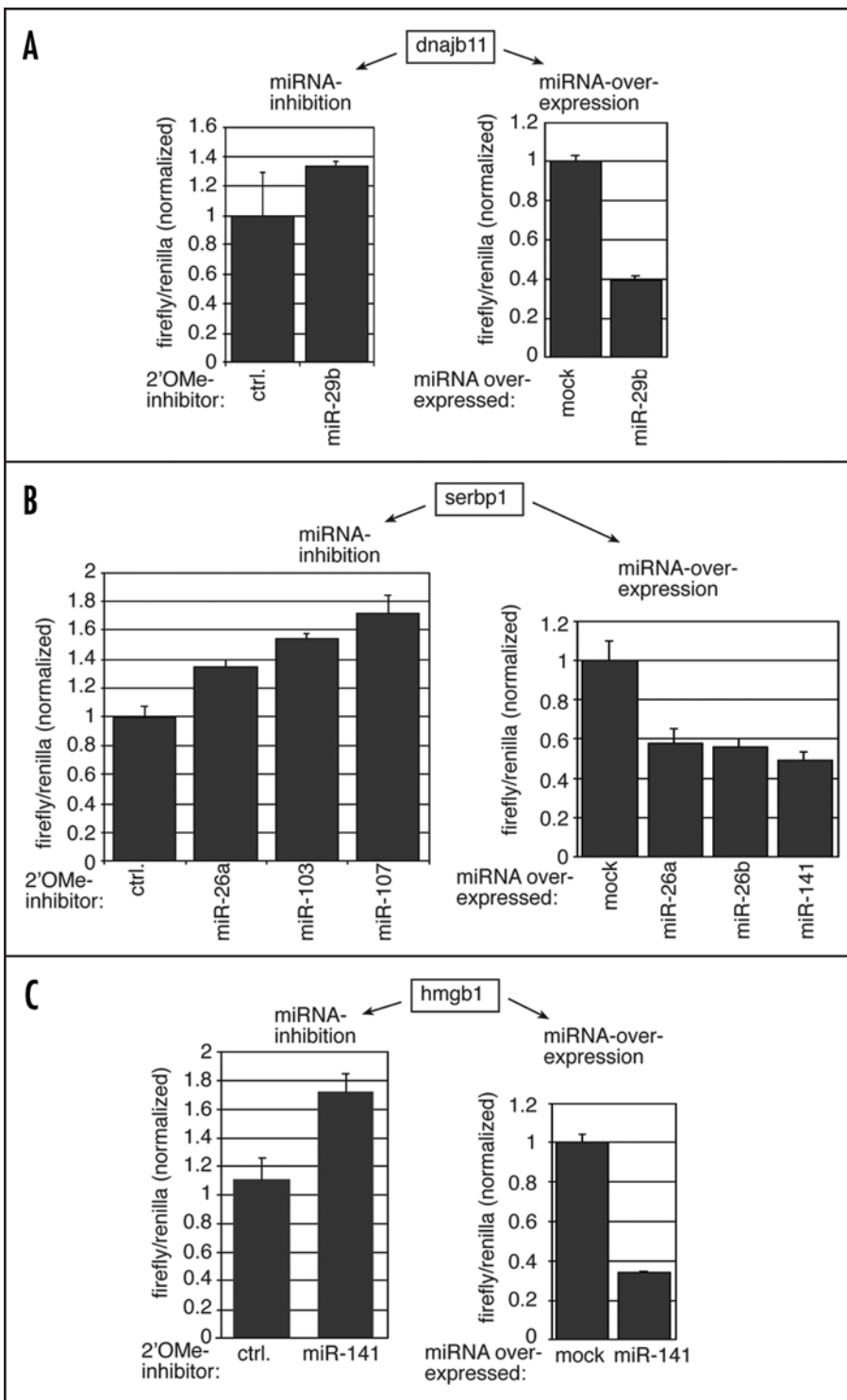


Figure 2. For legend, see page e8.

panels). Inhibitors against miRNAs that are not predicted to regulate the analyzed mRNAs served as controls. Strikingly, inhibition of miR-29b led to an enhanced luciferase activity compared to the control transfection when fused to the full length 3'UTR of *dnajb11*, an mRNA that encodes for a hsp40 variant indicating the *dnajb11* is indeed a miRNA target (Fig. 2A). Similar results were obtained when inhibitors against miRNAs that have been predicted to regulate *serbp1* (Fig. 3B), *hmgb1* (Fig. 3C), *raver2* (Fig. 3D) and *sfpq*

(Fig. 3E) were co-transfected with reporter plasmids containing the full length 3'UTRs of these mRNAs. Notably, we were not able to validate *stmn1* as miRNA target (data not shown). Therefore, our data suggest that the majority of the Ago1-bound mRNAs that have been validated are indeed under the control of endogenous miRNAs.

Inhibition of specific endogenous miRNAs resulted in enhanced expression of the above-mentioned Ago1-bound mRNAs. If these mRNAs are indeed under the control of the miRNA pathway, we hypothesized that forced over-expression of those miRNAs may lead to a decreased expression of Ago1-bound mRNAs. We cloned different miRNA hairpins into the pSUPER vector to allow for over-expression. Strikingly, when we express miR-29b the expression of a luciferase reporter containing the full-length *dnajb11* 3'UTR was reduced to about 40% indicating that *dnajb11* is indeed regulated by miR-29b (Fig. 2A, right panel). Similarly, when over-expressing miR-26a, miR-26b and miR-141 the expression of a luciferase reporter containing the full-length 3'UTR of *serbp1* was strongly reduced indicating that *serbp1* is under the control of the miRNA pathway (Fig. 2B). Similar results were obtained with *hmgb1* (Fig. 2C), *raver2* (Fig. 2D) and *sfpq* (Fig. 2E).

In summary, two independent validation approaches clearly demonstrate that all Ago1-bound mRNAs that have been tested are indeed miRNA targets suggesting a high number of miRNA targets in our libraries. We also provide a novel tool to specifically identify miRNA targets from individual human cell lines or tissues.

DISCUSSION

Ago proteins specifically recognize and bind both ends of small non-coding RNAs and are therefore considered as key factors in RNA silencing 14-16. Moreover, structural studies demonstrated that Ago proteins might not only interact with the small RNA but also with target RNAs that are regulated. Using a biochemical approach, we purified Ago-mRNPs from human cells and identified about 600 Ago1-bound and about 600 Ago2-bound mRNAs. Since it cannot be excluded that our libraries also contain mRNAs that un-specifically co-purify, we eliminated the single hits from the list to obtain all mRNAs that are enriched in the libraries. Using a luciferase-based reporter system, we have analyzed six Ago1-bound mRNAs and have validated five of them as miRNA targets. It is therefore tempting to speculate that a high percentage of our purified mRNAs are indeed miRNA targets. Notably, we have not validated Ago2-bound mRNAs yet. However, due to the specificity of the antibodies (Fig. 1A), it is likely that miRNA targets are enriched in the Ago2-associated mRNA fraction as well. Large-scale validation

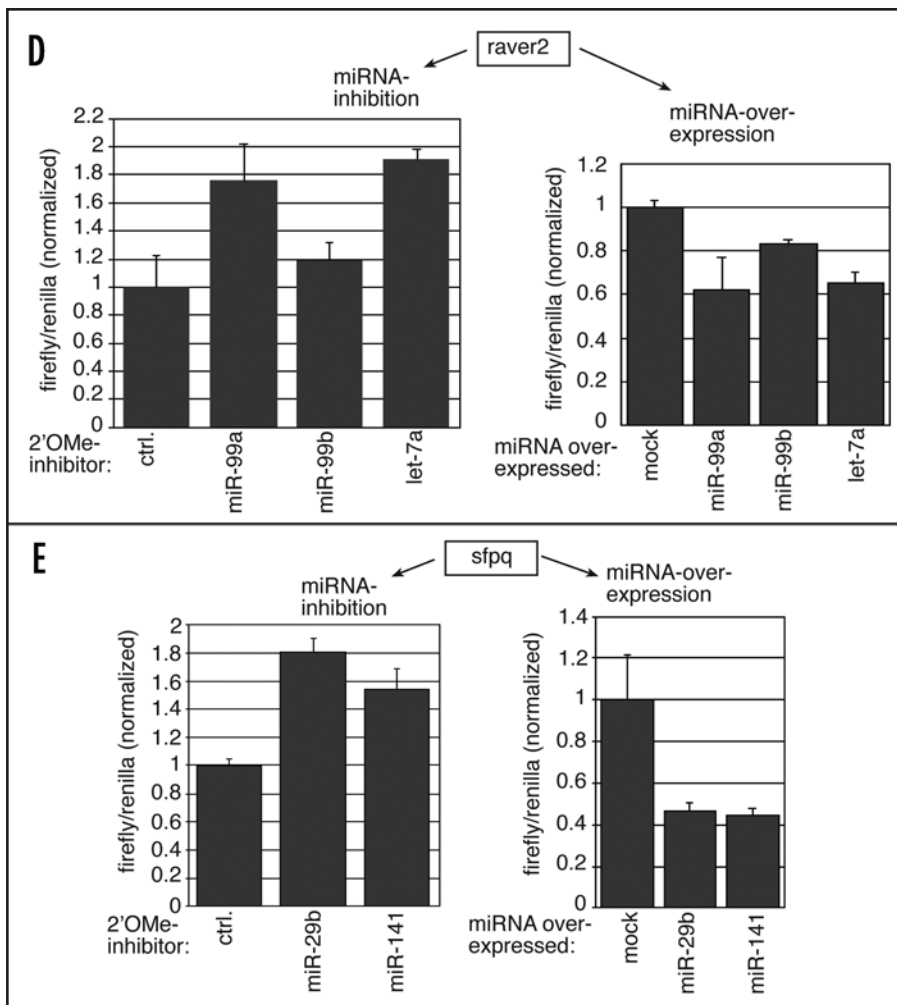


Figure 2. Validation of miRNA targets that are associated with human Ago1 mRNPs. (A) A luciferase reporter construct containing the full length 3'UTR of *dnajb11* was co-transfected either with a 2'O-methylated inhibitor antisense to miR-29b (left panel) or a plasmid over-expressing miR-29b (right panel). The empty vector served as control. Firefly luciferase expression was normalized to Renilla luciferase expression. Error bars are derived from three individual experiments. (B) Experiments were performed as in (A). The full-length 3'UTR of *serbp1* was fused to firefly luciferase. Inhibitors against miR-26a, miR-103 and miR-107 were co-transfected (left panel). MiR-26a, miR-26b and miR-141 were over-expressed (right panel). (C) Experiments were performed as in (A). The full length 3'UTR of *hmgb1* was fused to firefly luciferase. An inhibitor against miR-141 was co-transfected (left panel). MiR-141 was over-expressed (right panel). (D) Experiments were performed as in (A). The full-length 3'UTR of *raver2* was fused to firefly luciferase. Inhibitors against miR-99a, miR-99b and let-7a were co-transfected (left panel). MiR-99a, miR-99b and let-7a were over-expressed (right panel). (E) Experiments were performed as in (A). The full-length 3'UTR of *sfpq* was fused to firefly luciferase. Inhibitors against miR-29b and miR-141 were co-transfected (left panel). MiR-29b and miR-141 were overexpressed (right panel).

approaches will be needed to clearly show that the identified Ago-bound mRNAs are regulated by the miRNA pathway.

Among our purifications we find very abundant mRNA including many that encode for ribosomal proteins. Such highly abundant mRNAs very often co-precipitate un-specifically. However, several lines of evidence argue against high background in our purifications. First, we do not find visible amounts of mRNAs that co-purify with the monoclonal anti-FLAG antibody (Fig. 1B) indicating that most of the Ago1 and Ago2-associated mRNAs are specific and not just bound to the beads. Second, among the Ago1 and Ago2 mRNP purifications we find low abundant mRNAs with higher frequency than

for example messages for ribosomal proteins. Third, beside a few overlapping mRNAs in the Ago1- and Ago2-bound mRNA fractions, we find many mRNAs that are specific to one or the other Ago protein again arguing against general mRNA background in our purifications.

The limited number of overlapping mRNAs could be considered as general background. However, it is equally reasonable that those mRNAs are targeted both by Ago1 and Ago2 since it has been suggested by computer predictions that individual mRNAs might be targeted by multiple miRNAs. An exhaustive sequencing approach of Ago-bound cDNA libraries in conjunction with large-scale validation approaches will be a powerful tool to identify all mRNAs that are targeted by the miRNA pathway. Analysis of target mRNAs that are not predicted as miRNA targets yet will also help to understand how the miRNA pathway in general and individual Ago proteins in particular function in gene silencing.

Most interestingly, only about 60% of the Ago-bound mRNAs, which have been identified in this study, are predicted by the three most widely used prediction algorithms Miranda, targetScan and pictar (tables 1 and 2).³⁰⁻³² Assuming that the mRNA background in our purifications is low, our data suggest that the currently used miRNA target prediction algorithms may miss a significant number of miRNA targets. Moreover, many prediction programs do not cover all cellular RNAs including mitochondrial RNAs due to incomplete databases. It is therefore reasonable that we find mRNAs in our purifications that are not predicted as miRNA targets. However, only a comprehensive validation of the isolated mRNAs will allow for a conclusive comparison of bioinformatics and biochemical miRNA target identification approaches.

Detailed bioinformatic as well as biochemical analysis of biochemically-identified mRNAs will lead to a better understanding of how miRNPs function and how such particles are embedded into larger regulatory networks. It is reasonable that other protein factors bind to miRNA targets and either inhibit miRNA association or enhance miRNA and therefore Ago binding. Such factors might be specific to individual mRNAs that are targeted by miRNAs. The limited number of putative miRNA targets that we provide in this study is a perfect starting point to analyze consensus sequences for RNA binding proteins in the vicinity of predicted miRNA binding site.

Note

Supplemental materials can be found at:
www.landesbioscience.com/supplement/beitzingerRNA4-2-sup.pdf

References

1. Ambros V. The functions of animal microRNAs. *Nature* 2004; 431:350-5.
2. Bartel DP. MicroRNAs: genomics, biogenesis, mechanism, and function. *Cell* 2004; 116:281-97.
3. Chen PY, Meister G. microRNA-guided posttranscriptional gene regulation. *Biol Chem* 2005; 386:1205-18.
4. Borchert GM, Lanier W, Davidson BL. RNA polymerase III transcribes human microRNAs. *Nat Struct Mol Biol* 2006; 13:1097-101.
5. Lee Y, Kim M, Han J, Yeom KH, Lee S, Baek SH, Kim VN. MicroRNA genes are transcribed by RNA polymerase II. *Embo J* 2004; 23:4051-60.
6. Denli AM, Tops BB, Plasterk RH, Ketting RF, Hannon GJ. Processing of primary microRNAs by the Microprocessor complex. *Nature* 2004; 432:231-5.
7. Gregory RI, Yan KP, Amuthan G, Chendrimada T, Doratotaj B, Cooch N, Shiekhattar R. The Microprocessor complex mediates the genesis of microRNAs. *Nature* 2004; 432:235-40.
8. Landthaler M, Yalcin A, Tuschl T. The human DiGeorge syndrome critical region gene 8 and Its D. melanogaster homolog are required for miRNA biogenesis. *Curr Biol* 2004; 14:2162-7.
9. Lee Y, Ahn C, Han J, Choi H, Kim J, Yim J, Lee J, Provost P, Radmark O, Kim S, Kim VN. The nuclear RNase III Drosha initiates microRNA processing. *Nature* 2003; 425:415-9.
10. Meister G, Tuschl T. Mechanisms of gene silencing by double-stranded RNA. *Nature* 2004; 431:343-9.
11. Tomari Y, Zamore PD. Perspective: machines for RNAi. *Genes Dev* 2005; 19:517-29.
12. Pillai RS, Bhattacharyya SN, Filipowicz W. Repression of protein synthesis by miRNAs: how many mechanisms? *Trends Cell Biol* 2007; 17:118-26.
13. Peters L, Meister G. Argonaute proteins: mediators of RNA silencing. *Mol Cell* 2007; 26:611-23.
14. Hall TM. Structure and function of argonaute proteins. *Structure* 2005; 13:1403-8.
15. Patel DJ, Ma JB, Yuan YR, Ye K, Pei Y, Kuryavyi V, Malinina L, Meister G, Tuschl T. Structural biology of RNA silencing and its functional implications. *Cold Spring Harb Symp Quant Biol* 2006; 71:81-93.
16. Song JJ, Joshua-Tor L. Argonaute and RNA—getting into the groove. *Curr Opin Struct Biol* 2006; 16:5-11.
17. Liu J, Carmell MA, Rivas FV, Marsden CG, Thomson JM, Song JJ, Hammond SM, Joshua-Tor L, Hannon GJ. Argonaute2 is the catalytic engine of mammalian RNAi. *Science* 2004; 305:1437-41.
18. Meister G, Landthaler M, Patkaniowska A, Dorsett Y, Teng G, Tuschl T. Human Argonaute2 Mediates RNA Cleavage Targeted by miRNAs and siRNAs. *Mol Cell* 2004; 15:185-97.
19. Hutvagner G, Zamore PD. A microRNA in a multiple-turnover RNAi enzyme complex. *Science* 2002; 297:2056-60.
20. Olsen PH, Ambros V. The lin-4 regulatory RNA controls developmental timing in *Caenorhabditis elegans* by blocking LIN-14 protein synthesis after the initiation of translation. *Dev Biol* 1999; 216:671-80.
21. Seggerson K, Tang L, Moss EG. Two genetic circuits repress the *Caenorhabditis elegans* heterochronic gene lin-28 after translation initiation. *Dev Biol* 2002; 243:215-25.
22. Maroney PA, Yu Y, Fisher J, Nilsen TW. Evidence that microRNAs are associated with translating messenger RNAs in human cells. *Nat Struct Mol Biol* 2006; 13:1102-7.
23. Nottrott S, Simard MJ, Richter JD. Human let-7a miRNA blocks protein production on actively translating polyribosomes. *Nat Struct Mol Biol* 2006; 13:1108-14.
24. Petersen CP, Bordeleau ME, Pelletier J, Sharp PA. Short RNAs repress translation after initiation in mammalian cells. *Mol Cell* 2006; 21:533-42.
25. Humphreys DT, Westman BJ, Martin DI, Preiss T. MicroRNAs control translation initiation by inhibiting eukaryotic initiation factor 4E/cap and poly(A) tail function. *Proc Natl Acad Sci U S A* 2005; 102:16961-6.
26. Pillai RS, Bhattacharyya SN, Artus CG, Zoller T, Cougot N, Basyuk E, Bertrand E, Filipowicz W. Inhibition of translational initiation by Let-7 MicroRNA in human cells. *Science* 2005; 309:1573-6.
27. Chendrimada TP, Finn KJ, Ji X, Baillat D, Gregory RI, Liebhaber SA, Pasquinelli AE, Shiekhattar R. MicroRNA silencing through RISC recruitment of eIF6. *Nature* 2007.
28. Thermann R, Hentze MW. *Drosophila* miR2 induces pseudo-polysomes and inhibits translation initiation. *Nature* 2007.
29. Kiriakidou M, Tan GS, Lamprinak S, De Planell-Saguer M, Nelson PT, Mourelatos Z. An mRNA m(7)G Cap Binding-like Motif within Human Ago2 Represses Translation. *Cell* 2007; 129:1141-51.
30. John B, Enright AJ, Aravin A, Tuschl T, Sander C, Marks DS. Human MicroRNA targets. *PLoS Biol* 2004; 2:e363.
31. Krek A, Grun D, Poy MN, Wolf R, Rosenberg L, Epstein EJ, MacMenamin P, da Piedade I, Gunsalus KC, Stoffel M, Rajewsky N. Combinatorial microRNA target predictions. *Nat Genet* 2005; 37:495-500.
32. Lewis BP, Shih I, Jones-Rhoades MW, Bartel DP, Burge CB. Prediction of mammalian microRNA targets. *Cell* 2003; 115:787-98.
33. Stark A, Brennecke J, Russell RB, Cohen SM. Identification of *Drosophila* microRNA targets. *PLoS Biol* 2003; 1:397-409.
34. Didiano D, Hobert O. Perfect seed pairing is not a generally reliable predictor for miRNA-target interactions. *Nat Struct Mol Biol* 2006; 13:849-51.
35. Song JJ, Smith SK, Hannon GJ, Joshua-Tor L. Crystal structure of Argonaute and its implications for RISC slicer activity. *Science* 2004; 305:1434-7.
36. Yuan YR, Pei Y, Ma JB, Kuryavyi V, Zhadina M, Meister G, Chen HY, Dauter Z, Tuschl T, Patel DJ. Crystal Structure of *A. acolicus* Argonaute, a Site-Specific DNA-Guided Endoribonuclease, Provides Insights into RISC-Mediated mRNA Cleavage. *Mol Cell* 2005; 19:405-19.

Proteomic and functional analysis of Argonaute-containing mRNA–protein complexes in human cells

Julia Höck¹, Lasse Weinmann¹, Christine Ender¹, Sabine Rüdell¹, Elisabeth Kremmer², Monika Raabe³, Henning Urlaub³ & Gunter Meister^{1*}

¹Laboratory of RNA Biology, Max Planck Institute of Biochemistry, Martinsried, Germany, ²GSF—Institute of Molecular Immunology, Munich, Germany, and ³Bioanalytical Mass Spectrometry Group, Max Planck Institute of Biophysical Chemistry, Göttingen, Germany

Members of the Argonaute (Ago) protein family associate with small RNAs and have important roles in RNA silencing. Here, we analysed Ago1- and Ago2-containing protein complexes in human cells. Separation of Ago-associated messenger ribonucleoproteins (mRNPs) showed that Ago1 and Ago2 reside in three complexes with distinct Dicer and RNA-induced silencing complex activities. A comprehensive proteomic analysis of Ago-containing mRNPs identified a large number of proteins involved in RNA metabolism. By using co-immunoprecipitation experiments followed by RNase treatment, we biochemically mapped interactions within Ago mRNPs. Using reporter assays and knockdown experiments, we showed that the putative RNA-binding protein RBM4 is required for microRNA-guided gene regulation.

Keywords: Argonaute proteins; gene silencing; microRNA; RNA interference

EMBO reports (2007) 8, 1052–1060. doi:10.1038/sj.embor.7401088

INTRODUCTION

RNA silencing is a conserved gene-silencing pathway that is triggered by double-stranded RNA (dsRNA). DsRNA molecules are processed to small interfering RNAs (siRNAs) or microRNAs (miRNAs), which are then assembled into various effector complexes, including the RNA-induced silencing complex (RISC). MiRNA precursors (pre-miRNAs) are excised from primary transcripts by a nuclear complex containing the RNase III enzyme Droscha and the dsRNA-binding domain protein DGCR8/Pasha. Pre-miRNAs are subsequently exported to the cytoplasm by the export receptor exportin 5, where dsRNAs and pre-miRNAs are further

processed by the RNase III enzyme Dicer to duplexes of approximately 22 nucleotides. In a manner similar to Droscha, Dicer functions with the dsRNA-binding domain proteins TRBP (human immunodeficiency virus transactivating response RNA binding protein) and PACT (PKR activator; reviewed by Meister & Tuschl, 2004; Filipowicz *et al*, 2005; Zamore & Haley, 2005). Only one strand of the siRNA–miRNA duplex intermediate is loaded into the silencing effector complex to become the guide strand. SiRNAs and miRNAs either guide the sequence-specific degradation of complementary RNAs or inhibit the translation of partly complementary target messenger RNAs (Pillai *et al*, 2007). Recently, a third pathway of miRNA function has been identified in *Drosophila*, in which miRNAs guide the degradation of not perfectly complementary target mRNAs by recruiting de-adenylation and de-capping enzymes (Behm-Ansmant *et al*, 2006; Wu *et al*, 2006).

Members of the Argonaute (Ago) protein family are crucial components of RNA silencing effector complexes. Ago proteins contain PAZ and PIWI domains, and structural studies of archaeal Ago proteins show striking similarity between the PIWI domain and RNase H. Further functional analyses have shown that some Ago proteins contain endonucleolytic activity (Parker & Barford, 2006; Peters & Meister, 2007). Recently, another Ago domain, which binds to the m⁷G cap of mRNAs, was identified (Kiriakidou *et al*, 2007).

Biochemical purifications of Ago1 and Ago2 complexes from HeLa cell lysates identified the DEXD box protein MOV10 (Moloney leukaemia virus 10 homologue) and a protein termed TNRC6B (trinucleotide repeat containing 6B) as new components of the Ago complex (Eulalio *et al*, 2007a). Interestingly, TNRC6B is highly homologous to TNRC6A (GW182), which constitutes a marker protein for cytoplasmic processing bodies (P-bodies). P-bodies are cellular sites of RNA metabolism, and it has been shown that Ago proteins also localize to P-bodies (Eulalio *et al*, 2007a). MiRNAs and artificially bulged miRNA target mRNAs are also found in P-bodies, and it has been suggested that localization of mRNAs to P-bodies might prevent their translation (Liu *et al*, 2005; Pillai *et al*, 2005). Furthermore, a recent study showed that the P-body component RCK/p54 (DEAD box polypeptide 6) is required for miRNA-guided translational repression in human cells (Chu & Rana, 2006). Further studies showed that P-bodies are

¹Laboratory of RNA Biology, Max Planck Institute of Biochemistry, Am Klopferspitz 18, 82152 Martinsried, Germany

²GSF—Institute of Molecular Immunology, Marchioninistrasse 25, 81377 Munich, Germany

³Bioanalytical Mass Spectrometry Group, Max Planck Institute of Biophysical Chemistry, Am Fassberg 11, 37077 Göttingen, Germany

*Corresponding author. Tel: +49 89 8578 3420; Fax: +49 89 8578 3430; E-mail: meister@biochem.mpg.de

formed as a consequence of gene silencing, but their integrity is not required for gene silencing (Eulalio *et al*, 2007b).

Here, we report the biochemical identification and isolation of human Ago1 and Ago2 protein complexes. We identify three distinct Ago1 and Ago2 complexes, which we refer to as Ago complexes I–III. Using a comprehensive proteomic approach, we have identified the protein composition of the Ago complexes. Among these interactors, we found RBM4 (RNA binding motif protein 4) and show that it is required for small RNA-guided gene silencing.

RESULTS AND DISCUSSION

Human AGO1 and AGO2 associate with mRNPs

Previously, it has been shown that mammalian Ago proteins and miRNAs sediment with polyribosomes (Kim *et al*, 2004; Nelson *et al*, 2004; Maroney *et al*, 2006; Nottrott *et al*, 2006). In many studies, however, the majority of Ago proteins and miRNAs migrate together with messenger ribonucleoproteins (mRNPs; Kim *et al*, 2004; Nelson *et al*, 2004). For a detailed characterization of Ago protein complexes, we revisited Ago sedimentation in polyribosome fractionations (Fig 1A). Extracts from human embryonic kidney (HEK) 293 cells were separated on a sucrose gradient ranging from 17% to 51%. Fractions were analysed by western blotting against the ribosomal protein S6 (rpS6) to identify ribosome-containing fractions. RpS6 was detected in fractions 10–12, representing ribosomal subunits as well as monosomes, and in fractions 14–26, indicative of polyribosomes. Probing with antibodies against AGO1 showed that human AGO1 predominantly migrated in the fractions with low sucrose density. In addition, a small portion of AGO1 was found in higher molecular weight fractions that also contained polyribosomes (fractions 18–24).

To investigate AGO-containing mRNPs, we established gradient conditions that allowed further separation of the mRNP pool (Fig 1B). HEK 293 cell lysate was loaded onto a 15–55% sucrose gradient and fractionated by centrifugation for 18 h; AGO proteins were then analysed as above. Both AGO1 and AGO2 sedimented in three distinct complexes, which we refer to as AGO complexes I–III. A large portion of AGO1 or AGO2 was found in complex I, which has a molecular mass of about 250–350 kDa (lanes 2–7). Complex II constitutes a second prominent peak, which sediments similarly to a 19S particle and is about 600–700 kDa in size (lanes 10–13). Complex III peaks in fractions 15 and 16 are indicative of a molecular mass of more than 900 kDa or 25–30S (lanes 15, 16).

The co-migration of AGO proteins with mRNPs in polyribosome gradients prompted us to investigate whether Ago complexes I–III contain mRNAs and form mRNPs (Fig 1C). HEK 293 cell lysates preincubated with or without RNase A were separated as described previously. AGO1 complexes II–III were clearly visible in the untreated lysates (upper panel), but not in the RNase-treated extracts (lower panel). Together, our data show that human AGO1 and AGO2 associate with three distinct RNA–protein complexes. Furthermore, AGO complexes II and III are sensitive to RNase treatment, suggesting that these complexes form mRNPs.

AGO complex III co-sediments with the KRAS mRNA

Next, we investigated whether AGO complexes II and III contain miRNA target mRNAs. We transfected a luciferase reporter construct carrying the 3′-untranslated region (3′-UTR) of KRAS (Kirsten rat sarcoma viral oncogene homologue), which has been shown to be translationally regulated by let-7a in human cells

(Johnson *et al*, 2005). Cell lysates were separated on a 15–55% sucrose gradient. RNA was extracted from individual fractions and analysed by quantitative reverse transcription–PCR (qRT–PCR; Fig 1D). Strikingly, we detected high amounts of KRAS mRNA co-sedimenting with AGO complex III, suggesting that AGO complex III forms large mRNPs with miRNA target mRNAs.

AGO complexes I–III associate with miRNAs

A detailed molecular characterization of the AGO complexes I–III requires immunoprecipitations and functional analyses of the precipitates. As the antibodies used for western blotting proved to be too inefficient for immunoprecipitation, we recapitulated AGO protein complex associations using Flag/haemagglutinin (HA)-tagged AGO proteins (Flag/HA–AGO; Fig 2A). Flag/HA–AGO1 and Flag/HA–AGO2 were expressed in HEK 293 cells and the lysates were separated by centrifugation as described above. Individual fractions were analysed using HA antibodies. Consistently, the same distinct AGO1 and AGO2 complexes as in wild-type HEK 293 lysates were observed, indicating that Flag/HA–AGO1 and Flag/HA–AGO2 associated with native protein complexes and could therefore be used for further analyses.

As AGO proteins are the binding partners of mature miRNAs, we analysed the miRNA content of various AGO complexes. HEK 293 lysates containing Flag/HA–AGO1 or Flag/HA–AGO2 were separated as described above. Proteins were immunoprecipitated from each fraction using Flag antibodies, and the associated RNA was extracted and analysed by semiquantitative RT–PCR for miR-16 or let-7a (Fig 2B). Notably, both miR-16 and let-7a were found in all AGO-containing fractions, whereas only weak signals were found in other fractions (Fig 2B). Together, the three distinct human AGO1 and AGO2 complexes associate with mature miRNAs.

Analysis of AGO-associated RISC and Dicer activity

AGO2 is the endonucleolytic component of human RISC (Liu *et al*, 2004; Meister *et al*, 2004); therefore, we investigated which of the observed AGO2 complexes associates with RISC activity. Lysate from HEK 293 cells transfected with Flag/HA–AGO2 was fractionated and immunoprecipitated as described above. Individual immunoprecipitates were incubated with a ³²P-cap-labelled RNA complementary to endogenous miR-19b (Fig 2C). Fractions 3–6, as well as the total lysate, showed strong cleavage activity, whereas no cleavage activity was observed in higher molecular weight fractions, indicating that AGO2 complex I represents active human RISC.

It has been shown that human AGO proteins associate stably with Dicer and that this complex is able to generate small RNAs from dsRNA precursors (Gregory *et al*, 2005; Meister *et al*, 2005). Therefore, we tested individual AGO complexes for Dicer activity. HEK 293 lysates containing Flag/HA–AGO1 were fractionated and immunoprecipitated using Flag antibodies. The immunoprecipitates were incubated with an internally ³²P-labelled miR-27a precursor and the cleavage products were analysed by 15% denaturing RNA polyacrylamide gel electrophoresis (Fig 2D). AGO1 complex I (fractions 3–7) and AGO1 complex III (fractions 15–17) were associated with Dicer activity, whereas only very weak Dicer activity was observed in AGO1 complex II (fractions 10–13). Together, we have shown AGO2 complex I is a low-molecular-weight RISC, whereas AGO complexes I and III are associated with Dicer. Interestingly, AGO complex II does not contain RISC and shows little detectable Dicer activity.

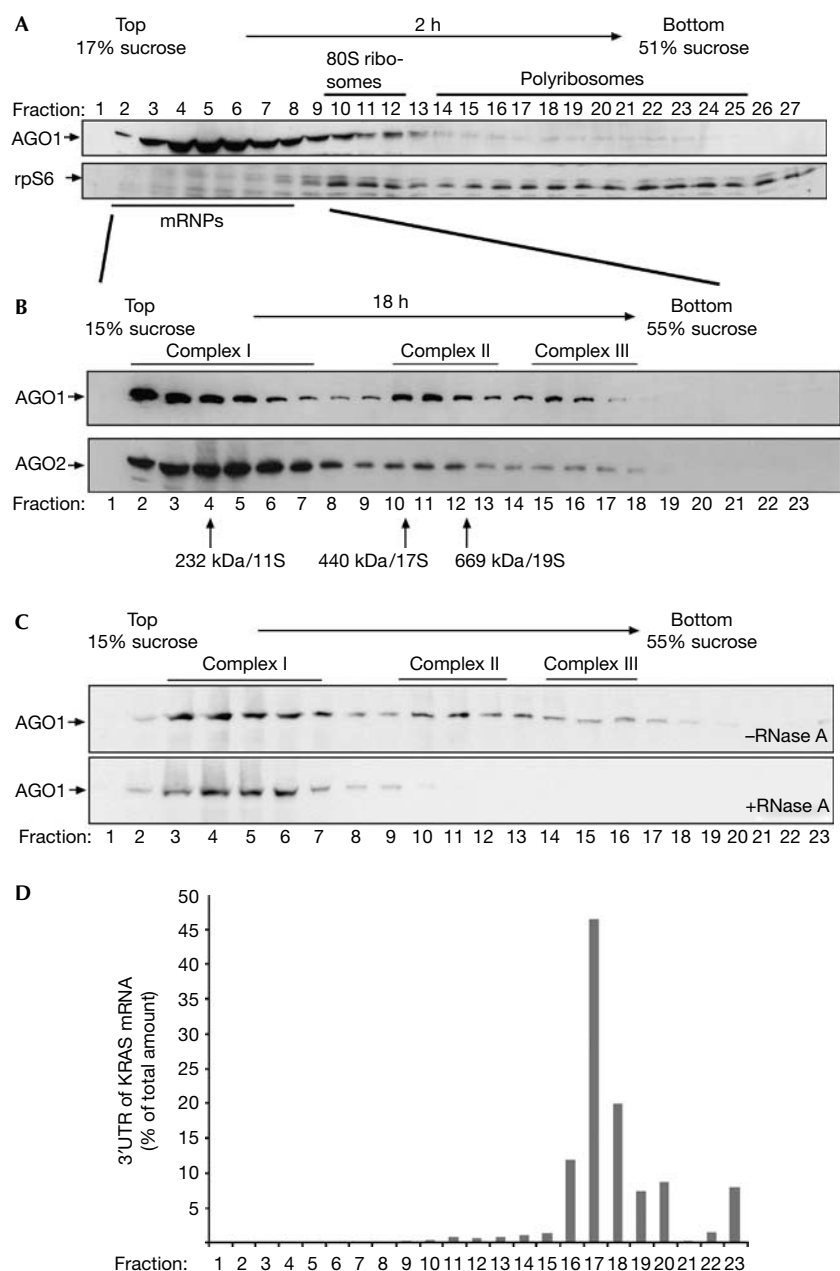


Fig 1 | Human AGO1 and AGO2 associate with distinct protein-RNA complexes. (A) Individual fractions of polyribosome gradients were analysed by western blotting against endogenous AGO1 (upper panel) or rpS6 (lower panel). (B) Lysates from wild-type HEK 293 cells were separated by sucrose density centrifugation under conditions that allow the separation of mRNPs. Endogenous AGO1 and AGO2 were analysed using specific antibodies. (C) Lysates were analysed as in (B). Lysates shown in the lower panel were treated with 100 µg/ml RNase A before centrifugation. (D) A reporter construct containing the KRAS 3'-UTR was transfected into HEK 293 cells and lysates were separated as in (B). Total RNA was extracted from the individual fractions and analysed by qRT-PCR. The distribution of the KRAS 3'-UTR is shown as a percentage of the total amount of the KRAS 3'-UTR. AGO, Argonaute; HEK, human embryonic kidney; KRAS, Kirsten rat sarcoma viral oncogene homologue; mRNPs, messenger ribonucleoproteins; qRT-PCR, quantitative reverse transcription-PCR; rpS6, ribosomal protein S6; 3'-UTR, 3'-untranslated region.

Proteomic analysis of AGO complexes I-III

We analysed the protein composition of AGO complexes I-III to identify cofactors that function together with AGO1 or AGO2. Flag/HA-AGO1 or Flag/HA-AGO2 was transiently expressed in HEK 293 cells, and the lysates were separated by gradient centrifugation.

Fractions 3-8, 10-13 and 15-18, representing AGO complexes I, II and III, respectively, were combined and AGO complexes were immunoprecipitated using Flag antibodies. The co-immunoprecipitated proteins were analysed using mass spectrometry (supplementary Fig 1 online). Antibodies that were not specific to the Flag tag

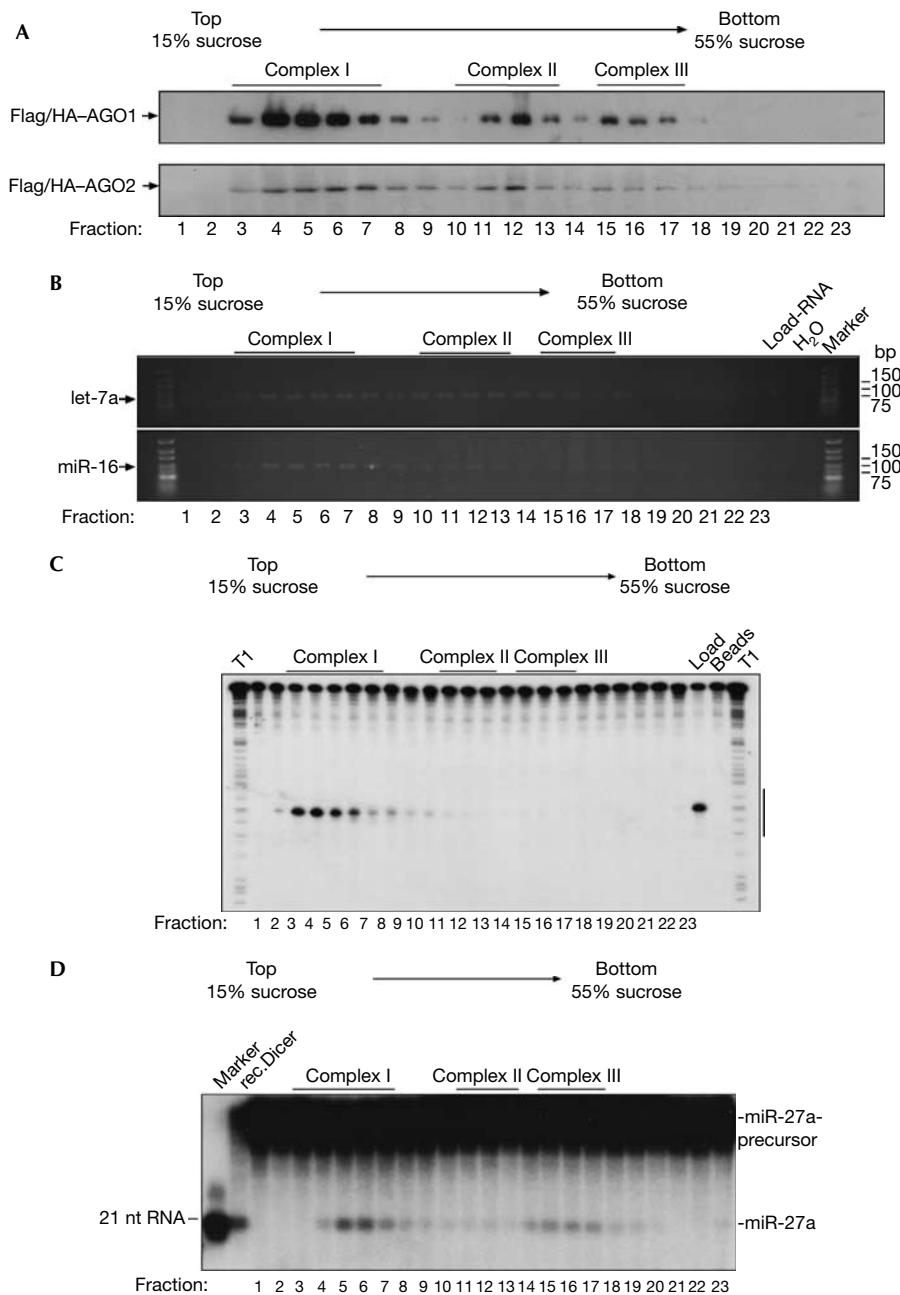


Fig 2 | Argonaute complexes associate with distinct Dicer and RISC activities. (A) HEK 293 cell extracts containing Flag/HA-AGO1 (upper panel) or Flag/HA-AGO2 (lower panel) were separated by gradient centrifugation. The presence of Flag/HA-AGO1 and Flag/HA-AGO2 was analysed by western blotting using HA antibodies. (B) Lysates from HEK 293 cells expressing Flag/HA-AGO1 or Flag/HA-AGO2 were separated as in (A). Fractions were immunoprecipitated using Flag antibodies. RNA was extracted and the presence of endogenous let-7a (upper panel) and miR-16 (lower panel) was determined using RT-PCR. (C) Lysates from Flag/HA-AGO2-transfected HEK 293 cells were separated and immunoprecipitated as described in (A). Immunoprecipitates were incubated with a ³²P-cap-labelled RNA, which contained a perfect complementary sequence to the endogenous miR-19b. Lanes indicated with T1 show RNase T1 digestions of the RNA substrates. The RNA sequence complementary to miR-19b is indicated by a black bar to the right. (D) Flag/HA-AGO1-containing HEK 293 lysate was separated and immunoprecipitated as described in (A). The immunoprecipitates or recombinant Dicer were incubated with an internally labelled pre-miR-27a substrate. A 21-nucleotide marker is shown to the left. AGO, Argonaute; HA, haemagglutinin; HEK, human embryonic kidney; qRT-PCR, quantitative reverse transcription-PCR; RISC, RNA-induced silencing complex.

were used for control purifications (supplementary Fig 2 online). After investigating only a few visible bands in our previous study (Meister *et al*, 2005), our aim was now to analyse all proteins that

were present in the AGO immunoprecipitates. Table 1 shows a list of proteins that were specifically found in AGO precipitations, but not in control purifications (see also the supplementary tables online).

Table 1 | Proteins associated with human AGO1 and AGO2

Name	Domains/motif	AGO1 complex	AGO2 complex	Accession no.
<i>Proteins involved in gene silencing</i>				
Dicer	DEAD box, RNase III, PAZ, dsRBD, DUF	I, III	I, III*	gi 21665773/gi 5019620
TNRC6B	RRM	—	I	gi 14133235
MOV10	DExH box	III	III	gi 14424568
TRBP	dsRBD	I*	I*	gi 107904
Gemin3	DEAD box		II*	gi 14209614
Gemin4	Leucine zipper	II*, III	II, III	gi 7657122
<i>DEAD/DEAH box-containing proteins</i>				
RNA helicase A (RHA)/DHX9	DEAH box, helicase domain, dsRBD, DUF1605	II, III	II, III	gi 1806048/gi 1082769
DHX30	DEAH box, helicase domain, dsRBD, DUF1605	II, III	II, III	gi 20336294
RENT1/Upf1	DEAD box, exoV	III	—	gi 1575536
DHX36	DEAH box, helicase domain, DUF1605	II*, III*	II*	gi 7959237/gi 23243423
DDX21/RNA helicase GuA	DEAD box, helicase domain, GUCT	II, III	II	gi 2135315
DDX50/RNA helicase GuB	DEAD box, helicase domain, GUCT, RESIII	III	—	gi 55664207
DDX46	DEAH box, helicase domain, DUF1605	II*	II*	gi 2696613
DDX48	DEAD box, helicase domain	II*, III	—	gi 496902
DDX18	DEAD box, helicase domain	III	—	gi 1498229
DDX5/p68	DEAD box, helicase domain	—	II*	
DDX39/BAT1	DEAD box, helicase domain	III*	II*	gi 1905998
DDX47	DEAD box, helicase domain, apolipoprotein L	III	—	gi 20149629
<i>Heterogeneous nuclear ribonucleoprotein particles</i>				
hnRNP-U	SAP, SPRY, SCOP	II, III	II, III	gi 32358
hnRNP-U-like	SAP, SPRY, SCOP	I*	—	gi 3319956
hnRNP-H2/H'	RRM, RNPf zinc finger	II*	—	gi 6065880
hnRNP-F	RRM, RNPf zinc finger	II*	I*	gi 16876910
hnRNP-C	RRM	II, III	II, III	gi 13937888/gi 14250048
hnRNP-E2	KH1, KH2	III*	—	
NSAP1	Phox-like, PX-associated motif, RRM	II, III	—	gi 5031512
hnRNP-L	Enoyl-CoA hydratase/isomerase, RRM	III*	—	gi 1152777
<i>Messenger RNA-binding proteins</i>				
Poly-A-binding proteins	RRM	II, III	II, III	gi 46367787/gi 693937
Nuclear cap-binding protein 80 kDa	MIF4G	III	—	gi 3153873
YB-1	Cold-shock domain	II	II, III	gi 181486/gi 55451
FMRp	Agenet, KH1	III*	—	gi 182673
FXR1	Agenet, KH1	—	III	gi 1730139
FXR2	Agenet, KH1	III	—	gi 4758410
ZBP-1	RRM, KH1	II, III	III	gi 7141072/gi 56237027
ZBP-3	RRM, KH1	III	—	gi 30795212
HuR	RRM	III*	—	gi 1022961
RBM4	RRM, zinc finger	—	III*	gi 4506445

Table 1 | Continued

Name	Domains/motif	AGO1 complex	AGO2 complex	Accession no.
<i>Proteins involved in RNA metabolism</i>				
NF90/ILF3/NFAR-1	dsRBD, DZF	II, III	II	gi 1082856/gi 5006602
NF45/ILF2	DZF	II, III	II, III	gi 532313
SART3	Lsm interaction motif, RRM	I, II, III	—	gi 7661952
RBM10	D111/G-patch, RRM, zinc finger, Ran binding	—	I*, II*	gi 12644371
Fibrillarin	Fibrillarin motif	—	II*, III*	gi 182592
NOP56	Pre-mRNA processing RNP, NOP5NT, NOSIC	III	—	gi 2230878
Nucleolin	RRM	III	—	gi 128841
eIF2b δ	Initiation factor 2B	I*	—	gi 6563202
eIF4b	RRM	—	I*	gi 288100
FLJ20758	Pentatricopeptide repeat	II	II	gi 38683855
<i>Other proteins</i>				
Myb-binding protein 1a	DNA polymerase V	III	III*	gi 7657351
Matrin 3	RRM, zinc finger	III*	III*	gi 6563246
Motor protein	—	II, III	—	gi 516764
ZNF326	AKAP95	II, III	—	gi 31807861/gi 47125447
Ku70	Ku70/80 motif, DNA-binding SAP	—	II*	gi 57165052
DDB1	CPSF A subunit	I	I*	gi 418316
RuvB-like II	AAA ATPase, Tip49b	I	I, II	gi 5730023/gi 12653319
Coatomer protein	WD-40, COPB2	III	II	gi 1002369

*Identified by a single peptide.

As expected from the Dicer activity assays, we found Dicer only in AGO1/2 complexes I and III, whereas TRBP was identified only in AGO complex I. TNRC6B, MOV10, RHA (DEAH box polypeptide 9), Gemin3 and Gemin4, which have been found in AGO complexes previously (Mourelatos *et al*, 2002; Meister *et al*, 2005; Robb & Rana, 2007), were also among the identified proteins. Proteins that have not yet been implicated in RNA silencing in mammals were grouped according to their domains and function (Table 1). Among the DEAD/DEAH box helicases, we found DDX5, an orthologue of *Drosophila* p68, which has been shown to associate with *Drosophila* Ago2 (Meister & Tuschl, 2004), and DDX18, a putative helicase that has been implicated in Drosha function (Gregory *et al*, 2004). Consistent with the hypothesis that AGO complexes II and III are mRNPs, we found various isoforms of poly-A-binding proteins, indicating that mRNAs were present in the purifications. Strikingly, we found many mRNA-binding proteins that are involved in translational regulation, including FMRp and its homologues FXR1 and FXR2. It was reported previously that FMRp associates with Ago proteins as well as miRNAs in both human and *Drosophila* cells (Meister & Tuschl, 2004). Further identified proteins with regulatory functions in translation are NSAP1/SYNCRIP, YB-1, HuR, RBM4, ZBP1 and ZBP3. We also found various ribosomal proteins in the Ago complexes (supplementary tables online), suggesting that ribosomal proteins might have other functions as components of mRNPs.

Next, using western blotting, we examined whether the identified factors specifically co-sediment with AGO-containing fractions in sucrose gradients (Fig 3A). Consistent with the proteomic data, hnRNP-U, NF-90, ZBP1 and ZBP3 co-migrated with both AGO complexes II and III, whereas TRBP was found in low-molecular-weight fractions co-migrating with AGO complex I; however, NF-45 and YB-1 were detected in fractions containing AGO complex III. For a more comprehensive analysis, we expressed Flag/HA-tagged DDX47, DDX36, DDX30, RHA (DHX9), hnRNP-C, HuR as well as SART3 and investigated co-sedimentation with AGO proteins. All tagged proteins migrated in fractions also containing AGO complexes II and III. Notably, we found a larger portion of the tagged proteins migrating at the top of the gradient, presumably owing to overexpression.

To validate a specific association with AGO complexes, we carried out co-immunoprecipitations (Fig 3B) and Flag/HA-AGO1 or Flag/HA-AGO2 was immunoprecipitated from HEK 293 lysates using Flag antibodies. RNase A-treated and untreated samples (supplementary Fig 3 online) were analysed using western blotting. hnRNP-C1/C2, ZBP1, ZBP3 and YB-1 disappeared from the Flag/HA-AGO1/2 immunoprecipitates when RNase A was added, indicating that the tested proteins were not associated with AGO proteins through protein-protein interactions, but bound to the same RNAs. NF-90, SART3, DDX5 and DDB-1 immunoprecipitated with Flag/HA-AGO1/2 in the presence of RNase A,

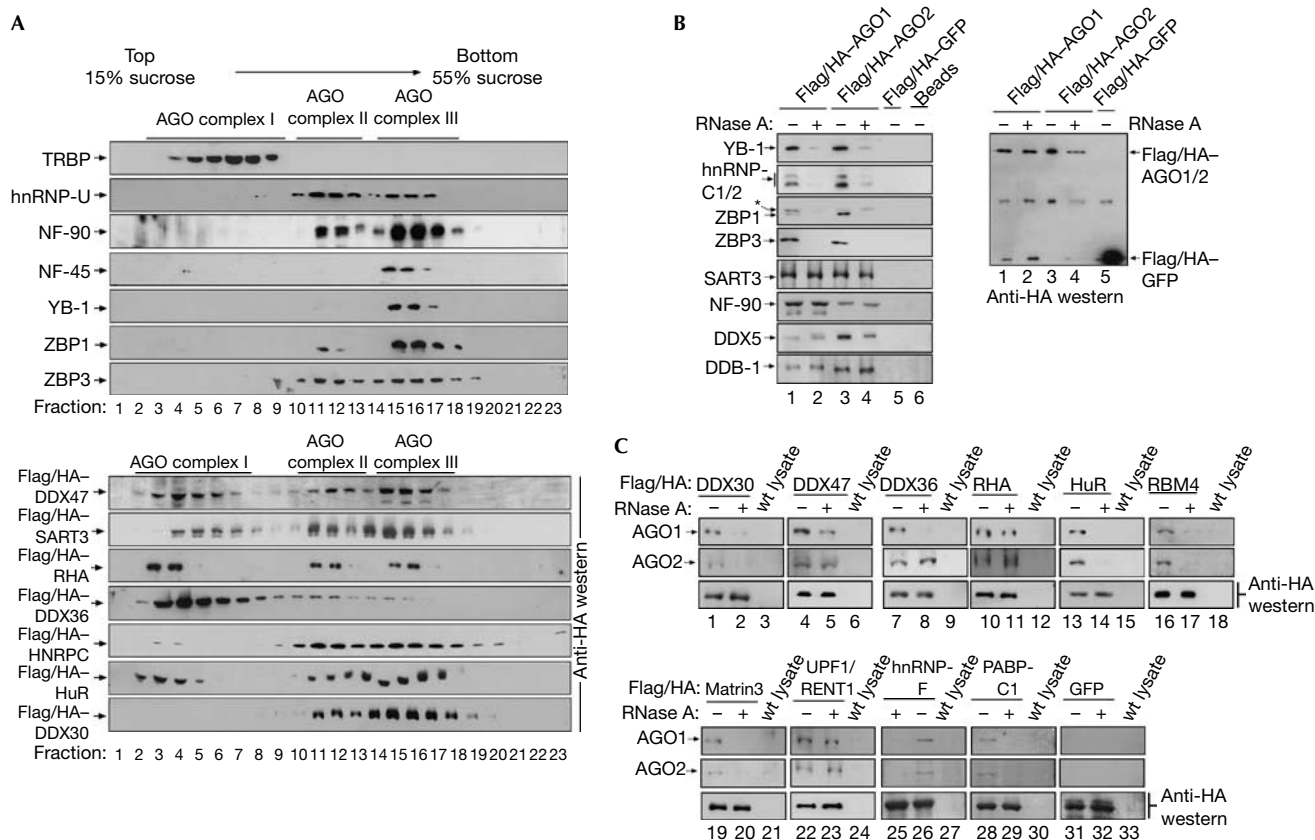


Fig 3 | Proteins identified by mass spectrometry interact with Argonaute complexes. (A) HEK 293 cell extracts were separated by gradient centrifugation and fractions were analysed by western blotting against the proteins indicated to the left (upper panels). HEK 293 cells were transiently transfected with Flag/HA-tagged expression constructs as indicated to the left and analysed by western blotting using HA antibodies. (B) HEK 293 cells were transfected as indicated. AGO complexes were immunoprecipitated using Flag antibodies and probed using specific antibodies with (lanes 2 and 4) or without (lanes 1 and 3) RNase A treatment (left panel). The asterisk denotes unspecific interactions of the ZBP1 antibody. A western blot using HA antibodies is shown to the right. (C) HEK 293 cells expressing Flag/HA-tagged proteins were treated as indicated. Immunoprecipitations and RNase treatment were carried out as in (A). Wild-type HEK 293 lysate was used as a control. Interactions were analysed by western blotting against AGO1 (upper panels), AGO2 (middle panels) or HA (control; lower panels). AGO, Argonaute; GFP, green fluorescent protein; HA, haemagglutinin; HEK, human embryonic kidney; hnRNP, heterogeneous nuclear ribonucleoprotein particles; TRBP, human immunodeficiency virus transactivating response RNA binding protein.

which is indicative of protein–protein interactions. To analyse a specific AGO association of mRNP components for which no specific antibodies were available, we expressed Flag/HA-tagged fusions (Fig 3C). The tagged proteins were immunoprecipitated using Flag antibodies and the precipitates were analysed by western blotting using HA (lanes 1–33, lower panel), AGO1 (upper panel) or AGO2 (middle panel) antibodies. Endogenous AGO1 and AGO2 clearly co-precipitated with all Flag/HA-tagged proteins (lanes 1–33). The binding of DDX30, HuR, RBM4, hnRNP-F, PABP-C1 and Matrin3 to AGO1 and AGO2 complexes was sensitive to RNase A treatment, whereas the binding of DDX36, DDX47, RHA and UPF1/RENT1 was not, suggesting protein–protein interactions.

RBM4 is required for miRNA-guided gene silencing

To investigate the relevance of identified AGO mRNP components for miRNA function, we generated a luciferase construct containing a

perfectly complementary miR-21 target site in the 3'-UTR (Fig 4A). As expected, knockdown of AGO1, AGO3 and AGO4 had no effect, whereas siRNAs against AGO2 or TNRC6B led to a significant increase of luciferase expression. No effect was observed with a mutated miR-21-binding site (supplementary Fig 4 online). Strikingly, knockdown of RBM4 resulted in a strong increase of luciferase activity, indicating that RBM4 modulates miR-21-guided RNA cleavage. Notably, the interaction of RBM4 and AGO2 is reduced when RNase A is added (Fig 3C). It is reasonable to assume that miRNA degradation by RNase A affects AGO2 interactions. Alternatively, RBM4 could also enhance the binding of AGO proteins to mRNAs by increasing the accessibility of miRNA target sites.

Next, we analysed whether RBM4 is also required for the regulation of natural miRNA targets (Fig 4B). A luciferase construct containing the KRAS 3'-UTR was transfected into HEK 293 cells in which let-7a was inhibited or TNRC6B, YB-1, RBM4, ZBP3 or FMRp was depleted by RNA interference. Knockdown of

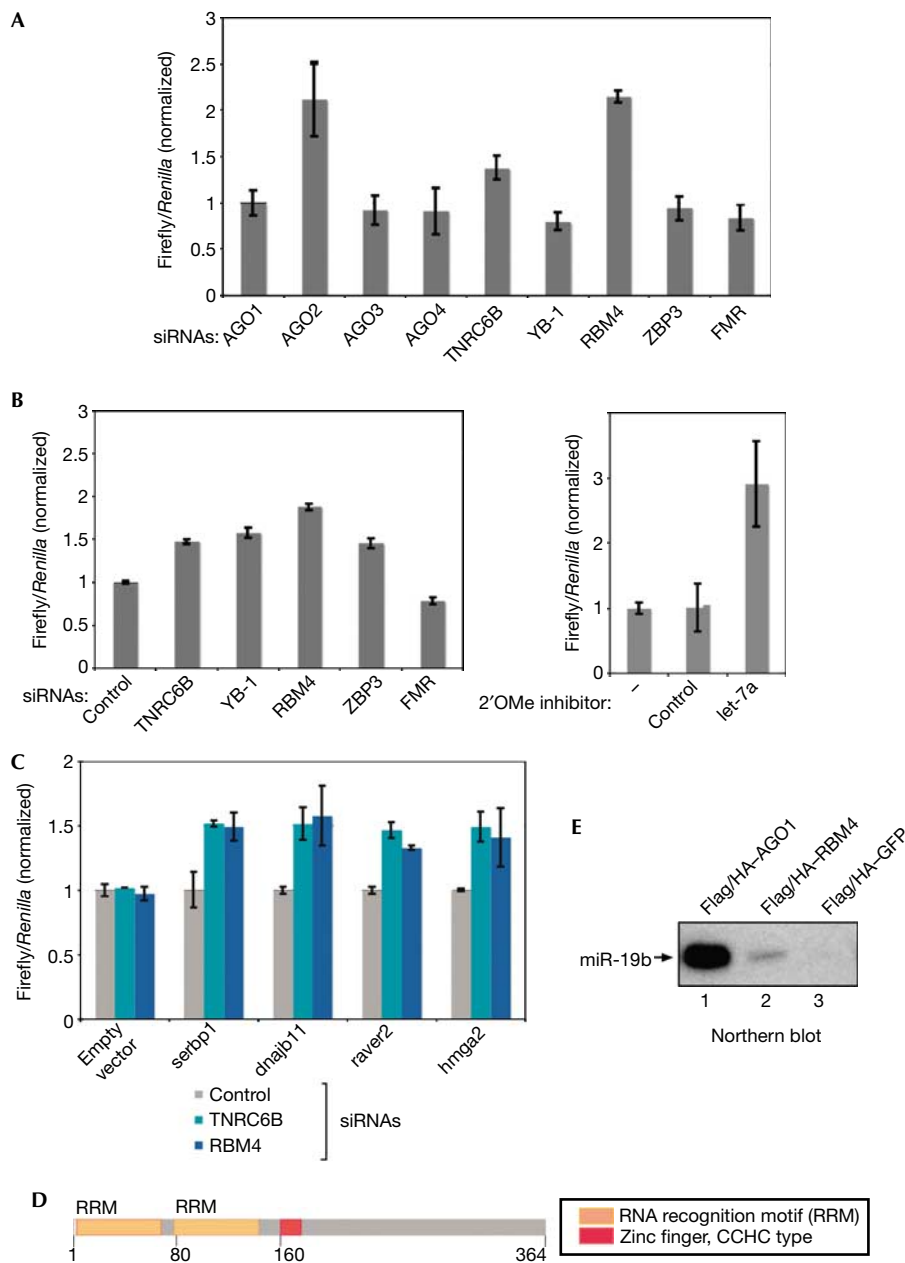


Fig 4 | RNA binding motif protein 4 is required for microRNA-guided gene silencing. (A) SiRNAs against the indicated proteins were pre-transfected into HeLa cells. After 2 days, a luciferase reporter containing a complementary binding site for miR-21 was transfected. (B) Experiments were carried out as described in (A). A luciferase reporter construct containing the 3'-UTR of KRAS was used (left panel). 2'OMe inhibitors of the indicated miRNAs were pre-transfected into HeLa cells (right panel). (C) Experiments were carried out as in (A). Luciferase reporter constructs carrying the 3'-UTRs of the indicated mRNAs were transfected and normalized to control siRNA. (D) Schematic illustration of RBM4. (E) Lysates from HEK 293 cells transfected with the indicated constructs were immunoprecipitated using Flag antibodies, and northern blotting against miR-19b was performed. GFP, green fluorescent protein; HEK, human embryonic kidney; KRAS, Kirsten rat sarcoma viral oncogene homologue; miRNA, microRNA; RBM4, RNA binding motif protein 4; siRNAs, small interfering RNAs; TNRC6B, trinucleotide repeat containing 6B; UTR, untranslated region.

TNRC6B, RBM4, YB-1 and ZBP3 resulted in stronger luciferase activity. Overexpression of RBM4 but not ZBP3 led to decreased luciferase activity (supplementary Fig 6 online), suggesting that RBM4 functions on the 3'-UTR of KRAS.

Recently, hmga2, serbp, dnajb11 and raver2 have been identified and validated as miRNA targets (Beitzinger *et al*, 2007; May

et al, 2007). Therefore, we transfected luciferase reporter constructs containing the respective 3'-UTRs and measured luciferase activity in an RBM4- or TNRC6B-knockdown background (Fig 4C). Indeed, luciferase activity was significantly increased in the RBM4- or TNRC6B-knockdown cells, indicating that RBM4 functions on different miRNA targets. As RBM4 contains two RNA

recognition motifs (Fig 4D), we investigated whether RBM4 co-immunoprecipitates with miRNAs (Fig 4E). Flag/HA-RBM4 was immunoprecipitated using Flag antibodies and the associated RNA was extracted. Strikingly, miR-19b was detected in the Flag/HA-RBM4 precipitate, whereas no miR-19b was precipitated in a control reaction.

Our data indicate that RBM4 co-immunoprecipitates with miRNAs and functions in AGO-mediated gene silencing; therefore, we have identified a new component of human gene silencing.

METHODS

Cell extracts and gradient centrifugation. Polyribosome fractionation from HEK 293 cells was carried out according to Pillai *et al* (2005). For complex purification and co-immunoprecipitations, HEK 293 cells were lysed in buffer containing 25 mM Tris-HCl (pH 7.4), 150 mM KCl, 0.5% NP-40, 2 mM EDTA, 1 mM NaF, 0.5 mM dithiothreitol and protease inhibitors (Roche, Penzberg, Germany) and centrifuged at 10,000g for 10 min at 4 °C. For fractionations, gradients from 15% (w/v) to 55% (w/v) sucrose in 150 mM KCl, 25 mM Tris (pH 7.4) and 2 mM EDTA were used. Lysates were separated by centrifugation at 30,000 r.p.m. for 18 h in an SW41 rotor at 4 °C. To determine indicated *S* values, catalase (11S), apoferritin (17S) and thyroglobin (19S) were used. For the analysis of RNA-dependent interactions, extracts were preincubated with 100 µg/ml RNase A (Qiagen, Hilden, Germany) at 4 °C for 1 h.

Immunoprecipitation of Flag/HA-tagged AGO complexes. AGO-containing gradient fractions were pooled and incubated with 100 µl Flag M2 agarose beads (Sigma, Taufkirchen, Germany) for 2 h at 4 °C. Beads were subsequently washed with immunoprecipitation buffer (300 mM NaCl, 5 mM MgCl₂, 0.1% NP-40 and 50 mM Tris-HCl, pH 7.5) and phosphate-buffered saline (PBS).

Co-immunoprecipitation experiments. Lysates were incubated with 30 µl Flag M2 agarose at 4 °C for 1.5 h, and washed with IP buffer and PBS. Beads were distributed equally into two tubes and 1.5 ml PBS or PBS containing 100 µg/ml RNase A was added. After incubation at 4 °C for 1.5 h, beads were washed with PBS and denatured by adding 25 µl of protein sample buffer.

Supplementary information is available at *EMBO reports* online (<http://www.emboreports.org>).

ACKNOWLEDGEMENTS

We thank S. Behrens for NF-45/NF-90-specific antibodies, S. Hüttelmaier for ZBP1/3-specific antibodies and S. Jentsch for support. Our research was supported by the Max-Planck-Society, Deutsche Forschungsgemeinschaft (DFG) grant ME 2064/2-1 and European Union grant LSHG-CT-2005-037900. L.W. receives a fellowship of the Boehringer Ingelheim Funds.

REFERENCES

Behm-Ansmant I, Rehwinkel J, Doerks T, Stark A, Bork P, Izaurralde E (2006) mRNA degradation by miRNAs and GW182 requires both CCR4:NOT deadenylase and DCP1:DCP2 decapping complexes. *Genes Dev* **20**: 1885–1898

Beitzinger M, Peters L, Zhu JY, Kremmer E, Meister G (2007) Identification of human microRNA targets from isolated Argonaute protein complexes. *RNA Biol* **4**: e1–e9

Chu CY, Rana TM (2006) Translation repression in human cells by microRNA-induced gene silencing requires RCK/p54. *PLoS Biol* **4**: e210

Eulalio A, Behm-Ansmant I, Izaurralde E (2007a) P bodies: at the crossroads of post-transcriptional pathways. *Nat Rev Mol Cell Biol* **8**: 9–22

Eulalio A, Behm-Ansmant I, Schweitzer D, Izaurralde E (2007b) P-body formation is a consequence, not the cause, of RNA-mediated gene silencing. *Mol Cell Biol* **27**: 3970–3981

Filipowicz W, Jaskiewicz L, Kolb FA, Pillai RS (2005) Post-transcriptional gene silencing by siRNAs and miRNAs. *Curr Opin Struct Biol* **15**: 331–341

Gregory RI, Yan KP, Amuthan G, Chendrimada T, Doratotaj B, Cooch N, Shiekhattar R (2004) The Microprocessor complex mediates the genesis of microRNAs. *Nature* **432**: 235–240

Gregory RI, Chendrimada TP, Cooch N, Shiekhattar R (2005) Human RISC couples microRNA biogenesis and posttranscriptional gene silencing. *Cell* **123**: 631–640

Johnson SM, Grosshans H, Shingara J, Byrom M, Jarvis R, Cheng A, Labourier E, Reinert KL, Brown D, Slack FJ (2005) RAS is regulated by the let-7 microRNA family. *Cell* **120**: 635–647

Kim J, Krichevsky A, Grad Y, Hayes GD, Kosik KS, Church GM, Ruvkun G (2004) Identification of many microRNAs that copurify with polyribosomes in mammalian neurons. *Proc Natl Acad Sci USA* **101**: 360–365

Kiriakidou M, Tan GS, Lamprinak S, De Planell-Saguer M, Nelson PT, Mourelatos Z (2007) An mRNA m(7)G cap binding-like motif within human ago2 represses translation. *Cell* **129**: 1141–1151

Liu J, Carmell MA, Rivas FV, Marsden CG, Thomson JM, Song JJ, Hammond SM, Joshua-Tor L, Hannon GJ (2004) Argonaute2 is the catalytic engine of mammalian RNAi. *Science* **305**: 1437–1441

Liu J, Valencia-Sanchez MA, Hannon GJ, Parker R (2005) MicroRNA-dependent localization of targeted mRNAs to mammalian P-bodies. *Nat Cell Biol* **7**: 719–723

Maroney PA, Yu Y, Fisher J, Nilsen TW (2006) Evidence that microRNAs are associated with translating messenger RNAs in human cells. *Nat Struct Mol Biol* **13**: 1102–1107

Mayr C, Hemann MT, Bartel DP (2007) Disrupting the pairing between let-7 and Hmga2 enhances oncogenic transformation. *Science* **315**: 1576–1579

Meister G, Tuschl T (2004) Mechanisms of gene silencing by double-stranded RNA. *Nature* **431**: 343–349

Meister G, Landthaler M, Patkaniowska A, Dorsett Y, Teng G, Tuschl T (2004) Human argonaute2 mediates RNA cleavage targeted by miRNAs and siRNAs. *Mol Cell* **15**: 185–197

Meister G, Landthaler M, Peters L, Chen PY, Urlaub H, Luhrmann R, Tuschl T (2005) Identification of novel argonaute-associated proteins. *Curr Biol* **15**: 2149–2155

Mourelatos Z, Dostie J, Paushkin S, Sharma A, Charroux B, Abel L, Rappsilber J, Mann M, Dreyfuss G (2002) miRNPs: a novel class of ribonucleoproteins containing numerous microRNAs. *Genes Dev* **16**: 720–728

Nelson PT, Hatzigeorgiou AG, Mourelatos Z (2004) miRNP:mRNA association in polyribosomes in a human neuronal cell line. *RNA* **10**: 387–394

Nottrott S, Simard MJ, Richter JD (2006) Human let-7a miRNA blocks protein production on actively translating polyribosomes. *Nat Struct Mol Biol* **13**: 1108–1114

Parker JS, Barford D (2006) Argonaute: a scaffold for the function of short regulatory RNAs. *Trends Biochem Sci* **31**: 622–630

Peters L, Meister G (2007) Argonaute proteins: mediators of RNA silencing. *Mol Cell* **26**: 611–623

Pillai RS, Bhattacharyya SN, Artus CG, Zoller T, Cougot N, Basyuk E, Bertrand E, Filipowicz W (2005) Inhibition of translational initiation by let-7 MicroRNA in human cells. *Science* **309**: 1573–1576

Pillai RS, Bhattacharyya SN, Filipowicz W (2007) Repression of protein synthesis by miRNAs: how many mechanisms? *Trends Cell Biol* **17**: 118–126

Robb GB, Rana TM (2007) RNA helicase a interacts with RISC in human cells and functions in RISC loading. *Mol Cell* **26**: 523–537

Wu L, Fan J, Belasco JG (2006) MicroRNAs direct rapid deadenylation of mRNA. *Proc Natl Acad Sci USA* **103**: 4034–4039

Zamore PD, Haley B (2005) Ribo-gnome: the big world of small RNAs. *Science* **309**: 1519–1524



RNA

A PUBLICATION OF THE RNA SOCIETY

Strand-specific 5'-O-methylation of siRNA duplexes controls guide strand selection and targeting specificity

Po Yu Chen, Lasse Weinmann, Dimos Gaidatzis, et al.

RNA 2008 14: 263-274

Access the most recent version at doi:[10.1261/rna.789808](https://doi.org/10.1261/rna.789808)

References

This article cites 82 articles, 28 of which can be accessed free at:
<http://rnajournal.cshlp.org/content/14/2/263.full.html#ref-list-1>

Email alerting service

Receive free email alerts when new articles cite this article - sign up in the box at the top right corner of the article or [click here](#)

To subscribe to *RNA* go to:
<http://rnajournal.cshlp.org/subscriptions>

Strand-specific 5'-O-methylation of siRNA duplexes controls guide strand selection and targeting specificity

PO YU CHEN,^{1,2,4} LASSE WEINMANN,^{2,4} DIMOS GAIDATZIS,³ YI PEI,^{1,5} MIHAELA ZAVOLAN,³ THOMAS TUSCHL,¹ and GUNTER MEISTER²

¹Laboratory of RNA Molecular Biology, Howard Hughes Medical Institute, The Rockefeller University, New York, New York, 10021, USA

²Munich Center for Integrated Protein Science (CIPSM), Max Planck Institute of Biochemistry, D-82152 Martinsried, Germany

³Bioinformatics, Biozentrum der Universität Basel and Swiss Institute of Bioinformatics, CH-4056 Basel, Switzerland

ABSTRACT

Small interfering RNAs (siRNAs) and microRNAs (miRNAs) guide catalytic sequence-specific cleavage of fully or nearly fully complementary target mRNAs or control translation and/or stability of many mRNAs that share 6–8 nucleotides (nt) of complementarity to the siRNA and miRNA 5' end. siRNA- and miRNA-containing ribonucleoprotein silencing complexes are assembled from double-stranded 21- to 23-nt RNase III processing intermediates that carry 5' phosphates and 2-nt overhangs with free 3' hydroxyl groups. Despite the structural symmetry of a duplex siRNA, the nucleotide sequence asymmetry can generate a bias for preferred loading of one of the two duplex-forming strands into the RNA-induced silencing complex (RISC). Here we show that the 5'-phosphorylation status of the siRNA strands also acts as an important determinant for strand selection. 5'-O-methylated siRNA duplexes refractory to 5' phosphorylation were examined for their biases in siRNA strand selection. Asymmetric, single methylation of siRNA duplexes reduced the occupancy of the silencing complex by the methylated strand with concomitant elimination of its off-targeting signature and enhanced off-targeting signature of the phosphorylated strand. Methylation of both siRNA strands reduced but did not completely abolish RNA silencing, without affecting strand selection relative to that of the unmodified siRNA. We conclude that asymmetric 5' modification of siRNA duplexes can be useful for controlling targeting specificity.

Keywords: RNA interference; RNAi; off-target effects; gene silencing; siRNA; RISC

INTRODUCTION

Duplexes of 21-nucleotide (nt) small interfering RNAs trigger RNA interference (RNAi) in mammalian cells and are widely used for functional genetic studies or screens in cultured cells (for reviews, see Dorsett and Tuschl 2004; Echeverri and Perrimon 2006; Fuchs and Boutos 2006; Root et al. 2006; Krausz 2007). siRNA duplexes are designed to mimic the RNase III processing intermediates of naturally expressed dsRNAs, such as miRNAs, to

effectively enter the RNAi pathway (for reviews, see Bartel 2004; Meister and Tuschl 2004; Filipowicz et al. 2005; Tomari and Zamore 2005). Naturally processed siRNAs or miRNAs carry 5' phosphates and 3'-hydroxyl groups and have symmetric 2-nt 3' overhangs (Elbashir et al. 2001; Lau et al. 2001). Synthetic siRNA duplexes with 5'-hydroxyl ends are rapidly phosphorylated inside cells by the cellular kinase Clp1 (Weitzer and Martinez 2007). Some classes of small RNAs are additionally 2'-O-methylated at their 3' ends, depending on the species (Ebhardt et al. 2005; Yu et al. 2005; Vagin et al. 2006; Horwich et al. 2007; Kirino and Mourelatos 2007; Ohara et al. 2007; Pelisson et al. 2007; Saito et al. 2007). Mammalian miRNAs or siRNAs are not methylated, but the germline-specifically expressed piRNAs are 3'-end modified (Kirino and Mourelatos 2007; Ohara et al. 2007).

One strand of the siRNA duplex or miRNA/miRNA* molecule is assembled into an effector complex or RISC, while the other strand is degraded during the assembly process (Hutvagner and Zamore 2002; Martinez et al.

⁴These authors contributed equally to this work.

⁵Present address: RNA Therapeutics, Merck & Co., Inc., WP26-410, West Point, PA 19486, USA.

Reprint requests to: Thomas Tuschl, Howard Hughes Medical Institute, Laboratory of RNA Molecular Biology, The Rockefeller University, 1230 York Avenue, Box 186, New York, NY 10021, USA; e-mail: ttuschl@rockefeller.edu; fax: (212) 327-7652; or Gunter Meister, Munich Center for Integrated Protein Science (CIPSM), Max Planck Institute of Biochemistry, Am Klopferspitz 18, D-82152 Martinsried, Germany; e-mail: meister@biochem.mpg.de; fax: 49-89-8578-3430.

Article published online ahead of print. Article and publication date are at <http://www.rnajournal.org/cgi/doi/10.1261/rna.789808>.

2002a). The effector complex contains at its heart an Ago/PIWI protein member (Hammond et al. 2001; Martinez et al. 2002a). Ago/PIWI proteins contain a conserved Piwi-Argonaute-Zwille (PAZ) and PIWI domain (for reviews, see Carmell et al. 2002; Peters and Meister 2007). The PAZ domain, which is also present in Dicer, specifically binds the characteristic 2-nt 3' overhangs of RNase-III-processed dsRNAs (Song et al. 2003; Yan et al. 2003; Lingel et al. 2004; Ma et al. 2004). The PIWI domain contains a RNA 5'-phosphate binding (MID domain) and a RNase H domain (Parker et al. 2004, 2005; Song et al. 2004; Ma et al. 2005; Rivas et al. 2005; Yuan et al. 2005, 2006; Song and Joshua-Tor 2006). The MID domain anchors the 5' end of the guide small RNAs (Ma et al. 2005; Parker et al. 2005; Rivas et al. 2005), and presumably also plays a role during RISC-loading by receiving and binding the guide strand 5' phosphate (Nykänen et al. 2001).

Protein factors critically involved in siRNA or miRNA silencing complex assembly were first identified in *Drosophila melanogaster*. Duplex siRNAs are recognized by the heterodimer of RNase III Dcr-2 and the dsRNA-binding-domain protein R2D2, both of which are critical for formation of the Ago2-containing RISC (Liu et al. 2003, 2006). miRNA maturation in *D. melanogaster* is catalyzed by a heterodimeric complex of RNase III Dcr-1 and the dsRNA-binding-domain protein Loquacious/R3D1 (Förstemann et al. 2005; Jiang et al. 2005; Saito et al. 2005). R2D2 preferably binds the thermodynamically more stable end of the siRNA duplex and thereby directs strand selection (Tomari et al. 2004b). The assembly of RISC is ATP dependent, at least to a certain degree (for reviews, see Filipowicz 2005; Preall and Sontheimer 2005). In mammalian systems, Dicer, the dsRNA-binding proteins TARBP2 and/or PACT, and an Ago protein appear to form the RISC-loading complex (Chendrimada et al. 2005; Gregory et al. 2005; Haase et al. 2005; Maniataki and Mourelatos 2005; Lee et al. 2006).

Two pathways are known for the transition of the duplex siRNAs or miRNA/miRNA* processing intermediate into a single-stranded RNA-containing effector complex (Matranga et al. 2005; Rand et al. 2005; Leuschner et al. 2006). The first pathway requires near-perfect base-pairing of the small RNA strands and depends on the RNase H activity intrinsic to a subset of the siRNA-binding Ago proteins (Liu et al. 2004; Meister et al. 2004; Parker et al. 2004, 2005; Rand et al. 2004; Song et al. 2004; Ma et al. 2005; Miyoshi et al. 2005; Rivas et al. 2005; Yuan et al. 2005). RNase H active Ago proteins are able to receive the duplex siRNAs and guide the cleavage of the nonretained siRNA strand (often referred to as passenger, nonguide, or sense siRNA) (Matranga et al. 2005; Rand et al. 2005; Leuschner et al. 2006). Upon release of the cleavage products, the retained guide (or anti-sense) siRNA is able to recognize complementary or partially complementary

mRNA targets. The second RISC loading pathway is used, when duplex siRNA or miRNA/miRNA* duplexes either encounter a RNase-H-deficient Ago protein member or when the duplexes are imperfectly paired across the center and cleavage site (like most miRNA/miRNA* duplexes), thereby preventing RNase H cleavage (Matranga et al. 2005). Presumably, a RNA helicase activity residing or transiently associating with the RISC-loading complex catalyzes the second RISC loading process (Tomari et al. 2004a; Meister et al. 2005; Robb and Rana 2007).

The duplex-initiated RISC assembly process appears to be bypassed if high concentrations of single-stranded siRNAs are added to cell lysates or transfected into cells (Martinez et al. 2002a). The role and the requirement for a 5' phosphate in reconstituting RISC and its activity, however, remained somewhat controversial (Liu et al. 2004; Song et al. 2004; Ma et al. 2005).

The specificity of small-RNA-guided mRNA degradation was examined in detail including mRNA array analysis (Jackson et al. 2003; Lin et al. 2005; Birmingham et al. 2006; Jackson et al. 2006b). These studies revealed "off-targeting" activities of siRNAs that could not be separated from the "on-targeting" activity by simply decreasing the siRNA concentration. Some of the off-targets contained sequence segments of extensive complementarity to the siRNA, but many other off-targets showed only partial complementarity within their 3'-untranslated region (UTR) to the siRNAs, notably at the 5' end of the siRNA guide strand. The latter observation was reminiscent of miRNA "seed" sequence (comprising positions 1–8) mediated target mRNA regulation (Lai 2002; Lewis et al. 2003; Stark et al. 2003; Rajewsky and Socci 2004; Lim et al. 2005; Linsley et al. 2007). Off-target signatures can be identified for both the sense and the anti-sense siRNA strands, although strand biases during the assembly of RISC affect the targeting efficiencies of the two strands (Khvorova et al. 2003; Schwarz et al. 2003). In selecting siRNA sequences one takes now into consideration the differential thermodynamic stability of the siRNA ends to favor the incorporation of the target mRNA complementary guide siRNA (for review, see Pei and Tuschl 2006). Other strategies proposed to control off-targeting activities included the introduction of 2'-O-methyl-ribose residues into the seed sequences of the siRNAs, which reduces off-targeting without detectable drop in on-targeting (Jackson et al. 2006a).

Here we study the role of the 5'-terminal phosphate during RISC assembly from duplex and single-stranded siRNAs using 5'-O-methyl-modified siRNAs. We show that the 5'-phosphorylation status within a duplex siRNA is an important determinant of strand incorporation into RISC, and we demonstrate that selective 5'-O-methylation can be used to control strand-specific off-targeting activity. The phosphorylation status of single-stranded siRNAs has little impact on the nonnatural RISC assembly and the subsequent activity of RISC.

RESULTS

5' phosphates are required for reconstitution of RISC from double-stranded but not single-stranded siRNAs

To revisit the requirements for 5' phosphates described for reconstituting RISC in *D. melanogaster* (Nykänen et al. 2001) or human cell lysates (Martinez et al. 2002a; Liu et al. 2004; Song et al. 2004; Ma et al. 2005), we prepared single- and double-stranded siRNAs with uridine and thymidine 5'-end modifications (Fig. 1A). 5'-O-methyl-thymidine is currently the only nucleotide readily available for solid-phase synthesis to render the ribose 5' ends of siRNAs refractory to phosphorylation in cell lysates (Nykänen et al. 2001). HeLa cells and lysates contain hClp1 kinase, which rapidly phosphorylates 5'-hydroxyl termini of dsRNA or dsDNA as well as single-stranded RNA (Martinez et al. 2002a; Weitzer and Martinez 2007). To control for the concomitant introduction of a 5-methyl group with 2'-deoxythymidine incorporation into RNA, we also prepared siRNAs with 5'-hydroxyl-2'-deoxythymidine, 5'-hydroxyl-uridine, and 5'-phosphorylated uridine-containing siRNAs.

HeLa S100 cell lysates were incubated with double-stranded siRNA derivatives followed by addition of 5' ³²P-labeled complementary target mRNA segments. Irrespective of the modification of the sense (passenger) strand, 5'-hydroxyl- or 5'-phosphate-modified anti-sense strands mediate target RNA cleavage. In contrast, 5'-O-methylated anti-sense siRNA showed substantially reduced activity (Fig. 1B). The siRNA duplexes were cognate to firefly luciferase (*Pp-luc*) mRNA, and they were cotransfected with plasmids encoding the *Pp-luc* target and sea pansy control luciferase (*Rr-luc*) genes into HeLa cells. Consistent with the biochemical results, only the duplex with 5'-O-methyl-modified anti-sense strand showed reduced silencing activity (Fig. 1C). Together, these observations were pointing to a role of the 5' phosphate of the anti-sense strand during RISC loading or RISC activity.

Two possibilities can be envisioned responsible for the reduced silencing activity of 5'-O-methylated anti-sense strand duplex siRNAs: (1) loading of the anti-sense strand into RISC was compromised, and/or (2) the anti-sense strand-loaded RISC had reduced activity because of conformational restraints imposed by an unoccupied Ago2 5'-phosphate binding pocket (Liu et al. 2004; Ma et al. 2005; Parker et al. 2005; Rivas et al. 2005). We therefore tested if we were able to load RISC using the single-stranded anti-sense siRNAs. Because single-stranded siRNAs are more susceptible to nucleases present in cell lysates than duplex siRNAs, we immunopurified FLAG/HA-affinity-tagged Ago2 protein complexes from HEK 293 cell lysates, and subsequently incubated them with single-stranded siRNAs and target RNA substrate. Surprisingly, the single-stranded siRNAs reconstituted RISC activity irrespective of their 5' modification status (Fig. 1D).

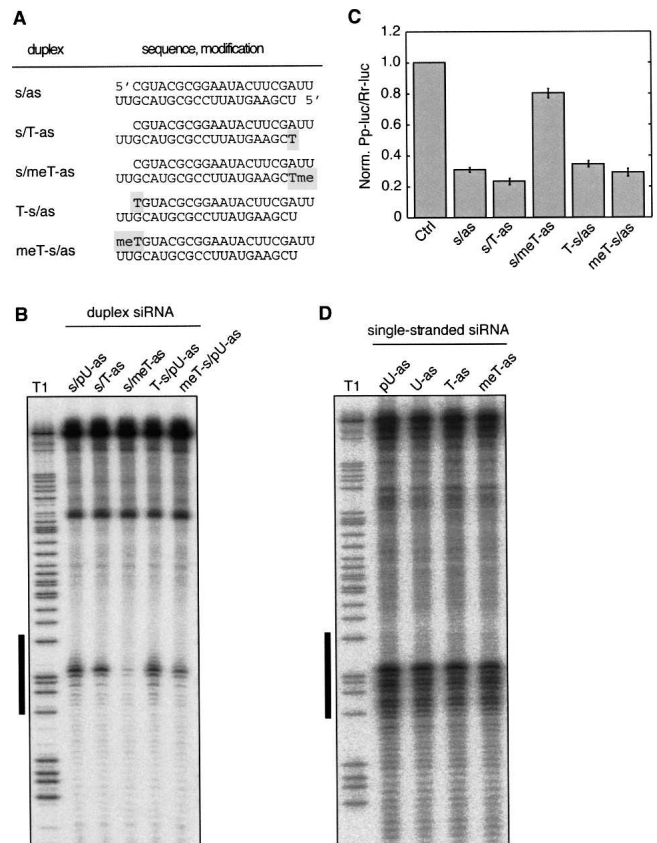


FIGURE 1. 5' phosphates are required for reconstitution of RISC from double-stranded but not single-stranded siRNAs. (A) Schematic presentation of the luciferase duplex siRNAs used in B and C. (B) HeLa S100 extract was incubated with the siRNAs shown in A. After preincubation, a ³²P-cap-labeled RNA substrate was added, and the cleaved RNA fragments were analyzed on a denaturing sequencing gel. T1 refers to partial nuclease T1 digestion of the target RNA. The black line to the left indicates the segment of the target RNA covered by the used siRNAs. (C) The effect of duplexes 1–5 and a control siRNA duplex on inhibition of the firefly luciferase (*Pp-luc*) expression relative to *Renilla* luciferase (*Rr-luc*) in a dual-luciferase assay. The ratios of the signals of *Pp-luc/Rr-luc* for duplexes 1–5 were normalized to that of the control siRNA. The plotted data were averaged from three independent experiments \pm SD. (D) FLAG/HA-tagged Ago2 was transiently transfected into HEK 293 cells. Tagged proteins were immunoprecipitated from the lysates using anti-FLAG beads, and RISC activity was reconstituted by adding single-stranded siRNA against the luciferase mRNA either with a 5' phosphate (lane 1), without a 5' phosphate (lane 2), with a 5'-hydroxyl-2'-dT (lane 3), or with a 5'-methoxy-2'-dT (lane 4). The beads were subsequently incubated with a ³²P-cap-labeled RNA substrate and analyzed by denaturing RNA-PAGE followed by phospho-imaging. T1 refers to partial nuclease T1 digestion of the luciferase target RNA. p indicates 5' phosphate; Me, 5'-O-methyl group.

These data suggest that the 5' phosphate plays an important role during the process of RISC loading, that a 5'-phosphate-sensing mechanism can be bypassed using single-stranded siRNAs, and that the Ago2 5'-phosphate binding pocket does not need to be occupied to mediate target mRNA cleavage.

Asymmetric 5'-O-methylation of duplex siRNAs directs strand selection during RISC formation

The loss of silencing activity of duplex siRNAs in which only the anti-sense strand was 5'-O-methyl-modified could be due either to preferential loading of the sense strand into RISC under these conditions or to a defective recognition of the siRNA duplex by some RNAi machinery protein at a stage prior to RISC assembly. To monitor the asymmetry of siRNA strand incorporation and target RNA cleavage, we synthesized two pairs of siRNA duplexes that were predicted to be symmetrically and asymmetrically incorporated into RISC based on the differences in thermodynamic

stability at their duplex termini (Khvorova et al. 2003; Schwarz et al. 2003).

We first characterized biochemically the symmetric siRNA duplex (Fig. 2A) by incubating it in lysates from HEK 293 cells transiently transfected with FLAG/HA-affinity-tagged Ago2. HEK 293 cells were chosen because they are efficiently transfected at large scale with FLAG/HA-Ago2 expression plasmids. The siRNAs that coimmunoprecipitated with FLAG/HA-Ago2 were analyzed by Northern blotting using probes complementary to either the anti-sense or the sense strand. Signals for the anti-sense strand were detected when the siRNA duplex contained

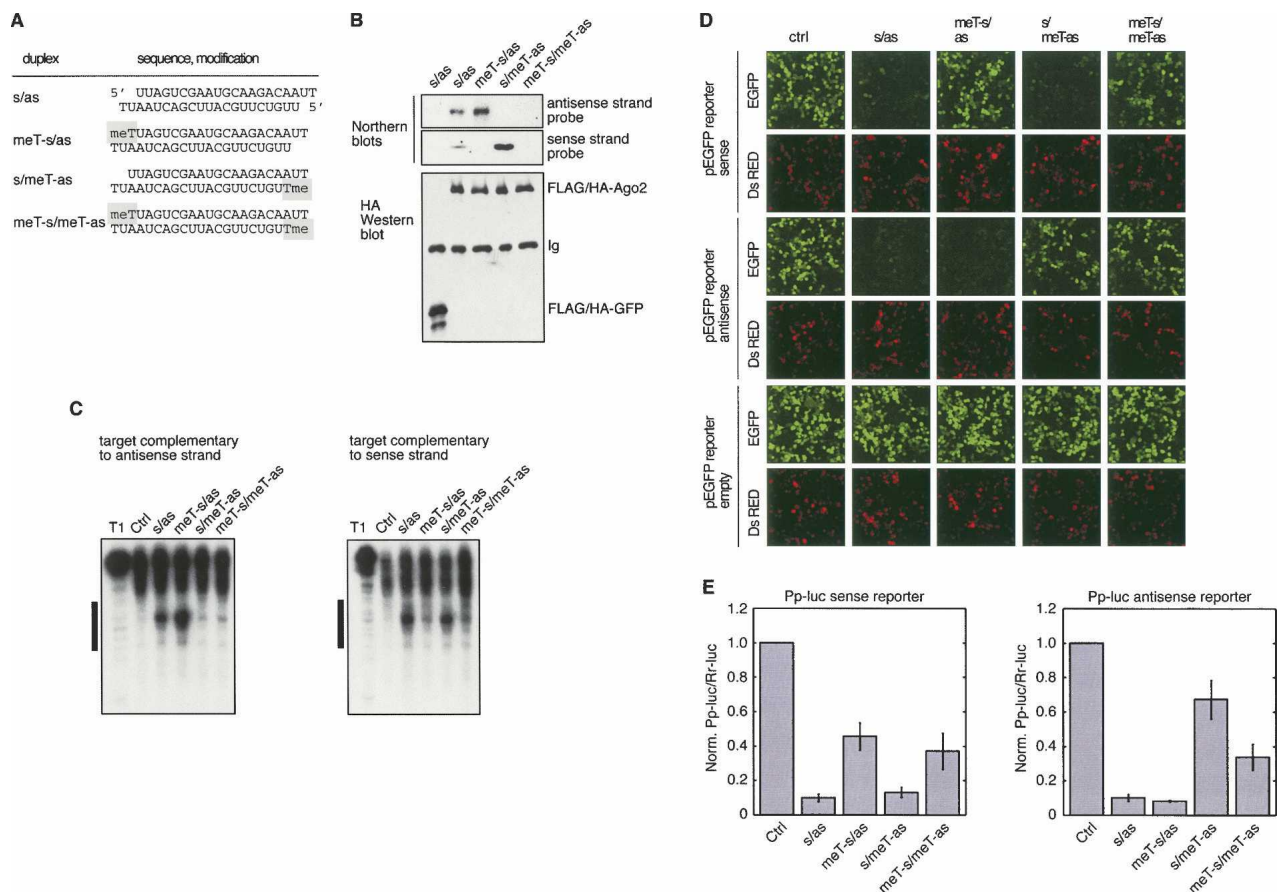


FIGURE 2. siRNA 5'-O-methylation inhibits RISC loading and RISC activity. (A) Schematic presentation of the symmetric RISC loading siRNA duplexes used in B, C, D, and E. (B) FLAG/HA-Ago2 and FLAG/HA-EGFP were transiently transfected into HEK 293 cells. Cell lysates were preincubated with siRNA duplexes allowing for RISC loading. RISCs were immunoprecipitated using anti-FLAG antibodies, and the precipitated proteins were analyzed using anti-HA antibodies (lower panel). Ig indicates the heavy chain of the immunoglobulin. The bound siRNA strands were examined by Northern blotting (upper panel). (C) HeLa cell extracts were preincubated with the indicated siRNA duplexes allowing for RISC loading. Control (Ctrl) refers to luciferase siRNA duplex. ³²P-cap-labeled substrates either complementary to the sense strand or the anti-sense strand were subsequently added and the cleaved RNA products were analyzed by 4% denaturing RNA PAGE. T1 indicates digestion of the substrate using nuclease T1. The bar to the left of the image indicates the sequence of the substrate RNA, which is complementary to the used siRNAs. (D) 5'-O-methylated siRNAs inhibits RNAi in living cells. Plasmids encoding EGFP, EGFP fused to a complementary target site for the anti-sense strand or EGFP fused to a complementary target site for the sense strand were cotransfected with control (ctrl), luciferase siRNAs, or the indicated siRNA duplex. A plasmid encoding the Ds Red gene was cotransfected and served as a transfection control. (E) Plasmids containing either a *Pp*-luciferase gene fused to a complementary target site for the anti-sense strand or a complementary target site for the sense strand of the siRNA were cotransfected with *Rr*-luciferase and the indicated siRNAs. GFP siRNA was utilized as control (ctrl) siRNA. The *Pp*-luc/*Rr*-luc ratios were normalized to that of the control siRNAs.

unmodified or 5'-O-methyl sense strand but not when the anti-sense strand was 5'-O-methylated (Fig. 2B). Signals for the sense strand were detected when the siRNA duplex contained unmodified or 5'-O-methyl anti-sense strand but not when the sense strand was 5'-O-methylated (Fig. 2B). We then confirmed that symmetrically or asymmetrically loaded FLAG/HA-Ago2 immunoprecipitates cleaved siRNA-complementary ³²P-cap-labeled target RNAs (Tuschl et al. 1999) as expected from their strand-loading ratios determined by Northern blotting (Fig. 2C).

To measure the cell-based silencing activities from the assembly of the anti-sense and the sense siRNA strand into RISC, we introduced anti-sense and sense-complementary sequence segments into the 3' UTR of EGFP as well as *Pp-luc* reporters. The results were consistent with our biochemical observations in HEK 293 lysates (Fig. 2D,E). Symmetric 5'-O-methylation of both siRNA strands lead to an overall reduced gene silencing activity in the luciferase reporter assay, without changing the symmetry of the residual cleavage activity when compared with the unmodified siRNA duplex. In contrast, a single asymmetric modification did not alter the activity attributable to the unmodified siRNA strand. Together, these observations indicate that the RISC assembly of symmetrical siRNA duplexes can be influenced using asymmetric 5'-O-methylation, whereby the methylation of one strand directs incorporation of the complementary strand into RISC.

We next evaluated whether strand selection of a thermodynamically asymmetrical siRNA duplex could be controlled by 5'-O-methylation (Fig. 3A). The activities of the modified and unmodified siRNA duplexes were determined using the EGFP and luciferase reporter assay described above (Fig. 3B,C). The unmodified siRNA duplex preferentially repressed the target complementary to the sense strand, as expected from the design of the siRNA. The 5'-O-methylation of the anti-sense siRNA reduced its cleavage activity about twofold. Reciprocally, 5'-O-methylation of the sense siRNA strand reduced its cleavage activity two-fold, while the anti-sense strand cleavage activity was significantly increased. Similar to the observations made for the symmetric siRNA duplex above, double 5'-O-methylation weakened the silencing activity of both the anti-sense and sense strands. These observations indicate that 5'-O-methylation of siRNA strands can influence siRNA strand incorporation into RISC, even in the context of a thermodynamically asymmetrical siRNA.

Strand-specific 5'-O-methylation also controls siRNA off-targeting activity

Off-target effects are, like on-target effects, strictly sequence-specific and caused either by near-perfect complementarity between the central region of the siRNA and its targets or by seed-sequence complementarity between the siRNA and the target 3' UTR (Jackson et al. 2003,

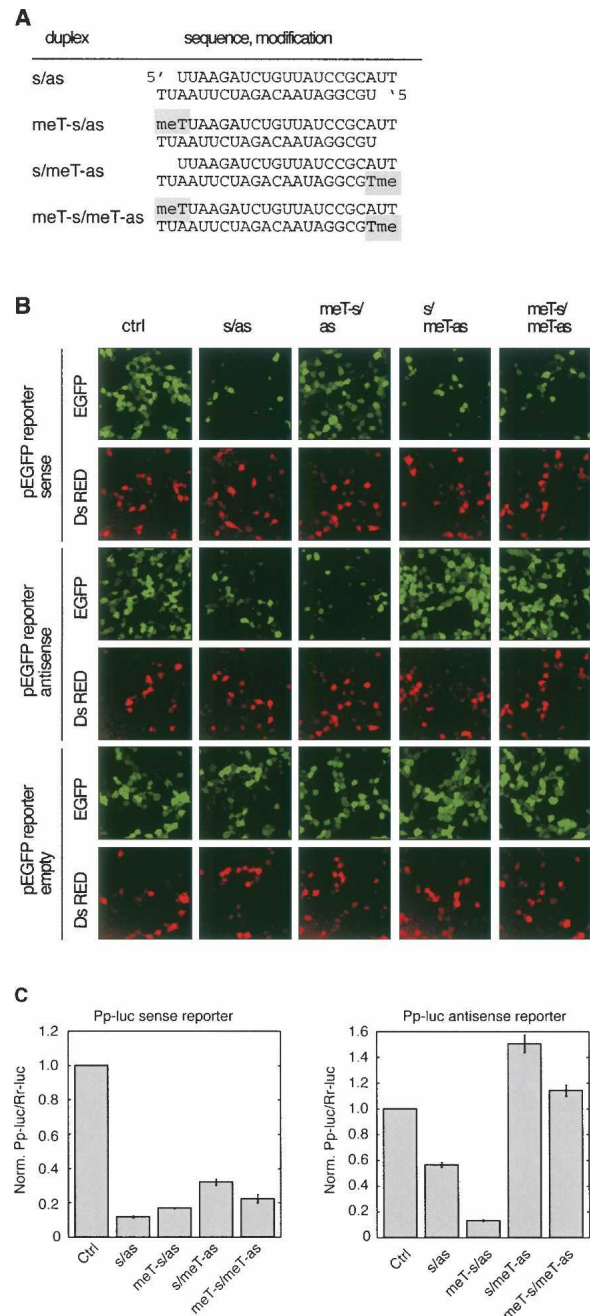


FIGURE 3. siRNA 5'-O-methylation inhibits RISC loading and RISC activity. (A) Schematic presentation of the asymmetric RISC loading siRNA duplexes used in B and C. (B) The same experiments and controls described in Figure 2D were carried out using the asymmetrically RISC loading siRNAs duplex as well as complementary EGFP target constructs. (C) The same experiments and controls described in Figure 2E were performed using the asymmetrical RISC loading siRNAs.

2006b; Birmingham et al. 2006). To assess if strand selection from asymmetrically 5'-O-methylated siRNA duplexes could be used for controlling siRNA off-targeting activity, we determined the gene expression profiles of HeLa

cells transfected with 5'-O-methylated or unmodified siRNA duplexes. The symmetrical siRNA duplex, whose both sense and anti-sense strands are incorporated into RISC, was selected for the analysis (Fig. 2A).

The choice of cell line and transfection reagents was critical for identifying siRNA-strand-specific off-targets. We first tested Lipofectamine 2000 Transfection Reagent (Invitrogen) in HEK 293 cells, but variations in gene expression, caused presumably by mild toxicity of the formulated transfection reagent, made it impossible to detect siRNA-sequence-dependent off-target signatures. Next, we tested Lipofectamine RNAiMAX transfection reagent (Invitrogen) in HEK 293 cells. Though the siRNA and mock transfection yielded reproducible and stable expression profiles, we did not detect any off-targeting signature using either Affymetrix or Agilent mRNA microarrays (data not shown). Finally, we examined HeLa cells transfected with Lipofectamine RNAiMAX using Affymetrix microarrays, and we were able to identify the expected off-targeting effects. Using the same approach, we also detected the previously reported off-targets of a siRNA duplex targeting the PIK3CB gene (PIK3CB-6340) (Jackson *et al.* 2006b), indicating that our Affymetrix array platform was sufficiently sensitive for off-target analysis in this cell type.

The off-target effects were quantified by analyzing the frequency of seed-complementary sites (where the seed was defined as nucleotides 1–7, 2–8, or 1–8 of the siRNA) for real and randomized siRNAs within the 3' UTRs of mRNAs that were down-regulated 1 d after siRNA transfection (Fig. 4). Consistent with our biochemical analysis, which indicated that both strands of our unmodified siRNA duplex were loaded into RISCs, we found seed-complementary site enrichment for both siRNA strands. 5'-O-methylation

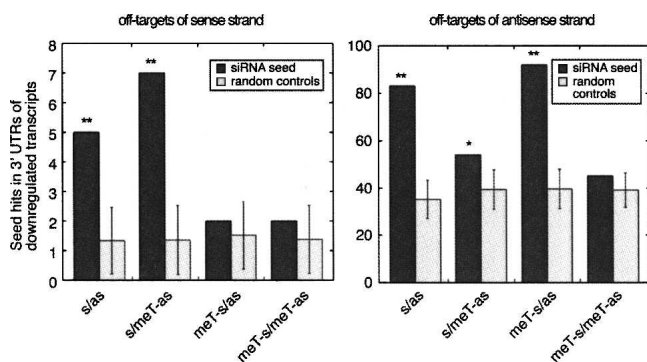


FIGURE 4. siRNA off-target analysis of the symmetric RISC loading siRNA duplexes. Enrichment of “seed”-complementary sequences for sense (*left* panel) and anti-sense (*right* panel) strands relative to random controls in the 3' UTRs of transcripts that are down-regulated upon siRNA transfection (see Materials and Methods). Dark gray and light gray bars show the number of occurrences of seed-complementary sites for the siRNAs used in the study and random controls, respectively. Double and single stars indicate enrichments that are significant at 0.01 and 0.05 level.

of the sense strand increased the off-targeting activity of the anti-sense strand, while decreasing its own off-targeting activity, and vice versa. Note that the sense strand has intrinsically fewer off-targets compared with the anti-sense strand. This is because the sense strand contains a CG dinucleotide in its seed sequence and CG-containing motifs are underrepresented in the genome compared to other dinucleotides. The random controls for the sense strand, being selected to have a similar number of seed-complementary sites in the entire set of 3' UTRs as the sense strand, also have low numbers of seed matches in the set of down-regulated UTRs. This leads to a higher variance in the expected number of seed-complementary sites for the sense compared with the anti-sense strand. Nonetheless, the seed enrichment for the sense strand is statistically significant in the case of the s/as and s/meT-as constructs. These analyses thus indicate that chemical modification can limit the off-targeting activity to only one strand of the siRNA duplex.

Comparison of the effects of 5'-O-methylation and duplex-destabilizing mutations on strand selection

The differential thermodynamic stability of siRNA duplex termini impacts siRNA strand selection (Khvorova *et al.* 2003; Schwarz *et al.* 2003). Thermodynamic biases can be introduced by varying the G/C content of the termini of the siRNA duplex or by placing destabilizing, non-Watson–Crick base pairs (mismatches) at one of the termini. We therefore wanted to compare the strand bias introduced by 5'-O-methylation with that introduced by mismatches using the asymmetrical siRNA duplex described above, whose sense strand is preferentially incorporated into RISC.

We placed mismatches in the G/C-rich terminus by altering the sequence of the anti-sense siRNA from positions 1 to 5 (Fig. 5A). According to the current model of strand selection, destabilizing the G/C-rich termini should lower the bias for incorporation of the sense strand of this siRNA duplex and should enhance the incorporation of the anti-sense strand into RISC. What we observed was that mismatches only minimally reduced the activity of the sense siRNA-containing RISC measured by the sense reporter, while 5'-O-methylation of the sense siRNA showed a more pronounced effect (Fig. 5B).

Anti-sense siRNA strand incorporation was determined by the anti-sense reporter assay. Mismatches introduced by altering the sequence of the anti-sense siRNA trivially lead to mismatches between the anti-sense siRNA and its reporter, resulting in the lack of cleavage activity for mutants of positions 3–5 of the anti-sense siRNA. Mutations placed at position 1 or 2 of the anti-sense siRNA showed similar activity as the unmodified siRNA duplex, consistent with unaltered behavior of the sense reporter, indicating that mismatches at position 1 or 2 were insufficient to alter asymmetry of RISC assembly. In contrast, the 5'-O-methylation of the sense strand, led to a much

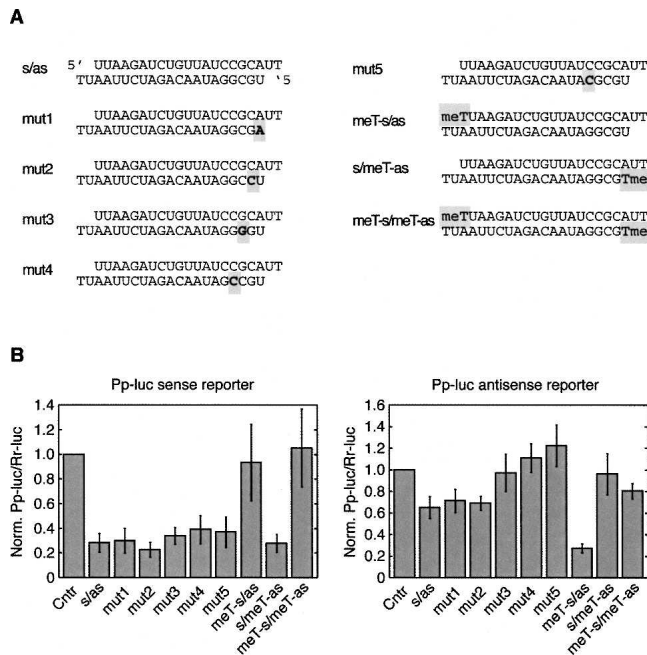


FIGURE 5. Influence of thermodynamic stability vs. 5'-O-methyl modification. (A) Schematic presentation of the asymmetric RISC loading siRNA duplexes used in B. (B) Plasmids containing either a *Pp*-luciferase gene fused to a complementary target site for the antisense strand or a complementary target site for the sense strand of the siRNA were cotransfected with *Rr*-luciferase and the indicated siRNAs. GFP siRNA was utilized as control (Ctrl) siRNA.

more pronounced activity of the anti-sense siRNA. Together, these experiments showed that 5'-O-methylation of the 5' end of siRNAs was more effective in changing strand preferences compared with alterations of thermodynamic stability induced by duplex-destabilizing mismatches.

DISCUSSION

Our analysis describes for the first time the consequences of strand-specific 5'-O-methyl-modification of siRNA duplexes on the assembly and activity of RISC. 5'-O-methylation of the terminal ribose blocked the phosphorylation of siRNAs by cellular kinases (Nykänen et al. 2001; Martinez et al. 2002b; Weitzer and Martinez 2007). The requirement for 5' phosphates during the assembly of RISC was noted previously using symmetrically 5'-O-methylated siRNA duplexes in *D. melanogaster* embryo lysates (Nykänen et al. 2001), and similarly, we also found that double 5'-O-methyl modification reduced RISC assembly in human cells. Strikingly, the placement of a single 5'-O-methyl only reduced the incorporation of the methylated strand without impairing the incorporation of the unmodified siRNA strand. It even appeared that modification of the sense siRNA strand enhanced the incorporation of the unmodified anti-sense strand, and vice versa. The effect of the 5'-O-methyl modification was also strong enough to

counteract the otherwise strong strand preference of an asymmetrically loading siRNA duplex. This observation emphasizes the importance of 5'-phosphate recognition during RISC assembly and its potential use for siRNA design and application.

The molecular events responsible for 5' phosphate recognition during RISC assembly remain to be defined. Presumably the contacts are made while placing the 5' phosphate of the guide siRNA strand into the 5'-phosphate binding pocket of Ago (Ma et al. 2005; Parker et al. 2005). The sensing of the 5' phosphate also appears to take place in the context of a duplex siRNA or a partially unwound duplex siRNA, because artificial loading of RISC with single-stranded 5'-O-methyl-modified or unmodified siRNAs was possible and led to similar RISC-mediated cleavage activities. Interestingly, a bulky 5'-fluorescein modification coupled via a 5'-phosphodiester linkage to the guide strand of a siRNA duplex did not affect its silencing efficiency (Harborth et al. 2003). It will be interesting to explore the effects of other 5'-hydroxyl modifications, for example, bulky alkyl groups (e.g., tertiary butyl), on RISC assembly.

Although siRNA duplexes are widely used in research as reagents for gene silencing, sequence-specific off-target effects can be problematic. Off-target effects are typically caused by siRNA sense and anti-sense strands, and the strand-specific reduction of off-target effects using 5'-O-methyl modifications will help to improve siRNA specificity. However, 5'-O-methylation will only eliminate off-target effects caused by the 5'-O-methylated strand of the siRNA duplex. Moreover, this may also lead to an enhanced off-target effect of the unmodified strand as its loading into RISC may increase; it should nonetheless allow for lowering the dose of siRNAs needed in gene silencing experiments and will aid in controlling potential side effects caused by competition of siRNA with miRNA pathways (Grimm et al. 2006).

Because not all siRNAs that are cognate to a given target mRNA are equally effective, computational tools have been developed based on experimental data to increase the likelihood of selecting effective siRNAs (for review, see Pei and Tuschl 2006). Though these methods facilitate selection of functional siRNAs, they do not yet alleviate the need for experimental validation. 5'-O-methylation of the passenger strand adds an additional constraint and might be useful in the context of generating genome-wide siRNA libraries, where the validation of each single siRNA is technically not feasible. Depending on the assay, high-throughput RNAi screens are sensitive to seed-sequence-mediated off-targeting effects (Lin et al. 2005), and reducing the likelihood for contributions of the passenger siRNA is useful.

Although it has been proposed that thermodynamic asymmetry can be readily introduced into siRNAs using LNAs (Elmén et al. 2005), minimizing the degree of

chemical modification needed to control asymmetry may be beneficial from the point of view of manufacturing or potential therapeutic use. It was also interesting to observe that the introduction of conventional mismatches for destabilizing one of the siRNA termini was less effective than the selective placement of a 5'-O-methyl group.

In summary, in this study we describe a novel approach of biasing siRNA strand selection from duplex siRNA based on 5'-phosphate sensing during RISC assembly.

MATERIALS AND METHODS

Oligonucleotide synthesis

siRNAs were chemically synthesized using RNA phosphoramidites (Pierce) on an Äkta Oligopilot 10 DNA/RNA synthesizer (GE Healthcare Life Sciences) at a 1 μ mol scale. The synthesis, deprotection and precipitation were performed according to the manufacturer's protocol. 5'-O-methylated siRNAs were purchased from Dharmacon. The sequences of the siRNAs used in this study are as follows: luciferase siRNA anti-sense strand, 5'-UCGAAGUAAUCCGCGUACGUU, sense strand, 5'-CGUACGCGGAAUACUUCGAUU; GFP siRNA anti-sense strand, 5'-GGC AAGCUGACCCUGAAGUUT, sense strand, 5'-ACUUCAGGGU CAGCUUGCCUT; symmetrically RISC-loaded siRNA anti-sense strand, 5'-UUGUCUUGCAUUCGACUAAUT, sense strand, 5'-UUAGUCGAAUGCAAGACAAUT; and asymmetrically RISC-load siRNA anti-sense strand, 5'-UUAAGAUCUGUUAUCCGC AUT, sense strand, 5'-UGCGGAUACAGAUCUUAUT. For analysis of the importance of the 5' phosphate, the 5' uridine residues were substituted by 5'-O-methyl-2'-deoxythymidine or 2'-deoxythymidine as control.

Plasmids

The mammalian expression plasmids for FLAG/HA-tagged Ago2 and GFP were previously described (Meister et al. 2004) and are available from www.addgene.org. Reporter plasmids for measuring RISC activity of anti-sense and sense siRNA strands were generated as follows: Complementary pairs of DNA oligonucleotides bearing the siRNA target sequence and flanking SacI and NaeI restriction sites were annealed, digested with SacI and NaeI, and cloned into the 3' UTR of the reporter vectors, using the SacI and NaeI sites of the pMIR-REPORT plasmid (Ambion) or the SacI and SmaI sites of the pEGFP-C2 plasmid (Clontech), respectively. Prior to this procedure, the pEGFP-C2 plasmid was modified by the insertion of a stop codon into the BglII site. The oligos containing the siRNA target sequences were as follows:

Target complementary to symmetric RISC loading anti-sense siRNA strand, 5'-CGCTGAGCTCATCGCCACCTGTTTAAG CCTTAGTCGAATGCAAGACAAATTAGACCTACGCACTCC AGGCCGGCTCGC and 5'-GCGAGCCGGCCTGGAGTGCGT AGGTCTAATTTGCTTGCATTTCGACTAAGGCTTAAACAA GGTGGCGATGAGCTCAGCG;

Target complementary to symmetric RISC loading sense siRNA strand, 5'-CGCTGAGCTCATCGCCACCTGTTTAAGCCTT GTCTTGCATTTCGACTAAATTAGACCTACGCACTCCAGGC CGGCTCGC and 5'-GCGAGCCGGCCTGGAGTGCGTAGGT

CTAATTTAGTCGAATGCAAGACAAAGGCTTAAACAAGGTG GCGATGAGCTCAGCG;

Target complementary to asymmetric RISC loading anti-sense siRNA strand, 5'-CGCTGAGCTCATCGCCACCTGTTTAAG CCGCGGATAACAGATCTTAAATTAGACCTACGCACTCC AGGCCGGCTCGC and 5'-GCGAGCCGGCCTGGAGTGCGT AGGTCTAATTTAAGATCTGTTATCCGCGGCTTAAACAA GGTGGCGATGAGCTCAGCG; and

Target complementary to asymmetric RISC loading sense siRNA strand, 5'-CGCTGAGCTCATCGCCACCTGTTTAAGCCTT TAAGATCTGTTATCCGCATTAGACCTACGCACTCCAGGC CGGCTCGC and 5'-GCGAGCCGGCCTGGAGTGCGTAGGT CTAATGCGGATAACAGATCTTAAAGGCTTAAACAAGGTG GCGATGAGCTCAGCG.

Plasmids for in vitro transcription of RNA cleavage substrates were generated by cloning of the annealed oligodeoxynucleotides into the SacI/SmaI sites of the pIVEX2.4d plasmid (Roche).

In vitro transcription of RISC cleavage substrates

DNA templates for in vitro transcription of RNA cleavage substrates were generated by linearization of the respective pIVEX2.4d plasmids using BamHI restriction enzyme digestion. The linearized plasmid was used for run-off in vitro transcription using T7 RNA polymerase (Fermentas) according to the manufacturer's protocol. The transcripts were purified by denaturing PAGE, visualized by UV-shadowing, excised, and eluted overnight in 0.3 M NaCl at 4°C. The eluted RNA was precipitated by addition of 3 volumes of ethanol and collected by centrifugation. The cleavage substrate complementary to the luciferase targeting siRNAs was ³²P-cap-labeled (Martinez et al. 2002a), and the cleavage was assayed as described previously (Meister et al. 2004). The sense and anti-sense ³²P-cap-labeled cleavage substrates were 188 nt and 195 nt, respectively.

Northern blotting

The oligodeoxynucleotide probes 5'-TTAGTCGAATGCAAGACAA, and 5'-TTGTCTTGCATTTCGACTAA were used for detection of the symmetrically RISC-loading siRNAs. Probes were radioactively labeled with T4 polynucleotide kinase (New England Biolabs) using [γ -³²P]-ATP. RNA samples were separated by 15% denaturing PAGE and transferred to a nylon membrane (Hybond-N+, Amersham) by semi-dry electroblotting. The membrane was then subjected to UV cross-linking using the auto-crosslink function on the Stratalinker (Stratagene) and subsequently baked for 1 h at 80°C. The membrane was incubated with 15 mL of prehybridization buffer (5 \times SSC/20 mM sodium phosphate buffer (pH 7.2)/7% SDS/1 \times Denhardt's solution/3 mg of sonicated salmon sperm DNA) in a hybridization oven for 1 h rotating at 50°C. The prehybridization solution was then replaced with 15 mL of hybridization buffer containing 3,000,000 cpm of ³²P-radiolabeled DNA probe and incubated overnight at 50°C. The membrane was washed twice with 100 mL of wash solution I (5 \times SSC/1% SDS) at 50°C for 10 min followed by a single wash step with wash solution II (1 \times SSC/1% SDS) at 50°C. The membrane was wrapped in plastic wrap and exposed to a film for 2 d.

Tissue culture and transfections

HEK 293 cells were cultured in Dulbecco's modified Eagle's medium (DMEM) supplemented with 10% fetal bovine serum (FBS), 100 unit/mL penicillin, and 100 μ g/mL streptomycin at 37°C in a 5% CO₂-containing atmosphere. The stably transfected HeLa S3 FLAG/HA-Ago2 cell line (Meister et al. 2004) was cultured under the same conditions with the addition of 0.5 mg/mL G418. HEK 293 cells were cotransfected with reporter or control plasmids and siRNAs using Lipofectamine 2000 (Invitrogen) according to the manufacturer's protocol in a 24-well format 24 h after seeding. Transfected cells were analyzed for luciferase activity or GFP fluorescence 24 h after transfection. For immunoprecipitation experiments, HEK 293 cells were transfected using the calcium chloride method. Cells were plated to 40% confluency 3–4 h before transfection on a 15-cm dish. Twenty micrograms of plasmid DNA were diluted in 858 μ L of water and 122 μ L 2M CaCl₂. One milliliter of 2 \times HEPES-buffered saline (274 mM NaCl, 1.5 mM Na₂HPO₄, 54.6 mM HEPES-KOH at pH 7.1) was added drop-wise under gentle agitation. The transfection solution was then sprinkled onto the cells.

Microscopy

HEK 293 cells were seeded on coverslips and were cotransfected with either empty pEGFP-C2 as control or pEGFP-C2 bearing the target complementary to siRNA strand-specific sequences (0.2 μ g/well), pDsRedmonomer-C1 (Clontech; 0.1 μ g/well) and siRNA (20 pmol/well). After 24 h, cells were fixed in PBS with 4% formaldehyde for 30 min at room temperature, washed twice with PBS, and mounted on slides using Vectashield mounting medium (Vector Laboratories). Images were recorded using a Leica TCS SP2 confocal laser microscope and a 20 \times immersion oil objective. For GFP and DsRed images, 10 z-sections of the cells were recorded and processed to average projections using the Leica confocal software.

Dual luciferase assays

For experiments described in Figure 1C, 7000 HEK 293 cells per well were transferred into 96-well plates the day before transfection. The cells were then cotransfected with 0.2 μ g pGL2-control (Promega), 0.02 μ g pRL-TK (Promega), and 3.75 pmol siRNA duplexes (final concentration 25 nM) with Lipofectamine 2000 (Invitrogen; 0.75 μ L). Luciferase activities were measured 20 h after transfection using the Dual Luciferase Assay Kit (Promega) and a Bio-Tek Clarity luminometer. The ratios of the signals of firefly (*Pp*) luciferase to seapansy (*Rr*) luciferase were calculated and normalized by dividing by the ratio for control siRNA against FLJ30525.3. The plotted data were averaged from triplicates \pm SD. For Figures 2–5, HEK 293 cells were cultured in 24-well plates and each cotransfected with either empty pMIR-REPORT (*Pp*-luc) control plasmid or pMIR-REPORT bearing the target complementary to siRNA strand-specific sequences (0.2 μ g/well), pRL-SV40 control vector (*Rr*-luc) (Promega) (0.1 μ g/well), and siRNA (20 pmol/well). The cells were lysed and assayed 24 h post-transfection following the Dual-Luciferase Reporter Assay system (Promega) instructions. Samples were analyzed on a Mithras LB 940 Multimode Microplate Reader (Berthold Technologies). All samples were assayed in triplicates.

Western blotting, extract preparation, and immunoprecipitation

Western blotting was performed as previously described (Meister et al. 2004). For immunoprecipitation, HEK 293 cells transiently transfected with FLAG-/HA-tagged Ago2 and HeLa S3 cells stably transfected with FLAG/HA-tagged Ago2 were harvested from 15 cm plates 48 h post-transfection. The cells were washed with PBS (pH 7.4) and subjected to lysis with 700 μ L of lysis buffer (150 mM KCl, 25 mM Tris-HCl at pH 7.4, 2 mM EDTA at pH 8.0, 1 mM NaF, 0.5 mM DTT, 0.05% NP40, 0.5 mM AEBSF) for 10 min at 4°C. The cells were subsequently scraped off of the plate and centrifuged at 17,200g for 10 min. The supernatant was incubated with 15 μ L of anti-FLAG M2 agarose beads (Sigma), which were activated by washing once with 0.1 M glycine-HCl (pH 2.5) and equilibrated by washing with 1.5 M Tris-HCl (pH 8.8), for 3 h at 4°C with rotation. The beads were collected and washed three times with 300 mM NaCl/5 mM MgCl₂/0.05% NP40/50 mM Tris-HCl (pH 7.5) and once with PBS (pH 7.5). To isolate the RISC-incorporated siRNA, the beads were then incubated in 300 μ L of proteinase K solution consisted of 2 \times proteinase K buffer (300 mM NaCl/25 mM EDTA at pH 8.0/2% SDS/200 mM Tris-HCl at pH 7.5 and proteinase K at 1 mg/mL concentration) for 10 min at 37°C. The RNA was phenol/chloroform-extracted and ethanol precipitated.

RNA cleavage assays

In vitro transcribed cleavage substrates were 5'-cap labeled as described previously (Martinez et al. 2002a). In a typical RNA cleavage reaction, 100 nM of siRNA was incubated in a 15 μ L reaction containing 50% HeLa S100 extract, 1 mM ATP, 0.2 mM GTP, 10 U/mL RNasin (Promega), 100 mM KCl, 1.5 mM MgCl₂, 0.5 mM DTT, 10 mM HEPES-KOH (pH 7.9) at 30°C. After 30 min, 5 nM of the cap-labeled cleavage substrate was added and further incubated for 1.5 h at 30°C. The reactions were stopped by adding 200 μ L of proteinase K buffer containing 1 mg/mL proteinase K. The RNA was subsequently isolated using phenol/chloroform extraction, and the cleavage products were analyzed by 8% denaturing RNA PAGE. The labeled RNA was detected by phosphoimaging and autoradiography.

Microarray mRNA expression analysis

HeLa cells were plated in a six-well plate with a volume of 2.5 mL at a density such that next day they are \sim 75% confluent for transfection. A transfection solution of 0.5 mL was utilized for transfection for the final siRNA duplex concentration of 50 nM using RNAiMAX (Invitrogen). Total RNA was extracted 24 h post-transfection with Trizol (Invitrogen) and purified using the RNeasy Mini Kit (Qiagen). Three micrograms of purified RNA was used to synthesize the first strand of cDNA using ArrayScript reverse transcriptase (Ambion, catalog no. 1791) and an oligo(dT) primer bearing a T7 promoter. The single-stranded cDNA was converted into dsDNA by DNA polymerase I in the presence of *Escherichia coli* RNase H and DNA ligase. After column purification, the dsDNA was served as a template for in vitro transcription in a reaction containing biotin-labeled UTP, unlabeled NTPs, and T7 RNA polymerase. The amplified, biotin-labeled, anti-sense RNA (aRNA) was purified, and quality was assessed using the Agilent 2100 Bioanalyzer and the RNA 6000 Nano kit. Twenty

micrograms of labeled aRNA were fragmented, and 15 μ g of the fragmented aRNA was hybridized to Affymetrix Human Genome U133 Plus 2.0 Array for 16 h at 45°C as described in the Affymetrix Technical Analysis Manual (Affymetrix). After hybridization, Gene Chips were stained with streptavidin-phycoerythrin, followed by an antibody solution (anti-streptavidin), and a second streptavidin-phycoerythrin solution, with all liquid handling performed by a GeneChip Fluidics Station 450. Gene Chips were then scanned with the Affymetrix GeneChip Scanner 3000. Agilent Whole Human Genome Oligonucleotide Microarray (catalog no. 4112F) analysis was performed by Cogenics.

Computational analyses of putative off-targets

We normalized the probe intensities for the five microarrays (transfection reagent only, symmetric RISC loading sense/anti-sense, MeO-sense/anti-sense, sense/MeO-anti-sense, MeO-sense/MeO-anti-sense siRNA duplexes) using the bioconductor (see <http://www.bioconductor.org> and Gentleman et al. 2004) and gcRMA software (Wu et al. 2004). To quantify off-target effects based on the frequency of seed-complementary sites in the 3' UTRs, we selected, for each gene measured by the microarray, the transcript with median 3'-UTR length. This data set consisted of 14,997 transcripts. From all the probe sets corresponding unambiguously to a given gene, we selected the one that responded best (exhibited the highest variance) across a large number of experiments performed on the Affymetrix platform that we used. This probe set was used to monitor the per-transcript expression level across our experiments. From each experiment (sense/anti-sense versus mock transfection, MeO-sense/anti-sense versus mock transfection, sense/MeO-anti-sense versus mock transfection, MeO-sense/MeO-anti-sense versus mock transfection), we extracted the top 1%, i.e., 149, most down-regulated transcripts and computed the number of occurrences of matches to the 1–7, 2–8, 1–8 nucleotide positions of both the sense and the anti-sense strands in these set of transcripts. We compared these numbers with the number of occurrences expected for “random siRNAs,” which we calculated as follows. For each of the anti-sense and the sense strand, we determined the number of occurrences of seed-complementary sites in the entire set of 3' UTRs. From all octameric sequences, we then selected the 5% (3277) whose reverse complements occurred with a frequency closest to that of siRNA-complementary sites in the entire set of 3' UTRs. These served as “random siRNA controls.” We determined the number of occurrences of seed-complementary sites of these random siRNAs in the down-regulated set of 3' UTRs. To correct for slight variations in this number that can be expected simply because the frequency of seed-complementary sites for real and random siRNAs in the 3' UTRs overall are not identical, we adjusted the observed counts by a factor equal to the ratio of observed occurrences of the real siRNA-complementary sites to the random siRNA-complementary sites in the entire set of 3' UTRs. We used the distribution of the values determined for random siRNAs to estimate the *P*-value of the number of occurrences of real siRNA-complementary sites.

ACKNOWLEDGMENTS

We thank S. Rottmüller for technical assistance; P. Linsley, A. Jackson, and J. Burchard for guidance on the technical aspects of microarray-based off-targeting analysis; C. Ender and An. Frohn

for critically reading the manuscript; and S. Jentsch for support. We also acknowledge W. Zhang and C. Zhao for Affymetrix array profiling carried out in the Rockefeller University Genomics Resource Center. L.W. is recipient of a fellowship from the Boehringer-Ingelheim Funds, and D.G. is supported by the Swiss Institute of Bioinformatics. Y.P. was supported by the Ruth L. Kirschstein Fellowship from NIH/National Institute of General Medical Sciences. This work was also supported by the Max Planck Society, HHMI and NIH grant R01 GM068476-01.

Received August 21, 2007; accepted October 24, 2007.

REFERENCES

- Bartel, D.P. 2004. MicroRNAs: Genomics, biogenesis, mechanism, and function. *Cell* **116**: 281–297.
- Birmingham, A., Anderson, E.M., Reynolds, A., Ilsley-Tyree, D., Leake, D., Fedorov, Y., Baskerville, S., Maksimova, E., Robinson, K., Karpilow, J., et al. 2006. 3'-UTR seed matches, but not overall identity, are associated with RNAi off-targets. *Nat. Methods* **3**: 199–204.
- Carmell, M.A., Xuan, Z., Zhang, M.Q., and Hannon, G.J. 2002. The Argonaute family: Tentacles that reach into RNAi, developmental control, stem cell maintenance, and tumorigenesis. *Genes & Dev.* **16**: 2733–2742.
- Chendrimada, T.P., Gregory, R.I., Kumaraswamy, E., Norman, J., Cooch, N., Nishikura, K., and Shiekhattar, R. 2005. TRBP recruits the Dicer complex to Ago2 for microRNA processing and gene silencing. *Nature* **436**: 740–744.
- Dorsett, Y. and Tuschl, T. 2004. siRNAs: Applications in functional genomics and potential as therapeutics. *Nat. Rev. Drug Discov.* **3**: 318–329.
- Ebhardt, H.A., Thi, E.P., Wang, M.B., and Unrau, P.J. 2005. Extensive 3' modification of plant small RNAs is modulated by helper component-proteinase expression. *Proc. Natl. Acad. Sci.* **102**: 13398–13403.
- Echeverri, C.J. and Perrimon, N. 2006. High-throughput RNAi screening in cultured cells: A user's guide. *Nat. Rev. Genet.* **7**: 373–384.
- Elbashir, S.M., Lendeckel, W., and Tuschl, T. 2001. RNA interference is mediated by 21 and 22 nt RNAs. *Genes & Dev.* **15**: 188–200.
- Elmén, J., Thonberg, H., Ljungberg, K., Frieden, M., Westergaard, M., Xu, Y., Wahren, B., Liang, Z., Ørum, H., Koch, T., et al. 2005. Locked nucleic acid (LNA) mediated improvements in siRNA stability and functionality. *Nucleic Acids Res.* **33**: 439–447. doi: 10.1093/nar/gki193.
- Filipowicz, W. 2005. RNAi: The nuts and bolts of the RISC machine. *Cell* **122**: 17–20.
- Filipowicz, W., Jaskiewicz, L., Kolb, F.A., and Pillai, R.S. 2005. Post-transcriptional gene silencing by siRNAs and miRNAs. *Curr. Opin. Struct. Biol.* **15**: 331–341.
- Förstemann, K., Tomari, Y., Du, T., Vagin, V.V., Denli, A.M., Bratu, D.P., Klattenhoff, C., Theurkauf, W.E., and Zamore, P.D. 2005. Normal microRNA maturation and germ-line stem cell maintenance requires Loquacious, a double-stranded RNA-binding domain protein. *PLoS Biol.* **3**: e236. doi: 10.1371/journal.pbio.0030236.
- Fuchs, F. and Boutros, M. 2006. Cellular phenotyping by RNAi. *Brief Funct. Genomic Proteomic* **5**: 52–56.
- Gentleman, R.C., Carey, V.J., Bates, D.M., Bolstad, B., Dettling, M., Dudoit, S., Ellis, B., Gautier, L., Ge, Y., Gentry, J., et al. 2004. Bioconductor: Open software development for computational biology and bioinformatics. *Genome Biol.* **5**: R80. doi: 10.1186/gb-2004-5-10-r80.
- Gregory, R.I., Chendrimada, T.P., Cooch, N., and Shiekhattar, R. 2005. Human RISC couples microRNA biogenesis and post-transcriptional gene silencing. *Cell* **123**: 631–640.

- Grimm, D., Streetz, K.L., Jopling, C.L., Storm, T.A., Pandey, K., Davis, C.R., Marion, P., Salazar, F., and Kay, M.A. 2006. Fatality in mice due to oversaturation of cellular microRNA/short hairpin RNA pathways. *Nature* **441**: 537–541.
- Haase, A.D., Jaskiewicz, L., Zhang, H., Laine, S., Sack, R., Gatignol, A., and Filipowicz, W. 2005. TRBP, a regulator of cellular PKR and HIV-1 virus expression, interacts with Dicer and functions in RNA silencing. *EMBO Rep.* **6**: 961–967.
- Hammond, S.M., Boettcher, S., Caudy, A.A., Kobayashi, R., and Hannon, G.J. 2001. Argonaute2, a link between genetic and biochemical analyses of RNAi. *Science* **293**: 1146–1150.
- Harborth, J., Elbashir, S.M., Vandeburgh, K., Manninga, H., Scaringe, S.A., Weber, K., and Tuschl, T. 2003. Sequence, chemical, and structural variation of small interfering RNAs and short hairpin RNAs and the effect on mammalian gene silencing. *Antisense Nucleic Acid Drug Dev.* **13**: 83–105.
- Horwich, M.D., Li, C., Matranga, C., Vagin, V., Farley, G., Wang, P., and Zamore, P.D. 2007. The *Drosophila* RNA methyltransferase, DmHen1, modifies germline piRNAs and single-stranded siRNAs in RISC. *Curr. Biol.* **17**: 1265–1272.
- Hutvagner, G. and Zamore, P.D. 2002. A microRNA in a multiple-turnover RNAi enzyme complex. *Science* **297**: 2056–2060.
- Jackson, A.L., Bartz, S.R., Schelter, J., Kobayashi, S.V., Burchard, J., Mao, M., Li, B., Cavet, G., and Linsley, P.S. 2003. Expression profiling reveals off-target gene regulation by RNAi. *Nat. Biotechnol.* **21**: 635–637.
- Jackson, A.L., Burchard, J., Leake, D., Reynolds, A., Schelter, J., Guo, J., Johnson, J.M., Lim, L., Karpilow, J., Nichols, K., et al. 2006a. Position-specific chemical modification of siRNAs reduces “off-target” transcript silencing. *RNA* **12**: 1197–1205.
- Jackson, A.L., Burchard, J., Schelter, J., Chau, B.N., Cleary, M., Lim, L., and Linsley, P.S. 2006b. Widespread siRNA “off-target” transcript silencing mediated by seed region sequence complementarity. *RNA* **12**: 1179–1187.
- Jiang, F., Ye, X., Liu, X., Fincher, L., McKearin, D., and Liu, Q. 2005. Dicer-1 and R3D1-L catalyze microRNA maturation in *Drosophila*. *Genes & Dev.* **19**: 1674–1679.
- Khvorova, A., Reynolds, A., and Jayasena, S.D. 2003. Functional siRNAs and miRNAs exhibit strand bias. *Cell* **115**: 209–216.
- Kirino, Y. and Mourelatos, Z. 2007. Mouse Piwi-interacting RNAs are 2'-O-methylated at their 3' termini. *Nat. Struct. Mol. Biol.* **14**: 347–348.
- Krausz, E. 2007. High-content siRNA screening. *Mol. Biosyst.* **3**: 232–240.
- Lai, E.C. 2002. Micro RNAs are complementary to 3'-UTR sequence motifs that mediate negative post-transcriptional regulation. *Nat. Genet.* **30**: 363–364.
- Lau, N.C., Lim, L.P., Weinstein, E.G., and Bartel, D.P. 2001. An abundant class of tiny RNAs with probable regulatory roles in *Caenorhabditis elegans*. *Science* **294**: 858–862.
- Lee, Y., Hur, I., Park, S.Y., Kim, Y.K., Suh, M.R., and Kim, V.N. 2006. The role of PACT in the RNA silencing pathway. *EMBO J.* **25**: 522–532.
- Leuschner, P.J., Ameres, S.L., Kueng, S., and Martinez, J. 2006. Cleavage of the siRNA passenger strand during RISC assembly in human cells. *EMBO Rep.* **7**: 314–320.
- Lewis, B.P., Shih, I., Jones-Rhoades, M.W., Bartel, D.P., and Burge, C.B. 2003. Prediction of mammalian microRNA targets. *Cell* **115**: 787–798.
- Lim, L.P., Lau, N.C., Garrett-Engele, P., Grimson, A., Schelter, J.M., Castle, J., Bartel, D.P., Linsley, P.S., and Johnson, J.M. 2005. Microarray analysis shows that some microRNAs downregulate large numbers of target mRNAs. *Nature* **433**: 769–773.
- Lin, X., Ruan, X., Anderson, M.G., McDowell, J.A., Kroeger, P.E., Fesik, S.W., and Shen, Y. 2005. siRNA-mediated off-target gene silencing triggered by a 7 nt complementation. *Nucleic Acids Res.* **33**: 4527–4535. doi: 10.1093/nar/gki762.
- Lingel, A., Simon, B., Izaurralde, E., and Sattler, M. 2004. Nucleic acid 3'-end recognition by the Argonaute2 PAZ domain. *Nat. Struct. Mol. Biol.* **11**: 576–577.
- Linsley, P.S., Schelter, J., Burchard, J., Kibukawa, M., Martin, M.M., Bartz, S.R., Johnson, J.M., Cummins, J.M., Raymond, C.K., Dai, H., et al. 2007. Transcripts targeted by the microRNA-16 family cooperatively regulate cell cycle progression. *Mol. Cell. Biol.* **27**: 2240–2252.
- Liu, Q., Rand, T.A., Kalidas, S., Du, F., Kim, H.E., Smith, D.P., and Wang, X. 2003. R2D2, a bridge between the initiation and effector steps of the *Drosophila* RNAi pathway. *Science* **301**: 1921–1925.
- Liu, J., Carmell, M.A., Rivas, F.V., Marsden, C.G., Thomson, J.M., Song, J.J., Hammond, S.M., Joshua-Tor, L., and Hannon, G.J. 2004. Argonaute2 is the catalytic engine of mammalian RNAi. *Science* **305**: 1437–1441.
- Liu, X., Jiang, F., Kalidas, S., Smith, D., and Liu, Q. 2006. Dicer-2 and R2D2 coordinately bind siRNA to promote assembly of the siRISC complexes. *RNA* **12**: 1514–1520.
- Ma, J.B., Ye, K., and Patel, D.J. 2004. Structural basis for overhang-specific small interfering RNA recognition by the PAZ domain. *Nature* **429**: 318–322.
- Ma, J.B., Yuan, Y.R., Meister, G., Pei, Y., Tuschl, T., and Patel, D.J. 2005. Structural basis for 5'-end-specific recognition of guide RNA by the *A. fulgidus* Piwi protein. *Nature* **434**: 666–670.
- Maniataki, E. and Mourelatos, Z. 2005. A human, ATP-independent, RISC assembly machine fueled by pre-miRNA. *Genes & Dev.* **19**: 2979–2990.
- Martinez, J., Patkaniowska, A., Urlaub, H., Lührmann, R., and Tuschl, T. 2002a. Single-stranded anti-sense siRNAs guide target RNA cleavage in RNAi. *Cell* **110**: 563–574.
- Martinez, L.A., Naguibneva, I., Lehmann, H., Vervisch, A., Tchenio, T., Lozano, G., and Harel-Bellan, A. 2002b. Synthetic small inhibiting RNAs: efficient tools to inactivate oncogenic mutations and restore p53 pathways. *Proc. Natl. Acad. Sci.* **99**: 14849–14854.
- Matranga, C., Tomari, Y., Shin, C., Bartel, D.P., and Zamore, P.D. 2005. Passenger-strand cleavage facilitates assembly of siRNA into Ago2-containing RNAi enzyme complexes. *Cell* **123**: 607–620.
- Meister, G. and Tuschl, T. 2004. Mechanisms of gene silencing by double-stranded RNA. *Nature* **431**: 343–349.
- Meister, G., Landthaler, M., Patkaniowska, A., Dorsett, Y., Teng, G., and Tuschl, T. 2004. Human Argonaute2 mediates RNA cleavage targeted by miRNAs and siRNAs. *Mol. Cell* **15**: 185–197.
- Meister, G., Landthaler, M., Peters, L., Chen, P.Y., Urlaub, H., Lührmann, R., and Tuschl, T. 2005. Identification of novel Argonaute-associated proteins. *Curr. Biol.* **15**: 2149–2155.
- Miyoshi, K., Tsukumo, H., Nagami, T., Siomi, H., and Siomi, M.C. 2005. Slicer function of *Drosophila* Argonautes and its involvement in RISC formation. *Genes & Dev.* **19**: 2837–2848.
- Nykänen, A., Haley, B., and Zamore, P.D. 2001. ATP requirements and small interfering RNA structure in the RNA interference pathway. *Cell* **107**: 309–321.
- Ohara, T., Sakaguchi, Y., Suzuki, T., Ueda, H., and Miyachi, K. 2007. The 3' termini of mouse Piwi-interacting RNAs are 2'-O-methylated. *Nat. Struct. Mol. Biol.* **14**: 349–350.
- Parker, J.S., Roe, S.M., and Barford, D. 2004. Crystal structure of a PIWI protein suggests mechanisms for siRNA recognition and slicer activity. *EMBO J.* **23**: 4727–4737.
- Parker, J.S., Roe, S.M., and Barford, D. 2005. Structural insights into mRNA recognition from a PIWI domain-siRNA guide complex. *Nature* **434**: 663–666.
- Pei, Y. and Tuschl, T. 2006. On the art of identifying effective and specific siRNAs. *Na. Methods* **3**: 670–676.
- Pelisson, A., Sarot, E., Payen-Groschene, G., and Bucheton, A. 2007. A novel repeat-associated small interfering RNA-mediated silencing pathway downregulates complementary sense gypsy transcripts in somatic cells of the *Drosophila* ovary. *J. Virol.* **81**: 1951–1960.
- Peters, L. and Meister, G. 2007. Argonaute proteins: Mediators of RNA silencing. *Mol. Cell* **26**: 611–623.
- Preall, J.B. and Sontheimer, E.J. 2005. RNAi: RISC gets loaded. *Cell* **123**: 543–545.

- Rajewsky, N. and Socci, N.D. 2004. Computational identification of microRNA targets. *Dev. Biol.* **267**: 529–535.
- Rand, T.A., Ginalski, K., Grishin, N.V., and Wang, X. 2004. Biochemical identification of Argonaute 2 as the sole protein required for RNA-induced silencing complex activity. *Proc. Natl. Acad. Sci.* **101**: 14385–14389.
- Rand, T.A., Petersen, S., Du, F., and Wang, X. 2005. Argonaute2 cleaves the anti-guide strand of siRNA during RISC activation. *Cell* **123**: 621–629.
- Rivas, F.V., Tolia, N.H., Song, J.J., Aragon, J.P., Liu, J., Hannon, G.J., and Joshua-Tor, L. 2005. Purified Argonaute2 and an siRNA form recombinant human RISC. *Nat. Struct. Mol. Biol.* **12**: 340–349.
- Robb, G.B. and Rana, T.M. 2007. RNA helicase A interacts with RISC in human cells and functions in RISC loading. *Mol. Cell* **26**: 523–537.
- Root, D.E., Hacohen, N., Hahn, W.C., Lander, E.S., and Sabatini, D.M. 2006. Genome-scale loss-of-function screening with a lentiviral RNAi library. *Nat. Methods* **3**: 715–719.
- Saito, K., Ishizuka, A., Siomi, H., and Siomi, M.C. 2005. Processing of pre-microRNAs by the Dicer-1-Loquacious complex in *Drosophila* cells. *PLoS Biol.* **3**: e235. doi: 10.1371/journal.pbio.0030235.
- Saito, K., Sakaguchi, Y., Suzuki, T., Siomi, H., and Siomi, M.C. 2007. Pimet, the *Drosophila* homolog of HEN1, mediates 2'-O-methylation of Piwi-interacting RNAs at their 3' ends. *Genes & Dev.* **21**: 1603–1608.
- Schwarz, D.S., Hutvagner, G., Du, T., Xu, Z., Aronin, N., and Zamore, P.D. 2003. Asymmetry in the assembly of the RNAi enzyme complex. *Cell* **115**: 199–208.
- Song, J.J. and Joshua-Tor, L. 2006. Argonaute and RNA—Getting into the groove. *Curr. Opin. Struct. Biol.* **16**: 5–11.
- Song, J.J., Liu, J., Tolia, N.H., Schneiderman, J., Smith, S.K., Martienssen, R.A., Hannon, G.J., and Joshua-Tor, L. 2003. The crystal structure of the Argonaute2 PAZ domain reveals an RNA binding motif in RNAi effector complexes. *Nat. Struct. Biol.* **10**: 1026–1032.
- Song, J.J., Smith, S.K., Hannon, G.J., and Joshua-Tor, L. 2004. Crystal structure of Argonaute and its implications for RISC slicer activity. *Science* **305**: 1434–1437.
- Stark, A., Brennecke, J., Russell, R.B., and Cohen, S.M. 2003. Identification of *Drosophila* microRNA targets. *PLoS Biol.* **1**: 397–409. doi: 10.1371/journal.pbio.0000060.
- Tomari, Y., Du, T., Haley, B., Schwarz, D.S., Bennett, R., Cook, H.A., Koppetsch, B.S., Theurkauf, W.E., and Zamore, P.D. 2004a. RISC assembly defects in the *Drosophila* RNAi mutant armitage. *Cell* **116**: 831–841.
- Tomari, Y., Matranga, C., Haley, B., Martinez, N., and Zamore, P.D. 2004b. A protein sensor for siRNA asymmetry. *Science* **306**: 1377–1380.
- Tomari, Y. and Zamore, P.D. 2005. Perspective: Machines for RNAi. *Genes & Dev.* **19**: 517–529.
- Tuschl, T., Zamore, P.D., Lehmann, R., Bartel, D.P., and Sharp, P.A. 1999. Targeted mRNA degradation by double-stranded RNA in vitro. *Genes & Dev.* **13**: 3191–3197.
- Vagin, V.V., Sigova, A., Li, C., Seitz, H., Gvozdev, V., and Zamore, P.D. 2006. A distinct small RNA pathway silences selfish genetic elements in the germline. *Science* **313**: 320–324.
- Weitzer, S. and Martinez, J. 2007. The human RNA kinase hClp1 is active on 3' transfer RNA exons and short interfering RNAs. *Nature* **447**: 222–226.
- Wu, Z., Irizarry, R.A., Gentleman, R., Martinez-Murillo, F., and Spencer, F. 2004. A model-based background adjustment for oligonucleotide expression arrays. *J. Am. Stat. Assoc.* **99**: 909–917.
- Yan, K.S., Yan, S., Farooq, A., Han, A., Zeng, L., and Zhou, M.M. 2003. Structure and conserved RNA binding of the PAZ domain. *Nature* **426**: 468–474.
- Yu, B., Yang, Z., Li, J., Minakhina, S., Yang, M., Padgett, R.W., Steward, R., and Chen, X. 2005. Methylation as a crucial step in plant microRNA biogenesis. *Science* **307**: 932–935.
- Yuan, Y.R., Pei, Y., Ma, J.B., Kuryavyi, V., Zhadina, M., Meister, G., Chen, H.Y., Dauter, Z., Tuschl, T., and Patel, D.J. 2005. Crystal structure of *A. aeolicus* Argonaute, a site-specific DNA-guided endoribonuclease, provides insights into RISC-mediated mRNA cleavage. *Mol. Cell* **19**: 405–419.
- Yuan, Y.R., Pei, Y., Chen, H.Y., Tuschl, T., and Patel, D.J. 2006. A potential protein-RNA recognition event along the RISC-loading pathway from the structure of *A. aeolicus* Argonaute with externally bound siRNA. *Structure* **14**: 1557–1565.



RNA
A PUBLICATION OF THE RNA SOCIETY

A multifunctional human Argonaute2-specific monoclonal antibody

Sabine Rüdell, Andrew Flatley, Lasse Weinmann, et al.

RNA 2008 14: 1244-1253

Access the most recent version at doi:[10.1261/rna.973808](https://doi.org/10.1261/rna.973808)

References

This article cites 55 articles, 17 of which can be accessed free at:
<http://rnajournal.cshlp.org/content/14/6/1244.full.html#ref-list-1>

Article cited in:

<http://rnajournal.cshlp.org/content/14/6/1244.full.html#related-urls>

Email alerting service

Receive free email alerts when new articles cite this article - sign up in the box at the top right corner of the article or [click here](#)

To subscribe to RNA go to:
<http://rnajournal.cshlp.org/subscriptions>

METHOD

A multifunctional human Argonaute2-specific monoclonal antibody

SABINE RÜDEL,¹ ANDREW FLATLEY,² LASSE WEINMANN,¹ ELISABETH KREMMER,² and GUNTER MEISTER¹

¹Center for Integrated Protein Science Munich (CIPSM), Laboratory of RNA Biology, Max Planck Institute of Biochemistry, 82152 Martinsried, Germany

²Helmholtz Center Munich, Institute of Molecular Immunology, 81377 Munich, Germany

ABSTRACT

Small regulatory RNAs including small interfering RNAs (siRNAs), microRNAs (miRNAs), or Piwi interacting RNAs (piRNAs) guide regulation of gene expression in many different organisms. The Argonaute (Ago) protein family constitutes the cellular binding partners of such small RNAs and regulates gene expression on the levels of transcription, mRNA stability, or translation. Due to the lack of highly specific and potent monoclonal antibodies directed against the different Ago proteins, biochemical analyses such as Ago complex purification and characterization rely on overexpression of tagged Ago proteins. Here, we report the generation and functional characterization of a highly specific monoclonal anti-Ago2 antibody termed anti-Ago2(11A9). We show that anti-Ago2(11A9) is specific for human Ago2 and detects Ago2 in Western blots as well as in immunoprecipitation experiments. We further demonstrate that Ago2 can be efficiently eluted from our antibody by a competing peptide. Finally, we show that anti-Ago2(11A9) recognizes Ago2 in immunofluorescence experiments, and we find that Ago2 not only localizes to cytoplasmic processing bodies (P-bodies) and the diffuse cytoplasm but also to the nucleus. With the anti-Ago2(11A9) antibody we have generated a potent tool that is useful for many biochemical or cell biological applications.

Keywords: Argonaute proteins; microRNAs; RISC; RNAi; gene silencing

INTRODUCTION

RNA silencing, or RNA interference (RNAi), is an evolutionarily conserved gene silencing pathway that is triggered by dsRNA (Meister and Tuschl 2004). The dsRNA trigger molecules are processed to small interfering RNAs (siRNAs) or microRNAs (miRNAs), which are then assembled into various silencing effector complexes, including the RNA-induced silencing complex (RISC) (Meister and Tuschl 2004; Filipowicz et al. 2005; Zamore and Haley 2005). Effector complexes containing miRNAs are often referred to as miRNPs (Mourelatos et al. 2002). miRNA precursors (pre-miRNAs) are excised from primary transcripts by a nuclear endonucleolytic complex that contains the RNase III enzyme Droscha and the dsRNA-binding domain (dsRBD) protein DGCR8/Pasha (Chen and Meister 2005; Zamore and Haley 2005). Pre-miRNAs are subsequently exported to the cytoplasm by the export receptor Exportin5

for further maturation (Chen and Meister 2005; Zamore and Haley 2005). In the cytoplasm, dsRNA and pre-miRNAs are processed by the RNase III enzyme Dicer to duplexes of ~21–23 nucleotides (nt) (Meister and Tuschl 2004). Similar to Droscha, Dicer functions in concert with dsRBD proteins as well. In humans, the immunodeficiency virus *trans*-activating response RNA-binding protein (TRBP) interacts with Dicer and contributes to the processing of miRNA precursors (Chendrimada et al. 2005; Haase et al. 2005). Recently, the dsRBD protein PACT has been shown to functionally interact with human Dicer as well (Lee et al. 2006). In a subsequent assembly process, which is not yet fully understood and presumably involves the action of ATP dependent helicases, only one strand of the siRNA or miRNA duplex intermediate is loaded into the silencing effector complex to become the guide sequence (Meister and Tuschl 2004). Notably, the putative RNA helicases RNA Helicase A (RHA) as well as DDX5/p68 have recently been implicated in RISC loading (Robb and Rana 2007; Salzman et al. 2007). An alternative model for RISC loading and activation has been proposed. In this model, the sense strand of the siRNA (also termed nonguide or passenger strand) is cleaved by Ago2, and the short 10- to 12-nt long cleavage products dissociate from the RISC

Reprint requests to: Gunter Meister, Center for Integrated Protein Science Munich (CIPSM), Laboratory of RNA Biology, Max Planck Institute of Biochemistry, Am Klopferspitz 18, 82152 Martinsried, Germany; e-mail: meister@biochem.mpg.de; fax: +49 8578 3430.

Article published online ahead of print. Article and publication date are at <http://www.rnajournal.org/cgi/doi/10.1261/rna.973808>.

presumably without the help of helicases (Matranga et al. 2005; Rand et al. 2005; Leuschner et al. 2006). The identification of a complex consisting of Ago2, TRBP, and Dicer that can be loaded with dsRNA or pre-miRNAs without the help of assisting helicases supports the above-mentioned RISC loading model (Gregory et al. 2005). However, the loading of endonucleolytically inactive human Ago1, Ago3, and Ago4 complexes is not explained by such a model and presumably involves different pathways.

Depending on the complementarity between the small guide RNA and its target, siRNAs and miRNAs guide either the sequence-specific degradation of complementary RNA molecules or inhibit the translation of partially complementary target mRNAs (Pillai et al. 2007). Recently, a third pathway of miRNA function has been identified in *Drosophila* and zebrafish, in which miRNAs guide the degradation of imperfectly complementary target mRNAs by recruiting deadenylation and decapping enzymes (Behm-Ansmant et al. 2006; Giraldez et al. 2006).

Members of the Ago protein family are key components of RNA silencing effector complexes. Ago proteins contain piwi-argonaute-zwille (PAZ) and PIWI domains (Carmell et al. 2002; Peters and Meister 2007; Hutvagner and Simard 2008). Recently, structures of PIWI domains, isolated PAZ domains, as well as full-length archaeal Ago proteins have been solved by NMR and X-ray crystallography (Hall 2005; Parker and Barford 2006; Patel et al. 2006; Song and Joshua-Tor 2006). The PIWI domain structures of bacterial proteins revealed striking similarity to RNase H, and it has been demonstrated that these proteins contain endonucleolytic activity (Parker et al. 2004; Song et al. 2004). Studies on human Ago proteins revealed that Ago2 is the endonuclease that cleaves the target RNA in RNAi (Liu et al. 2004; Meister et al. 2004). The MID domain, which is located N-terminally of the PIWI domain, forms the 5' phosphate binding pocket for the small RNA that sets the register for target RNA cleavage (Ma et al. 2005; Parker et al. 2005). Recently, a conserved tyrosine residue within this binding pocket has been implicated in protein-protein interaction as well (Till et al. 2007). The previously characterized PAZ domain of Ago proteins specifically recognizes and binds the single-stranded 3' ends of small RNAs (Hall 2005; Song and Joshua-Tor 2006).

Besides Ago proteins as core components of RNA silencing effector complexes, additional proteins have been identified in different experimental systems (for review, see Peters and Meister 2007). In humans, interactions of Ago2 with FMRP (fragile X mental retardation protein) have been observed (Jin et al. 2004). Furthermore, human miRNAs reside in a defined 15S complex that contains Gemin3, Gemin4, and Ago2 (Mourelatos et al. 2002). Recently, biochemical purifications of Ago1 and Ago2 complexes from HeLa cell lysates identified the DExD box protein MOV10 and a protein termed TNRC6B as novel Ago complex components. The precise function of

these different proteins in the RNA silencing process, however, remains elusive (Meister et al. 2005). Interestingly, TNRC6B is highly homologous with TNRC6A (GW182), which has been implicated in small RNA-guided gene silencing in many different organisms and constitutes a marker protein for P-bodies (Ding et al. 2005; Jakymiw et al. 2005; Liu et al. 2005a; Behm-Ansmant et al. 2006). P-bodies are cellular sites of RNA metabolism (Eulalio et al. 2007a), and it has been shown that Ago proteins localize to P-bodies as well (Liu et al. 2005b; Meister et al. 2005; Sen and Blau 2005). Further studies revealed that miRNAs as well as target mRNAs are also found in P-bodies, and it has been suggested that localization of mRNAs to P-bodies may prevent their translation (Liu et al. 2005b; Pillai et al. 2005; Bhattacharyya et al. 2006). However, it has also been shown that P-bodies form as a consequence of miRNA-guided gene silencing but are not required for it (Eulalio et al. 2007b).

In human cells, Ago proteins are found in different protein complexes with distinct molecular weights (Martinez et al. 2002; Mourelatos et al. 2002; Hock et al. 2007). Furthermore, Ago proteins are embedded into large mRNA-protein structures, and it has been shown that miRNA-targeted mRNAs can be isolated and identified from purified Ago complexes (Beitzinger et al. 2007; Easow et al. 2007; Karginov et al. 2007). In combination with bioinformatic miRNA target prediction algorithms, such biochemical approaches provide a novel tool for fast and reliable miRNA target identification. However, due to the lack of potent and highly specific antibodies against human Ago proteins, many biochemical studies rely on overexpression of a tagged Ago version, which sometimes interferes with natural protein function.

Here, we report the generation and functional characterization of a monoclonal anti-Ago2 antibody. This antibody recognizes human Ago2 in Western blots and does not cross-react with other human Ago proteins. Furthermore, we demonstrate that the anti-Ago2 antibody specifically immunoprecipitates Flag/HA-tagged as well as endogenous Ago2 without precipitating other Ago proteins. Moreover, we show that bound Ago2 can be efficiently eluted from the antibody matrix by competition with a short peptide comprising the epitope of the antibody. Finally, we demonstrate that the anti-Ago2 antibody recognizes cellular Ago2 in immunofluorescence studies by presenting data on endogenous Ago2 distribution without overexpression.

RESULTS

Anti-Ago2(11A9) discriminates between Ago2 and other human Ago proteins in Western blots

Due to the lack of potent and specific antibodies, most of the biochemical studies on human Ago proteins used overexpressed, tagged Ago proteins. In order to better understand endogenous RISC function, we set out to

generate a specific monoclonal anti-Ago2 antibody. A peptide encompassing the very N-terminal end of human Ago2 that is not conserved in other human Ago proteins (Fig. 1A) was injected into rats for monoclonal antibody production. We obtained hybridoma clone 11A9, which reacted strongly in an initial ELISA screen coated with the injected peptide (data not shown). Next, we analyzed anti-Ago2(11A9) in Western blots. Flag/HA-tagged Ago1 through 4 (FH-Ago) were expressed in HEK 293 cells and immunoprecipitated using anti-Flag antibody-coated agarose beads (Fig. 1B). Similar amounts of FH-Ago1–4 as well as FH-GFP were blotted onto nitrocellulose membranes and subsequently probed with anti-HA (Fig. 1B, lanes 7–12) or anti-Ago2(11A9) antibodies (Fig. 1B, lanes 1–6). Strikingly, anti-Ago2(11A9) strongly reacted with FH-Ago2 in Western blots (Fig. 1B, lane 2), whereas FH-Ago1, 3, 4, or FH-GFP were not detected by the antibody. Similar results were obtained using myc-tagged Ago proteins (Fig. 1B, lanes 13–24), indicating that anti-Ago2(11A9) is highly specific for Ago2 in Western blots.

Next, we investigated the Western blotting specificity of anti-Ago2(11A9) in lysates from untreated cells (Fig. 1C). Total cell lysates from RPE-1, HEK 293, and HeLa cells were analyzed using anti-Ago2(11A9) (Fig. 1C, lanes 1–3). Anti-Ago2(11A9) detected one single band with a molecular weight of ~ 100 kDa, indicating that the antibody is highly specific for endogenous Ago2 as well. No signal was observed when lysate from the mouse neuroblastoma cell line N2A was analyzed, demonstrating that anti-Ago2(11A9) does not recognize mouse Ago2. For further validation of the antibody, we separated nuclear and cytoplasmic extracts from the above-mentioned cell lines (Fig. 1C, lanes 5–12). Consistently, anti-Ago2(11A9) recognized specifically Ago2 in the cytoplasmic fractions. Interestingly, Ago2 is also detected in the nuclear fractions, suggesting putative roles of Ago2 in the nucleus or associated cellular compartments. Notably, two additional bands of unknown identity were detected in the nuclear fractions, which most likely reflect cross-reactivity with nuclear proteins. However, these bands were not detected in total cell lysates, presumably due to lower amounts of nuclear proteins therein. Using anti-Ago2(11A9), we analyzed endogenous Ago2 levels in a variety of cell lines (Fig. 1D). Interestingly, anti-Ago2(11A9) detects an additional band migrating slower than Ago2 in some cell lines, which most likely reflects post-translational modification of Ago2.

In summary, we have generated a monoclonal antibody that is highly specific for human Ago2 in Western blots. This antibody is available from www.ascenion.de.

Anti-Ago2(11A9) specifically immunoprecipitates human RISC

In order to perform biochemical studies on endogenous RISC, we analyzed anti-Ago2(11A9) for its immunoprecip-

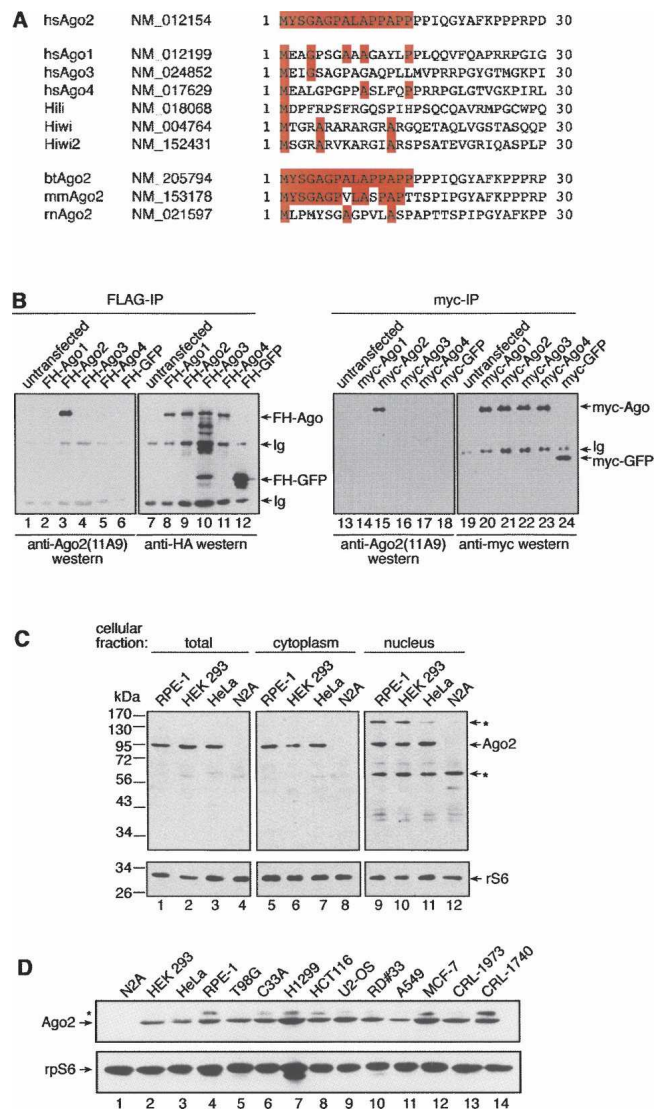


FIGURE 1. Anti-Ago2(11A9) is Ago2-specific in Western blots. (A) Amino acid alignment of the Ago2 peptide used for antibody generation. (B) Flag/HA-tagged Ago1 (FH-Ago1) through FH-Ago4 (lanes 1–5, 7–11), FH-GFP (lanes 6, 12), myc-Ago1 through 4 (lanes 13–17, 19–23), and myc-GFP (lanes 18, 24) were expressed in HEK 293 cells and immunoprecipitated using anti-Flag or anti-myc antibodies. Blotted immunoprecipitates were probed with anti-Ago2(11A9) (lanes 1–6, 13–18), anti-HA (lanes 7–12), or anti-myc antibodies (lanes 19–24). Ig indicates heavy and light chains of the immunoglobulins. (C) 30 μ g of total cell lysate (lanes 1–4), cytoplasmic extract (lanes 5–8), or nuclear extract (lanes 9–12) from RPE-1, HEK 293, or HeLa cells was blotted and probed with anti-Ago2(11A9). A Western blot using antibodies against the ribosomal protein S6 (rS6) served as a loading control (lower panel). (Asterisks) Unidentified proteins. (D) Total cell lysate from various cell lines was analyzed using anti-Ago2(11A9) (upper panel) or anti-rS6 (lower panel) as loading control. (Asterisk) Additional band recognized by anti-Ago2(11A9), which might correspond to post-translational modifications.

itation capabilities. Myc-tagged Ago1 through 4 were expressed in HEK 293 cells, and the lysates were subjected to anti-Ago2(11A9) immunoprecipitation (Fig. 2A). Immunoprecipitated proteins were further analyzed by Western blotting using anti-myc antibodies. The monoclonal anti-Ago2(11A9) antibody readily immunoprecipitated myc-Ago2 (Fig. 2A, lane 6) whereas no myc-Ago1, myc-Ago3, or myc-Ago4 (Fig. 2A, lanes 5,7,8) was immunoprecipitated. Our results clearly show that anti-Ago2(11A9) specifically recognizes and efficiently immunoprecipitates

myc-Ago2 and is therefore a valuable tool for biochemical analysis of human RISC.

Ago proteins are known to bind miRNAs (Peters and Meister 2007; Hutvagner and Simard 2008). Ago complex isolation followed by small RNA cloning and sequencing can be a useful tool for small RNA profiling in different cell lines or primary tissues, because Ago association indicates functional small RNA classes and clearly discriminates them from cellular RNA degradation products. Therefore, we analyzed if anti-Ago2(11A9) coimmunoprecipitates endogenous miRNAs. HEK 293 lysates were subjected to immunoprecipitation using anti-Ago2(11A9) (Fig. 2B). The coprecipitated RNA was separated by denaturing RNA PAGE and analyzed by Northern blotting using a probe complementary to miR-19b. MiR-19b was detectable in the total RNA sample (Fig. 2B, lane 1) and in the anti-Ago2(11A9) coimmunoprecipitate (Fig. 2B, lane 3). No miR-19b signal was observed in the anti-Flag control immunoprecipitation (Fig. 2B, lane 2). Similar results were obtained for many other miRNAs present in HEK 293 cells (data not shown).

It has been reported earlier that human Ago2 is the catalytic subunit of RISC (Liu et al. 2004; Meister et al. 2004). In order to analyze if anti-Ago2(11A9) immunoprecipitates functional RISC from human cell lysates, we performed *in vitro* cleavage assays (Fig. 2C). Ago2 was immunoprecipitated from untreated HEK 293 cell lysates using anti-Ago2(11A9) and incubated with a 32 P-cap-labeled substrate RNA containing a fully complementary binding site for endogenous miR-19b. Strikingly, a specific RISC cleavage product was observed only in the anti-Ago2(11A9) immunoprecipitate (Fig. 2C, lane 5), whereas no specific signal was detected in the control experiment (Fig. 2C, lane 4). Finally, we investigated if RISC activity can be reconstituted *in vitro* by using synthetic siRNAs in combination with anti-Ago2(11A9) immunoprecipitates (Fig. 2C). Endogenous Ago2 was immunoprecipitated using our monoclonal antibody and subsequently loaded with a synthetic single-stranded siRNA. The siRNA-primed Ago2 complex was further incubated with a radiolabeled target RNA containing a fully complementary target site for the synthetic siRNA. The immunoprecipitated Ago2 cleaved the target RNA (Fig. 2C, lane 2), whereas no specific cleavage signal was observed in the control immunoprecipitate (Fig. 2C, lane 1).

In summary, we have shown that our monoclonal anti-Ago2(11A9) antibody discriminates between Ago2 and other human Ago proteins in immunoprecipitation experiments and immunoprecipitates active RISC from untreated human cell lysates.

Native RISC isolation using peptide elution

Biochemical studies on RISC function such as kinetic measurements or proteomics often require soluble and pure complex isolations. This can be achieved by specific

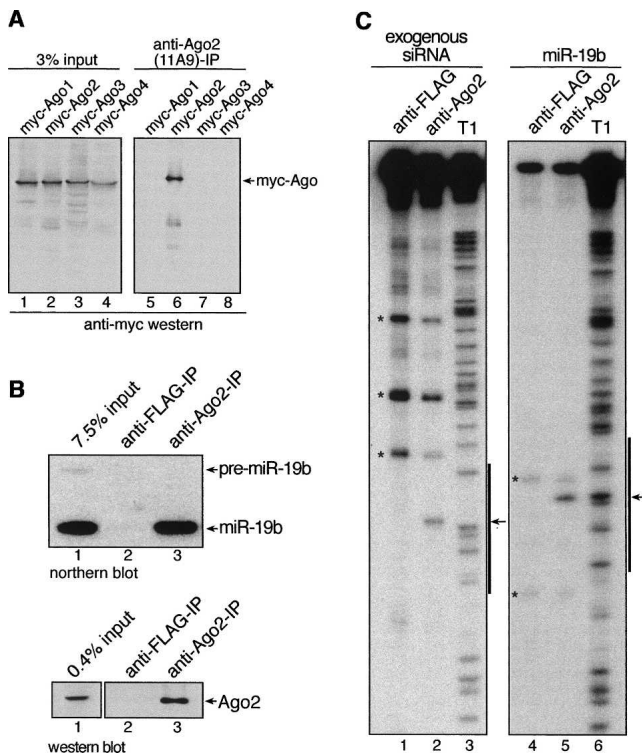


FIGURE 2. Anti-Ago2(11A9) specifically immunoprecipitates human Ago2 and therefore RISC. (A) myc-Ago1 through myc-Ago4 were expressed in HEK 293 cells and immunoprecipitated with anti-Ago2(11A9) (lanes 5–8). Immunoprecipitated proteins were analyzed by Western blotting using anti-myc antibodies. (Lanes 1–4) 3% of the lysate that has been used for the immunoprecipitations. (B) Endogenous Ago2 was immunoprecipitated from HEK 293 cell lysates using anti-Ago2(11A9) (lane 3). Associated RNA was extracted and analyzed by Northern blotting using a probe specific for the endogenous miR-19b (upper panel), while immunoprecipitated proteins were analyzed by Western blotting using anti-Ago2(11A9) (lower panel). An anti-Flag antibody served as negative control (lane 2). (Lane 1) 7.5% or 0.4% input. (C) Anti-Ago2(11A9) (lanes 2,5) or anti-Flag antibodies (lanes 1,4) were used for immunoprecipitation from untreated HEK 293 cell lysates. Immunoprecipitates were either preincubated with a single-stranded siRNA (lanes 1,2) or directly used for cleavage assays (lanes 4,5). 32 P-cap-labeled RNAs containing complementary target sites for the siRNA (lanes 1–3) or endogenous miR-19b (lanes 4–6) were used as RISC target RNAs. The cleavage products were analyzed by denaturing RNA PAGE followed by autoradiography. (T1 lanes) Nuclease T1 digestion of the substrate RNA. The small RNA target sites are indicated (black bars to the right of the gels), and the individual cleavage positions are marked (arrows). (Asterisks) Unspecific degradation products.

elution of affinity-captured proteins by adding a peptide encompassing the antibody epitope. We therefore set out to establish a protocol for native elution of Ago2 from the anti-Ago2(11A9) antibody matrix (Fig. 3A). We expressed FH-Ago2 in HEK 293 cells and immunoprecipitated tagged Ago2 with anti-Ago2(11A9). After stringent washing, a peptide encompassing the epitope of anti-Ago2(11A9) was added to compete for antibody binding (Fig. 3A). After 90 min of incubation with the Ago2 peptide, a considerable amount of bound Ago2 was eluted from the column (Fig. 3B, upper panel, lane 4), whereas no Ago2 was detected when the competing peptide was omitted from the reaction (Fig. 3B, middle panel). Similar results were obtained when endogenous Ago2 was immunoprecipitated from wild-type

HEK 293 cells (Fig. 3B, lower panel). Since antibody interactions are often sensitive to slight pH shifts, we repeated the experiment described above using different pH conditions to identify the optimal pH range for efficient elution (Fig. 3C). Lowering the pH from 7.5 to 7.0 had only a minor effect on the elution efficiency. However, at pH 8.0 almost all bound Ago2 was eluted from the column, indicating that RISC can be efficiently dissociated from the anti-Ago2(11A9) antibody. We next investigated if RISC activity is maintained during the above-mentioned elution procedure (Fig. 3D). Therefore, peptide-eluted RISC was incubated with a target RNA complementary to endogenous miR-19b, and the cleavage products were analyzed by denaturing RNA PAGE. Strikingly, only in the reaction where eluted RISC was present was a specific cleavage product detectable (Fig. 3D, lane 5), demonstrating that Ago2 complexes can be efficiently eluted by peptide competition.

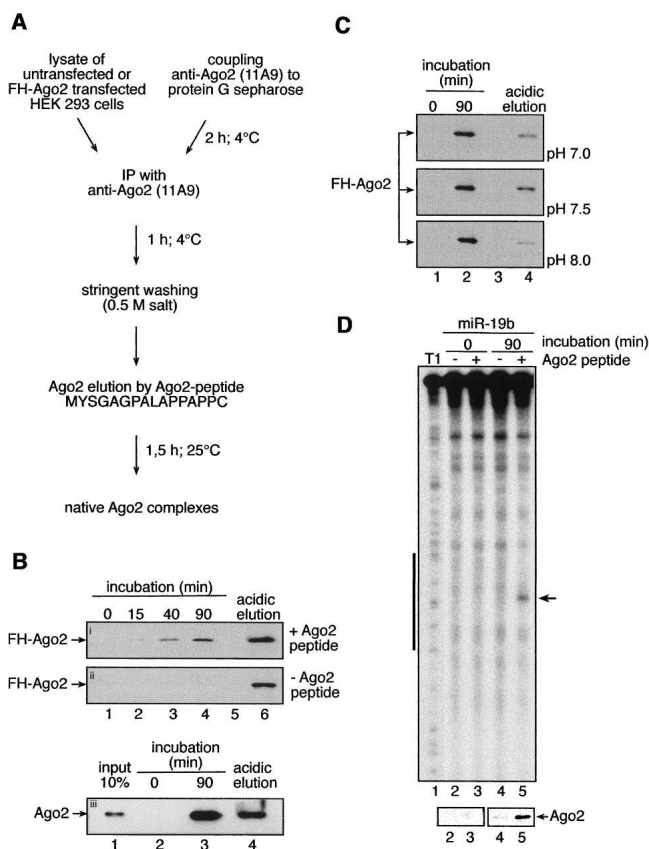


FIGURE 3. Peptide elution of Ago2 from anti-Ago2(11A9) antibodies. (A) Schematic representation of the experimental set up used in B–D. (B) FH-Ago2 was expressed in HEK 293 cells and immunoprecipitated using anti-Ago2(11A9). Antibody-bound Ago2 was incubated with (panel *i*) or without (panel *ii*) addition of an Ago2 peptide encompassing the anti-Ago2(11A9) epitope for the indicated time intervals. (Lane 6) Denaturing elution of remaining Ago2. In panel *iii*, untransfected HEK 293 cell lysate was used. (C) Experiments were performed as described in B using pH 7 (upper panel), pH 7.5 (middle panel), or pH 8 (lower panel) for elution. (D) Endogenous Ago2 was immunoprecipitated with anti-Ago2(11A9) and eluted as described in B. Eluates were incubated with a ³²P-cap-labeled target RNA complementary to endogenous miR-19b, and RISC cleavage assays were performed as described in Fig. 2C. (Lower panel) Western blot of the eluates.

Anti-Ago2(11A9) detects Ago2 in immunofluorescence experiments

Cellular Ago localization studies using immunofluorescence have been performed using tagged and overexpressed human Ago proteins or sera that have not been tested for cross-reactivity with other Ago proteins (Jakymiw et al. 2005; Liu et al. 2005b; Meister et al. 2005; Sen and Blau 2005). In order to find an antibody that specifically recognizes endogenous Ago2, we tested anti-Ago2(11A9) in immunofluorescence experiments using confocal microscopy (Fig. 4). HEK 293 (upper panels), HeLa (middle panels), or RPE-1 cells (lower panels) were fixed and stained with anti-Ago2(11A9) and anti-LSm4 antibodies. LSm4 is a component of the cellular RNA degradation machinery and served as a marker protein for P-bodies. In all three cell types, anti-Ago(11A9) showed a diffuse cytoplasmic staining. Moreover, distinct cytoplasmic foci that can be co-stained with anti-LSm4 antibodies and therefore indicate P-bodies are clearly visible (white arrows). Only a very weak background staining was observed when anti-Ago2(11A9) was omitted from the experiment (Fig. 4, panels 13,14). Interestingly, the confocal images from all three cell types revealed a detectable nuclear staining. In order to rule out that the nuclear signals are caused by anti-Ago2(11A9) cross-reactivities observed in Western blots (Fig. 1B), we performed an Ago2 knock down prior to anti-Ago2(11A9) staining (Fig. 4B). Notably, both the cytoplasmic and the nuclear staining disappeared after Ago2 knock down, indicating that the signals observed in anti-Ago2(11A9) stainings represent intracellular Ago2 localization.

DISCUSSION

Human RISC or Ago protein complexes have been purified using different biochemical approaches. RISC has been reconstituted on biotinylated siRNAs, or tagged Ago

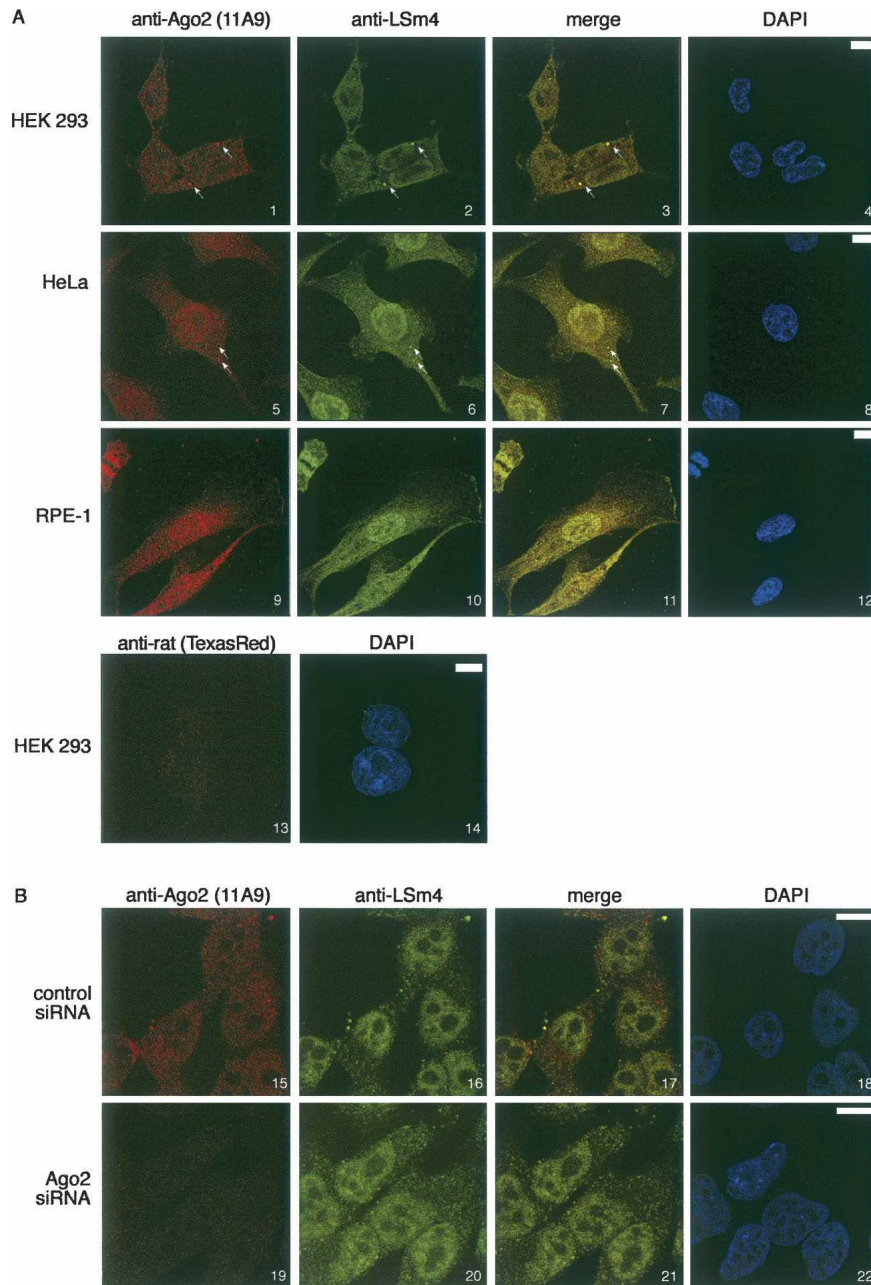


FIGURE 4. Anti-Ago2(11A9) detects endogenous Ago2 in immunofluorescence experiments. (A) HEK 293 cells (panels 1–4,13–14), HeLa cells (panels 5–8), or RPE-1 cells (panels 9–12) were fixed and stained with anti-Ago2(11A9) (panels 1,5,9,13) and anti-LSm4 antibodies (panels 2,6,10). (Panels 3,7,11) Merged images, (panels 4,8,12,14) DAPI staining. In panels 13 and 14, anti-Ago2(11A9) was omitted from the experiment. (B) HeLa cells were transfected with siRNAs against Ago2 (panels 19–22) or control siRNAs (panels 15–18). Cells were fixed and stained with anti-Ago2(11A9) (panels 15,19) or anti-LSm4 antibodies (panels 16,20). (Panels 18,22) DAPI stainings.

proteins were expressed and purified using affinity chromatography (Martinez et al. 2002; Gregory et al. 2005; Maniataki and Mourelatos 2005; Meister et al. 2005; Hock et al. 2007). Although these studies were very successful and key discoveries have been made, such approaches are for

three main reasons not ideal. First, overexpression of tagged Ago proteins may cause artificial protein–protein interactions. Second, tagging of proteins may interfere with function. This has not been observed for RISC activity when Ago2 was N-terminally tagged. However, it cannot be excluded that the tag affects other as yet unknown Ago2 functions. Third, and most importantly, tagged Ago proteins can only be introduced into transfectable cell lines. Very often, purification from primary cells or even tissue samples is more conclusive. Therefore, we have generated the monoclonal anti-Ago2(11A9) antibody in order to be independent of transfection and overexpression. We show that our monoclonal antibody is specific for Ago2 and does not react with the other highly conserved human Ago proteins. Moreover, anti-Ago2(11A9) immunoprecipitates active RISC from untreated cell lysates with high efficiency, providing a useful tool for Ago2 complex isolation from cells or tissues.

In many affinity purification protocols, the elution from the affinity matrix is often a critical step, because denaturing conditions often result in the elution of contaminants as well that bind unspecifically to the column. Strikingly, Ago2 can be efficiently eluted from the anti-Ago2(11A9) antibody by adding a peptide encompassing the epitope of the antibody, thus competing for binding.

Various small RNA cloning and sequencing approaches have been performed in organisms as diverse as plants, nematodes, flies, and mammals. Most of these studies were aiming at the identification of novel or differentially regulated miRNAs. However, by cloning from total RNA, cellular degradation products and other so far unidentified classes of small RNAs are cloned and sequenced as well. It is very often difficult to distinguish between degradation products and functional classes of small RNAs. Therefore, we

suggest that small RNA cloning approaches should be carried out from isolated Ago complexes, since associated small RNAs are most likely functional. Our monoclonal anti-Ago2 antibody provides a powerful tool for the identification of Ago2-associated functional small RNAs. Of

course, for comprehensive studies on Ago-associated small RNAs, potent antibodies directed against human Ago1, Ago3, and Ago4 will have to be generated in the future.

Ago complex purifications have recently been used for the identification of miRNA targets (Beitzinger et al. 2007; Easow et al. 2007; Karginov et al. 2007). Together with bioinformatic studies, such biochemical miRNA target identification approaches will be widely used in the future. In particular, more and more miRNA profiling studies aiming for the identification of differentially expressed miRNAs are carried out in many types of human tumors. Our antibody therefore provides a tool for the identification of miRNA targets from such cancerous human tissue.

Immunofluorescence studies revealed that human Ago proteins localize to P-bodies (Jakymiw et al. 2005; Liu et al. 2005b; Meister et al. 2005; Sen and Blau 2005; Leung et al. 2006). In many studies, a diffuse cytoplasmic staining has been observed as well. Due to the lack of potent anti-Ago antibodies for immunofluorescence experiments, these studies have been carried out using either tagged Ago proteins or poorly characterized anti-Ago sera. Strikingly, anti-Ago2(11A9) clearly detects Ago2 in P-bodies as well as a diffuse Ago2 distribution in the cytoplasm. Surprisingly, we also observed a nuclear staining with our antibody. Since such nuclear stainings have not been observed before, we performed an Ago2 knock down and found that both the cytoplasmic and the nuclear staining was strongly reduced. We conclude that the nuclear signal that we have observed represents a nuclear Ago2 pool. Notably, small RNAs as well as Ago proteins have indeed been implicated in nuclear functions before. It has been shown that siRNAs or miRNAs directed against nuclear RNAs guide efficient RNAi in nuclear extracts (Meister et al. 2004; Robb et al. 2005). Moreover, it has been suggested that siRNAs as well as Ago proteins guide transcriptional silencing processes on specific promoters in the nucleus (Morris et al. 2004; Janowski et al. 2006; Kim et al. 2006).

Taken together, we have generated a specific and efficient antibody against human Ago2 that will be highly valuable for the scientific community. Anti-Ago2(11A9) is available from www.ascenion.de.

MATERIALS AND METHODS

Cell lines and plasmids

Plasmids encoding Flag/HA-tagged proteins were described previously (Meister et al. 2004). For the expression of myc-tagged proteins, the corresponding cDNAs were cloned into a modified pCS2 plasmid kindly provided by Olaf Stemmann (Max Planck Institute of Biochemistry, Germany).

Cell culture and transfection

All cell lines used in this study were cultured in Dulbecco's modified Eagle's medium (PAA) supplemented with glucose

(4.5 g/L) and 10% (v/v) fetal bovine serum (Biochrom AG) in the presence of penicillin and streptomycin (Gibco).

After transfection by calcium phosphate procedure (Meister et al. 2005), HEK 293 cells were grown for an additional 48 h in 5% CO₂ atmosphere without medium exchange.

Extract preparations and Western blotting

For total cell extract, cells were scraped off the culture plates in lysis buffer (20 mM Tris-HCl, pH 7.5; 150 mM NaCl; 0.5% Nonidet P-40; 2 mM EDTA; 0.5 mM DTT; 1 mM NaF; and 1 mM Pefablock [Roche]) and centrifuged for 10 min at 17,000g.

Cytoplasmic and nuclear extract preparation according to Dignam et al. (1983) was modified as follows: Cells were trypsinized, washed once in PBS, resuspended in five volumes of hypotonic Roeder A buffer (10 mM HEPES, pH 7.9; 10 mM KCl; 1.5 mM MgCl₂; 0.5 mM DTT; and 1 mM Pefablock), and incubated for 10 min on ice. Swollen cells were homogenized with 10 strokes in two volumes Roeder A buffer, and the homogenate was centrifuged for 10 min at 900g. The remaining nuclei pellet was washed once in PBS and subsequently homogenized with 15 strokes in Roeder C buffer (20 mM HEPES, pH 7.9; 420 mM KCl; 1.5 mM MgCl₂; 0.5 mM DTT; 5% glycerine; 0.2 mM EDTA; and 1 mM Pefablock). Nuclear extract was cleared at 17,000g for 30 min.

For Western blot analysis, proteins were separated by 10% SDS-PAGE and transferred onto nitrocellulose membrane (Amersham Bioscience). Membranes were blocked for 30 min in Western blot wash buffer (30 mM Tris-HCl, pH 7.5; 150 mM NaCl; 0.25% [v/v] Tween-20) containing 10% (w/v) dry milk (Roth) and subsequently treated with the corresponding antibodies. The monoclonal anti-Ago2(11A9) was generated in cooperation with E. Kremmer as described previously (Beitzinger et al. 2007). Hybridoma supernatant was diluted 1:50 for Western blotting. Commercial antibodies additionally used include monoclonal anti-HA antibody (HISS Diagnostics), monoclonal anti-myc antibody (Abcam), and anti-S6 ribosomal protein antibody (Cell Signaling Technologies), as well as peroxidase-conjugated secondary anti-rat IgG antibody (Jackson Lab), anti-mouse IgG antibody (Sigma), and anti-rabbit IgG antibody (Sigma). They were diluted according to the manufacturers' recommendations for Western blotting.

Immunoprecipitations and peptide elution experiments

Tagged proteins were immunoprecipitated from total cell extract using anti-Flag- or anti-myc-conjugated agarose beads (both Sigma). For precipitation of untagged proteins, saturating amounts of the corresponding antibodies were coupled to protein G sepharose beads (Amersham Bioscience) for 2 h at 4°C prior to immunoprecipitation.

Beads and an excess of total extract were incubated for 90 min at 4°C under slight rotation. Precipitates were washed twice with IP wash buffer (IPB; 50 mM Tris-HCl, pH 7.5; 300 mM NaCl; 5 mM Mg₂Cl; and 0.05% Nonidet P-40), once with PBS, and finally transferred to a new tube and resuspended in the appropriate buffer.

Native RISC was captured with anti-Ago2(11A9) bound to protein G sepharose during a standard immunoprecipitation procedure (see above) and stringently washed: Twice with IPB containing 0.5 M NaCl, followed by a 40-min incubation in the

presence of 360 mM NaCl at 4°C under rotation, and one final washing with 0.5 M NaCl. RISC precipitates were equilibrated in PBS and eluted with 100 µg of synthetic Ago2 peptide in IPB per 25 µL of beads at 25°C and 600 rpm for 90 min. Eluate was collected with a polyrep column (Biorad) equilibrated with IPB. Ago2 complexes that remained on the beads were finally eluted with 0.1 M glycine pH 2.3 and neutralized immediately after with 1 M Tris-HCl, pH 8.0.

To test the effect of different pH values on RISC elution, Ago2 peptide was solved in IPB of the respective pH.

For time course experiments, the elution reaction was incubated directly in the polyrep column. For each time point, the eluate was collected and an aliquot stored at -20°C while the remaining reaction mixture was re-added into the column.

In vitro RISC assays

Preparation of cap-³²P-labeled RNA used as RISC substrate was described earlier (Martinez et al. 2002). The sequence of the exogenous siRNA used in Figure 2C is UCGAAGUAUCCGC GUACGUdT (Meister et al. 2004). Assays were performed with 40% (v/v) RISC either eluted or bound to beads in a total volume of 25 µL with 40 mM KCl, 4 mM Mg₂Cl₂, 5 mM DTT, 1 mM ATP, 0.2 mM GTP, and 1.2 U RiboLock RNase inhibitor (Fermentas). After adding 1 µL of substrate RNA (1.5 Bq/cm²), samples were incubated for 90 min at 30°C. RNA extraction and analysis was described before (Meister et al. 2004).

Northern blotting

Total RNA was extracted from HEK 293 cells according to Lagos-Quintana et al. (2001). Coimmunoprecipitated RNA was isolated by Proteinase K (AppliChem) treatment, followed by two extraction steps using first acidic phenol and second chloroform. For RNA precipitation, aqueous phase was mixed with three volumes of absolute ethanol and incubated overnight at -20°C. Without any additional washing, RNA was finally solved in formamide loading dye, separated by electrophoresis on 15% denaturing polyacrylamide gels, and transferred to Hybond-N membrane (Amersham Bioscience) by semidry blotting for 25 min with 5 V. Membranes were dried, UV treated, and incubated for 1 h at 80°C. Prehybridization was performed in 5× SSC; 20 mM Na₂HPO₄, pH 7.2; 7% (w/v) SDS; Denhardt's solution (0.02% [w/v] bovine serum albumin V; 0.02% [w/v] Polyvinylpyrrolidone K30; 0.02% [w/v] Ficoll 400), and 0.1 mg/mL sonicated salmon sperm DNA for 1 h at 45°C before a 5'-³²P-labeled probe (see below) was added overnight. Subsequently, the membrane was washed in 10-min intervals twice with 5× SSC; 1% (w/v) SDS and once with 1× SSC; 1% (w/v) SDS. Exposure to Kodak BioMax MS films was performed with an intensifying screen (Kodak) at -80°C.

For Northern probe preparation, 20 pmol synthetic DNA-oligonucleotides (Metabion) reverse complementary to miR-19b were radiolabeled in a T4-Polynucleotide kinase (Fermentas) reaction in the presence of γ-³²P-ATP (GE Healthcare) according to standard protocols and subsequently purified by gel filtration using MicroSpin G-25 columns (Amersham Bioscience).

Immunofluorescence

Cells were grown to 60%–70% confluency on cover slips and fixed with 3.7% formaldehyde in PBS. After 15 min of fixation, the

reaction was stopped by addition of 100 mM glycine solved in PBS. Subsequently, cells were incubated 10 min in PBS with 3% (w/v) bovine serum albumin (BSA, Roth) and 0.2% (v/v) Triton X 100 to make them permeable as well as to block unspecific antibody binding. After rinsing with 0.1% (v/v) Tween-20 and 0.2% (w/v) BSA, primary antibodies were added for 1 h. After intensive washing, secondary antibodies were added for another hour in the dark. DNA was stained with DAPI at a final concentration of 1 µg/mL for a few minutes. Immunofluorescence was observed and recorded using a LEICA TCS SP2 Confocal Laser Scanning microscope and Leica Confocal Software softWoRx. Monoclonal anti-LSm4 antibody was purchased from Geneway, FITC-conjugated anti-chicken IgY antibody from Sigma, and TexasRed-conjugated anti-rat IgG antibody from Vector Laboratories.

siRNA transfection

HeLa cells were reverse transfected with siRNAs in six-well plates at 40 nM final concentration using RNAiMAX (Invitrogen), according to the manufacturer's instructions. After 2 d, cells were seeded to cover slips in six-well plates. Cells were fixed 5 d post-transfection and stained for Ago2 and LSm4 (see above). The following siRNAs were used (sense, antisense): Ago2 siRNA, 5'-GCACGGAAGUCCAUCUGAAUU, 5'-UUCAGAUGGACUCC GUGCUU; non-silencing control siRNA, 5'-UUGUCUUGCAU UCGACUAAUT, 5'-UUAGUCGAAUGCAAGACAAUT.

ACKNOWLEDGMENTS

We thank Sabine Rottmüller for technical assistance, Ralf Zenke for help with the confocal microscope, Christian Pohl for discussion, and Stefan Jentsch for support. This work was supported in part by the Deutsche Forschungsgemeinschaft (DFG, Me2064/2-1), the European Union (LSHG-CT-2006-037900), and the Max Planck Society. L.W. received a fellowship from the Boehringer Ingelheim Fonds.

Received December 21, 2007; accepted February 18, 2008.

REFERENCES

- Behm-Ansant, I., Rehwinkel, J., Doerks, T., Stark, A., Bork, P., and Izaurralde, E. 2006. mRNA degradation by miRNAs and GW182 requires both CCR4:NOT deadenylase and DCP1:DCP2 decapping complexes. *Genes & Dev.* **20**: 1885–1898.
- Beitzinger, M., Peters, L., Zhu, J.Y., Kremmer, E., and Meister, G. 2007. Identification of human microRNA targets from isolated Argonaute protein complexes. *RNA Biol.* **4**: 76–84.
- Bhattacharyya, S.N., Habermacher, R., Martine, U., Closs, E.I., and Filipowicz, W. 2006. Relief of microRNA-mediated translational repression in human cells subjected to stress. *Cell* **125**: 1111–1124.
- Carmell, M.A., Xuan, Z., Zhang, M.Q., and Hannon, G.J. 2002. The Argonaute family: Tentacles that reach into RNAi, developmental control, stem cell maintenance, and tumorigenesis. *Genes & Dev.* **16**: 2733–2742.
- Chen, P.Y. and Meister, G. 2005. microRNA-guided post-transcriptional gene regulation. *Biol. Chem.* **386**: 1205–1218.
- Chendrimada, T.P., Gregory, R.I., Kumaraswamy, E., Norman, J., Cooch, N., Nishikura, K., and Shiekhattar, R. 2005. TRBP recruits the Dicer complex to Ago2 for microRNA processing and gene silencing. *Nature* **436**: 740–744.
- Dignam, J.D., Lebovitz, R.M., and Roeder, R.G. 1983. Accurate transcription initiation by RNA polymerase II in a soluble extract

- from isolated mammalian nuclei. *Nucleic Acids Res.* **11**: 1475–1489. doi: 10.1093/nar/11.5.1475.
- Ding, L., Spencer, A., Morita, K., and Han, M. 2005. The developmental timing regulator AIN-1 interacts with miRISCs and may target the argonaute protein ALG-1 to cytoplasmic P bodies in *C. elegans*. *Mol. Cell Biol.* **19**: 437–447.
- Easow, G., Teleman, A.A., and Cohen, S.M. 2007. Isolation of microRNA targets by miRNP immunopurification. *RNA* **13**: 1198–1204.
- Eulalio, A., Behm-Ansmant, I., and Izaurralde, E. 2007a. P bodies: At the crossroads of post-transcriptional pathways. *Nat. Rev. Mol. Cell Biol.* **8**: 9–22.
- Eulalio, A., Behm-Ansmant, I., Schweizer, D., and Izaurralde, E. 2007b. P-body formation is a consequence, not the cause, of RNA-mediated gene silencing. *Mol. Cell Biol.* **27**: 3970–3981.
- Filipowicz, W., Jaskiewicz, L., Kolb, F.A., and Pillai, R.S. 2005. Post-transcriptional gene silencing by siRNAs and miRNAs. *Curr. Opin. Struct. Biol.* **15**: 331–341.
- Giraldez, A.J., Mishima, Y., Rihel, J., Grocock, R.J., Van Dongen, S., Inoue, K., Enright, A.J., and Schier, A.F. 2006. Zebrafish MiR-430 promotes deadenylation and clearance of maternal mRNAs. *Science* **312**: 75–79.
- Gregory, R.I., Chendrimada, T.P., Cooch, N., and Shiekhattar, R. 2005. Human RISC couples microRNA biogenesis and post-transcriptional gene silencing. *Cell* **123**: 631–640.
- Haase, A.D., Jaskiewicz, L., Zhang, H., Laine, S., Sack, R., Gatignol, A., and Filipowicz, W. 2005. TRBP, a regulator of cellular PKR and HIV-1 virus expression, interacts with Dicer and functions in RNA silencing. *EMBO Rep.* **6**: 961–967.
- Hall, T.M. 2005. Structure and function of argonaute proteins. *Structure* **13**: 1403–1408.
- Hock, J., Weinmann, L., Ender, C., Rudel, S., Kremmer, E., Raabe, M., Urlaub, H., and Meister, G. 2007. Proteomic and functional analysis of Argonaute-containing mRNA–protein complexes in human cells. *EMBO Rep.* **8**: 1052–1060.
- Hutvagner, G. and Simard, M.J. 2008. Argonaute proteins: Key players in RNA silencing. *Nat. Rev. Mol. Cell Biol.* **9**: 22–32.
- Jakymiw, A., Lian, S., Eystathiou, T., Li, S., Satoh, M., Hamel, J.C., Fritzler, M.J., and Chan, E.K. 2005. Disruption of GW bodies impairs mammalian RNA interference. *Nat. Cell Biol.* **7**: 1267–1274.
- Janowski, B.A., Huffman, K.E., Schwartz, J.C., Ram, R., Nordsell, R., Shames, D.S., Minna, J.D., and Corey, D.R. 2006. Involvement of AGO1 and AGO2 in mammalian transcriptional silencing. *Nat. Struct. Mol. Biol.* **13**: 787–792.
- Jin, P., Zarnescu, D.C., Ceman, S., Nakamoto, M., Mowrey, J., Jongens, T.A., Nelson, D.L., Moses, K., and Warren, S.T. 2004. Biochemical and genetic interaction between the fragile X mental retardation protein and the microRNA pathway. *Nat. Neurosci.* **7**: 113–117.
- Karginov, F.V., Conaco, C., Xuan, Z., Schmidt, B.H., Parker, J.S., Mandel, G., and Hannon, G.J. 2007. A biochemical approach to identifying microRNA targets. *Proc. Natl. Acad. Sci.* **104**: 19291–19296.
- Kim, D.H., Villeneuve, L.M., Morris, K.V., and Rossi, J.J. 2006. Argonaute-1 directs siRNA-mediated transcriptional gene silencing in human cells. *Nat. Struct. Mol. Biol.* **13**: 793–797.
- Lagos-Quintana, M., Rauhut, R., Lendeckel, W., and Tuschl, T. 2001. Identification of novel genes coding for small expressed RNAs. *Science* **294**: 853–858.
- Lee, Y., Hur, I., Park, S.Y., Kim, Y.K., Suh, M.R., and Kim, V.N. 2006. The role of PACT in the RNA silencing pathway. *EMBO J.* **25**: 522–532.
- Leung, A.K., Calabrese, J.M., and Sharp, P.A. 2006. Quantitative analysis of Argonaute protein reveals microRNA-dependent localization to stress granules. *Proc. Natl. Acad. Sci.* **103**: 18125–18130.
- Leuschner, P.J., Ameres, S.L., Kueng, S., and Martinez, J. 2006. Cleavage of the siRNA passenger strand during RISC assembly in human cells. *EMBO Rep.* **7**: 314–320.
- Liu, J., Carmell, M.A., Rivas, F.V., Marsden, C.G., Thomson, J.M., Song, J.J., Hammond, S.M., Joshua-Tor, L., and Hannon, G.J. 2004. Argonaute2 is the catalytic engine of mammalian RNAi. *Science* **305**: 1437–1441.
- Liu, J., Rivas, F.V., Wohlschlegel, J., Yates 3rd, J.R., Parker, R., and Hannon, G.J. 2005a. A role for the P-body component GW182 in microRNA function. *Nat. Cell Biol.* **7**: 1161–1166.
- Liu, J., Valencia-Sanchez, M.A., Hannon, G.J., and Parker, R. 2005b. MicroRNA-dependent localization of targeted mRNAs to mammalian P-bodies. *Nat. Cell Biol.* **7**: 719–723.
- Ma, J.B., Yuan, Y.R., Meister, G., Pei, Y., Tuschl, T., and Patel, D.J. 2005. Structural basis for 5′-end-specific recognition of guide RNA by the *A. fulgidus* Piwi protein. *Nature* **434**: 666–670.
- Maniataki, E. and Mourelatos, Z. 2005. A human, ATP-independent, RISC assembly machine fueled by pre-miRNA. *Genes & Dev.* **19**: 2979–2990.
- Martinez, J., Patkaniowska, A., Urlaub, H., Lührmann, R., and Tuschl, T. 2002. Single-stranded antisense siRNAs guide target RNA cleavage in RNAi. *Cell* **110**: 563–574.
- Matranga, C., Tomari, Y., Shin, C., Bartel, D.P., and Zamore, P.D. 2005. Passenger-strand cleavage facilitates assembly of siRNA into Ago2-containing RNAi enzyme complexes. *Cell* **123**: 607–620.
- Meister, G. and Tuschl, T. 2004. Mechanisms of gene silencing by double-stranded RNA. *Nature* **431**: 343–349.
- Meister, G., Landthaler, M., Patkaniowska, A., Dorsett, Y., Teng, G., and Tuschl, T. 2004. Human Argonaute2 mediates RNA cleavage targeted by miRNAs and siRNAs. *Mol. Cell Biol.* **15**: 185–197.
- Meister, G., Landthaler, M., Peters, L., Chen, P.Y., Urlaub, H., Lührmann, R., and Tuschl, T. 2005. Identification of novel argonaute-associated proteins. *Curr. Biol.* **15**: 2149–2155.
- Morris, K.V., Chan, S.W., Jacobsen, S.E., and Looney, D.J. 2004. Small interfering RNA-induced transcriptional gene silencing in human cells. *Science* **305**: 1289–1292.
- Mourelatos, Z., Dostie, J., Paushkin, S., Sharma, A., Charroux, B., Abel, L., Rappsilber, J., Mann, M., and Dreyfuss, G. 2002. miRNPs: A novel class of ribonucleoproteins containing numerous microRNAs. *Genes & Dev.* **16**: 720–728.
- Parker, J.S. and Barford, D. 2006. Argonaute: A scaffold for the function of short regulatory RNAs. *Trends Biochem. Sci.* **31**: 622–630.
- Parker, J.S., Roe, S.M., and Barford, D. 2004. Crystal structure of a PIWI protein suggests mechanisms for siRNA recognition and slicer activity. *EMBO J.* **23**: 4727–4737.
- Parker, J.S., Roe, S.M., and Barford, D. 2005. Structural insights into mRNA recognition from a PIWI domain–siRNA guide complex. *Nature* **434**: 663–666.
- Patel, D.J., Ma, J.B., Yuan, Y.R., Ye, K., Pei, Y., Kuryavii, V., Malinina, L., Meister, G., and Tuschl, T. 2006. Structural biology of RNA silencing and its functional implications. *Cold Spring Harb. Symp. Quant. Biol.* **71**: 81–93.
- Peters, L. and Meister, G. 2007. Argonaute proteins: Mediators of RNA silencing. *Mol. Cell Biol.* **26**: 611–623.
- Pillai, R.S., Bhattacharyya, S.N., Artus, C.G., Zoller, T., Cougot, N., Basyuk, E., Bertrand, E., and Filipowicz, W. 2005. Inhibition of translational initiation by Let-7 MicroRNA in human cells. *Science* **309**: 1573–1576.
- Pillai, R.S., Bhattacharyya, S.N., and Filipowicz, W. 2007. Repression of protein synthesis by miRNAs: How many mechanisms? *Trends Cell Biol.* **17**: 118–126.
- Rand, T.A., Petersen, S., Du, F., and Wang, X. 2005. Argonaute2 cleaves the anti-guide strand of siRNA during RISC activation. *Cell* **123**: 621–629.
- Robb, G.B. and Rana, T.M. 2007. RNA helicase A interacts with RISC in human cells and functions in RISC loading. *Mol. Cell Biol.* **26**: 523–537.
- Robb, G.B., Brown, K.M., Khurana, J., and Rana, T.M. 2005. Specific and potent RNAi in the nucleus of human cells. *Nat. Struct. Mol. Biol.* **12**: 133–137.

- Salzman, D.W., Shubert-Coleman, J., and Furneaux, H. 2007. P68 RNA helicase unwinds the human let-7 microRNA precursor duplex and is required for let-7-directed silencing of gene expression. *J. Biol. Chem.* **282**: 32773–32779.
- Sen, G.L. and Blau, H.M. 2005. Argonaute 2/RISC resides in sites of mammalian mRNA decay known as cytoplasmic bodies. *Nat. Cell Biol.* **7**: 633–636.
- Song, J.J. and Joshua-Tor, L. 2006. Argonaute and RNA—Getting into the groove. *Curr. Opin. Struct. Biol.* **16**: 5–11.
- Song, J.J., Smith, S.K., Hannon, G.J., and Joshua-Tor, L. 2004. Crystal structure of Argonaute and its implications for RISC slicer activity. *Science* **305**: 1434–1437.
- Till, S., Lejeune, E., Thermann, R., Bortfeld, M., Hothorn, M., Enderle, D., Heinrich, C., Hentze, M.W., and Ladurner, A.G. 2007. A conserved motif in Argonaute-interacting proteins mediates functional interactions through the Argonaute PIWI domain. *Nat. Struct. Mol. Biol.* **14**: 897–903.
- Zamore, P.D. and Haley, B. 2005. Ribo-gnome: The big world of small RNAs. *Science* **309**: 1519–1524.

Fluorescence correlation spectroscopy and fluorescence cross-correlation spectroscopy reveal the cytoplasmic origination of loaded nuclear RISC *in vivo* in human cells

Thomas Ohrt¹, Jörg Mütze¹, Wolfgang Staroske¹, Lasse Weinmann², Julia Höck², Karin Crell¹, Gunter Meister² and Petra Schwille^{1,*}

¹BIOTEC, Biophysics, Dresden University of Technology, Dresden and ²Laboratory of RNA Biology, Max Planck Institute of Biochemistry, Martinsried, Germany

Received August 13, 2008; Revised and Accepted September 25, 2008

ABSTRACT

Studies of RNA interference (RNAi) provide evidence that in addition to the well-characterized cytoplasmic mechanisms, nuclear mechanisms also exist. The mechanism by which the nuclear RNA-induced silencing complex (RISC) is formed in mammalian cells, as well as the relationship between the RNA silencing pathways in nuclear and cytoplasmic compartments is still unknown. Here we show by applying fluorescence correlation and cross-correlation spectroscopy (FCS/FCCS) *in vivo* that two distinct RISC exist: a large ~3 MDa complex in the cytoplasm and a 20-fold smaller complex of ~158 kDa in the nucleus. We further show that nuclear RISC, consisting only of Ago2 and a short RNA, is loaded in the cytoplasm and imported into the nucleus. The loaded RISC accumulates in the nucleus depending on the presence of a target, based on an miRNA-like interaction with impaired cleavage of the cognate RNA. Together, these results suggest a new RISC shuttling mechanism between nucleus and cytoplasm ensuring concomitant gene regulation by small RNAs in both compartments.

INTRODUCTION

Small RNAs have emerged as key regulators of gene expression, acting in an evolutionary conserved group of gene-silencing pathways found in eukaryotes (1–3). The short ~19–24 nucleotide (nt) long dsRNA silencing triggers are produced from endogenous or exogenous dsRNA substrates of various secondary structure (4–7).

Short interfering RNAs (siRNAs) consist of a dsRNA with a stem of ~19 nt containing a 5'-phosphate and 2 nt overhangs at both 3'-ends (5,7). To function as targeting cofactors, siRNAs are bound by the RISC-loading complex (RLC) consisting of Dicer, TRBP and a member of the Argonaute (Ago) family (6,8,9). The siRNA-duplexes are separated into single strands as they assemble into an Argonaute protein, the core of the RNA-induced-silencing complex (RISC) (10). The RLC specifically incorporates the strand with the lowest thermodynamic stability at the 5'-end of the duplex, termed 'guide' strand, into Argonaute, thereby forming activated RISC whereas the 'passenger' strand is removed from the complex and degraded (11–13). Depending on the extent of complementarity between the guide RNA and the target mRNA sequence, in conjunction with the associated Argonaute family member, RISC can silence gene expression by endonucleolytic cleavage, translational repression, deadenylation, decapping and/or by translocation into P-bodies (14–16). Furthermore, it has been shown that siRNAs as well as the nuclear encoded miRNAs, another class of small dsRNA silencing triggers, depend on Exp5 mediated nuclear export for cytoplasmic localization and efficient silencing (17,18).

Nuclear functions for Ago proteins have also been reported, such as in *Schizosaccharomyces pombe*, where Ago is involved in heterochromatin formation to promote transcriptional gene silencing and in other organisms including plants, *Drosophila* and *Caenorhabditis elegans* (19–21). Although Ago proteins have been found in cytoplasmic and nuclear extracts from mammalian cells, it could not be excluded experimentally that the nuclear extracts were contaminated by Ago proteins associated with the nuclear envelope (22,23). Further indications

*To whom correspondence should be addressed. Tel: +49 351 46340328; Fax: +49 351 46340342; Email: schwille@biotec.tu-dresden.de
Correspondence may also be addressed to Thomas Ohrt. Tel: +49 351 46340324; Fax: +49 351 46340342; Email: thomas.ohrt@biotec.tu-dresden.de

The authors wish it to be known that, in their opinion, the first two authors should be regarded as joint First Authors

© 2008 The Author(s)

This is an Open Access article distributed under the terms of the Creative Commons Attribution Non-Commercial License (<http://creativecommons.org/licenses/by-nc/2.0/uk/>) which permits unrestricted non-commercial use, distribution, and reproduction in any medium, provided the original work is properly cited.

for the presence of Ago proteins in the nucleus are that the small nuclear RNAs (snRNAs) 7SK and U6 could be knocked down with siRNAs (23). Also, it has been shown that exogenously introduced siRNAs complementary to target sequences within gene promoters (agRNAs, antigene siRNAs) can either inhibit (transcriptional gene silencing, TGS) or activate gene transcription in an Argonaute protein dependent manner in mammalian cells (24–26). The Argonaute proteins bind to an antisense transcript or extended 5'-untranslated region of the mRNA that overlaps the gene promoter thereby mediating the formation of complexes with proteins and chromosomal DNA necessary for the activation of transcription or TGS in mammalian cells (27,28). However, endogenous, small dsRNA triggers involved in transcription regulation still need to be identified. In addition, it is unknown where the nuclear RISC is assembled and how the cell ensures the nuclear localization of agRNA-loaded RISC. The knowledge of the localization of its assembly, e.g. whether nuclear RISC is specifically loaded inside the nucleus or originates from cytoplasmic loaded RISC is important to better understand RNAi-mediated gene regulation and the interconnection between the cytoplasmic and nuclear RNAi pathways.

In this study, we used fluorescence correlation spectroscopy (FCS) and fluorescence cross-correlation spectroscopy (FCCS) to quantitatively analyse siRNA incorporation levels in Ago2 proteins and RISC-complex sizes concomitant in the cytoplasm and nucleus *in vivo*. FCS and FCCS are highly sensitive and specific optical techniques used for the study of dynamics and interactions of individual fluorescently labelled molecules in solution or living cells (for details see Methods section and Supplementary data) (29–31).

We provide the first direct characterization of nuclear RISC and show that cytoplasmic RNA-induced silencing complex (cRISC) and nuclear RNA-induced silencing complex (nRISC) are two, clearly distinguishable RISC complexes *in vivo*. Analyzing the asymmetric incorporation of fluorescently labelled siRNAs into nRISC and cRISC, we found that nRISC originates almost predominantly from loaded cRISC. Consequently, nRISC and cRISC are interconnected by the dynamic exchange of RISCs between the cytoplasm and the nucleus.

MATERIALS AND METHODS

Cell culture

ER293 cells stably transfected with the pERV3 vector (Stratagene) were cultured at 37°C in DMEM (high glucose, Sigma) with 10% FCS (PAA Laboratories GmbH), 2 mM glutamine (Gibco) and 0.3 mg/ml G418 (50 mg/ml, Gibco).

For the generation of the stable EGFP-Ago2 cell line, the pEGSH-EGFP-Ago2 vector was linearized with AseI. ER293 cells were seeded at 4×10^4 cells/ml, 24 h before transfection. Transfection was carried out using linearized DNA and Lipofectamine 2000 (Invitrogen) according to the manufacturer's protocols. After 24 h cells were treated with 0.4 mg/ml selection antibiotic Hygromycin B

(50 mg/ml, Gibco) for 3 weeks. Cells were diluted to 1 cell/0.2 ml and transferred onto 96-well plates for recloning. Wells with single colonies were cultured, resulting in EGFP-Ago2 positive clones that were confirmed via western blot, immunofluorescence and PCR. The generated cell line 10G stably expressing EGFP-Ago2 was cultured at 37°C in DMEM (high glucose, Sigma) with 10% fetal calf serum, 2 mM glutamine, 0.3 mg/ml G418 and 0.4 mg/ml Hygromycin B. All cells were regularly passaged at subconfluency and were plated with $1-5 \times 10^4$ cells/ml density.

siRNA sequences and calculation of the 5'-end free energy

All siRNA strands were obtained from IBA GmbH. The RNA oligonucleotides were synthesized with a 5'-phosphate and a 3'-amino group on a C6-carbon linker and were labelled with Cy5 succinimidyl ester (Cy5-NHS, Amersham Biosciences) as described previously (17). The nucleotides 18–21 were 2'-*O*-methyl modified to protect the label from degradation except for silencing assays where the siRNAs were not modified. Target-RNA and siRNA sequences are listed in the Supplementary data.

For siRNA control experiments, we used Silencer™ Negative control #2 (NegsiRNA) from Ambion.

The free energies of the first 4 bp of each siRNA strand of the duplex at the 5'-end was calculated in kcal/mol by using the nearest-neighbour method and the mfold algorithm (32,33).

Microinjection

For microinjection, $7-9 \times 10^4$ ER293/10G cells were transferred onto MatTek chambers coated with Fibronectin (25 µg/ml in PBS including CaCl₂ and MgCl₂, Roche) 24 h before microinjection. The micropipette (Femtotip 2, Eppendorf) is loaded with 1.5–4 µM labelled siRNAs (WGA 2.25 µg/µl, Biomeda) in 110 mM K-gluconate; 18 mM NaCl; 10 mM HEPES pH 7.4 and 0.6 mM MgSO₄. The micromanipulator consists of a FemtoJet and InjectMan NI2 which is mounted directly on a microscope. Working pressure for injection was between 25 and 80 hPa for 0.1 s and a holding pressure of 15 hPa.

Fluorescence correlation spectroscopy setup

Fluorescence correlation spectroscopy and laser scanning microscopy (LSM) were carried out on a commercial system consisting of a LSM510 and a ConfoCor3 (Zeiss, Jena, Germany). The 488 nm line of a Ar-Ion laser and the 633 nm line of a HeNe laser were attenuated by an acousto-optical tunable filter to 3.5 and 1.05 kW/cm² and directed via a 488/633 dichroic mirror onto the back aperture of a Zeiss C-Apochromat 40×, N.A. = 1.2, water immersion objective. Fluorescence emission light was collected by the same objective and split into two spectral channels by a second dichroic (LP635). To remove any residual laser light, a 505–610 nm bandpass or 655 nm longpass emission filter, respectively, was employed. The fluorescence was recorded by avalanche photodiode detectors (APDs) in each channel. For EGFP-Ago2 autocorrelation measurements, a mirror substituted the second dichroic and a 505-nm longpass emission filter was used

in a one channel setup. Out-of-plane fluorescence was reduced with a 70- μm pinhole. The fluorescence signals were software-correlated and evaluated with MATLAB (Mathworks, Natick, MA, USA) by using weighted Marquardt non-linear least-square fitting routine.

Laser scanning microscopy was performed using the APD's of the ConfoCor3 on the same setup. Cell measurements were performed in air-buffer (150 mM NaCl, 20 mM HEPES pH 7.4, 15 mM glucose, 15 $\mu\text{g}/\text{ml}$ BSA, 10 mM trehalose, 5.4 mM KCl, 0.85 mM MgCl_2 , 0.7 mM CaCl_2) at RT.

Preparation and fractionation of cell extracts

Fractionated cell extracts were prepared from 10G, 293 and ER293 cells from four confluent T175 chambers essentially performed as previously described by Robb *et al.* (23). Sucrose gradients were exactly performed as has been described in (34).

Immunoprecipitation

ER293 and 10G cells were lysed with IP buffer (0.5% NP-40, 150 mM KCl, 25 mM Tris-HCl pH 7.5, 2 mM EDTA, 1 mM NaF, 0.5 mM DTT, protease inhibitors, Roche) and centrifuged at 10000g for 10 min. Extracts were incubated with anti-GFP (Roche) or anti-p53 for 2 h at 4°C. Antibodies were pulled down with protein G Sepharose 4 fast flow beads (GE Healthcare) for 1 h at 4°C. Beads were subsequently washed with buffer (0.1% NP-40, 300 mM KCl, 25 mM Tris-HCl pH 7.5, 2 mM EDTA, 1 mM NaF, 0.5 mM DTT, protease inhibitors, Roche) and with PBS.

Western blotting

For western blot analysis, the cells were lysed with $\times 1.5$ loading buffer for denaturing polyacrylamide gel electrophoresis. For immunoblotting, proteins were run on 7.5–10% PAGE and transferred onto Protran[®] Nitrocellulose Transfer Membrane (Schleicher & Schuell). Antibodies: α -EGFP (Abcam ab290, 1:2000), α -Ago2 clone 11A9 (1:50), α -GAPDH (Abcam 9484, 1:2000), α -Actin (Abcam AC15). Immunoreactive signals were detected using ECL[™] Western Blotting Detection Reagents according to the manufacturer's protocol (Amersham Biosciences).

qPCR

Total RNA was isolated using the Prep Ease kit (USB, USA), according to the manufacturer's instructions, using DNaseI digestion on column. cDNA was synthesized with random hexamer primers from 2 μg of total RNA using the First Strand cDNA synthesis kit (Fermentas, Canada), according to the manufacturer's protocol. qPCR was performed on a MyiQ cycler (BioRad, USA) using the Mesa Green qPCR mastermix (Eurogentec, Belgium) with primers at 100 nM final concentration and a two-step PCR protocol (5 min initial denaturation at 95°C, 40 cycles with 10 s at 95°C and 1 min elongation at 60°C). The primers were (forward, reverse): GAPDH, 5' TGGTATCGTGGA AGGACTCATGAC, 5' ATGCCAGTGAGCTTCCCGT

TCAGC; 7SK, 5' CCTGCTAGAACCTCCAAACAAG, 5' GCCTCATTTGGATGTGTCTG. Data were evaluated using the $\Delta\Delta\text{Ct}$ method.

RESULTS

To investigate RISC by FCS/FCCS *in vivo*, we created a 293 based cell line, in which hAgo2 is tagged with the enhanced green fluorescent protein (EGFP). For this study, hAgo2 was chosen, because it has been demonstrated that it is involved in nuclear RNAi, is associated with siRNAs and miRNAs, endonucleolytically active and that tagging hAgo2 on the N-terminus with EGFP had no effect on hAgo2 RNAi activity and sub-cellular localization (35,36). The characterization of the newly generated cell line 10G revealed that the EGFP-Ago2 protein reproduces the enzymatic activity, protein/RNA interactions, sub-cellular localization, expression level and function of endogenous hAgo2 protein (Supplementary Figure S1A–D).

Nuclear RISC differs from cytoplasmic RISC

Although the human RISC complex has been intensely studied, the protein composition is still not entirely clear, with reported molecular weights from ~ 160 kDa to ~ 2 MDa (37,38). The huge deviation in molecular mass might depend on extract generation or on the experimental procedure for their estimation. To avoid preparation artefacts, we measured hAgo2 containing RISC complexes in thermal equilibrium *in vivo* in 10G cells and determined the molecular mass of the individual RISC in different cellular compartments by FCS (for details see Supplementary materials). The autocorrelation curves of EGFP in 293 cells resulted in almost identical diffusion times in the cytoplasm and the nucleus of $\tau_{\text{EGFP}(\text{cytopl})} = (354 \pm 13) \mu\text{s}$ and $\tau_{\text{EGFP}(\text{nuc})} = (368 \pm 8) \mu\text{s}$, corresponding to a diffusion coefficient of $D_{\text{EGFP}(\text{cytopl})} = (25.5 \pm 0.9) \mu\text{m}^2/\text{s}$ and $D_{\text{EGFP}(\text{nuc})} = (24.5 \pm 0.5) \mu\text{m}^2/\text{s}$, indicating that the viscosity and therefore the motility is approximately the same in both compartments (Figure 1A) (39). In contrast, measurements in 10G cells displayed a significant difference in diffusion time for EGFP-Ago2 between the cytoplasm ($\tau_{\text{EGFP-Ago2}(\text{cytopl})} = (1678 \pm 58) \mu\text{s}$, $D_{\text{EGFP-Ago2}(\text{cytopl})} = (5.4 \pm 0.2) \mu\text{m}^2/\text{s}$) and the nucleus ($\tau_{\text{EGFP-Ago2}(\text{nuc})} = (657 \pm 22) \mu\text{s}$, $D_{\text{EGFP-Ago2}(\text{nuc})} = (13.7 \pm 0.5) \mu\text{m}^2/\text{s}$). With respect to EGFP, these diffusion times correspond to a molecular weight of (3.0 ± 0.6) MDa for cRISC and (158 ± 26) kDa for nRISC. While the obtained molecular weight for cRISC is in the range of a previously isolated RISC of about 2 MDa (37), the molecular weight of nRISC resembles almost the distinct EGFP-Ago2 alone. It should be noted that the molecular mass for cRISC could be overestimated due to a higher effective viscosity a larger molecule experiences in a crowded environment. Yet, due to the ~ 20 -fold difference in molecular mass, we conclude that cRISC represents a different complex compared to nRISC. Further analyses of the measurements indicate that within the accuracy of the FCS technique no distinct

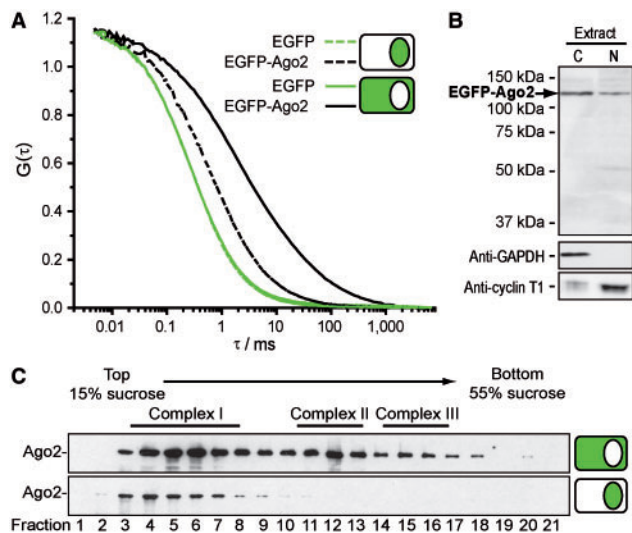


Figure 1. Nuclear RISC differs from cytoplasmic RISC. (A) Normalized FCS curves of EGFP-Ago2 as measured in the nucleus (dashed black line) and cytoplasm (black line) of 10G cells. The graph exhibits the autocorrelation functions $G(\tau)$ at lag time τ (for more details on FCS and the autocorrelation function see Supplementary materials). Curves are the average of at least 10 measurements. As control, FCS curves were recorded for EGFP alone in ER293 cells (nucleus: green dashed line, cytoplasm: green line). (B) Western blot of 10G nuclear and cytoplasmic extracts for EGFP-Ago2. To show the purity of the nuclear and cytoplasmic fractions, western blot analysis was performed with α -Cyclin T1 and α -GAPDH antibody. (C) HEK 293 cytoplasmic and nuclear extracts were separated by sucrose density centrifugation under conditions that allow the separation of different hAgo2 containing mRNPs that were analysed by western blot with specific α -hAgo2 antibody.

EGFP-Ago2 is present in the cytoplasm (Supplementary data).

Western blot analysis of nuclear and cytoplasmic 10G-extracts with an EGFP-specific antibody yielded a single specific band for EGFP-Ago2 at 130 kDa, demonstrating the absence of contaminating EGFP-Ago2 fragments in the nucleus (Figure 1B). Therefore, nRISC is not formed by a truncated version of EGFP-Ago2. To corroborate the FCS data, sucrose gradients with nuclear and cytoplasmic extracts from 293 cells were performed. The cytoplasmic extracts displayed the aforementioned hAgo2 containing complexes I–III with a large portion of complexes being bigger than 350 kDa. The large complexes II–III were missing in nuclear extracts (Figure 1C). The same result was obtained for hAgo1 (data not shown). The discrepancy between the obtained molecular weights and the proportions of different RISC in sucrose density gradients and FCS measurements lie within the different experimental techniques. Whereas FCS is a real-time acquisition technique *in vivo*, the gradient extract preparation includes a centrifugation step which excludes the analysis of high molecular weight complexes. Furthermore, the sucrose gradients are performed over a period of 20 h which might lead to the disassembly of the majority of RISC complexes. However, the results obtained by FCS are supported by sucrose gradients illustrating the absence of higher molecular weight complexes in the nucleus.

To characterize the sub-cellular distribution of hAgo2 containing complexes, we quantified the amount of EGFP-Ago2 in the nucleus and the cytoplasm by FCS and imaging. EGFP-Ago2 preferentially localized to the cytoplasm with a cytoplasmic to nuclear ratio of $(4.2 \pm 0.5):1$ determined by FCS and $(4.7 \pm 0.5):1$ determined by imaging (for details see Supplementary materials). The higher value for imaging might be caused by the accumulation of EGFP-Ago2 into P-bodies, which are not accessible with FCS.

We could directly characterize RISC sizes in the nucleus in thermal equilibrium by FCS *in vivo* without preparation artefacts and contaminations by cRISC. Our data demonstrate that cytoplasmic EGFP-Ago2 is part of a large complex and differs from nRISC which most probably represents the discrete EGFP-Ago2 protein. We obtained a cytoplasmic to nuclear EGFP-Ago2 concentration of ~ 4 – 5 , indicating that hAgo2 is not as underrepresented in the nucleus as estimated by previous imaging studies. This might result from the high expression levels in transient systems in previous reports, compared to the almost endogenous expression levels of EGFP-Ago2 in 10G cells (35,36).

Asymmetric guide strand incorporation into nuclear and cytoplasmic RISC

The incorporation of siRNAs into nRISC and the effects of target interactions on the distribution of activated RISC in the cytoplasm and the nucleus in mammalian cells are largely unknown. To assess siRNA incorporation levels and asymmetric loading of the guide strand into RISC by FCCS *in vivo* (for details see Supplementary materials), we covalently labelled siRNAs on the 3'-end of the guide or passenger strand with Cy5 (illustrated in Figure 2C and D top) and delivered them directly into 10G cells via microinjection to avoid siRNA segregation within endocytic compartments. This resulted in silencing active and homogeneous localized cytoplasmic siRNAs required for FCCS (17). The siRNA siTK3 targets the mRNA of Renilla luciferase encoded on the plasmid pRL-TK. The 5'-end hybridization energy of siTK3 was calculated as described (12) to define the guide and passenger strand of the siTK3 duplex (Figure 2A). The siTK3 siRNA was used as it displayed high levels of Renilla luciferase silencing, demonstrating the incorporation of the guide strand into endogenous RISC (Figure 2B).

Microinjection of the passenger strand labelled siTK3 resulted in cross-correlation amplitudes between 0% and 5% in the cytoplasm and nucleus up to 12 h, indicating the exclusion of the passenger strand from RISC (Figure 2C). On the contrary, guide strand labelled siTK3 lead to significant cross-correlation amplitudes in the nucleus and the cytoplasm gradually increasing for up to 6 h with a slight decline thereafter (Figure 2D). As the relative amplitude of the cross-correlation function is directly proportional to the concentration of double labelled species, this result demonstrates the specific incorporation of the guide strand into nuclear and cytoplasmic RISC whereas the passenger strand is excluded during the loading process. The specific incorporation of the guide strand could be

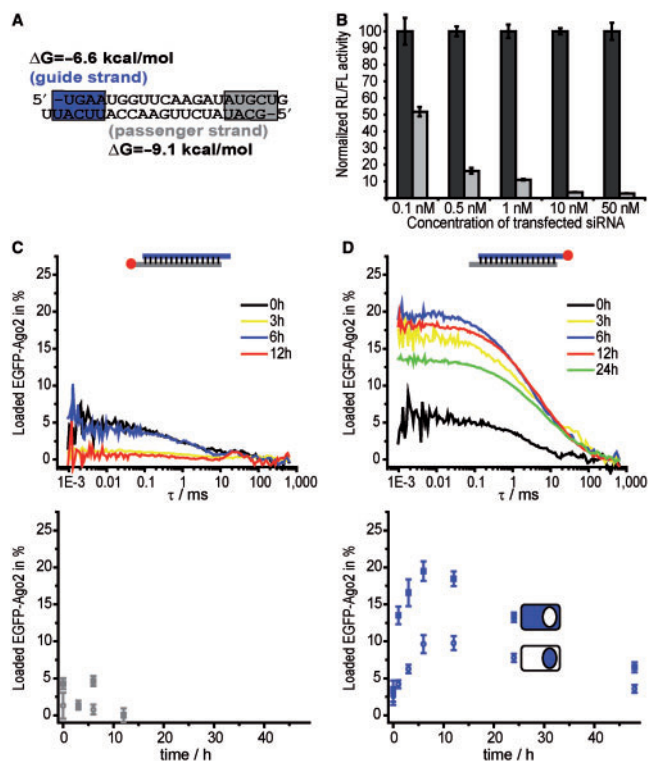


Figure 2. Asymmetric guide strand incorporation into nuclear and cytoplasmic RISC. (A) Illustration of the sequence and free energies of the siRNA siTK3. To follow the incorporation of the individual strands, the duplexes were either labelled on the 3'-end of the guide or passenger strand. (B) ER293 cells were transfected with the indicated amounts of siTK3 or NegsiRNA together with the fixed concentration of the pGL2-control and pRL-TK reporter plasmids. After 48 h, the ratios of target to control luciferase concentrations were normalized to the NegsiRNA control indicated in dark grey; siTK3 is indicated in grey. The plotted data were averaged from three different experiments \pm SD. (C) Normalized cross-correlation curves of EGFP-Ago2 and the labelled passenger strand of siTK3 in the cytoplasm for different incubation times after microinjection in 10G cells *in vivo* (top). Curves are the average of at least 10 measurements. The resulting cross-correlation amplitudes in the cytoplasm (filled boxes) and nucleus (open circles) are displayed in the bottom graph. (D) Normalized cross-correlation curves for the labelled guide strand of siTK3 in the cytoplasm (top). The bottom graph depicts the resulting cross-correlation for different incubation times in the cytoplasm (filled boxes) and nucleus (open circles) as indicated by the cartoon. Data are represented as mean \pm SEM.

observed down to a 5'-hybridization energy difference of 0.5 kcal/mol (siGL2) (data not shown). Interestingly, the incorporation levels in the nucleus and the cytoplasm synchronistically increased and declined, in the nucleus however to a lower level, reaching saturation after 6 h (Figure 2D, bottom panel). Similar results were obtained with other siRNAs: siTK2 (Supplementary Figure S3), siRNA targeting Firefly luciferase (siGL2) and siGAPDH (data not shown). Guide strand labelled siRNAs could be examined for longer time periods compared to passenger strand labelled siRNAs, due to the loss of the Cy5 signal in passenger strand containing cells. This most probably results from a stabilization of the guide strand caused by the interaction with RISC whereas the passenger strand gets degraded. Control experiments with GFP supplemented with guide strand labelled siTK3

exhibited no cross-correlation amplitude, whereas a double labelled control resulted in 80% cross-correlation amplitude *in vitro* (Supplementary Figure S4A and B).

For the first time, we could monitor the asymmetry dependent incorporation into nRISC and show that nuclear levels of guide strand incorporation correlate with cytoplasmic incorporation levels in time *in vivo*. The specific guide strand incorporation into nRISC provides additional evidence for the specific loading and function of nRISC.

nRISC loading levels are affected by target RNA interactions

The snRNA 7SK can be specifically silenced with an siRNA (23). In the previous section, we showed that siRNAs can be detected in nRISC independently of endogenous targets. To elucidate the effect of a nuclear target, we microinjected guide or passenger strand labelled si7SK1 (23) targeting 7SK snRNA. In conformity with our previous experiments, the asymmetric incorporation of the guide strand into cytoplasmic and nuclear RISC was observed, whereas the passenger strand was excluded from both complexes (Figure 3A). Interestingly, the si7SK1 loaded RISC accumulated much stronger in the nucleus between 1 h and 6 h after microinjection compared to all siRNAs tested (Figure 3A and B). Knock down of 7SK snRNA with two unrelated siRNAs 48 h before microinjection resulted in a decrease in cross-correlation amplitude that resembles the values of siTK3 (Figure 3C) and other siRNAs (data not shown) indicating a target dependent si7SK1-loaded RISC accumulation in the nucleus. A control transfection with NegsiRNA did not affect si7SK1-RISC accumulation in the nucleus (Figure 3C). Interestingly, another siRNA targeting 7SK snRNA (si7SK2) did not result in increased cross-correlation amplitudes in the nucleus, suggesting that the presence of a nuclear target *per se* is not sufficient for target dependent nRISC accumulation (Figure 3B and C). The target sites of the two siRNAs within 7SK snRNA structure are different (40), si7SK1 hybridizes with its seed sequence in a single stranded loop where the cleavage site is masked in a dsRNA stretch, whereas si7SK2 binds to a relatively unstructured part of 7SK snRNA (Figure 3D). By analyzing the silencing efficiency of si7SK1 and 2, we found that si7SK2 silences 7SK snRNA down to 20% whereas si7SK1 resulted in ~60% of relative 7SK levels (Figure 3E). It has been shown that dsRNA structures in close proximity to the cleavage site from the 3'-end inhibit cleavage (41). Furthermore, a target site in a small loop structure leads to steric problems resulting in reduced cleavage rates. These results are consistent with our silencing data (Figure 3E). To test the idea that binding of RISC to its target RNA without endonucleolytic cleavage leads to accumulation of loaded RISC in the nucleus, we compared an siRNA forming a central bulge (si7SK3-bulge) with the target site in an unstructured part of the 7SK snRNA to its perfect matching siRNA (si7SK3). The silencing efficiencies of the two siRNAs were analysed by qRT-PCR. Si7SK3 efficiently

silenced 7SK down to 16% whereas a central mismatch at position 9–11 completely impaired silencing (si7SK3-bulge; Figure 3E). Evaluation of the incorporation levels in the cytoplasm and the nucleus also displayed the accumulation of silencing impaired si7SK3-bulge loaded RISC in the nucleus, whereas the perfect match siRNA resulted in a 2-fold lower cross-correlation amplitude inside the nucleus. The cytoplasmic incorporation levels were not affected (Figure 3F). Additionally, the inhibition of target RNA cleavage by the si7SK3-bulge resulted in higher incorporation levels in the nucleus compared to the si7SK1 for incubation times longer than 6 h (Supplementary Figure S5A). The si7SK1 nuclear cross-correlation amplitude decreased after 6 h, a result of reduced levels of 7SK RNA due to the marginal silencing activity of si7SK1 during the time course compared to si7SK3-bulge with impaired cleavage. The analysis of the cytoplasmic to nuclear ratio of EGFP-Ago2 concentration did not show significant changes that can be related to the accumulation of EGFP-Ago2 loaded with si7SK3 and si7SK3-bulge siRNA in the nucleus (Supplementary Figure S5B). Therefore, we could show that EGFP-Ago2 levels remain stable, leading only to the accumulation of the particularly loaded RISCs in the nucleus.

We also analysed the sub-cellular localization of si7SK1 in living cells by quantifying fluorescence intensity.

We could not detect increased levels of si7SK1 RNA labelled on either strands in the nucleus of 10G or ER293 cells compared to other siRNAs (Supplementary Figure S5C). The analysis of siRNA sub-cellular localization by imaging does not correlate with target RNA localization, since the majority of siRNAs is not bound by the RLC/RISC and therefore the sub-cellular localization is mainly affected by Exp5 mediated export illustrated by siRNA incorporation levels of <35%.

Taken together, our data show that nRISC loaded with a specific guide RNA can accumulate in a target and duration of the interaction dependent fashion, indicating that this process is dynamic and does not result from a stable fraction of RISC in the nucleus. The nuclear hAgo2 protein concentration seems to be highly regulated, since a 2-fold increase of specifically loaded nRISC did not change the overall cytoplasmic to nuclear concentration ratio of EGFP-Ago2.

Cleavage impaired RISC-target interactions mediate RISC accumulation in the nucleus

To directly investigate the effect of RISC-target-RNA interactions in the nucleus and cytoplasm by FCCS, we microinjected a 50 nt long RNA into 10G cells that is labelled with Cy5 on the 5'-end, contains the siTK3 target site and is modified with 2'-*O*-methyl on each end

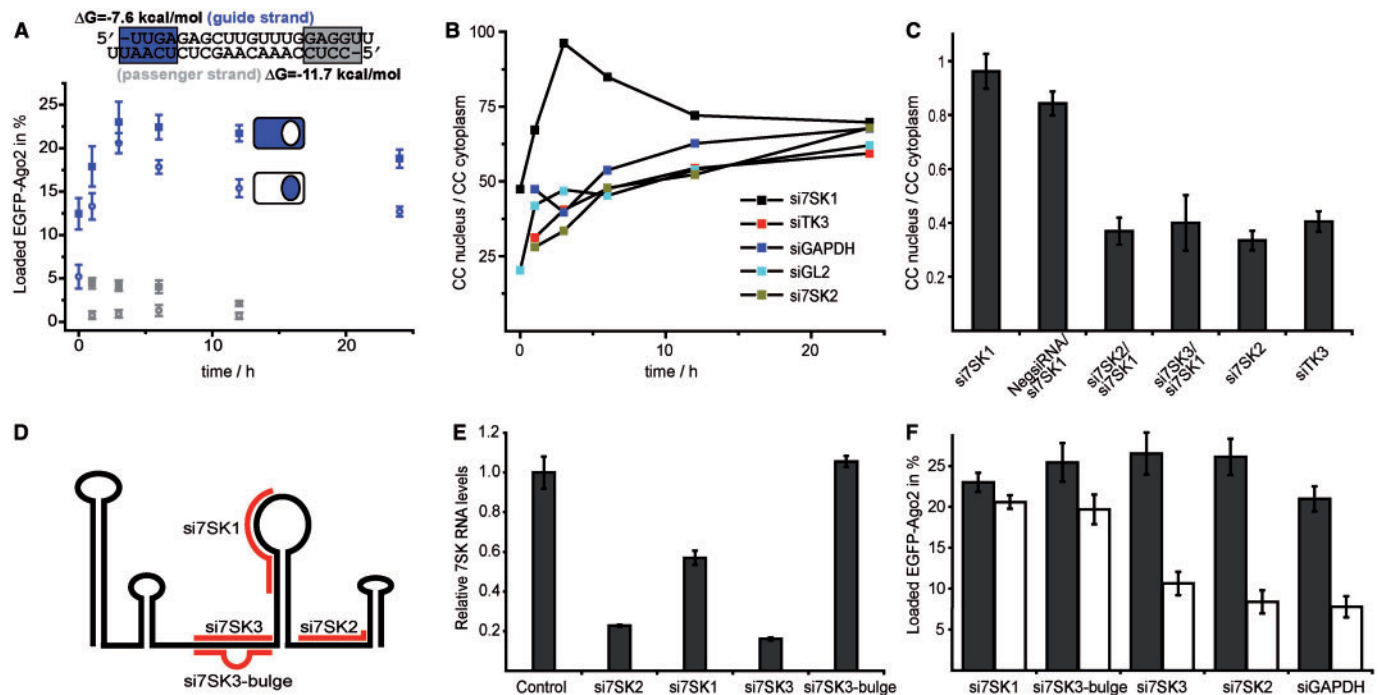


Figure 3. nRISC loading levels are affected by target RNA interactions. (A) Cross-correlation amplitude in the cytoplasm (filled boxes) and nucleus (open circles) of the nuclear targeting siRNA 7SK1 for different incubation times. Values were obtained by either labelling the guide strand (blue) or passenger strand (grey) and measuring in at least 10 cells. The sequence and free energies of the siRNA is illustrated. (B) Cross-correlation experiments of the nuclear targeting siRNA 7SK1 as shown in (A), graphed as ratio of the cross correlation in the nucleus over the cross-correlation in the cytoplasm. In addition, the ratios of other tested siRNAs are plotted. (C) Target specificity of the nuclear accumulation of the siRNA 7SK1. Plotted are the cross-correlation ratios nucleus to cytoplasm after 3 h of incubation for 7SK1 and for 7SK1 after the transfection (48 h) of a NegsiRNA, the siRNA 7SK2 and 7SK3. Additionally, the ratios for si7SK2 and siTK3 are depicted for comparison. (D) Schematic overview of the target sites of the used 7SK siRNAs used to analyse the influence of target interaction. (E) Quantitative PCR (qPCR) analysis of 7SK snRNA knockdown with different indicated siRNA duplexes. (F) Cross-correlation amplitude in the cytoplasm (filled bars) and nucleus (open bars) after 3 h of incubation for the siRNAs 7SK1, 7SK3-bulge, 7SK3, 7SK2 and for comparison GAPDH. Mean values \pm SEM.

to protect the target-RNA molecule against cellular RNases. The interaction of the EGFP-labelled RISC containing an unlabelled siRNA with the target-RNA can then be visualized by increased cross-correlation amplitudes (Figure 4A). The target-RNA localized to the cytoplasm and displayed a slight accumulation of fluorescence signal in the nucleus and even stronger in nucleolar structures (Figure 4B). FCCS measurements in non-transfected

and NegsiRNA transfected 10G cells after 1 and 3 h of target-RNA delivery showed no interaction of RISC with the target-RNA illustrating assay specificity and the absence of miRNA target sites within the target-RNA (Figure 4C). Longer incubation times were not tested as already 30% of target-RNA was degraded after 3 h in S20 extracts as determined by PAGE (data not shown). Despite that, transfection of perfectly matching siTK3 resulted in very low levels of EGFP-Ago2-target-RNA interactions (Figure 5C). In contrast, transfection of siTK3-B2 which forms a central bulge with the siTK3-target site yielded high levels of RISC-bound target-RNA in the cytoplasm. In the nucleus however, levels were 3-fold lower after 1 h with an increase after 2 and 3 h almost reaching cytoplasmic interaction levels (Figure 4C). The complete inactivation of the siTK3-B2 cleavage activity was verified by a dual luciferase assay (Figure 4D).

These results demonstrate (i) the localization of functional guide strand loaded RISC to the nucleus, (ii) the short interaction time of RISC loaded with a perfectly matching guide strand with the target-RNA and that (iii) bulges in the centre of the guide-target-RNA hybridizations increase the lifetime of RISC-target-RNA interaction, resulting in the accumulation of the complex in the nucleus over time. This is in strong agreement with our previous results showing the accumulation of specifically loaded RISC in a target- and duration of the interaction dependent fashion. Therefore, the target-dependent accumulation of nRISC is caused by the stable interaction of RISC with its target and not by the nuclear localization of

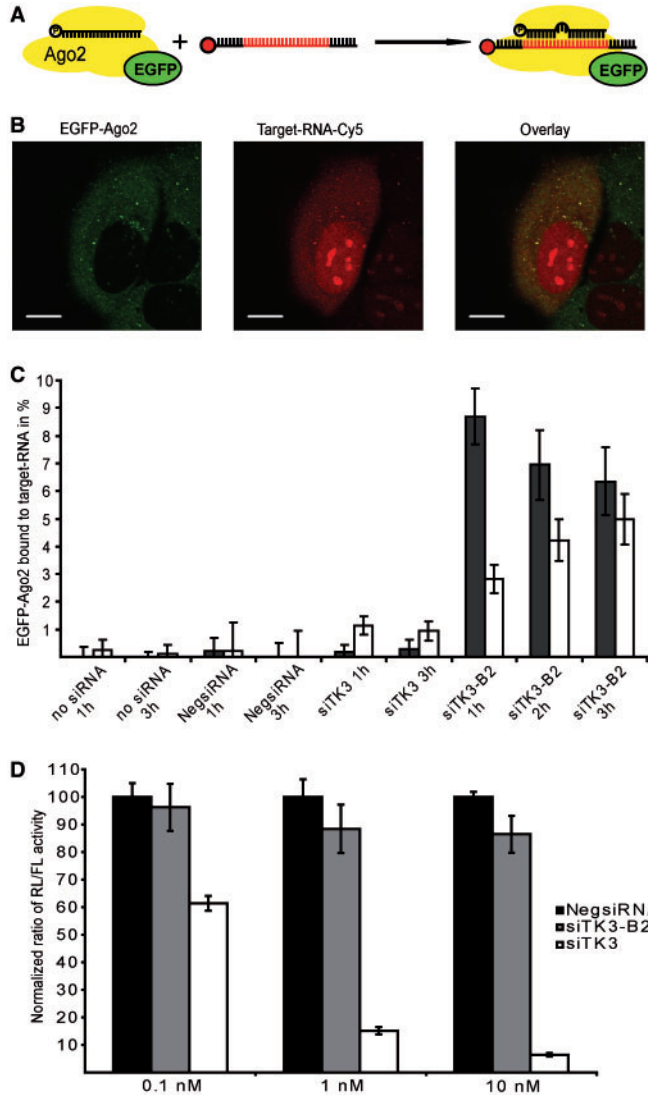


Figure 4. Cleavage impaired RISC-target interactions mediate RISC accumulation in the nucleus. (A) An outline of the experiment is illustrated. EGFP-Ago2 serves as a fluorescent label for RISC that can interact with the Cy5 labelled target-RNA. The interaction with the target-RNA is determined by FCCS *in vivo*. (B) LSM images of a target-RNA microinjected 10G cell (green: EGFP-Ago2, red: target-RNA, right panel: overlay). Scale bars indicate 10 μ m. (C) Cross-correlation measurements were performed 1 or 3 h after microinjection. Data are represented as mean \pm SEM, filled bars indicate measurements in the cytoplasm, open bars in the nucleus. (D) ER293 cells were transfected with the indicated amounts of NegsiRNA, siTK3 and siTK3-B2 together with the fixed concentration of the pGL2-Control and pRL-TK reporter plasmids. After 48 h, the ratios of target to control luciferase concentrations were normalized to the NegsiRNA control (black); siTK3-B2 (grey) and siTK3 (white). The plotted data were averaged from three different experiments \pm SD.

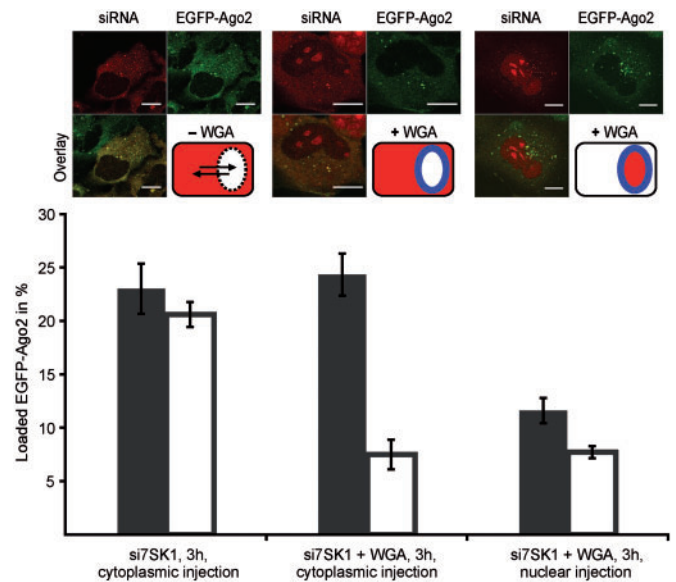


Figure 5. Nuclear activated RISC originates from the cytoplasm. The incorporation of the guide strand of 7SK1 into RISC was measured for a cytoplasmic microinjection, a cytoplasmic injection together with wheat germ agglutinin (WGA) to inhibit active transport through the nuclear pore and a nuclear injection of 7SK1 and WGA. LSM images (red: Cy5, green: EGFP, yellow: overlay) and cross-correlation measurement were taken 3 h after incubation. Scale bars indicated 10 μ m, data are represented as mean \pm SEM; filled bars indicate measurement in the cytoplasm, open bars in the nucleus.

7SK snRNA, again underlining the dynamic levels of specifically loaded nRISC.

Nuclear activated RISC originates from the cytoplasm

The fact that we could detect a target dependent accumulation of nRISC raises the question of the origination of nRISC. Two mechanisms are possible: First, RISC is loaded both inside the nucleus and the cytoplasm or second, RISC is loaded in the cytoplasm and can then be imported into the nucleus to regulate gene expression/function. The first hypothesis is less likely for several reasons. The nRISC that was characterized by FCS *in vivo* displayed a molecular mass of ~158 kDa which is too small for the RLC (containing EGFP-Ago2, TRBP and Dicer which should result in a complex of approximately 380 kDa). In addition, siRNAs are too short to contain localization signals, therefore the RLC is incapable to locate the appropriate cellular compartment for individual silencing triggers until RISC interacts with its target RNA. And last, miRNAs and siRNAs depend on their cytoplasmic localization, mediated by Exp5, for effective silencing to occur (17,18,42). To elucidate the cytoplasmic origin of nRISC, we microinjected si7SK1 into the cytoplasm of 10G cells and allowed for exchange between nucleus and cytoplasm. This resulted in a preferential cytoplasmic localization of the siRNAs with 24% of EGFP-Ago2 loading levels in the cytoplasm with the corresponding nuclear levels of 21% after 3 h (Figure 5). In the second experiment, we microinjected siRNAs into the cytoplasm together with wheat germ agglutinin (WGA), an inhibitor of nuclear pore-mediated active transport. The sub-cellular localization of the siRNAs was still preferentially in the cytoplasm, but due to their small size could still be detected in the nucleus (Figure 5). The cytoplasmic incorporation levels were unaffected compared to WGA-free microinjected cells showing that WGA did not interfere with the RISC loading process. The nuclear incorporation level decreased 3-fold down to 7%, indicating that most of nRISC is originating from the cytoplasm. The same decrease in EGFP-Ago2 nuclear incorporation levels were detected by nuclear microinjection of si7SK1 together with WGA. The drop of loaded EGFP-Ago2 with si7SK1 in the cytoplasm results from reduced siRNA levels in the cytoplasm mediated by WGA. The preferential delivery of siRNAs via microinjection into the nucleus could be detected by the higher fluorescence intensity in the nucleus in comparison with the cytoplasm (Figure 5). The same results were obtained for si7SK3-bulge (Supplementary Figure S6). The inhibitory function of injected WGA on import and export processes was verified with the stress kinase Mk2 tagged with EGFP. Upon stress this predominantly nuclear protein shuttles into the cytoplasm (43). We could show that EGFP-MK2 shuttles into the cytoplasm after treatments with Anisomycin for 3 h that could be stopped with the addition of Leptomycin B which is an inhibitor of the exporter of MK2 (Supplementary Figure S7A, upper panel and S7B). The microinjection with WGA inhibited the export of EGFP-MK2 very efficiently (Supplementary Figure S7A, bottom panel and S7B). Treatment with

cycloheximide did not change incorporation levels of EGFP-Ago2 in the nucleus, thereby excluding that the accumulation of specifically loaded RISC in the nucleus results from *de novo* synthesis of EGFP-Ago2 which is transported in the nucleus and subsequently loaded (Supplementary Figure S8).

Our results show that RISC is loaded in the cytoplasm and is imported into the nucleus. Therefore, the RLC is strictly localized in the cytoplasm. The accumulation of the si7SK1 and si7SK3-bulge siRNA indicates a dynamic exchange of RISC between the nucleus and the cytoplasm. Furthermore, the interaction with the target RNA seems to interfere with the export of RISC leading to the accumulation of this particularly loaded RISC in the nucleus. RISC shuttling between the cytoplasm and the nucleus represents a mechanism to access targets in both cellular compartments.

DISCUSSION

To summarize our findings, we propose the following model for human RISC loading and shuttling between the cytoplasm and the nucleus (Figure 6). (i) We could show for the first time that the RLC is localized and interacts with siRNAs/miRNAs exclusively in the cytoplasm. This is supported by Exp5 mediated nuclear export of small dsRNAs that actively reduces the concentration of silencing triggers in the nucleus and hence would lower the loading efficiency of nRISC (17,18). Consequently, miRNAs as well as siRNAs depend on the cytoplasmic localization for efficient silencing activity. The RLC senses the asymmetry of the duplex and specifically incorporates the guide strand into hAgo2, thereby forming cRISC. This process seems to be regulated, as FCCS measurements immediately after microinjection yielded low

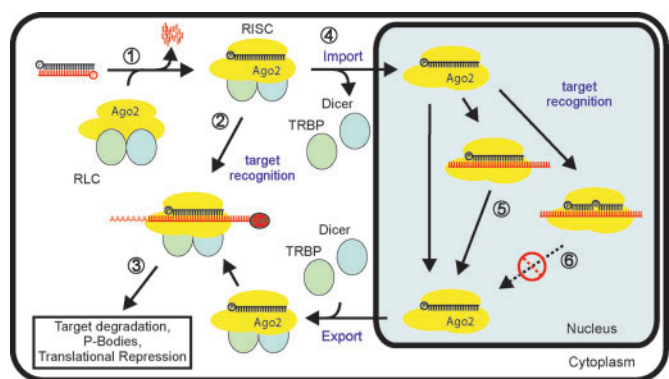


Figure 6. Model for human RISC loading and shuttling between the cytoplasm and the nucleus. (i) Asymmetric guide-strand incorporation is localized to the cytoplasm only, (ii) Guide-strand mediated target recognition in the cytoplasm, (iii) A perfect match results in RISC mediated target degradation, (iv) A fraction of cytoplasmic loaded RISC is imported into the nucleus to ensure cell wide target regulation. Cytoplasmic co-factors dissociate from hAgo2 protein, thereby forming nRISC, (v) Guide-strand mediated target recognition in the nucleus. A perfect RISC-target interaction leads to free RISC which can be exported into the cytoplasm, and (vi) whereas a miRNA-like interaction leads to the accumulation of RISC in the nucleus resulting in efficient regulation in the nucleus.

levels of loaded RISC. Most of the guide strands were incorporated within the first 3–12 h, followed by a decline for longer incubation times. (ii) We proved that the majority of activated cRISC remains in the cytoplasm as a complex of ~3MDa to regulate gene expression of mRNAs. (iii) In case of perfectly priming guide strands to target RNAs, cRISC catalyses RNA degradation. For miRNAs, cRISC remains bound to the mRNA to regulate its expression and/or translocation to P-bodies. (iv) Our results indicate a partial translocation of activated cRISC into the nucleoplasm thereby forming nRISC of ~158 kDa, most likely composed of only hAgo2. We were not able to monitor whether EGFP-Ago2 loses the RLC components Dicer, TRBP and other factors before or during the translocation, but RLC disassembly after guide strand incorporation is supported by previous reports *in vitro* (44,45). The partial translocation of loaded hAgo2 is in agreement with the findings by Robb *et al.* (23) who observed cleavage activity in cytoplasmic and nuclear extracts. (v) In contrast to Robb *et al.*, we were able to directly compare guide strand incorporation levels with hAgo2 concentration and intracellular localization as well as the interaction dynamics of RISC with its target RNA. We therefore could demonstrate that perfectly priming guide-target RNA hybridizations lead to target RNA cleavage, immediately causing RISC-target RNA-complex disassembly, resulting in free nRISC which is in agreement with the kinetic analysis of minimal RISC *in vitro* (41). (vi) On the contrary, cleavage impaired nRISC, e.g. caused by dsRNA regions or bulges, results in the accumulation of this particularly loaded RISC in the nucleus, facilitated by its prolonged interaction with the target RNA. Due to the artificially induced target-RNA-RISC accumulation, we can exclude that the target dependent accumulation of nRISC is facilitated by the strict nuclear localization of 7SK snRNA and therefore results from the stable interaction of RISC with its target. Since we never detected a concentration increase of nRISC, we reason that a stable equilibrium between n- and cRISC exists that is shifted for a particularly loaded nRISC depending on the target interaction.

Taken together, our results propose a RISC exchange/shuttling mechanism between the cytoplasm and the nucleus. Due to the absence of nuclear localization signals in siRNAs and miRNAs, this shuttling mechanism ensures the accessibility of activated RISC to target containing cellular compartments. The shuttling of hAgo2 into the nucleus also explains why agRNAs can function in the nucleus. Due to the identical localization patterns of hAgo1 and hAgo2 (23), we propose that nuclear hAgo1 also originates from the cytoplasm to mediate transcription activation or TGS. In agreement with our model, the findings that also let-7 miRNA is incorporated into nuclear hAgo2 and that computational approaches showed that many identified miRNAs have substantial complementarity to sequences within gene promoters provide further evidence for the existence of an endogenous RNA-mediated transcription regulation machinery originating from cytoplasmic activated Argonaute proteins (23,28).

In a previous report, Berezhna and colleagues observed by confocal imaging that siRNAs targeting 7SK and U6 snRNAs localize into the nucleus as duplexes whereas an siRNA targeting cytoplasmic hepatitis C virus replicon RNA dissociates into the cytoplasmic localized guide strand and a degraded passenger strand after transfection. From this Berezhna *et al.* (46) concluded the existence of a mechanism by which the RISC-loading machinery orchestrates a target-determined localization of siRNAs and provide evidence for RISC-loading in the nucleus. In contrast to their findings, we showed that the analysis of siRNA sub-cellular localization by imaging is mainly affected by Exp5 mediated export, since the majority of siRNAs is not bound by the RLC/RISC thereby excluding a target-determined localization. Further arguing against the target-determined siRNA localization hypothesis is the stable hAgo2 concentration that we observed in the nucleus independent of the incorporated guide strand and our direct evidence for exclusive cytoplasmic RISC-loading. In addition, RISC has been shown to identify its target and defines the silencing mode after the removal of the passenger strand depending on the complementarity to its target, supporting our observations (47). The localization of the complete siRNA duplex in the nucleus, as observed by Berezhna *et al.*, would imply that the RLC is able to sense whether the bound siRNA duplex has a nuclear or cytoplasmic target. However, siRNAs are only bound briefly to the RLC in form of a duplex as we could not detect significant levels of incorporated passenger strand in neither RISCs. Findings by Robb *et al.* (23) also showed the target independent localization of guide RNAs in nuclear extracts. In addition, we showed that nRISC consists of a distinct hAgo2 protein that cannot bind dsRNA (48).

Underlining our model, it was shown that miR-138 is restricted to distinct cell types, whereas its precursor pre-miR-138-2 is ubiquitously expressed and cytoplasmically localized, thus showing the regulation on the post-transcriptional level in the cytoplasm (49). In combination with our results that the RLC is restricted to the cytoplasm, this post-transcriptional control of miRNA maturation in the cytoplasm applies to the regulation of guide strand incorporation into c- and nRISC.

As the interaction of nRISC with its target seems to prevent its export, this mechanism might prevent specific RNA transcripts from entering the cytoplasm and associating with the translation machinery. Further studies on the effect of nRISC-target RNA interactions and the sequencing of miRNAs or other classes of small RNAs in nRISC are needed to unravel the biological role of the nuclear RNAi machinery.

The advantage of our newly established experimental platform is the detailed real-time monitoring of the incorporation process into RISC *in vivo*. It represents a unique tool to address so far inaccessible questions from a new perspective. Our FCCS assay is superior in studying the impact of siRNA sequence and structure on RISC loading and strand asymmetry compared to standard silencing readouts that are normally used in high-throughput assays. Therefore, our technique can contribute to the development of improved siRNA duplexes with different

functions suitable for the application as therapeutic agents. It can be used for screening chemicals that affect the activity of the RLC or the interaction of RISC with the target RNA which was not possible *in vivo* until now. Furthermore, the possibility of studying RISC-target interactions can lead to the engineering of RNAs that can inhibit specific RNA functions, structures or affect for example alternative splicing and other RNA dependent mechanism.

SUPPLEMENTARY DATA

Supplementary Data are available at NAR Online.

ACKNOWLEDGEMENTS

We thank J. Martinez for providing hAgo2 plasmid; M. Gaestel for providing the EGFP-MK2 plasmid; Cenix BioSciences GmbH for helpful support; Z. Petrasek and E. Petrov for helpful advice and discussions; P. Svoboda, D. Merkle and S. Mende for critically reading the manuscript.

FUNDING

DFG (SPP 1128); Max-Planck Society; Boehringer Ingelheim Fonds fellowship (to L.W.). Funding for open access charge: DFG (SPP 1128).

Conflict of interest statement. None declared.

REFERENCES

- Ambros, V. (2004) The functions of animal microRNAs. *Nature*, **431**, 350–355.
- Elbashir, S.M., Harborth, J., Lendeckel, W., Yalcin, A., Weber, K. and Tuschl, T. (2001) Duplexes of 21-nucleotide RNAs mediate RNA interference in cultured mammalian cells. *Nature*, **411**, 494–498.
- Fire, A., Xu, S., Montgomery, M.K., Kostas, S.A., Driver, S.E. and Mello, C.C. (1998) Potent and specific genetic interference by double-stranded RNA in *Caenorhabditis elegans*. *Nature*, **391**, 806–811.
- Bernstein, E., Caudy, A.A., Hammond, S.M. and Hannon, G.J. (2001) Role for a bidentate ribonuclease in the initiation step of RNA interference. *Nature*, **409**, 363–366.
- Elbashir, S.M., Lendeckel, W. and Tuschl, T. (2001) RNA interference is mediated by 21- and 22-nucleotide RNAs. *Genes Dev.*, **15**, 188–200.
- Ketting, R.F., Fischer, S.E., Bernstein, E., Sijen, T., Hannon, G.J. and Plasterk, R.H. (2001) Dicer functions in RNA interference and in synthesis of small RNA involved in developmental timing in *C. elegans*. *Genes Dev.*, **15**, 2654–2659.
- Watanabe, T., Totoki, Y., Toyoda, A., Kaneda, M., Kuramochi-Miyagawa, S., Obata, Y., Chiba, H., Kohara, Y., Kono, T., Nakano, T. *et al.* (2008) Endogenous siRNAs from naturally formed dsRNAs regulate transcripts in mouse oocytes. *Nature*, **453**, 539–543.
- Hutvagner, G., McLachlan, J., Pasquinelli, A.E., Balint, E., Tuschl, T. and Zamore, P.D. (2001) A cellular function for the RNA-interference enzyme Dicer in the maturation of the let-7 small temporal RNA. *Science*, **293**, 834–838.
- Gregory, R.I., Chendrimada, T.P., Cooch, N. and Shiekhattar, R. (2005) Human RISC couples microRNA biogenesis and posttranscriptional gene silencing. *Cell*, **123**, 631–640.
- Hammond, S.M., Bernstein, E., Beach, D. and Hannon, G.J. (2000) An RNA-directed nuclease mediates post-transcriptional gene silencing in *Drosophila* cells. *Nature*, **404**, 293–296.
- Khvorova, A., Reynolds, A. and Jayasena, S.D. (2003) Functional siRNAs and miRNAs exhibit strand bias. *Cell*, **115**, 209–216.
- Schwarz, D.S., Hutvagner, G., Du, T., Xu, Z., Aronin, N. and Zamore, P.D. (2003) Asymmetry in the assembly of the RNAi enzyme complex. *Cell*, **115**, 199–208.
- Tomari, Y. and Zamore, P.D. (2005) Perspective: machines for RNAi. *Genes Dev.*, **19**, 517–529.
- Bhattacharyya, S.N., Habermacher, R., Martine, U., Closs, E.I. and Filipowicz, W. (2006) Relief of microRNA-mediated translational repression in human cells subjected to stress. *Cell*, **125**, 1111–1124.
- Pillai, R.S., Bhattacharyya, S.N., Artus, C.G., Zoller, T., Cougot, N., Basyuk, E., Bertrand, E. and Filipowicz, W. (2005) Inhibition of translational initiation by Let-7 MicroRNA in human cells. *Science*, **309**, 1573–1576.
- Valencia-Sanchez, M.A., Liu, J., Hannon, G.J. and Parker, R. (2006) Control of translation and mRNA degradation by miRNAs and siRNAs. *Genes Dev.*, **20**, 515–524.
- Ohrt, T., Merkle, D., Birkenfeld, K., Echeverri, C.J. and Schwill, P. (2006) *In situ* fluorescence analysis demonstrates active siRNA exclusion from the nucleus by Exportin 5. *Nucleic Acids Res.*, **34**, 1369–1380.
- Yi, R., Doehle, B.P., Qin, Y., Macara, I.G. and Cullen, B.R. (2005) Overexpression of exportin 5 enhances RNA interference mediated by short hairpin RNAs and microRNAs. *RNA*, **11**, 220–226.
- Hall, I.M., Shankaranarayana, G.D., Noma, K., Ayoub, N., Cohen, A. and Grewal, S.I. (2002) Establishment and maintenance of a heterochromatin domain. *Science*, **297**, 2232–2237.
- Matzke, M.A. and Birchler, J.A. (2005) RNAi-mediated pathways in the nucleus. *Nat. Rev. Genet.*, **6**, 24–35.
- Volpe, T.A., Kidner, C., Hall, I.M., Teng, G., Grewal, S.I. and Martienssen, R.A. (2002) Regulation of heterochromatic silencing and histone H3 lysine-9 methylation by RNAi. *Science*, **297**, 1833–1837.
- Meister, G., Landthaler, M., Patkaniowska, A., Dorsett, Y., Teng, G. and Tuschl, T. (2004) Human Argonaute2 mediates RNA cleavage targeted by miRNAs and siRNAs. *Mol. Cell*, **15**, 185–197.
- Robb, G.B., Brown, K.M., Khurana, J. and Rana, T.M. (2005) Specific and potent RNAi in the nucleus of human cells. *Nat. Struct. Mol. Biol.*, **12**, 133–137.
- Janowski, B.A., Huffman, K.E., Schwartz, J.C., Ram, R., Nordsell, R., Shames, D.S., Minna, J.D. and Corey, D.R. (2006) Involvement of AGO1 and AGO2 in mammalian transcriptional silencing. *Nat. Struct. Mol. Biol.*, **13**, 787–792.
- Janowski, B.A., Younger, S.T., Hardy, D.B., Ram, R., Huffman, K.E. and Corey, D.R. (2007) Activating gene expression in mammalian cells with promoter-targeted duplex RNAs. *Nat. Chem. Biol.*, **3**, 166–173.
- Morris, K.V., Chan, S.W., Jacobsen, S.E. and Looney, D.J. (2004) Small interfering RNA-induced transcriptional gene silencing in human cells. *Science*, **305**, 1289–1292.
- Han, J., Kim, D. and Morris, K.V. (2007) Promoter-associated RNA is required for RNA-directed transcriptional gene silencing in human cells. *Proc. Natl Acad. Sci. USA*, **104**, 12422–12427.
- Schwartz, J.C., Younger, S.T., Nguyen, N.B., Hardy, D.B., Monia, B.P., Corey, D.R. and Janowski, B.A. (2008) Antisense transcripts are targets for activating small RNAs. *Nat. Struct. Mol. Biol.*, **15**, 842–848.
- Bacia, K., Kim, S.A. and Schwill, P. (2006) Fluorescence cross-correlation spectroscopy in living cells. *Nat. Methods*, **3**, 83–89.
- Kim, S.A., Heinze, K.G. and Schwill, P. (2007) Fluorescence correlation spectroscopy in living cells. *Nat. Methods*, **4**, 963–973.
- Haustein, E. and Schwill, P. (2004) Single-molecule spectroscopic methods. *Curr. Opin. Struct. Biol.*, **14**, 531–540.
- Mathews, D.H., Sabina, J., Zuker, M. and Turner, D.H. (1999) Expanded sequence dependence of thermodynamic parameters improves prediction of RNA secondary structure. *J. Mol. Biol.*, **288**, 911–940.
- Zuker, M. (2003) Mfold web server for nucleic acid folding and hybridization prediction. *Nucleic Acids Res.*, **31**, 3406–3415.
- Hock, J., Weinmann, L., Ender, C., Rudel, S., Kremmer, E., Raabe, M., Urlaub, H. and Meister, G. (2007) Proteomic and functional analysis of Argonaute-containing mRNA-protein complexes in human cells. *EMBO Rep.*, **8**, 1052–1060.
- Leung, A.K., Calabrese, J.M. and Sharp, P.A. (2006) Quantitative analysis of Argonaute protein reveals microRNA-dependent localization to stress granules. *Proc. Natl Acad. Sci. USA*, **103**, 18125–18130.

36. Sen, G.L. and Blau, H.M. (2005) Argonaute 2/RISC resides in sites of mammalian mRNA decay known as cytoplasmic bodies. *Nat. Cell Biol.*, **7**, 633–636.
37. Chendrimada, T.P., Finn, K.J., Ji, X., Baillat, D., Gregory, R.I., Liebhaber, S.A., Pasquinelli, A.E. and Shiekhattar, R. (2007) MicroRNA silencing through RISC recruitment of eIF6. *Nature*, **447**, 823–828.
38. Martinez, J. and Tuschl, T. (2004) RISC is a 5' phosphomonoester-producing RNA endonuclease. *Genes Dev.*, **18**, 975–980.
39. Chen, Y., Muller, J.D., Ruan, Q.Q. and Gratton, E. (2002) Molecular brightness characterization of EGFP in vivo by fluorescence fluctuation spectroscopy. *Biophys. J.*, **82**, 133–144.
40. Wassarman, D.A. and Steitz, J.A. (1991) Structural analyses of the 7SK ribonucleoprotein (RNP), the most abundant human small RNP of unknown function. *Mol. Cell Biol.*, **11**, 3432–3445.
41. Ameres, S.L., Martinez, J. and Schroeder, R. (2007) Molecular basis for target RNA recognition and cleavage by human RISC. *Cell*, **130**, 101–112.
42. Yi, R., Qin, Y., Macara, I.G. and Cullen, B.R. (2003) Exportin-5 mediates the nuclear export of pre-microRNAs and short hairpin RNAs. *Genes Dev.*, **17**, 3011–3016.
43. Engel, K., Kotlyarov, A. and Gaestel, M. (1998) Leptomycin B-sensitive nuclear export of MAPKAP kinase 2 is regulated by phosphorylation. *EMBO J.*, **17**, 3363–3371.
44. MacRae, I.J., Ma, E., Zhou, M., Robinson, C.V. and Doudna, J.A. (2008) In vitro reconstitution of the human RISC-loading complex. *Proc. Natl Acad. Sci. USA*, **105**, 512–517.
45. Maniataki, E. and Mourelatos, Z. (2005) A human, ATP-independent, RISC assembly machine fueled by pre-miRNA. *Genes Dev.*, **19**, 2979–2990.
46. Berezna, S.Y., Supekova, L., Supek, F., Schultz, P.G. and Deniz, A.A. (2006) siRNA in human cells selectively localizes to target RNA sites. *Proc. Natl Acad. Sci. USA*, **103**, 7682–7687.
47. Doench, J.G., Petersen, C.P. and Sharp, P.A. (2003) siRNAs can function as miRNAs. *Genes Dev.*, **17**, 438–442.
48. Rivas, F.V., Tolia, N.H., Song, J.J., Aragon, J.P., Liu, J., Hannon, G.J. and Joshua-Tor, L. (2005) Purified Argonaute2 and an siRNA form recombinant human RISC. *Nat. Struct. Mol. Biol.*, **12**, 340–349.
49. Obernosterer, G., Leuschner, P.J., Alenius, M. and Martinez, J. (2006) Post-transcriptional regulation of microRNA expression. *RNA*, **12**, 1161–1167.

A Human snoRNA with MicroRNA-Like Functions

Christine Ender,^{1,6} Azra Krek,^{2,3,6} Marc R. Friedländer,² Michaela Beitzinger,¹ Lasse Weinmann,¹ Wei Chen,⁴ Sébastien Pfeffer,⁵ Nikolaus Rajewsky,^{2,*} and Gunter Meister^{1,*}

¹Center for Integrated Protein Science Munich (CIPSM), Laboratory of RNA Biology, Max Planck Institute of Biochemistry, Am Klopferspitz 18, 82152 Martinsried, Germany

²Max Delbrück Center for Molecular Medicine, Robert-Rössle-Strasse 10, 13125 Berlin, Germany

³Department of Physics, New York University, 4 Washington Place, New York, NY 10003, USA

⁴Department of Human Molecular Genetics, Max Planck Institute of Molecular Genetics, Ihnestrasse 73, 14195 Berlin, Germany

⁵IBMP-CNRS, 12 Rue du General Zimmer, 67084 Strasbourg Cedex, France

⁶These authors contributed equally to this work

*Correspondence: rajewsky@mdc-berlin.de (N.R.), meister@biochem.mpg.de (G.M.)

DOI 10.1016/j.molcel.2008.10.017

SUMMARY

Small noncoding RNAs function in concert with Argonaute (Ago) proteins to regulate gene expression at the level of transcription, mRNA stability, or translation. Ago proteins bind small RNAs and form the core of silencing complexes. Here, we report the analysis of small RNAs associated with human Ago1 and Ago2 revealed by immunoprecipitation and deep sequencing. Among the reads, we find small RNAs originating from the small nucleolar RNA (snoRNA) ACA45. Moreover, processing of ACA45 requires Dicer activity but is independent of Drosha/DGCR8. Using bioinformatic prediction algorithms and luciferase reporter assays, we uncover the mediator subunit CDC2L6 as one potential mRNA target of ACA45 small RNAs, suggesting a role for ACA45-processing products in posttranscriptional gene silencing. We further identify a number of human snoRNAs with microRNA (miRNA)-like processing signatures. We have, therefore, identified a class of small RNAs in human cells that originate from snoRNAs and can function like miRNAs.

INTRODUCTION

Small noncoding RNAs, including microRNAs (miRNAs), short interfering RNAs (siRNAs), and Piwi-interacting RNAs (piRNAs), are important regulators of gene expression (Filipowicz et al., 2005; Meister and Tuschl, 2004; Seto et al., 2007). miRNAs and siRNAs guide sequence-specific cleavage, deadenylation, or translational repression of target mRNAs (Chen and Rajewsky, 2007; Pillai et al., 2007). piRNAs are specifically expressed in testes (Seto et al., 2007) and control retrotransposition in the mammalian germ line (Aravin et al., 2007).

In many gene-silencing pathways, small RNAs are generated from double-stranded RNA (dsRNA) molecules by distinct processing steps (Tomari and Zamore, 2005). miRNA genes are transcribed by RNA polymerases II or III as primary miRNAs that are further processed to hairpin-structured miRNA precursors

(pre-miRNAs) by the nuclear microprocessor complex containing the RNase III enzyme Drosha and its cofactor DGCR8 (Borchert et al., 2006; Denli et al., 2004; Gregory et al., 2004; Landthaler et al., 2004; Lee et al., 2003, 2004). Pre-miRNAs are transported to the cytoplasm, where the RNase III enzyme Dicer cleaves off the loop of the miRNA hairpin, thereby generating a short dsRNA of about 20–25 nucleotides (nt) in length (Bohnsack et al., 2004; Grishok et al., 2001; Hutvagner et al., 2001; Lund et al., 2004). Such dsRNA intermediates are subsequently unwound, and the single-stranded mature miRNA is incorporated into effector complexes often referred to as miRNPs (Mourelatos et al., 2002). In the siRNA pathway or RNA interference (RNAi), long dsRNA is processed by Dicer as well (Bernstein et al., 2001). The mature siRNA is incorporated into the RNA-induced silencing complex (RISC). The biogenesis of piRNAs is only poorly understood and probably does not require the function of Drosha or Dicer.

Argonaute (Ago) proteins are the cellular binding partners of small RNAs and form the core of gene silencing effector complexes (Parker and Barford, 2006; Peters and Meister, 2007). In humans, eight different Argonaute genes exist, which can be phylogenetically divided into four Ago and four Piwi subfamily members (Peters and Meister, 2007; Tolia and Joshua-Tor, 2007). Whereas Piwi proteins interact with piRNAs in the germ line (Seto et al., 2007), Ago subfamily members associate with miRNAs in somatic cells. Argonaute proteins are generally characterized by Piwi-Argonaute-Zwille (PAZ) and PIWI domains (Parker and Barford, 2006; Peters and Meister, 2007). A third domain, termed MID domain, anchors the 5' end of the small RNA (Ma et al., 2005; Parker et al., 2005). The PAZ domain binds the 3' end of the small RNA, and the PIWI domain, which is structurally similar to RNase H, cleaves the complementary target RNA (Parker and Barford, 2006; Patel et al., 2006; Tolia and Joshua-Tor, 2007). However, not all Argonaute proteins are endonucleases, although critical residues within the PIWI domain are conserved. In mammals, only Ago2 has been shown to act as endonuclease in RNAi (Liu et al., 2004; Meister et al., 2004). Argonaute proteins with endonuclease activity are often referred to as Slicers. Although Ago subfamily members have been extensively studied in the past, only little is known about their individual small RNA-binding specificities. It has been reported that all Ago proteins bind miRNAs or siRNAs indiscriminately of their

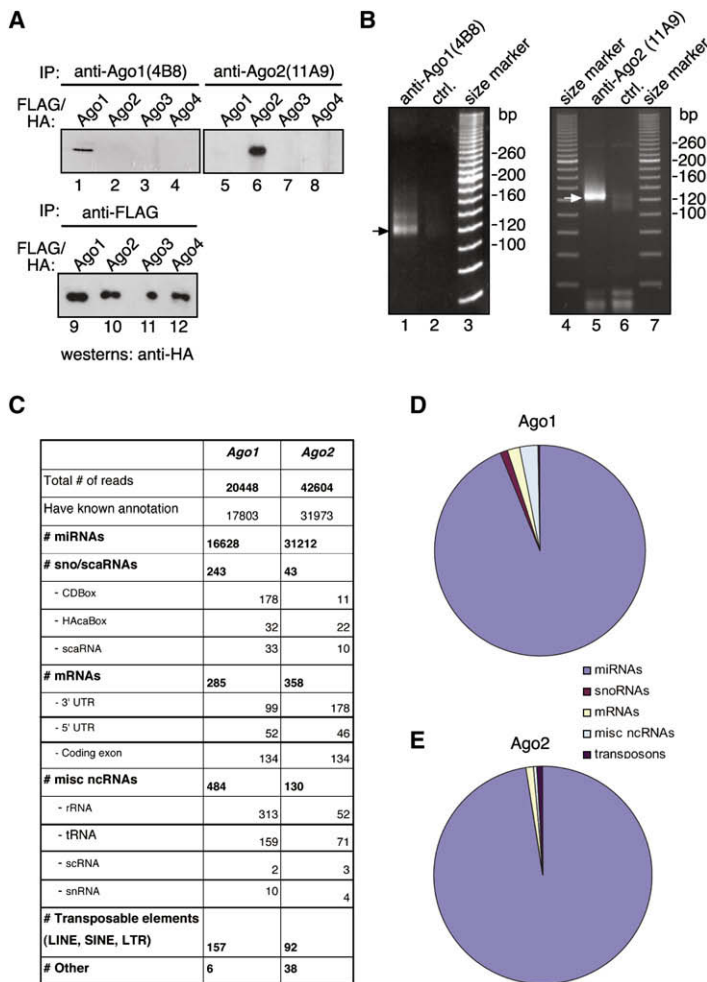


Figure 1. Small RNAs Associated with Ago1 and Ago2 Complexes

(A) Characterization of monoclonal anti-Ago1 and anti-Ago2 antibodies. FLAG/HA-tagged Ago1 through 4 were subjected to immunoprecipitations using anti-Ago1(4B8) (lanes 1–4), anti-Ago2(11A9) (lanes 5–8), and anti-FLAG (lanes 9–12). Immunoprecipitated FLAG/HA-Ago proteins were analyzed by western blotting using anti-HA antibodies.

(B) Endogenous Ago1 (lane 1) and Ago2 (lane 5) complexes were immunoprecipitated using the specific monoclonal antibodies described in (A). An anti-FLAG (lane 2) or an anti-GST antibody (lane 6) served as controls. Coimmunoprecipitated RNAs were extracted, cloned, and sequenced. Cloned PCR products containing 5' adaptors, poly(A) tails, and 3' adaptor sequences were loaded onto an agarose gel and visualized by ethidium bromide staining.

(C) Summary of the sequencing data obtained from deep sequencing of human Ago1 and Ago2 associated small RNAs.

(D and E) Schematic representation of individual small RNA classes that are associated with human Ago1 or Ago2 complexes.

RESULTS

Small RNAs Associated with Human Ago1 and Ago2

Different Ago proteins associate with the same miRNA species regardless of their sequence (Azuma-Mukai et al., 2008; Meister et al., 2004). However, the spectrum of Ago-associated small RNAs in human somatic cells is presently not known. Therefore, we used monoclonal antibodies specific to human Ago1 (Ago1 [4B8]) (Beitzinger et al., 2007) and Ago2 (Ago2 [11A9]) (Rudel et al., 2008) for Ago isolation from total HEK293 cell lysates (Figure 1A). Coimmunoprecipitated RNAs were extracted and cloned without size fractionation (Figure 1B). Using 454 deep sequencing, we obtained 20448 reads from the Ago1-associated and 42604 reads from the Ago2-associated small RNA libraries (Figures 1C–1E). Using a Dicer substrate identification algorithm (Friedländer et al., 2008), the presence of 166 known miRNAs in the combined Ago1 and Ago2 libraries was confirmed. We next investigated whether miRNAs are differentially bound to Ago1 or Ago2 in HEK293 cells (Table S1 available online). All miRNAs that are present in the libraries bind to Ago1 as well as Ago2. Similarly to the published data on Ago2 and Ago3 miRNA association (Azuma-Mukai et al., 2008), some miRNAs are more highly represented in one or the other library, suggesting a preferential Ago binding.

Processing of Functional Small RNAs from the Bona Fide snoRNA ACA45

In the Ago-associated RNA libraries, we have identified small RNAs with a length of about 20–22 nt that originate from snoRNAs particularly from ACA45 (Figure 2A). Notably, the sequenced reads derive only from the hairpin formed by the 3' half of ACA45. The found reads are conserved in mammals (Figure 2B), suggesting that they are, indeed, specific processing products.

Although ACA45 was identified in a screen for functional snoRNAs (Kiss et al., 2004), it is conceivable that it represents a miRNA gene that has been misannotated as snoRNA. Due to

sequence (Liu et al., 2004; Meister et al., 2004). However, a recent study analyzed small RNAs that are associated with human Ago2 and Ago3 and suggested that Ago proteins might have preferences for individual miRNA species, although all miRNAs that have been investigated bind to both Ago2 and Ago3 (Azuma-Mukai et al., 2008).

Here, we report the characterization of small RNAs associated with human Ago1 and Ago2 by immunoprecipitation and deep sequencing. We find that Ago1 and Ago2 bind to similar sets of miRNAs, although some miRNAs are more prominent in Ago2 libraries and vice versa. More importantly, we find small RNAs that originate from small nucleolar RNAs (snoRNAs). snoRNAs are nucleolar noncoding RNAs, which have important functions in the maturation of other noncoding RNAs such as ribosomal RNAs (rRNAs) or small nuclear RNAs (snRNAs) (Matera et al., 2007). We demonstrate that the bona fide snoRNA ACA45 is processed to small 20- to 25-nt-long RNAs that stably associate with Ago proteins. Processing is independent of the Drosha/DGCR8 complex but requires Dicer. Finally, we identify a cellular target mRNA that is regulated by the ACA45-derived small RNA, indicating that snoRNA-derived small RNAs can function like miRNAs.

their specific structures and functions, snoRNAs can be grouped in H/ACA and Box C/D class snoRNAs. snoRNAs associate with specific protein components such as GAR-1 (H/ACA) or fibrillarin (Box C/D) to form functional snoRNPs (Matera et al., 2007). In order to prove that ACA45 is, indeed, a functional snoRNA, we analyzed GAR-1 binding to ACA45 (Figure 2C). Endogenous GAR-1 was immunoprecipitated using anti-GAR-1 antibodies. Associated RNAs were extracted and further analyzed by northern blotting using the probe specific to ACA45. Indeed, full-length ACA45 was readily detectable in the anti-GAR-1 (lane 2), but not in control immunoprecipitates (lane 3). Our data, therefore, confirm that ACA45 represents a functional snoRNA.

We next validated the processing of ACA45 to small RNAs by northern blotting (Figure 2D). A probe complementary to the 5' arm (Figure 2A, indicated in blue) detected the full-length ACA45 snoRNA as well as a band of ~22–23 nt in total RNA, indicating that a portion of the cellular ACA45 pool is, indeed, processed to small RNAs. Using quantitative northern blotting, we analyzed ACA45 sRNA molecule numbers per cell (data not shown). We find that less than 1000 molecules are present per cell, which is similar to a low abundant miRNA (Lim et al., 2003). Since only a minor portion of ACA45 is processed to small RNAs, we next investigated whether ACA45 processing products are specifically enriched in Ago protein complexes (Figure 2E). Endogenous Ago1 (lane 2) or Ago2 (lane 4) were immunoprecipitated, and associated RNAs were analyzed by northern blotting against ACA45-processing products. Consistent with the cloning data, the small RNA derived from ACA45 was enriched in Ago1 as well as Ago2 immunoprecipitates, indicating that ACA45-processing products specifically associate with Ago proteins. Therefore, we refer to this functional small RNA as ACA45 small RNA (ACA45 sRNA).

ACA45 Small RNAs Can Function Like miRNAs

The striking similarity of ACA45-processing products to miRNA precursors prompted us to investigate whether ACA45 sRNAs are functionally similar to miRNAs. We generated a luciferase reporter construct containing a complementary binding site for the abundant 5' arm of the snoRNA precursor (Figure 3A). Luciferase activity was strongly increased when the endogenous ACA45-derived small RNAs were inhibited using 2'-O-methylated (2'-OMe) antisense inhibitors (Figure 3A). Moreover, luciferase activity was also increased when the RNAi endonuclease Ago2 was depleted (Figure 3B), indicating that small RNAs that are processed from ACA45 can function like miRNAs.

ACA45 Processing Is Independent of the Drosha/DGCR8 Complex but Requires Dicer

The cleavage signature of the stem-loop-structured processing intermediate is different than the typical 2 nt 3' overhangs generated by Drosha. Therefore, we analyzed whether ACA45 processing requires activity of the Drosha/DGCR8 complex using *in vitro* as well as *in vivo* approaches (Figures 3B and 3C). FLAG/HA(FH)-tagged DGCR8 was immunoprecipitated, and the immunoprecipitate was incubated with either a ³²P-labeled primary miR-27a transcript or ACA45. A specific cleavage product representing pre-miR-27a was observed in the anti-DGCR8 immunoprecipitates, whereas no signal was observed when

ACA45 was used as substrate. We further investigated Drosha requirements using the luciferase reporter construct described above (Figure 3B). Indeed, we did not observe elevated luciferase activity upon Drosha depletion (siRNAs have been validated in Landthaler et al. [2004]), whereas luciferase activity of a miR-19b-responsive reporter was significantly increased. Taken together, our results suggest that ACA45 processing is independent of the Drosha/DGCR8 complex.

Next, we investigated Dicer requirements for ACA45 processing. It has been demonstrated that Ago proteins form a stable complex with Dicer, and Dicer activity can be coimmunoprecipitated with antibodies against Ago proteins (Gregory et al., 2005; Maniataki and Mourelatos, 2005; Meister et al., 2005). Therefore, FH-tagged Ago proteins, as well as FH-Dicer, was immunoprecipitated from HEK293 lysates and incubated with ³²P-labeled pre-miR-27a or full-length ACA45 (Figure 3D). As expected, both FH-Ago2 and FH-Dicer immunoprecipitates efficiently processed the miR-27a precursor (Figure 3D, left panel). Furthermore, FH-Ago1, FH-Ago2, and FH-Dicer immunoprecipitates processed the ³²P-labeled full-length ACA45 as well (Figure 3D, right panel), suggesting that Dicer is required for the generation of ACA45 small RNAs. To further investigate Dicer's function in ACA45 processing, we analyzed whether Dicer alone is sufficient for ACA45 processing *in vitro*. ³²P-labeled ACA45 was incubated with increasing amounts of recombinant Dicer, and cleavage products were analyzed by RNA-PAGE (Figure 3E). Indeed, recombinant Dicer produced small RNAs from the full-length ACA45 in a concentration-dependent manner, suggesting that Dicer alone is sufficient for ACA45 processing. Notably, Dicer generates longer RNAs as well, which might represent processing intermediates (see asterisk in Figure 3D). Finally, we analyzed the role of Dicer in ACA45 processing *in vivo*. Total RNA from mouse embryonic stem (ES) cells carrying homozygous or heterozygous Dicer deletions (Murchison et al., 2005) was analyzed for the presence of ACA45 small RNAs by semiquantitative real-time PCR (qRT-PCR) (Figure 3F). Strikingly, no PCR product was detectable in the Dicer^{-/-} cells, whereas a PCR product originating from the ACA45 small RNA was readily detectable in Dicer^{+/-} cells. Notably, the full-length ACA45 was present in both Dicer^{-/-} and Dicer^{+/-} cells. Similar results were obtained when total RNA from Dicer^{-/-} and Dicer^{+/-} cells was analyzed by northern blotting using a probe complementary to the ACA45 small RNA (Figure 3G). In summary, our data indicate that Dicer processes ACA45 to small RNAs independently of the Drosha-containing microprocessor complex.

Validation of an Endogenous ACA45-Derived Small RNA Target

It is thought that complementary Watson-Crick base pairing of the seed (nucleotides 2–8 counted from the 5' end) is a key feature of miRNA:mRNA target recognition. It is also known that highly conserved 7-mers in 3'UTRs are often complementary to seed sequences of known miRNAs (Chen and Rajewsky, 2007). Remarkably, the seed of ACA45 22-nt-long processing product is perfectly complementary to a significantly conserved 3'UTR motif (top 3% of all possible seed sites). Using the miRNA target prediction algorithm PicTar (Krek et al., 2005), we have predicted target mRNAs for the ACA45-derived small RNA

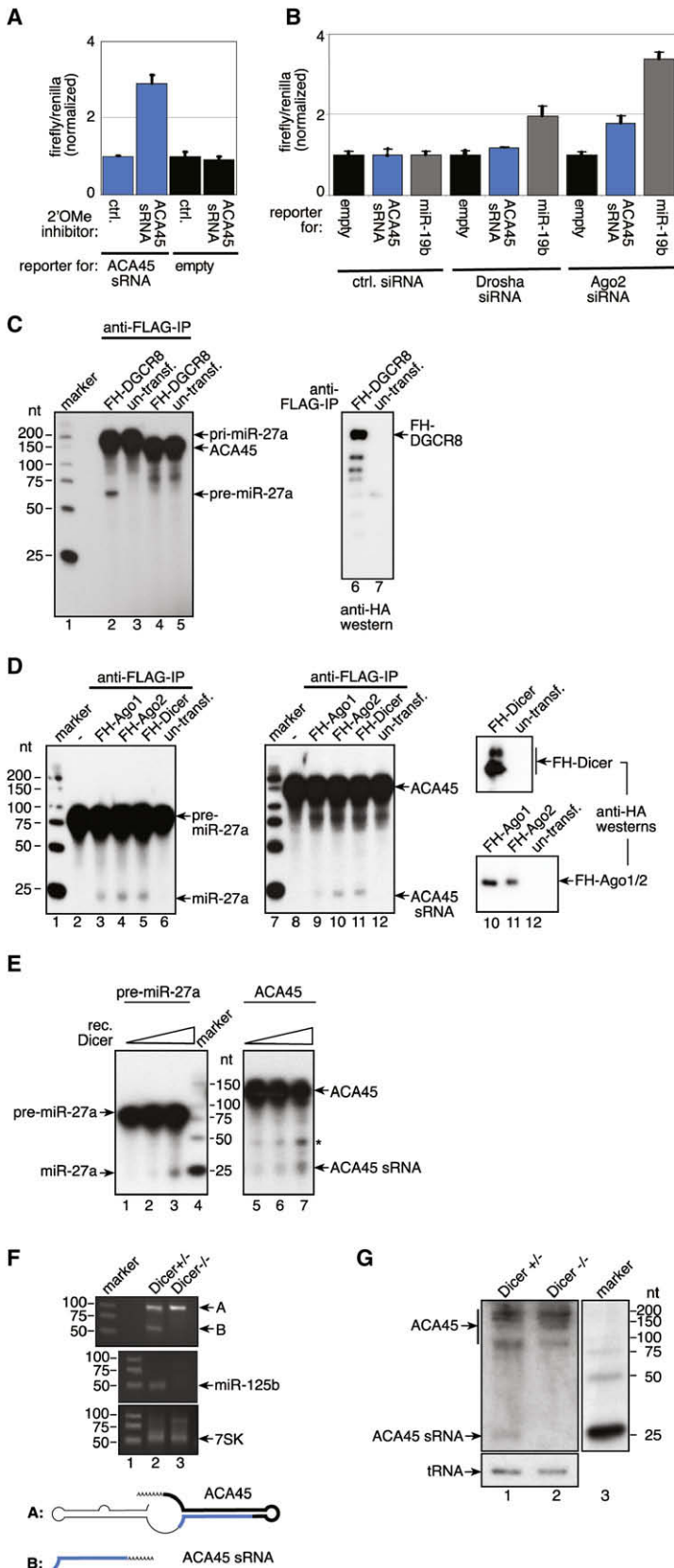


Figure 3. ACA45 Processing Requires Dicer but Is Independent of Drosha

(A) A luciferase reporter construct containing a perfectly complementary binding site for the ACA45 sRNA or the empty vector was cotransfected with 2'-O-methylated antisense inhibitors directed against the ACA45 sRNA.

(B) The luciferase reporter described in (A), the empty vector, and a luciferase reporter containing a complementary binding site to miR-19b were transfected into HEK293 cells that have been pre-transfected with control siRNAs, siRNAs directed against Drosha, and siRNAs against Ago2. Firefly luciferase activity was normalized to Renilla activity. Error bars are derived from four individual experiments.

(C) FH-DGCR8 or untreated cells were immunoprecipitated using anti-FLAG antibodies. Immunoprecipitates were incubated with ³²P-labeled pri-miRNA-27a (lanes 2 and 3) or ACA45 (lanes 4 and 5). Lane 1 represents a size marker, and lanes 6 and 7 represent the protein input.

(D) FH-Ago2 (lanes 4 and 10), FH-Ago1 (lanes 3 and 9), and FH-Dicer (lanes 5 and 11) were incubated with ³²P-labeled pre-miR-27a (lanes 2–6) or ACA45 (lanes 8–12) and analyzed by RNA PAGE. In lanes 6 and 12, lysate from untransfected HEK293 cells was used. Lanes 13–15 show anti-HA western blots of the protein input. Lanes 1 and 7 show size markers.

(E) ³²P-labeled pre-miR-27a (lanes 1–3) or ACA45 (lanes 5–7) were incubated with increasing amounts of recombinant Dicer. Cleavage products were analyzed by RNA PAGE. Lane 4 shows a size marker. A putative processing intermediate is indicated by an asterisk.

(F) Total RNA from Dicer^{+/-} (lane 2) or Dicer^{-/-} cells was analyzed by semi-qRT-PCR using primers specific for the ACA45 sRNA (upper panel), miR-125b (middle panel), and 7SK RNA (lower panel). The origin of the PCR products indicated as A and B are highlighted in bold below the figure.

(G) Total RNA from Dicer^{+/-} (lane 1) or Dicer^{-/-} (lane 2) cells was analyzed by northern blotting using probes specific for the ACA45 small RNA described above. Lane 3 shows a size marker.

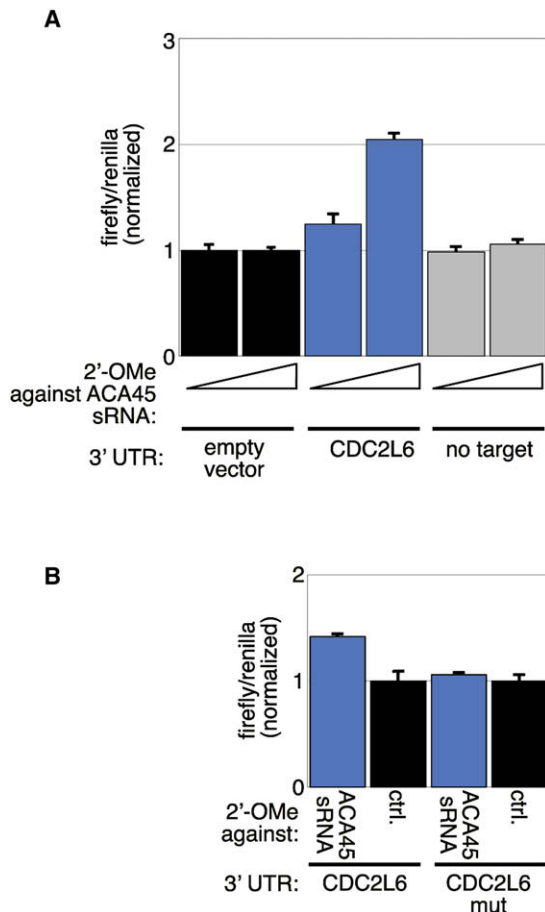


Figure 4. ACA45-Derived Small RNAs Regulated CDC2L6 Expression

(A) Luciferase reporter constructs containing the 3'UTR of CDC2L6 or BAP-1 (no target) or the empty vector were cotransfected with increasing concentrations of 2'-OMe inhibitors against the ACA45 sRNA. Firefly luciferase activity was normalized to Renilla activity. Error bars are derived from four individual experiments.

(B) Luciferase reporter constructs containing the 3'UTR of CDC2L6 or the CDC2L6 3'UTR with mutated ACA45 sRNA-binding sites were cotransfected with 2'-OMe inhibitors against the ACA45 sRNA. Firefly luciferase activity was normalized to Renilla activity. Error bars are derived from four individual experiments.

(data not shown). For experimental validation, we fused a number of 3'UTRs that we selected from the predicted target mRNAs to a luciferase reporter gene. Luciferase reporter constructs were cotransfected with 2'-OMe oligonucleotides antisense to the ACA45 small RNA. Many of the tested 3'UTRs, however, did not respond to the 2'-OMe inhibitors, suggesting that the small RNA does not target these mRNAs or that small RNA-target mRNA interactions are not relevant in the cell line that has been used (Figure 4A and data not shown). Strikingly, we found that activity of the luciferase reporter fused to the CDC2L6 (CDK11) 3'UTR is increased when the endogenous ACA45 small RNA is inhibited. The CDC2L6 gene product is a component of the mediator complex and, therefore, important for transcription (Conaway et al., 2005). For further validation of ACA45 sRNA

effects on CDC2L6 expression, we mutated all predicted ACA45 sRNA-binding sites in the CDC2L6 3'UTR (Figures 4B and S1). Indeed, a luciferase reporter containing the mutated CDC2L6 3'UTR was not upregulated when endogenous ACA45 sRNA was inhibited (Figure 4B), indicating that ACA45 sRNA seed sequence matches are important for CDC2L6 expression.

In summary, our data demonstrate that ACA45 is processed to a small RNA that can function like a miRNA on the endogenous target CDC2L6, identifying the ACA45 sRNA as a potential transcriptional regulator in human cells.

Cellular snoRNAs with miRNA Processing Signatures

The intriguing finding that ACA45 can function like a miRNA prompted us to analyze processing of other snoRNAs. We generated small RNA libraries from human Ago1–4 complexes and mapped the sequence reads to snoRNAs (the detailed composition of the Ago1–4 libraries are currently analyzed and will be published elsewhere). We find reads originating from stem-loop structures within the snoRNAs ACA47, ACA36b, U92, HBI-100, ACA56, ACA3, and ACA50 (Figure 6). Both arms of the individual stems are present in the libraries, and the sequence with the lower abundance is indicated as “star” sequences in Table S1 (see also Tables S2 and S3 for individual snoRNA-derived sequence reads and read lengths). Our data obtained from larger sequencing data sets suggest that processing of snoRNAs to functional small RNAs is not unique to ACA45 and can be observed for other snoRNAs as well.

DISCUSSION

snoRNAs form a highly abundant class of noncoding RNAs in many different organisms. snoRNAs localize to the nucleolus and guide specific modifications of rRNAs or snRNAs (Matera et al., 2007). Moreover, snoRNAs have also been implicated in alternative splicing events (Kishore and Stamm, 2006). Here, we show that the snoRNA ACA45 is processed to a small RNA that can function like a miRNA. ACA45 processing is independent of the Drosha-containing microprocessor complex but requires Dicer. At least in vitro, Dicer can process the full-length ACA45, although it does not structurally represent a classical Dicer substrate. In northern blots, however, the strongest signal originates from the full-length ACA45, and only a minor portion is processed to a small miRNA-like RNA. This observation is consistent with the finding that ACA45 exists as a functional snoRNA that forms snoRNPs with the protein factor GAR-1 (Matera et al., 2007). Therefore, we propose a model in which ACA45 is transcribed and functions in the nucleolus of human cells (Figure 5). However, a minor portion is transported to the cytoplasm by a so far unknown export receptor. In the cytoplasm, Dicer immediately processes the full-length snoRNA to a miRNA-like small RNA that functions in gene silencing. This hypothesis is supported by our finding that recombinant Dicer, as well as Dicer-containing Ago protein complexes, are capable of generating ACA45 small RNAs in vitro. However, it cannot be excluded that other nucleases contribute to ACA45 processing in the cytoplasm. Alternatively, ACA45 is cleaved in the nucleus already, and one half is recognized as miRNA precursor by the miRNA pathway. However, such a scenario might be unlikely because a nuclear

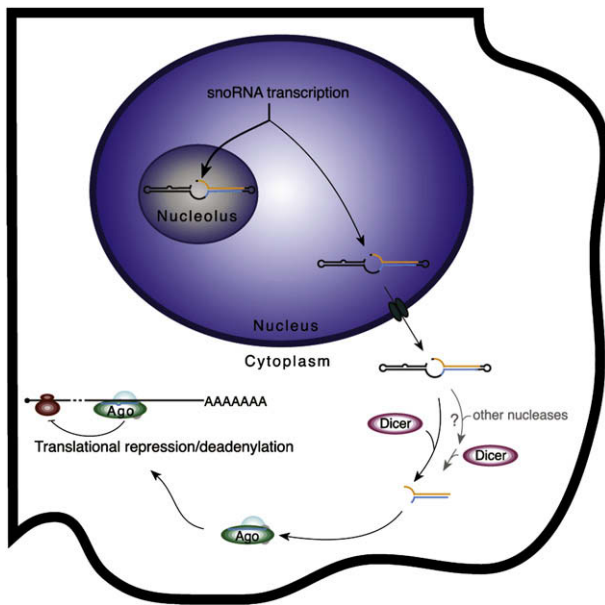


Figure 5. Model for ACA45 Processing and ACA45 sRNA Function in Human Cells

ACA45 snoRNA is transcribed in the nucleus, and the majority localizes to the nucleolus where it fulfills its specific functions by modifying other noncoding RNAs. However, a minor portion of ACA45 is exported to the cytoplasm, where Dicer, probably with the help of other nucleases, processes it to small RNAs that are specifically loaded into Ago protein-containing complexes. The ACA45-derived small RNA guides Ago protein complexes to partially complementary binding sites in the 3'UTR of target genes and represses its expression. AAAA, poly(A) tail.

cleavage activity might cleave the majority of the ACA45 pool, which is needed for classical snoRNA functions. Moreover, only one half of ACA45 would be exported by this model, although the other half folds like a typical miRNA precursor as well. Alternatively, a potential nuclear snoRNA cleavage activity could be physically separated from the snoRNAs as well. Further experiments aiming at the identification of specific snoRNA export pathways will help to elucidate the biogenesis pathways of small RNAs derived from snoRNAs.

Many small RNA cloning and sequencing projects have been carried out, but small RNAs derived from snoRNAs or other noncoding RNAs have not been reported. Here, we have immunoprecipitated endogenous Ago complexes, and it is very likely that small RNAs that associate with Ago proteins are functional RNA molecules rather than just degradation products. Most published cloning approaches size fractionated total RNA before cloning and, therefore, all unspecific degradation products are present in the libraries and it is difficult to find classes of functional small RNAs. Therefore, we suggest that cloning projects aiming at the identification of new classes of Ago-associated small noncoding RNAs of about 18–35 nt in length should be carried out from anti-Ago immunoprecipitations.

Using cloning and sequencing approaches, a variety of different snoRNA genes have been identified in the past (Bachelier et al., 2002). However, many of these snoRNA candidates have not been characterized in detail, and it is unknown whether or

not these candidates represent functional snoRNAs. Therefore, it is tempting to speculate that more snoRNAs are specifically processed to functional small RNAs. Indeed, by analyzing larger data sets, we find several small RNAs with miRNA-like processing signatures that originate from snoRNAs (Figure 6). These candidate sRNAs are derived from a subset of snoRNAs comprised of H/ACA snoRNAs and small Cajal body RNAs (scaRNAs), whose secondary structure is characterized by two hairpins linked by a hinge similar to ACA45 (Figure 2A). These findings support our hypothesis that a considerable number of snoRNAs are natural precursors for functional small RNAs. Moreover, we add another so far unrecognized function in post-transcriptional gene silencing to the list of snoRNA functions. A detailed functional characterization of all mammalian snoRNAs will help to elucidate the impact of snoRNA processing in RNA-guided gene silencing.

EXPERIMENTAL PROCEDURES

Ago Complex Purification

HEK293 cells were lysed in buffer containing 20 mM Tris HCl (pH 7.5), 150 mM NaCl, 0.25% NP-40, and 1.5 mM MgCl₂ and centrifuged at 10,000 × g for 10 min at 4°C.

For immunoprecipitation of endogenous Ago complexes, 100 μl protein G Sepharose (GE Healthcare) was washed with phosphate-buffered saline (PBS) and incubated with 10 ml anti-Ago1-4B8, anti-Ago2-11A9, anti-FLAG-3H3, or anti-GST at 4°C with gentle agitation overnight. After washes with PBS, beads were incubated with HEK293 cell lysate of 6 × 15 cm plates for 3 hr. Anti-Ago1-coated beads were extensively washed with 300 mM NaCl, 2.5 mM MgCl₂, 0.5% NP40, and 20 mM Tris-HCl (pH 7.5) followed by a wash with PBS. Anti-Ago2-coated beads were washed five times using RIPA buffer (50 mM Tris-HCl, 500 mM NaCl, 1% Nonidet P-40, 0.5% sodium deoxycholate, 0.1% SDS). RNA was isolated with 40 μg Proteinase K in 200 μl Proteinase K buffer (300 mM NaCl, 25 mM EDTA, 2% SDS, 200 mM Tris HCl [pH 7.5]) followed by Phenol/Chloroform extraction and Ethanol precipitation.

For immunoprecipitation of FLAG/HA-tagged Ago complexes, cell lysate from two 15 cm dishes were incubated with 20 μl FLAG M2 agarose beads (Sigma) for 2 hr at 4°C with rotation. Beads were extensively washed, and coimmunoprecipitated RNA was extracted as described above.

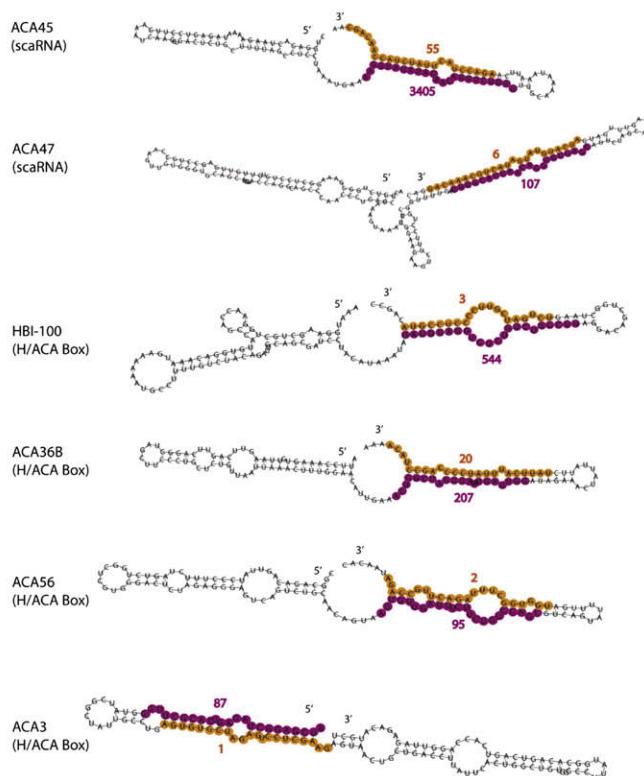
Small RNA Cloning

Small RNA cloning was carried out by Vertis Biotechnology (Weihenstephan, Germany) and has been described earlier (Tarasov et al., 2007). Without any size fractionation, extracted Ago-associated RNAs were poly(A)-tailed using poly(A) polymerase, and an adaptor was ligated to the 5' phosphate of the miRNAs: (5' end adaptor [43 nucleotides]: 5'-GCCTCCCTCGGCCATCAG CTNNNGACCTTGGCTGTCACTCA-3'). NNNN represents a "barcode" sequence. Next, first-strand cDNA synthesis was performed using an oligo(dT)-linker primer and M-MLV-RNase H reverse transcriptase (3' end oligo [dT] linker primer [61 bases]: 5'-GCCTTGCCAGCCCGCTCAGACGAGACATCGCCCG C[T]₂₅-3'). The resulting cDNAs were PCR amplified in 22 cycles using the high-fidelity Phusion polymerase (Finnzymes). The 120–135 bp amplification products were confirmed by polyacrylamide gel electrophoresis (PAGE) analysis. Both cDNAs pools were mixed in equal amounts and subjected to gel fractionation. The 120–135 bp fraction was electroeluted from 6% PAA-gels. After isolation with Nucleospin Extract II (Macherey and Nagel), cDNA pools were dissolved in 5 mM Tris/HCl (pH 8.5) with a concentration of 10 ng/μl and used in single-molecule sequencing. Massively parallel sequencing was performed by 454 Life Sciences (Branford, USA) using the Genome Sequencer 20 system as well as MWG Biotech (Germany). The complete sequencing data is available at the Gene Expression Omnibus (GEO, Accession number: GSE13370).

A

type	ID	tot. # reads	"mature" seq. [# of reads]	"star" seq. [# of reads]	3' overhang
scaRNA	ACA45	3516	aagguagauagaacaggucuu [3405]	agaccuacuaucaaccaacagc [55]	Y
scaRNA	ACA47	136	auugcaguaacaggugugagc [107]	aucaugauaugauacugcaaacag [6]	Y
scaRNA	U92	9	uaacggacagauacggggcagaca [5]	acugccuuuugaugacgggagc [4]	Y
H/ACA Box RNA	HBI-100	591	uaggagugucucugucggcu [544]	ucugaucgucccccaua* [3]	Y
H/ACA Box RNA	ACA36B**	269	acuggcuagggaaaauaugg [207]	uuucaaauuaccccagccuaca [20]	N
H/ACA Box RNA	ACA56	102	aguggugaguucucuguccagc [95]	uggugccuuuagacuugccaga [2]	N
H/ACA Box RNA	ACA3	98	aucgaggcuagagucagcuugg [87]	agugugcuagaguccuagaag [1]	Y
H/ACA Box RNA	ACA50	11	aagcacugccuuugaaccugaugu [8]	acggccaagcaacagugcuaga [3]	Y (5nt)

B



RNA Cleavage Experiments

In vitro transcribed pri-27a substrate used in this study was described previously in Landthaler et al. (2004) and Meister et al. (2005). The template for pre-27a transcription was created by annealing the following primers: 5'-T TAATACGACTCACTATAGCTGAGGAGCAGGGCTTAGCTGCTTGTGAGCAG GGTCCACACCAAGTCGTGTTACAGTGGCTAAGTTCCGCCCCCCAGC and 5'-GCTGGGGGGCGAACCTTAGCCACTGTGAACACGACTTGGTGTGACCC TGCTCACAAGCAGCTAAGCCCTGCTCCTCAGCTATAGTGTAGTTCGTATTA. ACA45 was cloned from genomic DNA using the primers 5'-ACGAGCTCCTGG AGACTAAGAAAATAGAGTCCCTGA and 5'-ACGGTACCTGCTGTTGGTAGT AAGTAGTCTTGAA, digested with *SacI* and *KpnI*, and inserted into the *SacI* and *KpnI* restriction sites of the pBluescript. Plasmid was linearized using the *KpnI* restriction site and in vitro transcribed as described in Landthaler et al. (2004). The construction of human FLAG/HA-Ago1, FLAG/HA-Ago2, and FLAG/HA-Dicer was reported earlier (Meister et al., 2005). FLAG/HA-DGCR8 was purchased from Addgene.

Figure 6. Several Human snoRNAs Show miRNA-Like Processing Signatures

(A) Small RNA reads originating from human snoRNAs that have been found in large sequencing data sets from Ago immunoprecipitates. The more abundant read is indicated as "mature," and the complementary strand is indicated as "star" read. All reads that have been found for individual snoRNAs are indicated as "total reads."

*The official genomic sequence is tctgatcgttcccctcc gta, but all of the reads mapping to this position have a mismatch, and all have "a" at position 18 and there is an annotated SNP at this position.

**The ACA36b sRNA candidate is identical to the annotated miRNA miR-664.

(B) Schematic representation of the secondary structure of full-length snoRNAs. Ago-associated reads are highlighted in purple and yellow.

Immunoprecipitations were performed as described above. For cleavage activity assays, 10 µl of Ago or Dicer complex-containing anti-FLAG beads were incubated in 20 µl PBS containing 5 mM ATP, 7.5 mM MgCl₂, 10 U/ml RNasin (Promega), and about 100 counts (~50 fmol) of internally labeled RNA for 1 hr at 37°C. The reaction was stopped by adding 200 µl proteinase K buffer (300 mM NaCl, 25 mM EDTA, 2% SDS, 200 mM Tris HCl [pH 7.5]) containing proteinase K (0.2 mg/ml). RNA was isolated with Phenol/Chloroform and analyzed by 8% or 12% denaturing RNA PAGE. Signals were detected by autoradiography.

Northern Blotting and Semiquantitative RT-PCR

Immunoprecipitated RNA and 30 µg total RNA isolated from HEK293 cells using Trifast (Peqlab) was separated by 12% denaturing RNA PAGE and transferred to a nylon membrane (GE Healthcare) by semidry electroblotting. Membranes were crosslinked by 1-ethyl-3-(3-dimethylaminopropyl) carbodiimide (EDC) chemical crosslink incubating for 1 hr at 50°C, prehybridized for 1 hr, and hybridized overnight at 50°C with probes complementary to snoRNA ACA45 or tRNA. The following probes have been used: 5'-AAGACCTGTCTA TCTACCT complementary to snoRNA ACA45 and 5'-C TGATGCTCTACCGACTGAGCTATCCGGGC complementary to lysine tRNA. After hybridization, membranes were washed twice 10 min with 5 × SSC and

once 10 min with 1 × SSC. Radioactive signals were detected by exposure of BioMax MS film (Kodak) using an intensifying screen (GE Healthcare).

For semiquantitative RT-PCR, extracted RNA was modified by addition of poly(A) tail using poly(A) tailing kit from Ambion. Reverse transcription was performed using the cDNA synthesis kit (Fermentas) with the universal RT primer 5' AACGAGACGACGACAGACTTTTTTTTTTTTTTTT (described in Hurteau et al. [2006]). DNA was amplified using Mesa Green qPCR MasterMix Plus (Eurogentec), a universal reverse primer identical to the 18 bp tag added during the RT step and the following specific primers: 5'-AAGGUAGAUAGAACAGGUCUUG for ACA45, 5'-TCCCTGAGACCCCTAACTTGTGA for miR-125b, and 5'-ACA CATCCAAATGAGGCG for 7SK. The PCR products were analyzed by 4% agarose gel electrophoresis.

Conserved Processing of ACA45

The human ACA45 sequence was obtained at the snoRNABase (<http://www-snoRNA.biotoul.fr/>). The ACA45 mouse, rat, and dog homologs were

identified by mapping the human sequence against each genome, retaining only unambiguous matches. Subsequently, a number of deep sequencing data sets were mapped to the ACA45 homologs. Each data set was mapped to the homolog of the species from which the data set originated, and only perfect matches were retained. The human data consisted of the data sets produced for this study using the 454 Life Sciences technology, as well as a data set produced by deep sequencing the small RNA fraction of HeLa cells using the Solexa/Illumina technology (GEO accession number GSE10829) (Friedländer et al., 2008). The mouse data sets were produced by deep sequencing small RNAs from mouse brain and kidney tissues using the 454 technology (unpublished data). The rat data set was produced by deep sequencing column-purified small RNAs from testes extracts using the 454 technology (GEO accession number GSE5026) (Lau et al., 2006). The dog data set was produced by sequencing small RNAs from dog lymphocytes using the Solexa technology (GEO accession number GSE10825) (Friedländer et al., 2008).

Computational Methods

A total of 64733 reads was obtained by deep sequencing the RNA that immunoprecipitated with Ago1 and Ago2. Of this, 20834 belonged to the Ago1 set and 43899 to the Ago2 set. Upon removal of adapters, the sequences shorter than 17 nt were discarded, resulting in 20448 and 42604 reads in Ago1 and Ago2 sets, respectively. These reads were mapped to human genome (hg 18, UCSC database [Karolchik et al., 2003]) using NCBI blastn (Altschul et al., 1990) with the minimum word length set to 7. The mapping with the best E value was associated with each read. The only mismatches allowed were the first nt at the 5' end or the last three nt at the 3' end of the read. In case a read mapped with the same E value to several locations, they were all taken into consideration. The genomic loci of best matches were annotated using the tables from UCSC database (Karolchik et al., 2003). A read was annotated as a DNA repeat (including LINE, SINE, LTR) only if the genomic locus it mapped to had no other annotation.

For purposes of identification of known and novel miRNAs, reads from the Ago1 and Ago2 libraries were combined and mapped to the human genome using NCBI megablast with the following options: $-W 12 -p 100$. Only perfect mappings (full length, 100% identity) were retained. These were used as input to miRDeep, an algorithm designed for the discovery of Dicer substrates such as miRNAs from deep sequencing data (Friedländer et al., 2008). The algorithm intersects the mappings with local genomic sequence to identify potential Dicer hairpin substrates. These are then scored according to the distribution of positions and frequencies of the reads mapped to the individual hairpin, using Bayesian statistics. The energetics and stability of the hairpins and the cross-species conservation of the seed sequence also contribute to the score. Human snoRNA sequences were downloaded from snoRNABase (Lestradre and Weber, 2006).

To map the total of 17362367 sequence reads obtained by sequencing Ago1–4 IP using Solexa technology to the genome, we used the locally developed suffix array-based tool (to be published elsewhere). Candidate snoRNAs with miRNA-like processing were selected (Table S1) if the combined Ago1–4 data set contained reads mapping to both strands of a hairpin and if these reads represented more than 85% of all reads mapping to a given snoRNA.

SUPPLEMENTAL DATA

The Supplemental Data include Supplemental Experimental Procedures, one figure, and three tables and can be found with this article at [http://www.molecule.org/supplemental/S1097-2765\(08\)00733-8](http://www.molecule.org/supplemental/S1097-2765(08)00733-8).

ACKNOWLEDGMENTS

We are grateful to Sabine Rottmüller and Bernd Haas for technical support, Vertis Biotechnologie AG (Weißenstephan, Germany) for small RNA cloning, and MWG biotech (Munich, Germany) for deep sequencing. We thank Sihem Cheloufi and Greg Hannon for providing RNA from *Dicer*^{-/-} as well as *Dicer*^{+/-} cells and Witold Filipowicz for the anti-GAR-1 antibody. Our research is supported by the Max Planck Society. This work was supported, in part, by EU grant LSHG-CT-2006-037900 (SIROCCO; G.M.) and the Deutsche Forschungsgemeinschaft (Me 2064/2-1 to G.M.).

Received: August 18, 2008

Revised: October 16, 2008

Accepted: October 27, 2008

Published: November 20, 2008

REFERENCES

- Altschul, S.F., Gish, W., Miller, W., Myers, E.W., and Lipman, D.J. (1990). Basic local alignment search tool. *J. Mol. Biol.* *215*, 403–410.
- Aravin, A.A., Sachidanandam, R., Girard, A., Fejes-Toth, K., and Hannon, G.J. (2007). Developmentally regulated piRNA clusters implicate MILI in transposon control. *Science* *316*, 744–747.
- Azuma-Mukai, A., Oguri, H., Mituyama, T., Qian, Z.R., Asai, K., Siomi, H., and Siomi, M.C. (2008). Characterization of endogenous human Argonautes and their miRNA partners in RNA silencing. *Proc. Natl. Acad. Sci. USA* *105*, 7964–7969.
- Bachellerie, J.P., Cavaille, J., and Huttenhofer, A. (2002). The expanding snoRNA world. *Biochimie* *84*, 775–790.
- Beitzinger, M., Peters, L., Zhu, J.Y., Kremmer, E., and Meister, G. (2007). Identification of human microRNA targets from isolated argonaute protein complexes. *RNA Biol.* *4*, 76–84.
- Bernstein, E., Caudy, A.A., Hammond, S.M., and Hannon, G.J. (2001). Role for a bidentate ribonuclease in the initiation step of RNA interference. *Nature* *409*, 363–366.
- Bohnsack, M.T., Czaplinski, K., and Gorlich, D. (2004). Exportin 5 is a RanGTP-dependent dsRNA-binding protein that mediates nuclear export of pre-miRNAs. *RNA* *10*, 185–191.
- Borchert, G.M., Lanier, W., and Davidson, B.L. (2006). RNA polymerase III transcribes human microRNAs. *Nat. Struct. Mol. Biol.* *13*, 1097–1101.
- Chen, K., and Rajewsky, N. (2007). The evolution of gene regulation by transcription factors and microRNAs. *Nat. Rev. Genet.* *8*, 93–103.
- Conaway, R.C., Sato, S., Tomomori-Sato, C., Yao, T., and Conaway, J.W. (2005). The mammalian Mediator complex and its role in transcriptional regulation. *Trends Biochem. Sci.* *30*, 250–255.
- Denli, A.M., Tops, B.B., Plasterk, R.H., Ketting, R.F., and Hannon, G.J. (2004). Processing of primary microRNAs by the Microprocessor complex. *Nature* *432*, 231–235.
- Filipowicz, W., Jaskiewicz, L., Kolb, F.A., and Pillai, R.S. (2005). Post-transcriptional gene silencing by siRNAs and miRNAs. *Curr. Opin. Struct. Biol.* *15*, 331–341.
- Friedländer, M.R., Chen, W., Adamidi, C., Maaskola, J., Einspanier, R., Knespel, S., and Rajewsky, N. (2008). Discovering microRNAs from deep sequencing data using miRDeep. *Nat. Biotechnol.* *26*, 407–415.
- Gregory, R.I., Yan, K.P., Amuthan, G., Chendrimada, T., Doratotaj, B., Cooch, N., and Shiekhattar, R. (2004). The Microprocessor complex mediates the genesis of microRNAs. *Nature* *432*, 235–240.
- Gregory, R.I., Chendrimada, T.P., Cooch, N., and Shiekhattar, R. (2005). Human RISC couples microRNA biogenesis and posttranscriptional gene silencing. *Cell* *123*, 631–640.
- Grishok, A., Pasquinelli, A.E., Conte, D., Li, N., Parrish, S., Ha, I., Baillie, D.L., Fire, A., Ruvkun, G., and Mello, C.C. (2001). Genes and mechanisms related to RNA interference regulate expression of the small temporal RNAs that control *C. elegans* developmental timing. *Cell* *106*, 23–34.
- Hurteau, G.J., Spivack, S.D., and Brock, G.J. (2006). Potential mRNA degradation targets of hsa-miR-200c, identified using informatics and qRT-PCR. *Cell Cycle* *5*, 1951–1956.
- Hutvagner, G., McLachlan, J., Pasquinelli, A.E., Bálint, E., Tuschl, T., and Zamore, P.D. (2001). A cellular function for the RNA interference enzyme Dicer in small temporal RNA maturation. *Science* *293*, 834–838.
- Karolchik, D., Baertsch, R., Diekhans, M., Furey, T.S., Hinrichs, A., Lu, Y.T., Roskin, K.M., Schwartz, M., Sugnet, C.W., Thomas, D.J., et al. (2003). The UCSC Genome Browser Database. *Nucleic Acids Res.* *31*, 51–54.

- Kishore, S., and Stamm, S. (2006). The snoRNA HBII-52 regulates alternative splicing of the serotonin receptor 2C. *Science* 311, 230–232.
- Kiss, A.M., Jady, B.E., Bertrand, E., and Kiss, T. (2004). Human box H/ACA pseudouridylation guide RNA machinery. *Mol. Cell. Biol.* 24, 5797–5807.
- Krek, A., Grun, D., Poy, M.N., Wolf, R., Rosenberg, L., Epstein, E.J., MacMenamin, P., da Piedade, I., Gunsalus, K.C., Stoffel, M., and Rajewsky, N. (2005). Combinatorial microRNA target predictions. *Nat. Genet.* 37, 495–500.
- Landthaler, M., Yalcin, A., and Tuschl, T. (2004). The human DiGeorge syndrome critical region gene 8 and its *D. melanogaster* homolog are required for miRNA biogenesis. *Curr. Biol.* 14, 2162–2167.
- Lau, N.C., Seto, A.G., Kim, J., Kuramochi-Miyagawa, S., Nakano, T., Bartel, D.P., and Kingston, R.E. (2006). Characterization of the piRNA complex from rat testes. *Science* 313, 363–367.
- Lee, Y., Ahn, C., Han, J., Choi, H., Kim, J., Yim, J., Lee, J., Provost, P., Radmark, O., Kim, S., and Kim, V.N. (2003). The nuclear RNase III Drosha initiates microRNA processing. *Nature* 425, 415–419.
- Lee, Y., Kim, M., Han, J., Yeom, K.H., Lee, S., Baek, S.H., and Kim, V.N. (2004). MicroRNA genes are transcribed by RNA polymerase II. *EMBO J.* 23, 4051–4060.
- Lestrade, L., and Weber, M.J. (2006). snoRNA-LBME-db, a comprehensive database of human H/ACA and C/D box snoRNAs. *Nucleic Acids Res.* 34, D158–D162.
- Lim, L.P., Lau, N.C., Weinstein, E.G., Abdelhakim, A., Yekta, S., Rhoades, M.W., Burge, C.B., and Bartel, D.P. (2003). The microRNAs of *Caenorhabditis elegans*. *Genes Dev.* 17, 991–1008.
- Liu, J., Carmell, M.A., Rivas, F.V., Marsden, C.G., Thomson, J.M., Song, J.J., Hammond, S.M., Joshua-Tor, L., and Hannon, G.J. (2004). Argonaute2 is the catalytic engine of mammalian RNAi. *Science* 305, 1437–1441.
- Lund, E., Guttinger, S., Calado, A., Dahlberg, J.E., and Kutay, U. (2004). Nuclear export of microRNA precursors. *Science* 303, 95–98.
- Ma, J.B., Yuan, Y.R., Meister, G., Pei, Y., Tuschl, T., and Patel, D.J. (2005). Structural basis for 5'-end-specific recognition of guide RNA by the *A. fulgidus* Piwi protein. *Nature* 434, 666–670.
- Maniataki, E., and Mourelatos, Z. (2005). A human, ATP-independent, RISC assembly machine fueled by pre-miRNA. *Genes Dev.* 19, 2979–2990.
- Matera, A.G., Terns, R.M., and Terns, M.P. (2007). Non-coding RNAs: lessons from the small nuclear and small nucleolar RNAs. *Nat. Rev. Mol. Cell Biol.* 8, 209–220.
- Meister, G., and Tuschl, T. (2004). Mechanisms of gene silencing by double-stranded RNA. *Nature* 431, 343–349.
- Meister, G., Landthaler, M., Patkaniowska, A., Dorsett, Y., Teng, G., and Tuschl, T. (2004). Human Argonaute2 mediates RNA cleavage targeted by miRNAs and siRNAs. *Mol. Cell* 15, 185–197.
- Meister, G., Landthaler, M., Peters, L., Chen, P.Y., Urlaub, H., Luhrmann, R., and Tuschl, T. (2005). Identification of novel argonaute-associated proteins. *Curr. Biol.* 15, 2149–2155.
- Mourelatos, Z., Dostie, J., Paushkin, S., Sharma, A., Charroux, B., Abel, L., Rappsilber, J., Mann, M., and Dreyfuss, G. (2002). miRNPs: a novel class of ribonucleoproteins containing numerous microRNAs. *Genes Dev.* 16, 720–728.
- Murchison, E.P., Partridge, J.F., Tam, O.H., Cheloufi, S., and Hannon, G.J. (2005). Characterization of Dicer-deficient murine embryonic stem cells. *Proc. Natl. Acad. Sci. USA* 102, 12135–12140.
- Parker, J.S., and Barford, D. (2006). Argonaute: a scaffold for the function of short regulatory RNAs. *Trends Biochem. Sci.* 31, 622–630.
- Parker, J.S., Roe, S.M., and Barford, D. (2005). Structural insights into mRNA recognition from a PIWI domain-siRNA guide complex. *Nature* 434, 663–666.
- Patel, D.J., Ma, J.B., Yuan, Y.R., Ye, K., Pei, Y., Kuryavyi, V., Malinina, L., Meister, G., and Tuschl, T. (2006). Structural biology of RNA silencing and its functional implications. *Cold Spring Harb. Symp. Quant. Biol.* 71, 81–93.
- Peters, L., and Meister, G. (2007). Argonaute proteins: mediators of RNA silencing. *Mol. Cell* 26, 611–623.
- Pillai, R.S., Bhattacharyya, S.N., and Filipowicz, W. (2007). Repression of protein synthesis by miRNAs: how many mechanisms? *Trends Cell Biol.* 17, 118–126.
- Rudel, S., Flatley, A., Weinmann, L., Kremmer, E., and Meister, G. (2008). A multifunctional human Argonaute2-specific monoclonal antibody. *RNA* 14, 1244–1253.
- Seto, A.G., Kingston, R.E., and Lau, N.C. (2007). The coming of age for Piwi proteins. *Mol. Cell* 26, 603–609.
- Tarasov, V., Jung, P., Verdoodt, B., Lodygin, D., Epanchintsev, A., Menssen, A., Meister, G., and Hermeking, H. (2007). Differential regulation of microRNAs by p53 revealed by massively parallel sequencing: miR-34a is a p53 target that induces apoptosis and G1-arrest. *Cell Cycle* 6, 1586–1593.
- Tolia, N.H., and Joshua-Tor, L. (2007). Slicer and the argonautes. *Nat. Chem. Biol.* 3, 36–43.
- Tomari, Y., and Zamore, P.D. (2005). Perspective: machines for RNAi. *Genes Dev.* 19, 517–529.

Importin 8 Is a Gene Silencing Factor that Targets Argonaute Proteins to Distinct mRNAs

Lasse Weinmann,¹ Julia Höck,¹ Tomi Ivacevic,⁴ Thomas Ohrt,² Jörg Mütze,² Petra Schwille,² Elisabeth Kremmer,³ Vladimir Benes,⁴ Henning Urlaub,⁵ and Gunter Meister^{1,*}

¹Laboratory of RNA Biology and Center for Integrated Protein Science Munich, Max Planck Institute of Biochemistry, Am Klopferspitz 18, 82152 Martinsried, Germany

²Biophysics, BIOTEC, Technische Universität Dresden, Tatzberg 47-51, 01307 Dresden, Germany

³Helmholtz Zentrum München, Marchioninistr. 25, 81377 Munich, Germany

⁴European Molecular Biology Laboratory, Meyerhofstr. 1, 69117 Heidelberg, Germany

⁵Bioanalytical Mass Spectrometry Group, Max Planck Institute of Biophysical Chemistry, Am Fassberg 11, 37077 Göttingen, Germany

*Correspondence: meister@biochem.mpg.de

DOI 10.1016/j.cell.2008.12.023

SUMMARY

Small regulatory RNAs including small interfering RNAs (siRNAs) and microRNAs (miRNAs) guide Argonaute (Ago) proteins to specific target RNAs leading to mRNA destabilization or translational repression. Here, we report the identification of Importin 8 (Imp8) as a component of miRNA-guided regulatory pathways. We show that Imp8 interacts with Ago proteins and localizes to cytoplasmic processing bodies (P bodies), structures involved in RNA metabolism. Furthermore, we detect Ago2 in the nucleus of HeLa cells, and knockdown of Imp8 reduces the nuclear Ago2 pool. Using immunoprecipitations of Ago2-associated mRNAs followed by microarray analysis, we further demonstrate that Imp8 is required for the recruitment of Ago protein complexes to a large set of Ago2-associated target mRNAs, allowing for efficient and specific gene silencing. Therefore, we provide evidence that Imp8 is required for cytoplasmic miRNA-guided gene silencing and affects nuclear localization of Ago proteins.

INTRODUCTION

Small noncoding RNAs including microRNAs (miRNAs), small interfering RNAs (siRNAs), and Piwi-interacting RNAs (piRNAs) are important regulators of gene expression in many different organisms (Filipowicz et al., 2005; Seto et al., 2007; Zamore and Haley, 2005). miRNA genes are transcribed by RNA polymerases II and III generating primary miRNA transcripts, which are further processed to stem-loop-structured miRNA precursors by the nuclear RNase III Drosha and its partner DGCR8/Pasha (Bushati and Cohen, 2007). Pre-miRNAs are exported to the cytoplasm where processing of Dicer, another RNase III enzyme, generates 21–23 nucleotide (nt) long double-stranded

(ds) miRNA/miRNA* intermediates with characteristic 2 nt 3' overhangs and 5' phosphate groups (Meister and Tuschl, 2004; Zamore and Haley, 2005). After further processing and/or unwinding steps, one strand gives rise to the mature miRNA and is incorporated into miRNA-protein complexes often referred to as miRNPs (Leuschner et al., 2006; Matranga et al., 2005; Mourelatos et al., 2002; Rand et al., 2005).

Members of the Argonaute protein family constitute the cellular binding partners of miRNAs as well as other small RNAs and are therefore key components of miRNPs. The human genome encodes for eight different Argonaute genes, which can be phylogenetically divided into four Ago and four Piwi subfamily members (Peters and Meister, 2007; Tolia and Joshua-Tor, 2007). Expression of the Piwi subfamily members HIWI1–3 and HILI seems to be restricted to testes, and different Piwi subfamily members bind to different classes of testes-specific piRNAs (Aravin et al., 2006; Girard et al., 2006). The mouse Piwi member MILI, for example, binds to a developmentally regulated piRNA cluster and influences transposon expression (Aravin et al., 2007). The individual members of the human Ago subfamily, namely Ago1–4, are ubiquitously expressed and most likely bind to similar populations of miRNAs.

Depending on the degree of complementarity between the miRNA and the target RNA, miRNAs guide sequence-specific cleavage, deadenylation, or translational repression of specific target mRNAs (Pillai et al., 2007). It has been shown by in vitro translation assays that miRNAs inhibit translation of reporter constructs at early stages of translational initiation (Mathonnet et al., 2007; Thermann and Hentze, 2007; Wakiyama et al., 2007; Wang et al., 2006). In contrast, on the basis of the finding that miRNAs cosediment with polysomes it has been proposed that miRNAs function on the level of translational elongation (Maroney et al., 2006; Olsen and Ambros, 1999; Seggerson et al., 2002). Other models of miRNA functions suggest rapid ribosome drop-off from mRNAs upon miRNA inhibition or miRNA-guided degradation of the nascent polypeptide chain by the proteasome (Nottrott et al., 2006; Petersen et al., 2006). mRNA profiling studies have recently shown that miRNAs affect

the stability of many mRNAs that contain imperfect miRNA binding sites. Moreover, it appears that miRNA effects on mRNA levels are as common as translational repression (Bagga et al., 2005). Consistently, miRNAs guide mRNA deadenylation processes followed by decapping and degradation (Behm-Ansmant et al., 2006; Giraldez et al., 2006; Humphreys et al., 2005; Wu et al., 2006).

While miRNA processing is well understood, target mRNA recognition and binding is only poorly understood. It has been demonstrated that HuR (ELAV1) can release miRNA repression of the CAT-1 mRNA upon cellular stress (Bhattacharyya et al., 2006). Moreover, a protein termed dead end 1 (Dnd1) can occupy miRNA binding sites on the 3' untranslated regions (UTRs) of specific target mRNAs and thus inhibit miRNA-guided gene silencing (Kedde et al., 2007). Although only a few mRNA binding proteins with effects on miRNA function have been identified thus far, it is very likely that many more protein factors exist that influence recruitment or stable binding of miRNPs to specific mRNAs.

Here, we report the identification of Imp8 as component of human Ago protein complexes. We show that Imp8 is required for binding of Ago proteins to a variety of mRNA targets and that depletion of Imp8 interferes with miRNA-guided gene silencing. Furthermore, we demonstrate that Imp8 modulates nuclear localization of Ago2. We have therefore identified Imp8 as specificity factor in the miRNA pathway, which may fulfill additional functions in nuclear Ago import.

RESULTS

Imp8 Interacts with Human Ago Proteins

Human Ago1 and Ago2 complexes have been analyzed biochemically in the past (Gregory et al., 2005; Hock et al., 2007; Liu et al., 2004; Meister et al., 2005). However, the function of Ago3 and Ago4 in human cells has not been addressed yet. Therefore, we performed biochemical purification studies using FLAG/HA (FH)-tagged Ago3 and Ago4. HEK293 cells were transfected with FH-Ago3 or FH-Ago4, and immunoprecipitates were analyzed by mass spectrometry (Figure 1A, Tables S1 and S2 available online). We found known Ago-associated proteins such as TNRC6B, but also a variety of factors that have not been linked to Ago function thus far. Among them, we found the Importin β -like import receptor Imp8 (Gorlich et al., 1997). Cosedimentation studies revealed that FH-Imp8 comigrates with Ago proteins in sucrose gradients (Figure S1). For in vitro interaction studies, recombinant GST-Imp8 was immobilized on glutathione-coated beads and incubated with [³⁵S]-labeled Ago1–4 (Figure 1B). All Ago proteins interacted with GST-Imp8 (lanes 1–4), whereas no signal was observed in control reactions where GST alone was immobilized (lanes 6–9). Next, we investigated the interaction of Ago proteins with Imp8 in vivo. HEK293 cells were cotransfected with myc-tagged Ago proteins and FH-Imp8. Consistent with the in vitro data, all myc-Ago proteins were readily detectable in the anti-FLAG immunoprecipitates (Figure 1C, lanes 2, 5, 8, and 11). No myc-Ago was detected in FH-GFP control experiments (lanes 3, 6, 9, and 12). Furthermore, treatment of the immunoprecipitates with RNase A demonstrated that interaction of Ago proteins with Imp8 is independent of RNA (lanes 1, 4, 7, and 10). In contrast, interaction of Ago2 with

the poly-A binding protein C1 (PABPC1) was impaired upon RNase A treatment (lane 13), demonstrating efficient RNase A digestion. In order to validate endogenous Imp8-Ago2 interactions, we generated a polyclonal antibody against Imp8. The purified anti-Imp8 serum immunoprecipitates transfected FH-Imp8 (Figure 1D, lane 2) and endogenous Imp8 (lane 4, lower panel). Moreover, with an antibody against Ago2 (Rüdel et al., 2008), endogenous Ago2 was detectable in the Imp8 immunoprecipitate (lane 4, upper panel). Import receptors require interaction with the GTPase Ran for cytoplasmic substrate binding and nuclear transport. Therefore, we added recombinant Ran or RanQ69L, a mutant that promotes the dissociation of the cargo-Importin complexes, to the FH-Imp8 immunoprecipitate (Figure 1E, lanes 2 and 3). RanQ69L strongly reduced Ago2 binding to Imp8 (lane 3) compared to Ran (lane 2) or a sample where no protein was added (lane 1), indicating that Ago proteins bind to Imp8 in a Ran-dependent manner. By using a proteomics approach, we have identified and validated Imp8 as Ago-interacting protein in human cells.

Imp8 and Ago Proteins Colocalize in P Bodies

Human Ago proteins localize to P bodies and stress granules (Leung et al., 2006; Liu et al., 2005; Sen and Blau, 2005). We therefore analyzed the subcellular localization of Imp8. FH-Imp8 was transfected into HEK293 cells, and fixed cells were stained with anti-HA antibodies (Figure 2A). FH-Imp8 was detectable in the nucleus as well as cytoplasmic structures that were positive for the P body marker LSm4, indicating that Imp8 localizes to P bodies. Moreover, Imp8 localizes to arsenite-induced stress granules, as indicated by the colocalization with the known stress granule marker FMRp. As control, FH-Importin 4 (Imp4) was analyzed, and it localizes neither to P bodies nor to stress granules (Figure S2). We next analyzed whether Ago proteins colocalize with Imp8 in P bodies (Figure 2B). Myc-Ago2 and FH-Imp8 were cotransfected and fixed cells were analyzed with anti-myc or anti-FLAG antibodies. Indeed, Ago2 colocalizes with Imp8 in P bodies, suggesting a function for Imp8 in RNA metabolism. Similar results were obtained when other human Ago proteins were analyzed (data not shown and Figure S3B). Consistently, the anti-Imp8 serum stained P bodies in cells expressing FH-Ago2 (Figure 2B, panels 5–8) or the known P body component FH-TNRC6B (panels 9–12) (Meister et al., 2005), indicating that endogenous Imp8 is present in P bodies as well.

The Ran-dependent interaction of Imp8 and Ago proteins prompted us to analyze whether localization of Imp8 to P bodies depends on Ran as well (Figure 2C). FH-Imp8 was cotransfected with myc-Ran (panels 1–4), myc-RanQ69L (panels 5–8), or myc-RanT24N (panels 9–12), a mutant that stabilizes importin-cargo interaction, into HEK293 cells and localization was analyzed with anti-HA antibodies. Coexpression of RanWT or RanT24N had no effect on Imp8 P body localization. However, cotransfection of RanQ69L, which promotes the dissociation of import receptors from their cargo proteins, resulted in disruption of Imp8 P body localization, whereas P body formation itself was not impaired, as indicated by LSm4 analysis. Interestingly, Ago protein localization remained unaffected when RanQ69L was expressed (Figure S3). Of note, in the RanQ69L expression experiments, FH-Imp8 could be detected in cytoplasmic granules that

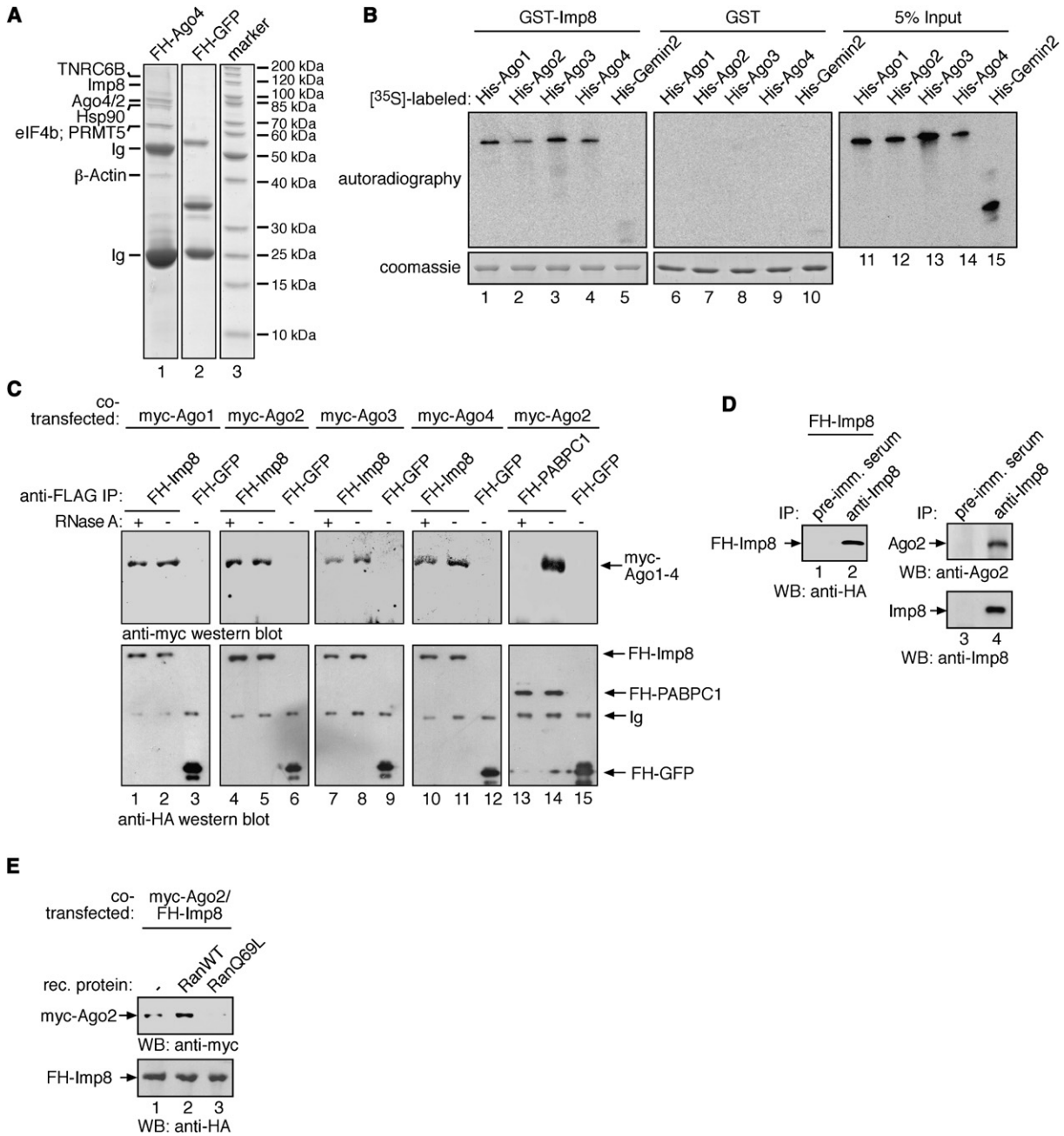


Figure 1. Imp8 Interacts with Human Ago1–4

(A) SDS-PAGE analysis of proteins interacting with human Ago4. FH-Ago4 or FH-GFP plasmids were transfected into HEK293 cells. FH-Ago4 (lane 1) and FH-GFP (lane 2) were immunoprecipitated from cell lysates, and immunoprecipitates were separated by SDS-PAGE. Lane 3 shows a molecular weight standard. Proteins interacting with FH-Ago4 but not with FH-GFP are shown to the left. A complete list of FH-Ago4- and FH-Ago3-interacting proteins is shown in [Tables S1 and S2](#). (B) GST-Imp8 (lanes 1–5) or GST alone (lanes 6–10) was immobilized on glutathione sepharose beads and incubated with [³⁵S]-methionine-labeled in vitro-translated His-Ago1–4 or His-Gemin2 control protein. Autoradiograms of bound [³⁵S]-labeled proteins (lanes 1–10) and radioactive input signals (lanes 11–15) are shown in the upper panels. Lower panels show coomassie stainings of coupled GST-Imp8 (lanes 1–5) or GST (lanes 6–10). (C) FH-Imp8, FH-GFP or FH-PABPC1 plasmids were cotransfected with myc-Ago1 (lanes 1–3), myc-Ago2 (lanes 4–6, 13–15), myc-Ago3 (lanes 7–9), or myc-Ago4 plasmids (lanes 10–12) into HEK293 cells. FH-tagged proteins were immunoprecipitated from cell lysates with anti-FLAG sepharose beads in the presence or absence of 20 μg/ml RNase A. The immunoprecipitate was analyzed by anti-myc western blotting (upper panel) and anti-HA western blotting (lower panel). Ig, Immunoglobulin heavy chain. (D) Left panel: HEK293 cells were transfected with FH-Imp8. Immunoprecipitation was performed from cell lysates using preimmune serum (lane 1) or anti-Imp8 (lane 2). FH-Imp8 was detected with anti-HA antibodies. Right panel: Lysate from untransfected HEK293 cells was immunoprecipitated with preimmune serum (lane 3) or anti-Imp8 (lane 4). The immunoprecipitate was analyzed by anti-Ago2 western blotting (upper panel) and anti-Imp8 western blotting (lower panel).

are clearly distinct from P bodies (panel 7) and might correspond to stress granules. Thus, Imp8 colocalizes with Ago proteins to P bodies in a Ran-dependent manner.

Imp8 Affects Nuclear Localization of Ago Proteins

Import receptors target cargo proteins to the nucleus. Since human Ago proteins have been shown to function in the nucleus (Janowski et al., 2006; Kim et al., 2006), we investigated nuclear Ago protein import (Figure 3). The monoclonal anti-Ago2 (11A9) antibody stained P bodies, as well as the diffuse cytoplasm and the nucleus of fixed HeLa cells (panels 1–4) (see Rüdell et al., 2008 for a detailed characterization of anti-Ago2 [11A9]). Knockdown of Ago2 led to a loss of the cytoplasmic and the nuclear signal, indicating that Ago2 is indeed in the nucleus (Rüdell et al., 2008). We quantified nuclear and cytoplasmic signals from average pixel intensities and calculated ratios of cytoplasmic versus nuclear Ago2 for each set of samples (Figure 3B). We found that upon Imp8 knockdown, the localization of Ago2 is shifted from the nucleus to the cytoplasm, whereas the total amount of soluble Ago2 remained unaffected (Figure 3B). Similar results were obtained when a HEK293 cell line stably expressing EGFP-Ago2 was analyzed by fluorescence correlation spectroscopy (Figure 3C) (Ohr et al., 2008). As control, Imp4 knockdown was performed, and it had no effect on nuclear EGFP-Ago2 localization. The used Imp4 siRNAs were as efficient as the Imp8 siRNAs (data not shown). In summary, we provide evidence that Imp8 can influence nuclear import of Ago proteins in human cells.

Imp8 Is Required for miRNA-Guided Gene Silencing

The interaction and colocalization of Ago proteins with Imp8 prompted us to analyze whether Imp8 is functionally involved in miRNA-guided gene silencing. We first analyzed the consequence of Imp8 depletion on sequence-specific cleavage of a luciferase reporter perfectly complementary to miR-21 (Figure 4A). As expected, knockdown of the slicer endonuclease Ago2 (Liu et al., 2004; Meister et al., 2004) led to a strong increase of luciferase expression. However, luciferase activity was not altered after Imp8 depletion, indicating that Imp8 is not required for Ago2-mediated cleavage of target RNA (for siRNA validation, see Figure S4).

Next, we investigated whether Imp8 is necessary for miRNA-guided silencing of known target mRNAs (Figure 4B). Luciferase reporters fused to full-length 3' UTRs of previously validated miRNA targets (Beitzinger et al., 2007) were transfected into HeLa cells where either Imp8 or as controls Ago2 or TNRC6B had been depleted by RNAi. Depletion of Ago2 or TNRC6B, which are required for miRNA function, resulted in elevated luciferase expression from all constructs. Strikingly, knockdown of Imp8 led to an increase of luciferase activity as well, indicating that Imp8 is required for repression of the tested 3' UTRs. We further tested whether the observed Imp8 effects on gene expression are linked to the miRNA pathway or whether Imp8 functions independently of Ago proteins on 3' UTRs. For further

studies, we used the 3' UTR of Hmga2, which is strongly derepressed when endogenous let-7a is inhibited with 2'-O-methylated antisense oligonucleotides (Figure 4C). Knockdown of TNRC6B or Imp8 led to increased luciferase activity similar to other miRNA targets. As specificity control, we mutated all let-7a binding sites in the Hmga2 reporter construct (Figures 4C and 4D and Figure S5). Indeed, the mutated 3' UTR did not respond to Imp8 knockdown anymore, indicating that Imp8 functions together with Ago proteins in the miRNA pathway. Since miRNAs can trigger target mRNA degradation, we investigated whether knockdown of Imp8 affects the level of endogenous miRNA target mRNAs (Figure 4E). We found that Imp8 depletion led to a moderate increase of some miRNA targets relative to GAPDH or β -Actin mRNAs (Figure S6). Thus, Imp8 is required for silencing of endogenous miRNA targets.

Imp8 Is Involved in Loading of Ago Complexes onto mRNA Targets

We next investigated individual steps of the miRNA pathway for Imp8 requirement. It has been suggested that Importin β -like proteins function as chaperones and increase the solubility of RNA binding proteins by preventing unspecific aggregation with nucleic acids (Jakel et al., 2002). Therefore, we analyzed soluble Ago protein levels after Imp8 knockdown in HeLa cells (Figure 5A). Cells transfected with siRNAs against Imp8 or control siRNAs were analyzed by western blotting with specific antibodies against endogenous Ago1–4 or β -actin as loading control. Because of the low Ago3 and Ago4 expression levels, Ago3 and Ago4 were immunoprecipitated prior to western blotting. Knockdown of Imp8 had no effect on the steady-state levels of soluble Ago proteins. Next, we analyzed Ago2 protein turnover using pulse-chase experiments (Figure 5B). HEK293 cells were cotransfected with a construct expressing FH-Ago2 and a plasmid expressing short hairpin RNAs (shRNAs) against Imp8 or control shRNAs. After 3 days, cells were pulsed with [³⁵S]-methionine-containing medium followed by chase in normal medium, and [³⁵S]-labeled Ago2 complexes were immunoprecipitated with anti-FLAG antibodies. Both in control and Imp8 knockdown cells, [³⁵S]-labeled Ago2 was strongly reduced after 13 hr chase. Therefore, our data suggest that Imp8 has no effect on the steady-state levels or turnover of Ago proteins in human cells.

Next, we asked whether Imp8 is involved in miRNA biogenesis, which would explain the effects of Imp8 on miRNA target expression (Figure 5C). HeLa cells were transfected with siRNAs directed against Dicer or Imp8, and total RNA was analyzed by northern blotting with probes specific for let-7a, miR-21, or miR-16. As expected, Dicer knockdown resulted in lower miRNA levels (lane 1). However, Imp8 knockdown had no effect on mature miRNA levels, suggesting that Imp8 is not involved in miRNA biogenesis (lanes 3 and 4). Using anti-Ago2 immunoprecipitations, we further investigated whether Imp8 affects the loading of Ago2 with miRNAs (Figure 5D). Endogenous Ago2 was immunoprecipitated from cell lysates transfected with

(E) myc-Ago2 and FH-Imp8 plasmids were cotransfected into HEK293 cells. FH-Imp8 was immunoprecipitated from cell lysates with anti-FLAG antibodies. The immunoprecipitate was incubated with PBS/5mM GTP containing either 100 μ M RanWT (lane 2), RanQ69L (lane 3) or no protein (lane 1). Myc-Ago2 and FH-Imp8 proteins were detected by western blotting (upper panel and lower panel).

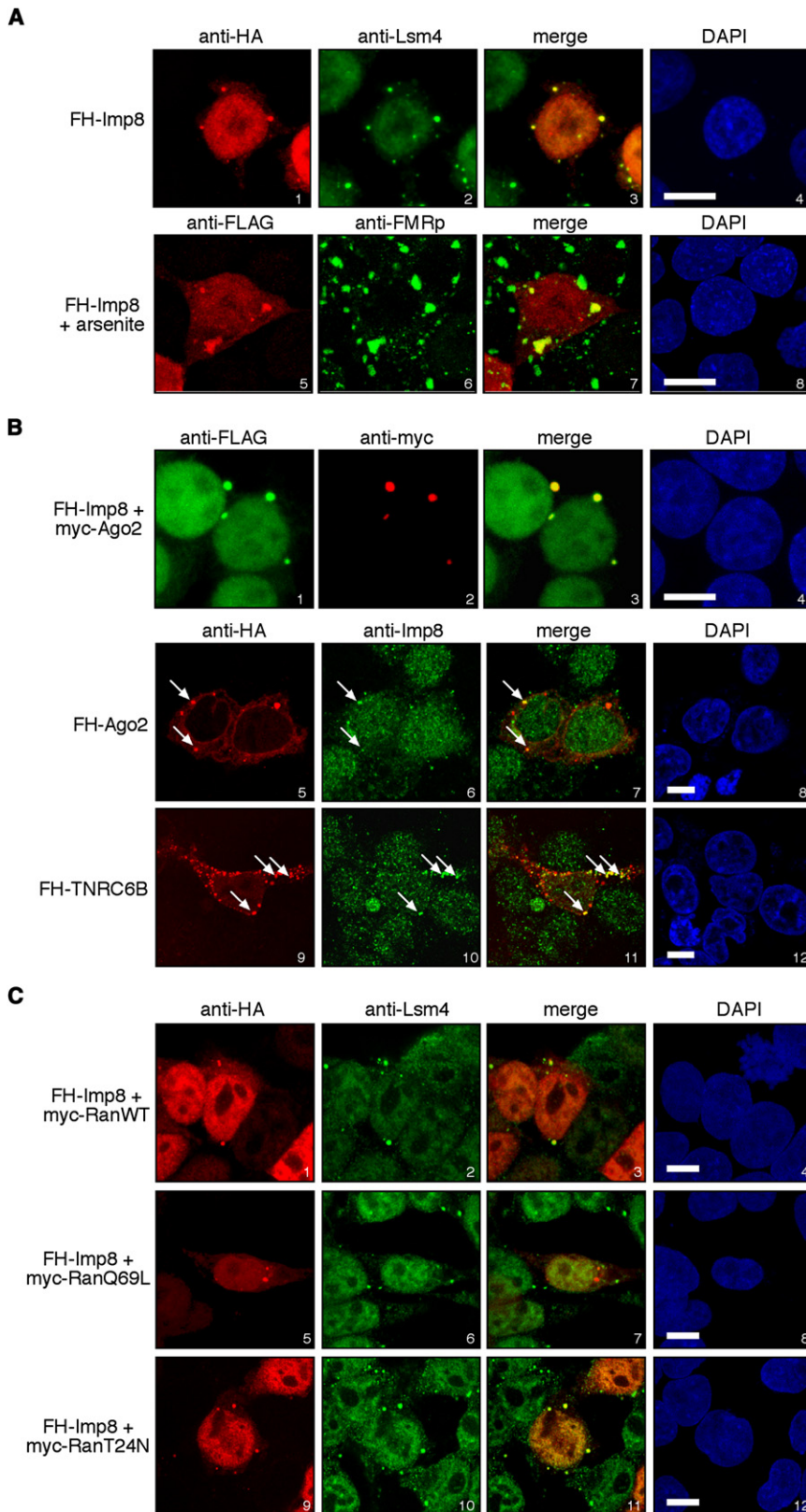


Figure 2. FH-Imp8 Localizes to P Bodies and Stress Granules

(A) HEK293 cells were transfected with FH-Imp8. Cells were fixed and stained for FH-Imp8 with anti-HA antibody (1) and for endogenous LSM4 (2). Lower panel: Cells were treated with 500 μ M sodium arsenite for 30 min, fixed, and stained for FH-Imp8 with anti-FLAG antibody (5) and for endogenous FMRp (6). DAPI was used as nuclear counterstain (4 and 8).

(B) Upper panel: HEK293 cells were transfected with FH-Imp8 and myc-Ago2, fixed, and stained with anti-FLAG antibody (1), anti-myc antibody (2), and DAPI (4). Lower panels: HEK293 cells were transfected with FH-Ago2 (5–8) or FH-TNRC6B (9–12), fixed, and stained with anti-HA antibody (5 and 9), anti-Imp8 antibody (6 and 10), and DAPI (8 and 12).

(C) HEK293 cells were cotransfected with FH-Imp8 and myc-RanWT (1–4), myc-RanQ69L (5–8), or myc-RanT24N (9–12), fixed, and stained with anti-HA antibody (1, 5, and 9), anti-LSM4 antibody (2, 6, and 10), and DAPI (4, 8, and 12). Scale bars represent 10 μ m.

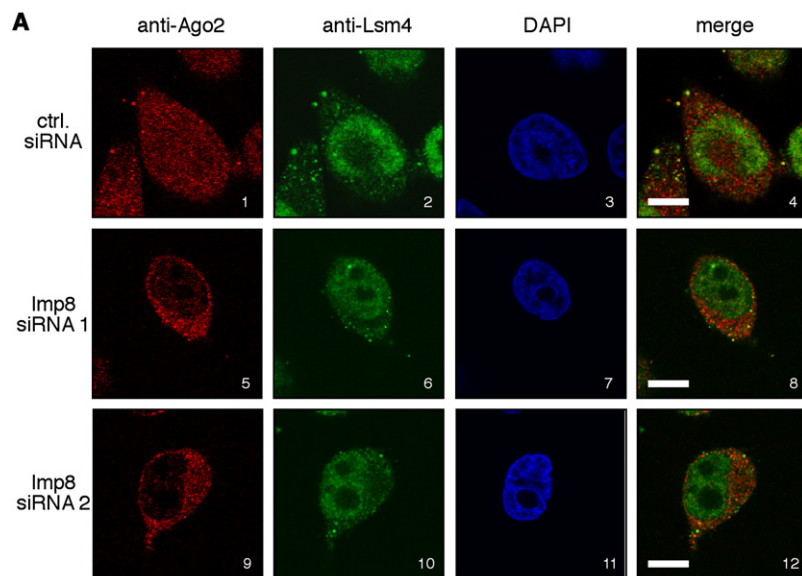
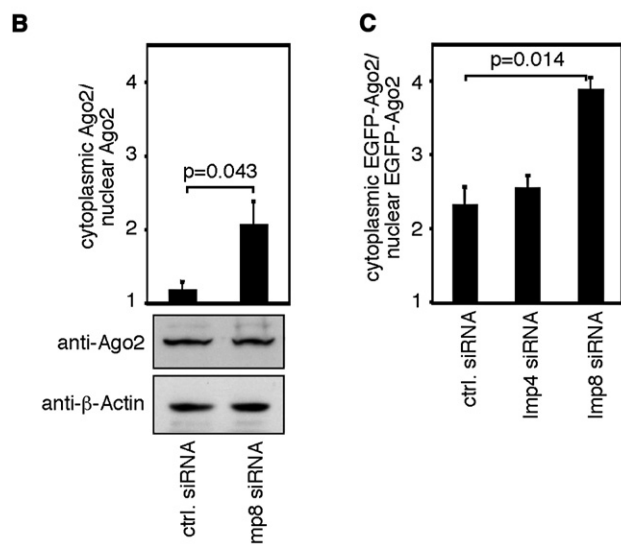


Figure 3. Imp8 Affects nuclear Localization of Ago Proteins

(A) HeLa cells were transfected with a control siRNA (1–4) or Imp8 siRNAs (5–8 and 9–12), fixed, and stained with anti-Ago2 (11A9) antibody (1, 5, and 9), anti-LSm4 antibody (2, 6, and 10), and DAPI (3, 7, and 11). The scale bar represents 10 μ m.

(B) Upper panel: Cells were treated as in (A), and nuclear and cytoplasmic Ago2 signal intensities were quantified from at least 15 cells per sample. The figure shows the mean ratio of cytoplasmic versus nuclear signal intensities \pm SEM. Lower panel: siRNA-transfected cells were lysed, and total Ago2 levels were assessed by western blotting, with β -Actin used as a loading control.

(C) A HEK2933 subline stably transfected with EGFP-Ago2 was transfected with a control siRNA, an Imp4 siRNA, or an Imp8 siRNA. The fluorescence intensities of cytoplasmic and nuclear EGFP-Ago2 were quantified with live microscopy, and mean ratios (\pm SEM) of cytoplasmic versus nuclear EGFP-Ago2 signals were calculated from 20 cells per sample.



control siRNAs (lanes 1 and 3) or siRNAs directed against Imp8 (lanes 2 and 4), and the presence of let-7a or miR-21 in the immunoprecipitate was analyzed by northern blotting. Knockdown of Imp8 did not change the levels of miRNAs coprecipitated with Ago2 complexes, suggesting that Imp8 is not required for loading of Ago proteins with miRNAs.

Finally, we analyzed Imp8 requirements for binding of Ago2 to miRNA target mRNAs (Figure 5E). We and others have reported earlier that Ago complexes stably associate with miRNA targets (Beitzinger et al., 2007; Easow et al., 2007; Karginov et al., 2007). Endogenous Ago2 complexes were immunoprecipitated with anti-Ago2 antibodies, and the coprecipitated mRNAs were further analyzed by quantitative real-time PCR (qRT-PCR). As expected, endogenous Hmga2 mRNA was strongly enriched in the anti-Ago2 immunoprecipitate. Specific binding was abrogated when either let-7a antisense inhibitor or an Ago2 siRNA was transfected, indicating that the enrichment in the immuno-

precipitate is miRNA specific and depends on the presence of Ago2. Strikingly, Hmga2 mRNA enrichment was significantly reduced ($p < 0.01$) when Imp8 was targeted by two different siRNAs, suggesting a role for Imp8 in recruiting Ago proteins to miRNA target mRNAs. Similar results were obtained when myc-Ago2 was analyzed (Figure 5F, left panel).

Our finding that Imp8 is required for Ago2 binding to miRNA targets as well as nuclear Ago import could potentially be explained by recruitment of Ago proteins to target mRNAs in the nucleus. In order to analyze binding of Ago2 to mRNAs in the nucleus, we fused Ago2 to a SV40-NLS, leading to Imp8-independent nuclear localization (Figure S7). Binding of SV40 NLS-Ago2 to the miRNA target HMGA2 is still dependent on Imp8 (Figure 5F, right panel, and Figure S8), suggesting that Imp8 functions in the miRNA pathway independently of nuclear

Ago import and that Ago proteins are loaded onto mRNAs in the cytoplasm.

Imp8 Is Required for Binding of Ago2 to a Large Set of Target mRNAs

Next, we analyzed Imp8 effects on global Ago2 transcript binding. Endogenous Ago2 was immunoprecipitated from cell lysates that were transfected with control siRNAs or siRNAs directed against Imp8. Coimmunoprecipitated mRNA was extracted and investigated by affimetrix microarray analysis (Figure 6A and Table S3). The Ago2-associated transcripts that were most enriched compared to total RNA levels were identified in the data set where control siRNAs had been transfected. Indeed, most of the top 30 Ago2-associated mRNAs are reduced in Ago2 immunoprecipitates from Imp8-depleted cells, indicating that Imp8 not only affects Ago2-binding to HMGA2 but also many other mRNA targets (Figure 6B).

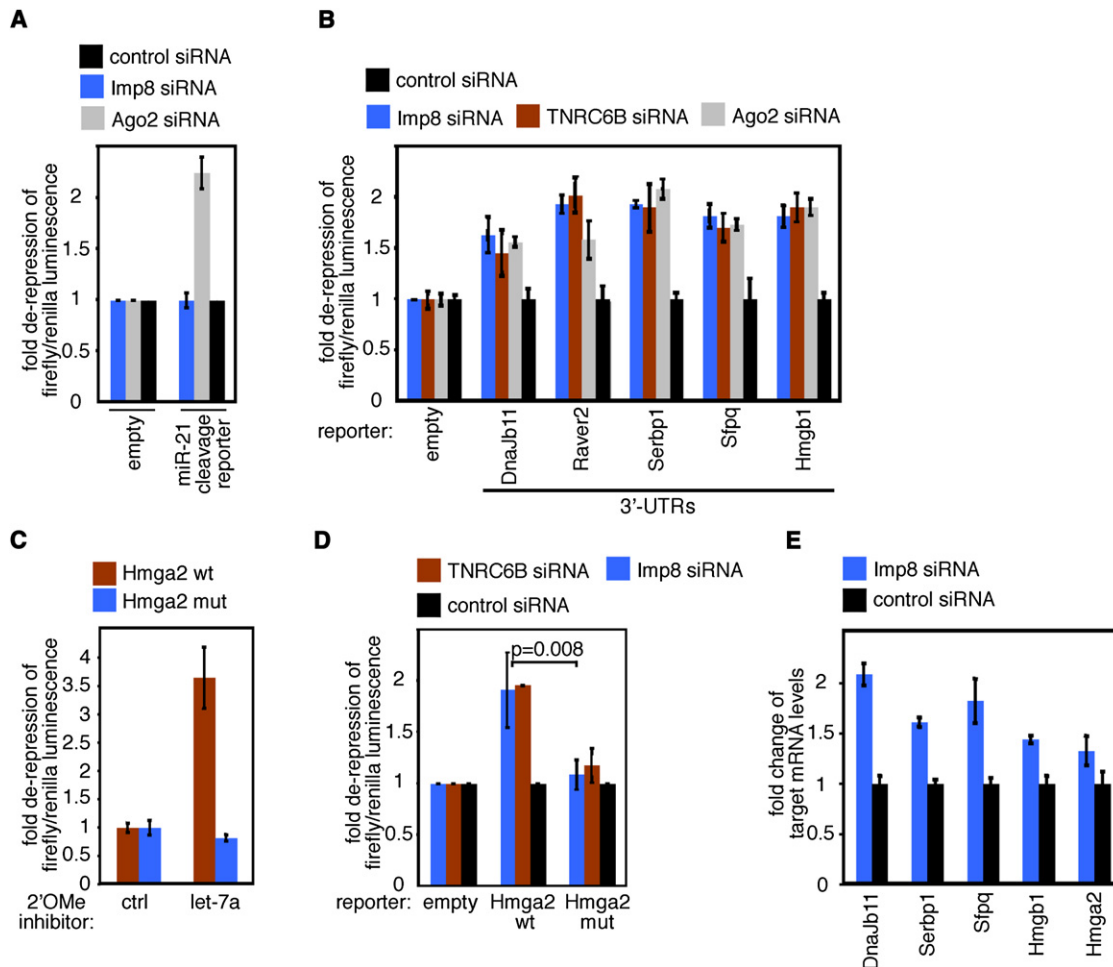


Figure 4. Imp8 Is Required for miRNA Function, but Not for RNAi

(A, B, and D) HeLa cells were sequentially transfected with the indicated siRNAs and pMIR-RL dual luciferase reporter plasmids. Firefly/renilla luminescence ratios are displayed as mean derepression of the reporter constructs (\pm SEM), which is calculated by normalization of the luminescence ratios of the construct of interest to the corresponding values of the empty plasmid.

(C) A Hmga2 3' UTR dual luciferase reporter construct or a corresponding reporter construct bearing mutated let-7 binding sites was cotransfected with either hsa-let-7a antisense 2'-O-methyl oligonucleotide or a control oligonucleotide into HeLa cells. Data are displayed as mean derepression of luciferase activity (\pm SEM), normalized to negative control oligonucleotide transfections.

(E) HeLa cells were transfected with Imp8 or control siRNAs. RNA was isolated and reverse transcribed, and miRNA target mRNA levels were quantified by qPCR. Data were normalized to GAPDH mRNA levels and to control siRNA-transfected samples.

The requirement of Imp8 for Ago2 mRNA binding was further validated by qRT-PCR (Figure 6C). Indeed, knockdown of Imp8 reduced the Ago2 association of all mRNAs that have been tested. Moreover, the 30 mRNAs analyzed in Figure 6B are significantly stabilized when TNRC6B, a component of the miRNA pathway guiding mRNA destabilization processes, is depleted (Figure 6D). In contrast, a control set of mRNAs, which is not specifically enriched on Ago2, was not stabilized upon TNRC6B knockdown (Figure 6D). These results strongly suggest that the analyzed Ago2-bound mRNAs are indeed targets of the miRNA pathway. This is further supported by the finding that miRNA seed sequence matches are enriched in Ago2-associated mRNAs (Figure 6E). In order to investigate the step at which Imp8 affects Ago2 mRNA target binding, endogenous Imp8 was immunoprecipitated and the associated mRNAs analyzed by

qRT-PCR (Figure 6F). None of the Ago2-associated mRNAs analyzed in Figure 6C, however, were enriched in the Imp8 immunoprecipitate, suggesting that Imp8 does not bind to Ago2 on mRNA targets. Alternatively, Imp8-miRNA target interactions may not be stable enough to resist immunoprecipitation conditions. Our data suggest that Imp8 is required for binding of Ago2 to a broad set of mRNAs. Thus, Imp8 is a general gene-silencing factor that regulates target mRNA repression on the level of miRNP-mRNA interactions.

DISCUSSION

Ago proteins bind to miRNAs and mediate repression of target mRNA expression. However, only little is known about how Ago proteins find their specific binding sites on the 3' UTRs of

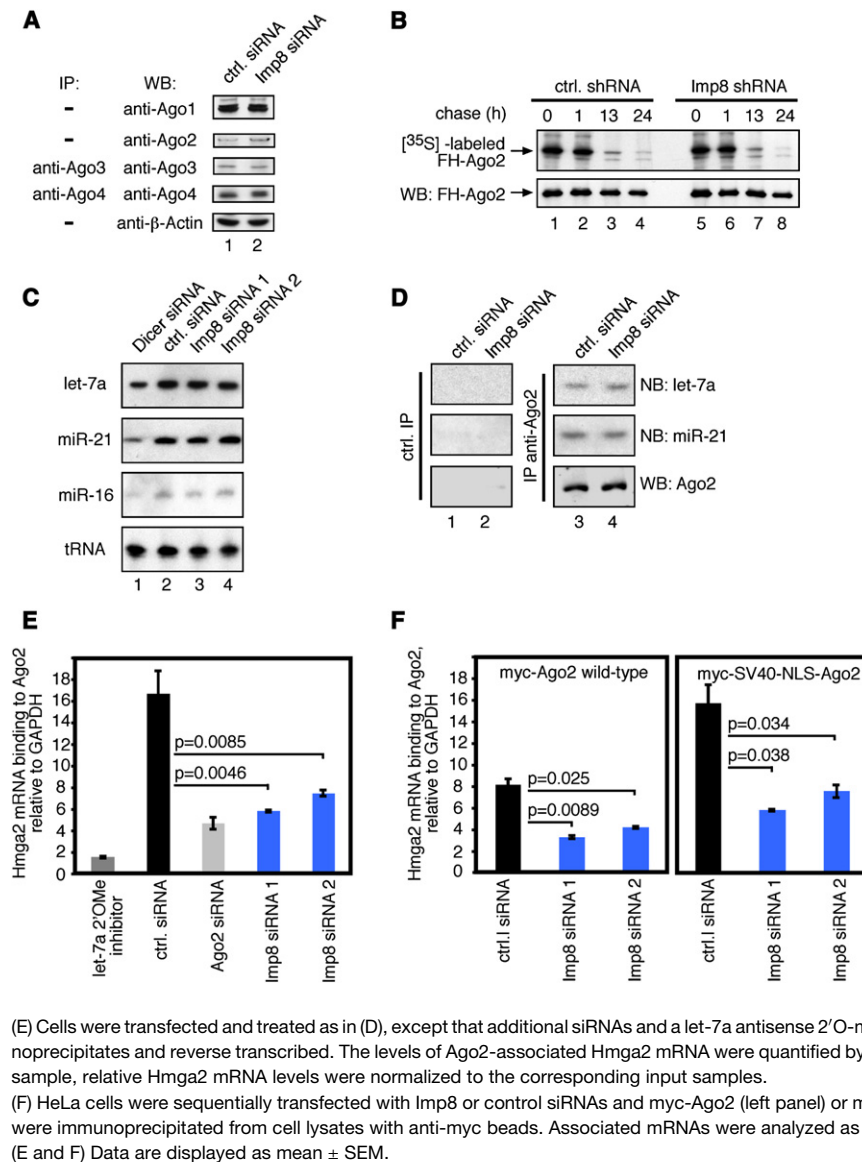


Figure 5. Imp8 Functions in Ago Protein Recruitment to Target mRNAs

(A) RNAi depletion of Imp8 does not affect soluble Ago protein levels in human cells. HeLa cells were transfected with a control siRNA (lane 1) or Imp8 siRNA (lane 2). Cells were lysed, and insoluble cellular fractions were pelleted by centrifugation. Supernatants were analyzed for Ago1/2 levels by SDS-PAGE/western blotting, with β -Actin used as loading control. Note that because of the low abundance of endogenous Ago3 and Ago4 in HeLa cells, Ago3 and Ago4 were immunoprecipitated with specific monoclonal antibodies prior to western blot analysis to obtain detectable signals. (B) Plasmids for the expression of FH-Ago2 and an Imp8 shRNA (lanes 5–8) or a control shRNA (lanes 1–4) were cotransfected into HEK293 cells. Cells were pulsed with medium containing [³⁵S]-labeled amino acids, incubated with nonradioactive chase points, and harvested at the indicated time points. FH-Ago2 was immunoprecipitated with anti-FLAG beads. The immunoprecipitate was analyzed for [³⁵S]-labeled FH-Ago2 (upper panel) and for total FH-Ago2 levels by western blotting (lower panel).

(C) HeLa cells were transfected with a Dicer siRNA (lane 1), control siRNA (lane 2), or Imp8 siRNAs (lanes 3–4). Total RNA was analyzed by denaturing RNA-PAGE/northern blotting for let-7a, miR-21, and miR-16, with lys-tRNA used as loading control.

(D) HeLa cells were transfected with a control siRNA (lanes 1 and 3) or Imp8 siRNA (lanes 2 and 4). IP was performed from cell lysates with a control antibody (lanes 1 and 2) or anti-Ago2 (11A9) monoclonal antibody (lanes 3 and 4). The immunoprecipitate was analyzed for Ago2 by western blotting (lower panel) and for let-7a and miR-21 by northern blotting (upper and middle panels, respectively).

target mRNAs. In this study, we provide evidence that Imp8 is required for efficient binding of Ago proteins to target mRNAs. We have identified Imp8 in proteomic analyses of Ago complex purifications (this study and Hock et al. [2007]) and show that Imp8 is required for binding of Ago2 to the let-7a target Hmga2. Imp8 knockdown had no effect on Ago stability, miRNA biogenesis, or miRNA loading onto Ago proteins. However, Hmga2 mRNA was strongly reduced in anti-Ago2 immunoprecipitations when Imp8 was depleted by RNAi, suggesting that Imp8 is involved in loading of Hmga2 mRNA with Ago2 complexes or in stabilizing the Ago2-target interaction. Similar results were obtained for many other mRNA targets, as shown by affymetrix arrays. However, we show that Imp8 is not stably associated with Ago2-bound mRNAs, suggesting that Imp8 may be required for efficient binding of Ago2 to target mRNAs rather than for stabilization of such interactions. We further show that depletion of Imp8 interferes with efficient miRNA

repression of many known miRNA targets. Therefore, we propose that Imp8 might be a general factor in the miRNA pathway. Specific factors negatively regulating miRNA binding to target 3' UTRs have been identified recently. It has been shown in liver cells that HuR (ELAV1), which binds to AU-rich elements on target mRNAs, antagonizes miR-122 repression on the CAT-1 3' UTR upon cellular stress (Bhattacharyya et al., 2006). Moreover, Dnd1, a protein expressed in primordial germ cells, prevents miRNA-guided repression by binding to the vicinity of miRNA binding sites (Kedde et al., 2007). In contrast, Imp8 is required for efficient binding of miRNAs to 3' UTRs and therefore functions in the opposite manner of factors such as HuR or Dnd1. Interestingly, Imp8 is not required for RNAi, suggesting that the assembly of miRNP-mRNA structures might be a highly coordinated process, which may differ from sequence-specific cleavage events. Notably, imb-5, the closest *C. elegans* homolog of human Imp8, has been identified in

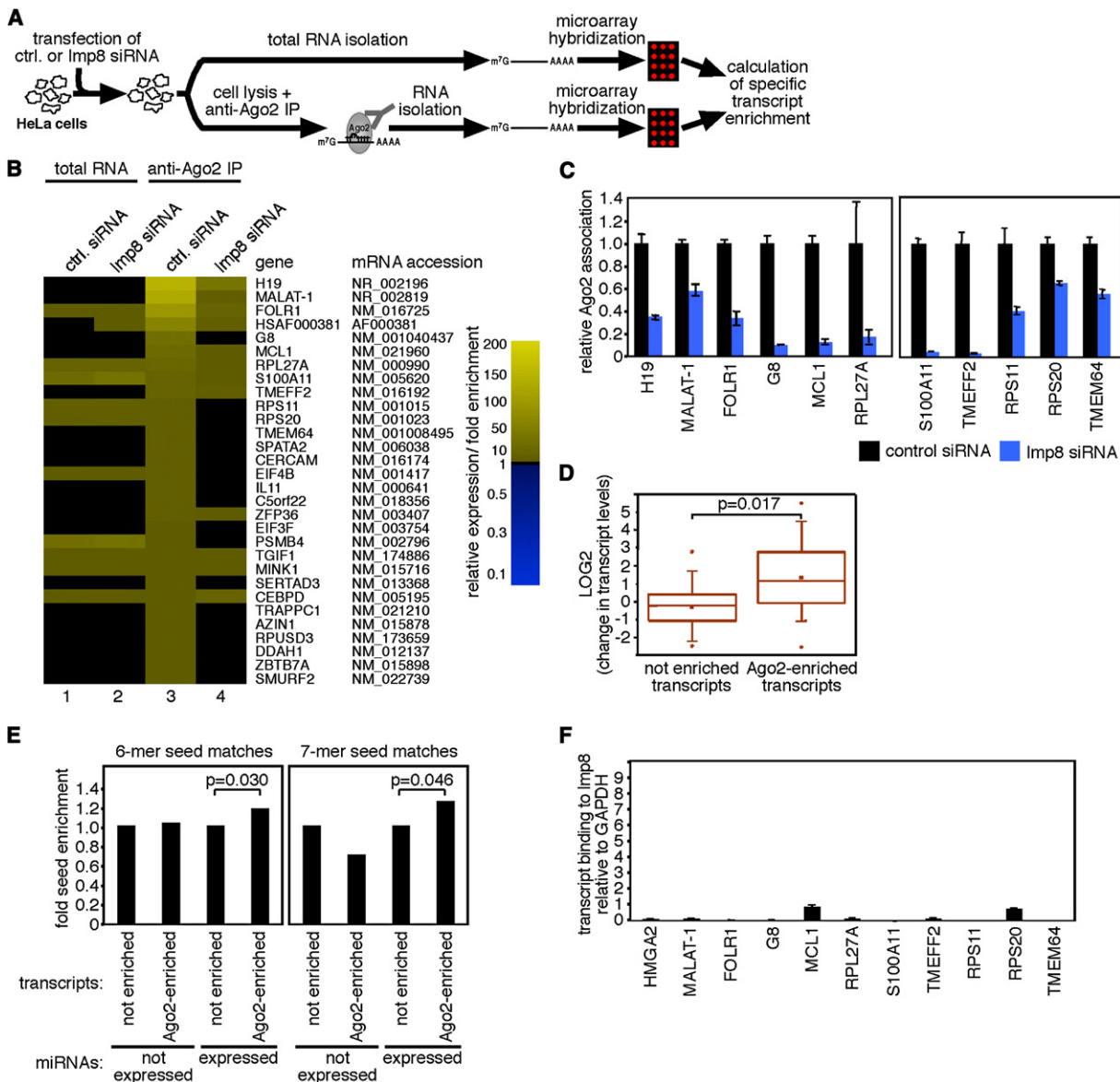


Figure 6. Imp8 Is Required for Binding of Ago2 to a Large Set of Target mRNAs

(A) HeLa cells were transfected with control or Imp8 siRNAs. Each sample was divided into two parts for total RNA extraction (upper arrow), and anti-Ago2 immunoprecipitation followed by RNA extraction (lower arrows). Total RNA samples and immunoprecipitated RNA samples were hybridized to separate Human Genome U133 Plus 2.0 Affymetrix microarrays. The specific enrichment of each individual transcript was calculated from its normalized measurement value in the immunoprecipitation sample, divided by its value in the total RNA sample.

(B) A heat map of 30 transcripts most highly enriched in anti-Ago2 immunoprecipitates from control siRNA-transfected cells. The heat map shows normalized measurements for total RNA from control siRNA-transfected cells (lane 1), Imp8 siRNA-transfected cells (lane 2), and Ago2-associated RNA from control siRNA-transfected cells (lane 3) and Imp8 siRNA-transfected cells (lane 4).

(C) Ago2 association of transcripts was validated by qRT-PCR and quantified relative to GAPDH and to input lysate samples. Ago2 association of transcripts in control siRNA transfected cells was normalized to 1.

(D) Box-whisker plot for log₂ changes in transcript abundance after TNRC6B knockdown. The plot shows the top 30 Ago2-associated transcripts (right side) and transcripts which are not specifically associated (enrichment = 1 ± 0.05; left side). Outliers are denoted by asterisks. Mean changes of Ago2-associated transcript levels are significant (p = 0.017; Student's t test from four microarray replicates from immunoprecipitated RNA).

(E) The number of 6-mer (left panel) and 7-mer (right panel) seed sequence matches was calculated for 3' UTRs of all transcripts more than 2-fold Ago2-enriched in at least three out of four microarray replicates compared to seven control groups of not enriched transcripts (enrichment = 1 ± 0.1). Enrichment was calculated for nine miRNAs highly expressed in HeLa cells and nine absent miRNAs, followed by normalization to 3' UTR length.

(F) HeLa cell lysates were immunoprecipitated with anti-Imp8 antibodies. RNA was isolated from immunoprecipitates, and the specific association of transcripts with Imp8 was calculated relative to the input sample and to GAPDH.

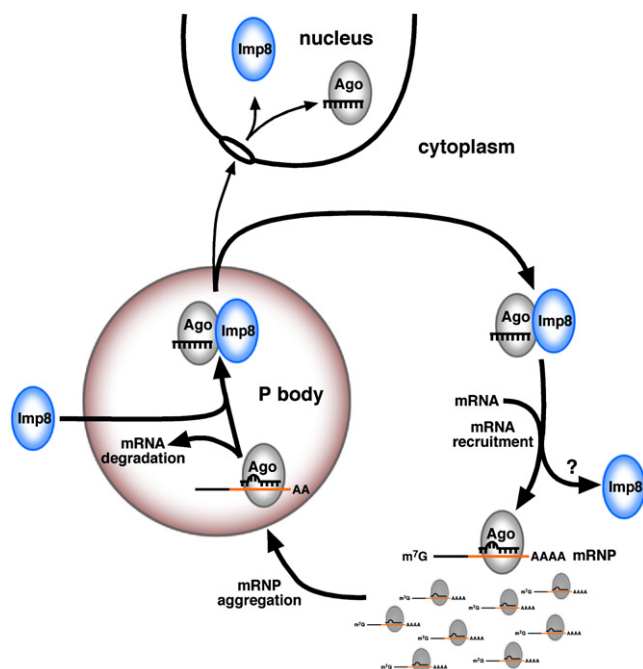


Figure 7. A Model for Imp8 Function

Imp8 may bind to Ago proteins in P bodies, followed by shuttling to the nucleus. Alternatively, Imp8 assists Ago protein recruitment to miRNA target mRNAs in the cytoplasm by delivering Ago proteins to target mRNAs, followed by dissociation of the Imp8-Ago protein complex and aggregation of repressed mRNPs. Please note that the Ran binding cycle was omitted from the figure for simplification.

a genetic screen for factors essential for small RNA-guided gene silencing (Kim et al., 2005).

Notably, among the most highly enriched Ago2-associated transcripts we found the noncoding RNAs H19 and MALAT-1. Most miRNA target predictions published thus far have been restricted to 3' UTRs of mRNAs. Our data suggest that other noncoding RNAs are targeted by miRNAs as well. On the basis of the analysis of Ago2-associated mRNAs, we suggest that miRNA target searches should be extended to the entire transcriptome and should include larger noncoding transcripts.

Interestingly, Imp8 localizes together with Ago proteins to P bodies in human cells. It is therefore tempting to speculate that Ago proteins bind to Imp8 in P bodies presumably after target mRNA degradation and that Imp8 subsequently transfers free Ago-miRNA complexes to new target mRNAs (Figure 7). Since Imp8 has no obvious RNA binding domain, Imp8 might transiently interact with other protein factors that interact with specific binding sites on target 3' UTRs. Alternatively, binding of Imp8 to Ago proteins may alter the structure of Ago proteins, allowing for efficient binding to target mRNAs.

Ago proteins have been implicated in transcriptional silencing processes in different organisms (Lippman and Martienssen, 2004). The intriguing finding that the import receptor Imp8 associated with human Ago complexes led us to investigate whether or not Ago proteins are imported into the nucleus. Using a monoclonal anti-Ago2 antibody, we provide evidence that Ago2 is indeed found in the nucleus of human cells. Moreover, depletion

of Imp8 reduced the pool of nuclear Ago2, suggesting that Imp8 is involved in targeting Ago proteins to the nucleus. Biochemical analyses have suggested before that miRNAs as well as Ago proteins localize and function in the nucleus (Meister et al., 2004; Robb et al., 2005). siRNAs directed against nuclear RNAs such as 7SK RNA efficiently reduced 7SK RNA levels in nuclear fractions, suggesting that Ago2-mediated cleavage of target RNA occurs in the nucleus (Robb et al., 2005). Notably, a significant portion of Ago2 remained in the nucleus after Imp8 depletion, suggesting that alternative nuclear import pathways for Ago proteins may exist. Human Ago proteins have been implicated in transcriptional silencing processes (Janowski et al., 2006, 2007; Kim et al., 2006; Morris et al., 2004). It is possible that the nuclear Ago pool might also be involved in small RNA-guided transcriptional silencing processes in human cells. It is also conceivable that novel nuclear Ago functions exist that have yet to be defined.

Our data strongly suggest that Imp8 plays a major role in Ago-mediated gene silencing (Figure 7). In the cytoplasm, Imp8 localizes together with Ago proteins to P bodies and is involved in efficient loading of Ago proteins onto a variety of different target mRNAs. Moreover, Imp8 may also direct Ago proteins to the nucleus of human cells. Currently, it is unclear which factors direct Imp8 for nuclear import and which factors for Ago protein loading onto mRNA targets. It is likely that other factors that are present in our proteomic data set might be involved in regulating Imp8 function in small RNA pathways.

EXPERIMENTAL PROCEDURES

Antibodies and Recombinant Proteins

The following antibodies were used: mouse-anti-HA (Covance, Princeton, NJ), rabbit-anti-FLAG (Sigma, St. Louis, MO), rabbit-anti-myc (Abcam, UK), mouse anti- β -Actin AC15 (Abcam, UK), chicken-anti-Lsm4 (Genway, San Diego, CA), anti-rabbit-HRP (Sigma), anti-mouse-HRP (Sigma), anti-rat-HRP (Jackson, West Grove, PA), goat-anti-rat-Texas Red, goat-anti-rabbit-Texas Red, horse-anti-mouse-fluorescein, horse-anti-mouse-Texas Red (all Vector Laboratories, Burlingame, CA), and anti-chicken-fluorescein (Sigma).

Anti-Ago2 clone 11A9 has been described elsewhere (Rüdel et al., 2008). Rat-anti-Ago1 clone 1C9, rat-anti-Ago3 clone 5A3, and rat-anti-Ago4 clone 6C10 were generated as described (Beitzinger et al., 2007). Anti-Imp8 polyclonal antiserum was generated by immunization of KLH-CMQSNNGRGEDEEEEDDDWD into rabbits. Purification of anti-Imp8 polyclonal antibody was performed with CNBr-activated Sepharose 4 Fast Flow (GE Healthcare) according to the manufacturer's instructions. Recombinant GST-Importin 8 dialyzed against coupling buffer (0.1 M NaHCO₃ [pH 8.3], 0.5 M NaCl) served as ligand.

Coupled sepharose beads were washed with 10 ml PBS and subsequently incubated with 10 ml serum overnight at 4°C. Serum was removed from the column by gravity flow, and beads were washed twice with 10 ml PBS. For elution of the purified antibody, 1 ml fractions of elution buffer (0.1 M Glycine [pH 2.3]) were added to the beads, and the column was emptied by gravity flow into reaction tubes containing 0.1 ml 1M Tris-HCl (pH 8.8) to neutralize the eluate.

Recombinant GST-Imp8 was expressed and purified as follows: pGEX6P1-Imp8 was transformed into *E. coli* BL21 Rosetta bacteria. Overnight cultures were diluted into fresh medium, grown to 0.8 OD₆₀₀, and induced at 18°C with 1 mM IPTG for 18 hr. Bacteria were disrupted by sonication in purification buffer [500 mM NaCl/50 mM Tris/HCl (pH 7.5)/5 mM MgCl₂/1 mM 4-(2-Aminoethyl) benzenesulfonyl fluoride hydrochloride (AEBFSF)], and debris was removed by centrifugation. Supernatants were incubated with Glutathione sepharose beads (GE healthcare) for 2 hr. Beads were washed twice with purification buffer (pH 8.0). GST-Imp8 was eluted in purification buffer (pH 8.0) containing 3 mg/ml glutathione and dialyzed against PBS.

Coimmunoprecipitation and Mass Spectrometry

For coimmunoprecipitation (Co-IP) experiments, 3 × 15 cm plates of HEK293 cells per sample were transfected with appropriate plasmids for 2 days. Cells were washed twice with PBS and lysed in 500 μl lysis buffer (150 mM KCl/25 mM Tris-HCl [pH 7.5]/2 mM ethylenediaminetetraacetic acid [EDTA]/1 mM NaF/0.5% NP-40/0.5 mM dithiothreitol [DTT]/0.5 mM AEBSF) per plate. Ribolock (Fermentas, 1 μl per ml of lysis buffer) was added for RNA IPs. Lysates were cleared by centrifugation at 16,000 g for 10 min. For IP of FLAG-tagged proteins, lysates were incubated with 60 μl anti-FLAG M2 agarose beads for 3 hr at 4°C with or without RNaseA (QIAGEN, 20 μg/ml). For IP of endogenous proteins, 6 ml monoclonal antibody-containing hybridoma supernatant was coupled to 60 μl protein G-Sepharose (GE Healthcare) for 2 hr at 4°C. Coupled beads were washed twice with PBS and subsequently incubated with cell lysate for 3 hr at 4°C. All IP samples were washed three times with IP wash buffer (300 mM NaCl/50 mM Tris [pH 7.5]/1 mM NaF, 0.01% NP-40/5 mM MgCl₂) and once with PBS. For the detection of proteins, beads were boiled in protein sample buffer. For the detection of associated RNAs, proteins were digested with 1 mg/ml proteinase K for 1 hr at 42°C, followed by phenol/chloroform/isopropyl alcohol extraction and precipitation of RNA in 80% ethanol at -20°C. Mass spectrometry of Ago complexes was performed as previously described (Hock et al., 2007).

Ago2-Associated mRNA Analysis

HeLa cells were reverse transfected in 10 cm plates with Imp8 or control siRNAs. For the analysis of mRNA binding to myc-tagged Ago2, cells were transfected 2 days later with 15 μg/plate pCS2-Ago2 or pCS2-SV40-NLS-Ago2 with Lipofectamine 2000 (Invitrogen) according to the manufacturer's instructions. Three days after plasmid transfection, cells were lysed and treated analogous to IP samples. IP for myc-tagged proteins was performed for 2.5 hr at 4°C with 40 μl anti-myc beads (Sigma) per sample. For analysis of mRNA binding to endogenous Ago2, siRNA-transfected cells were harvested 5 days after transfection and treated as described for IP samples. Immunoprecipitates were washed three times with IP wash buffer and once with PBS. IP samples and corresponding samples containing 10% of input lysate were proteinase K digested, followed by phenol/chloroform/isopropyl alcohol extraction and precipitation of RNA in 80% ethanol at -20°C. RNA was pelleted, dried, and treated with DNaseI (Fermentas) for 30 min at 37°C, followed by thermal inactivation of DNaseI. RNAs were detected via cDNA synthesis and qPCR. Hmga2 mRNA levels were normalized to GAPDH mRNA or Ile tRNA levels for input and IP samples. Specific binding of Hmga2 mRNA to Ago proteins was calculated from the relative Hmga2 mRNA abundance in IP samples, divided by the relative abundance in the corresponding input samples.

Microarray Hybridization and Data Analysis

RNA for microarray analysis was isolated with PrepEase Kit for total RNA (USB, Cleveland, OH) and phenol/chloroform/isopropyl alcohol extraction for IP samples. RNA was processed and hybridized with the Gene Chip (Affymetrix) kit and the hybridization procedure for eukaryotic samples, used according to the manufacturer's instructions. Samples were hybridized to Human Genome U133 Plus 2.0 arrays. All arrays were performed in at least two biological replicates.

Microarray data were analyzed with Agilent Genespring software. Expression values below 0.01 were set to 0.01. Each measurement was divided by the 50th percentile of all measurements in that sample. All IP samples were normalized to the corresponding total RNA samples: the IP sample from control siRNA-transfected cells was normalized against the median of the corresponding total RNA sample, and the IP sample from Imp8 siRNA-transfected cells was normalized against the median of the corresponding total RNA sample. Each measurement for each gene in the IP samples was divided by the median of that gene's measurements in the corresponding total RNA samples.

Using this normalization procedure, the normalized expression value of each transcript in IP samples directly reflects its over- or underrepresentation in the immunoprecipitated transcript pool relative to the total RNA pool. So that transcripts bound by Ago2 could be filtered, all transcripts with raw measurements over 50 that were more than 4-fold enriched in immunoprecipitates from control siRNA-transfected cells were displayed (Table S3). p values for

enriched transcripts were calculated on the basis of expression levels with the Genespring software.

ACCESSION NUMBERS

The microarray data sets reported in this paper have been deposited in Gene Expression Omnibus with the serial accession number GSE14054.

SUPPLEMENTAL DATA

Supplemental Data include Supplemental Experimental Procedures, eight figures, and four tables and can be found with this article online at [http://www.cell.com/supplemental/S0092-8674\(08\)01628-0](http://www.cell.com/supplemental/S0092-8674(08)01628-0).

ACKNOWLEDGMENTS

We thank Keiichi Ozono for pGEX-Imp4, Erich Nigg for pcDNA3.1-RanWT, -RanQ69L, and -RanT24N, Olaf Stemmann for pCS2, Simone Heubes for recombinant RanWT and RanQ69L, and Susanna Nagel for technical advice. Further, we thank Dirk Görlich, Witold Filipowicz, Michael Doyle, Laura Riolo-bos, Thomas Güttler, Sabine Rüdell, Michaela Beitzinger, and Christine Ender for helpful discussions, Thomas Tuschl and Tobias Walther for critical reading of the manuscript, Sabine Rottmüller and Bernd Haas for technical assistance, and Stefan Jentsch for support. Our research is funded by the Max Planck Society. This work was supported in part by the Deutsche Forschungsgemeinschaft (DFG, Me2064/2-1), the European Union (LSHG-CT-2006-037900), and the Max Planck Society. T.O. is funded by Deutsche Volkswagenstiftung I/79308. L.W. received a fellowship from the Boehringer Ingelheim Fonds.

Received: March 3, 2008

Revised: October 27, 2008

Accepted: December 8, 2008

Published online: January 22, 2009

REFERENCES

- Aravin, A., Gaidatzis, D., Pfeffer, S., Lagos-Quintana, M., Landgraf, P., Iovino, N., Morris, P., Brownstein, M.J., Kuramochi-Miyagawa, S., Nakano, T., et al. (2006). A novel class of small RNAs bind to MILI protein in mouse testes. *Nature* 442, 203–207.
- Aravin, A.A., Sachidanandam, R., Girard, A., Fejes-Toth, K., and Hannon, G.J. (2007). Developmentally regulated piRNA clusters implicate MILI in transposon control. *Science* 316, 744–747.
- Bagga, S., Bracht, J., Hunter, S., Massirer, K., Holtz, J., Eachus, R., and Pasquinelli, A.E. (2005). Regulation by let-7 and lin-4 miRNAs results in target mRNA degradation. *Cell* 122, 553–563.
- Behm-Ansmant, I., Rehwinkel, J., Doerks, T., Stark, A., Bork, P., and Izauralde, E. (2006). mRNA degradation by miRNAs and GW182 requires both CCR4:NOT deadenylase and DCP1:DCP2 decapping complexes. *Genes Dev.* 20, 1885–1898.
- Beitzinger, M., Peters, L., Zhu, J.Y., Kremmer, E., and Meister, G. (2007). Identification of human microRNA targets from isolated argonaute protein complexes. *RNA Biol.* 4, 76–84.
- Bhattacharyya, S.N., Habermacher, R., Martine, U., Closs, E.I., and Filipowicz, W. (2006). Relief of microRNA-mediated translational repression in human cells subjected to stress. *Cell* 125, 1111–1124.
- Bushati, N., and Cohen, S.M. (2007). microRNA functions. *Annu. Rev. Cell Dev. Biol.* 23, 175–205.
- Easow, G., Teleman, A.A., and Cohen, S.M. (2007). Isolation of microRNA targets by miRNP immunoprecipitation. *RNA* 13, 1198–1204.
- Filipowicz, W., Jaskiewicz, L., Kolb, F.A., and Pillai, R.S. (2005). Post-transcriptional gene silencing by siRNAs and miRNAs. *Curr. Opin. Struct. Biol.* 15, 331–341.

- Giraldez, A.J., Mishima, Y., Rihel, J., Grocock, R.J., Van Dongen, S., Inoue, K., Enright, A.J., and Schier, A.F. (2006). Zebrafish MiR-430 promotes deadenylation and clearance of maternal mRNAs. *Science* 312, 75–79.
- Girard, A., Sachidanandam, R., Hannon, G.J., and Carmell, M.A. (2006). A germline-specific class of small RNAs binds mammalian Piwi proteins. *Nature* 442, 199–202.
- Gorlich, D., Dabrowski, M., Bischoff, F.R., Kutay, U., Bork, P., Hartmann, E., Prehn, S., and Izaurralde, E. (1997). A novel class of RanGTP binding proteins. *J. Cell Biol.* 138, 65–80.
- Gregory, R.I., Chendrimada, T.P., Cooch, N., and Shiekhattar, R. (2005). Human RISC couples microRNA biogenesis and posttranscriptional gene silencing. *Cell* 123, 631–640.
- Hock, J., Weinmann, L., Ender, C., Rudel, S., Kremmer, E., Raabe, M., Urlaub, H., and Meister, G. (2007). Proteomic and functional analysis of Argonaute-containing mRNA-protein complexes in human cells. *EMBO Rep.* 8, 1052–1060.
- Humphreys, D.T., Westman, B.J., Martin, D.I., and Preiss, T. (2005). MicroRNAs control translation initiation by inhibiting eukaryotic initiation factor 4E/cap and poly(A) tail function. *Proc. Natl. Acad. Sci. USA* 102, 16961–16966.
- Jakel, S., Mingot, J.M., Schwarzmaier, P., Hartmann, E., and Gorlich, D. (2002). Importins fulfil a dual function as nuclear import receptors and cytoplasmic chaperones for exposed basic domains. *EMBO J.* 21, 377–386.
- Janowski, B.A., Huffman, K.E., Schwartz, J.C., Ram, R., Nordsell, R., Shames, D.S., Minna, J.D., and Corey, D.R. (2006). Involvement of AGO1 and AGO2 in mammalian transcriptional silencing. *Nat. Struct. Mol. Biol.* 13, 787–792.
- Janowski, B.A., Younger, S.T., Hardy, D.B., Ram, R., Huffman, K.E., and Corey, D.R. (2007). Activating gene expression in mammalian cells with promoter-targeted duplex RNAs. *Nat. Chem. Biol.* 3, 166–173.
- Karginov, F.V., Conaco, C., Xuan, Z., Schmidt, B.H., Parker, J.S., Mandel, G., and Hannon, G.J. (2007). A biochemical approach to identifying microRNA targets. *Proc. Natl. Acad. Sci. USA* 104, 19291–19296.
- Kedde, M., Strasser, M.J., Boldajpour, B., Vrielink, J.A., Slanchev, K., le Sage, C., Nagel, R., Voorhoeve, P.M., van Duijse, J., Orom, U.A., et al. (2007). RNA-binding protein Dnd1 inhibits microRNA access to target mRNA. *Cell* 131, 1273–1286.
- Kim, D.H., Villeneuve, L.M., Morris, K.V., and Rossi, J.J. (2006). Argonaute-1 directs siRNA-mediated transcriptional gene silencing in human cells. *Nat. Struct. Mol. Biol.* 13, 793–797.
- Kim, J.K., Gabel, H.W., Kamath, R.S., Tewari, M., Pasquinelli, A., Rual, J.F., Kennedy, S., Dybbs, M., Bertin, N., Kaplan, J.M., et al. (2005). Functional genomic analysis of RNA interference in *C. elegans*. *Science* 308, 1164–1167.
- Leung, A.K., Calabrese, J.M., and Sharp, P.A. (2006). Quantitative analysis of Argonaute protein reveals microRNA-dependent localization to stress granules. *Proc. Natl. Acad. Sci. USA* 103, 18125–18130.
- Leuschner, P.J., Ameres, S.L., Kueng, S., and Martinez, J. (2006). Cleavage of the siRNA passenger strand during RISC assembly in human cells. *EMBO Rep.* 7, 314–320.
- Lippman, Z., and Martienssen, R. (2004). The role of RNA interference in heterochromatic silencing. *Nature* 431, 364–370.
- Liu, J., Carmell, M.A., Rivas, F.V., Marsden, C.G., Thomson, J.M., Song, J.J., Hammond, S.M., Joshua-Tor, L., and Hannon, G.J. (2004). Argonaute2 is the catalytic engine of mammalian RNAi. *Science* 305, 1437–1441.
- Liu, J., Valencia-Sanchez, M.A., Hannon, G.J., and Parker, R. (2005). MicroRNA-dependent localization of targeted mRNAs to mammalian P-bodies. *Nat. Cell Biol.* 7, 719–723.
- Maroney, P.A., Yu, Y., Fisher, J., and Nilsen, T.W. (2006). Evidence that microRNAs are associated with translating messenger RNAs in human cells. *Nat. Struct. Mol. Biol.* 13, 1102–1107.
- Mathonnet, G., Fabian, M.R., Svitkin, Y.V., Parsyan, A., Huck, L., Murata, T., Biffo, S., Merrick, W.C., Darzynkiewicz, E., Pillai, R.S., et al. (2007). MicroRNA inhibition of translation initiation in vitro by targeting the cap-binding complex eIF4F. *Science* 317, 1764–1767.
- Matranga, C., Tomari, Y., Shin, C., Bartel, D.P., and Zamore, P.D. (2005). Passenger-strand cleavage facilitates assembly of siRNA into Ago2-containing RNAi enzyme complexes. *Cell* 123, 607–620.
- Meister, G., and Tuschl, T. (2004). Mechanisms of gene silencing by double-stranded RNA. *Nature* 431, 343–349.
- Meister, G., Landthaler, M., Patkaniowska, A., Dorsett, Y., Teng, G., and Tuschl, T. (2004). Human Argonaute2 mediates RNA cleavage targeted by miRNAs and siRNAs. *Mol. Cell* 15, 185–197.
- Meister, G., Landthaler, M., Peters, L., Chen, P.Y., Urlaub, H., Luhrmann, R., and Tuschl, T. (2005). Identification of novel argonaute-associated proteins. *Curr. Biol.* 15, 2149–2155.
- Morris, K.V., Chan, S.W., Jacobsen, S.E., and Looney, D.J. (2004). Small interfering RNA-induced transcriptional gene silencing in human cells. *Science* 305, 1289–1292.
- Mourelatos, Z., Dostie, J., Paushkin, S., Sharma, A., Charroux, B., Abel, L., Rapsilber, J., Mann, M., and Dreyfuss, G. (2002). miRNPs: a novel class of ribonucleoproteins containing numerous microRNAs. *Genes Dev.* 16, 720–728.
- Nottrott, S., Simard, M.J., and Richter, J.D. (2006). Human let-7a miRNA blocks protein production on actively translating polyribosomes. *Nat. Struct. Mol. Biol.* 13, 1108–1114.
- Ohr, T., Mutze, J., Staroske, W., Weinmann, L., Hock, J., Crell, K., Meister, G., and Schulle, P. (2008). Fluorescence correlation spectroscopy and fluorescence cross-correlation spectroscopy reveal the cytoplasmic origination of loaded nuclear RISC in vivo in human cells. *Nucleic Acids Res.* 36, 6439–6449.
- Olsen, P.H., and Ambros, V. (1999). The lin-4 regulatory RNA controls developmental timing in *Caenorhabditis elegans* by blocking LIN-14 protein synthesis after the initiation of translation. *Dev. Biol.* 216, 671–680.
- Peters, L., and Meister, G. (2007). Argonaute proteins: mediators of RNA silencing. *Mol. Cell* 26, 611–623.
- Petersen, C.P., Bordeleau, M.E., Pelletier, J., and Sharp, P.A. (2006). Short RNAs repress translation after initiation in mammalian cells. *Mol. Cell* 21, 533–542.
- Pillai, R.S., Bhattacharyya, S.N., and Filipowicz, W. (2007). Repression of protein synthesis by miRNAs: how many mechanisms? *Trends Cell Biol.* 17, 118–126.
- Rand, T.A., Petersen, S., Du, F., and Wang, X. (2005). Argonaute2 cleaves the anti-guide strand of siRNA during RISC activation. *Cell* 123, 621–629.
- Robb, G.B., Brown, K.M., Khurana, J., and Rana, T.M. (2005). Specific and potent RNAi in the nucleus of human cells. *Nat. Struct. Mol. Biol.* 12, 133–137.
- Rüdel, S., Flatley, A., Weinmann, L., Kremmer, E., and Meister, G. (2008). A multifunctional human Argonaute2-specific monoclonal antibody. *RNA* 14, 1244–1253.
- Seggerson, K., Tang, L., and Moss, E.G. (2002). Two genetic circuits repress the *Caenorhabditis elegans* heterochronic gene *lin-28* after translation initiation. *Dev. Biol.* 243, 215–225.
- Sen, G.L., and Blau, H.M. (2005). Argonaute 2/RISC resides in sites of mammalian mRNA decay known as cytoplasmic bodies. *Nat. Cell Biol.* 7, 633–636.
- Seto, A.G., Kingston, R.E., and Lau, N.C. (2007). The coming of age for Piwi proteins. *Mol. Cell* 26, 603–609.
- Thermann, R., and Hentze, M.W. (2007). Drosophila miR2 induces pseudopolysomes and inhibits translation initiation. *Nature* 447, 875–878.
- Tolia, N.H., and Joshua-Tor, L. (2007). Slicer and the argonautes. *Nat. Chem. Biol.* 3, 36–43.
- Wakiyama, M., Takimoto, K., Ohara, O., and Yokoyama, S. (2007). Let-7 microRNA-mediated mRNA deadenylation and translational repression in a mammalian cell-free system. *Genes Dev.* 21, 1857–1862.
- Wang, B., Love, T.M., Call, M.E., Doench, J.G., and Novina, C.D. (2006). Recapitulation of short RNA-directed translational gene silencing in vitro. *Mol. Cell* 22, 553–560.
- Wu, L., Fan, J., and Belasco, J.G. (2006). MicroRNAs direct rapid deadenylation of mRNA. *Proc. Natl. Acad. Sci. USA* 103, 4034–4039.
- Zamore, P.D., and Haley, B. (2005). Ribo-gnome: the big world of small RNAs. *Science* 309, 1519–1524.

Argonaute Proteins: Mediators of RNA Silencing

Lasse Peters¹ and Gunter Meister^{1,*}

¹Laboratory of RNA Biology, Max Planck Institute of Biochemistry, Am Klopferspitz 18, 82152 Martinsried, Germany

*Correspondence: meister@biochem.mpg.de

DOI 10.1016/j.molcel.2007.05.001

Small regulatory RNAs such as short interfering RNAs (siRNAs), microRNAs (miRNAs), and Piwi interacting RNAs (piRNAs) have been discovered in the past, and it is becoming more and more apparent that these small molecules have key regulatory functions. Small RNAs are found in all higher eukaryotes and play important roles in cellular processes as diverse as development, stress response, or transposon silencing. Soon after the discovery of small regulatory RNAs, members of the Argonaute protein family were identified as their major cellular protein interactors. This review focuses on the various cellular functions of mammalian Argonaute proteins in conjunction with the different small RNA species that are known today.

Introduction

Double-stranded (ds) RNA is the trigger molecule in small RNA-guided gene-silencing pathways that have been characterized in mammals thus far. Long dsRNA can derive from various sources such as simultaneous sense and antisense transcription of specific genomic loci or viral replication intermediates. The predominant form of dsRNA in mammalian cells, however, is derived from endogenously expressed miRNAs. miRNA genes are transcribed by RNA polymerase II and III (Borchert et al., 2006; Lee et al., 2004) as primary transcripts that are subsequently processed to stem-loop-structured miRNA precursors (pre-miRNAs) by the RNase III enzyme Drosha. Like all RNase III enzymes, Drosha leaves two nucleotide (nt) 3' overhangs and 5' phosphate groups. Pre-miRNAs are further transported to the cytoplasm via the export-receptor Exportin-5. Both long dsRNA and secondary fold-back structures such as hairpins are recognized and processed by the cytoplasmic RNase III enzyme Dicer (for a comprehensive overview, see Ambros [2004] and Meister and Tuschl [2004]). Dicer binds and cleaves dsRNA preferentially from the ends and generates a 21–25 nt long dsRNA with characteristic 5' phosphate groups and 2 nt 3' overhangs (Zhang et al., 2002, 2004). Both strands of such dsRNA intermediates are separated, and one strand is incorporated into an effector complex where it directly binds to a member of the Argonaute protein family. The RNA-induced silencing complex (RISC) contains a small RNA that guides the sequence-specific cleavage of complementary target RNAs, a process termed RNA interference or RNAi (Hammond et al., 2000; Martinez et al., 2002). Most mammalian miRNAs, however, do not guide cleavage of target mRNAs by RNAi-like mechanisms. In contrast, mammalian miRNAs predominantly repress gene expression on the level of translation or affect mRNA stability by guiding cellular decay processes, including mRNA deadenylation and decapping. To distinguish them from mRNA cleavage reactions mediated by

RISC, effector complexes containing miRNAs are often referred to as miRNPs (Mourelatos et al., 2002).

Recently, a novel class of small RNAs has been cloned from mammalian testes and termed Piwi interacting RNAs (piRNAs) because of their interaction with specific members of the Argonaute protein family (Aravin et al., 2006; Girard et al., 2006; Grivna et al., 2006; Lau et al., 2006). However, the biogenesis of piRNAs, including transcription and processing, as well as their cellular functions remains elusive.

In *Schizosaccharomyces pombe* (*S. pombe*), siRNAs derive from centromeric repeats and associate with Argonaute proteins to form the RNA-induced initiation of transcriptional gene silencing (RITS) complex (reviewed in Lippman and Martienssen [2004]). RITS guides methyltransferases to specific chromatic regions, allowing for the methylation of H3/lysine 9 (H3/K9) and therefore the establishment of silenced heterochromatin. Repeat-associated small interfering RNAs (rasiRNAs) have been discovered in various organisms, including flies and nematodes (Aravin et al., 2003; Sijen and Plasterk, 2003; Vagin et al., 2006). In mammals, a class of small RNAs that might be similar to rasiRNAs has been described recently (Watanabe et al., 2006; Yang and Kazanian, 2006). However, the function of this mammalian class of small RNAs remains unclear.

The Argonaute Protein Family

Argonaute proteins were named after the characteristic squid-like phenotype of plants lacking functional Argonaute proteins (Bohmert et al., 1998). In the past years, Argonaute proteins have been extensively studied in many different organisms, including *S. pombe*, *Caenorhabditis elegans* (*C. elegans*), *Drosophila melanogaster* (*D. melanogaster*), and various mammals. It is becoming more and more apparent that Argonaute proteins are key actors in many different RNA silencing pathways. Gene inactivation studies revealed that Argonaute proteins are

Table 1. Mouse and Human Argonaute Proteins

Argonaute Protein	Slicer Activity	Catalytic Triad	Associated Small RNAs	Reference(s)
Homo sapiens				
Ago1	–	DDR	si-, miRNAs	Liu et al., 2004; Meister et al., 2004
Ago2	+	DDH	si-, miRNAs	Liu et al., 2004; Meister et al., 2004
Ago3	–	DDH	si-, miRNAs	Liu et al., 2004; Meister et al., 2004
Ago4	–	DGR	si-, miRNAs	Liu et al., 2004; Meister et al., 2004
HIWI1	Not investigated	DDH	Not investigated	
HIWI2	Not investigated	DAH	Not investigated	
HIWI3	Not investigated	DDH	Not investigated	
HILI	Not investigated	DDH	Not investigated	
Mus musculus				
Ago1	Not investigated	DDR	Not investigated	
Ago2	Not investigated	DDH	Not investigated	
Ago3	Not investigated	DDH	Not investigated	
Ago4	Not investigated	DGR	Not investigated	
Ago5	Not investigated	NDH	Not investigated	
MIWI	Not investigated	DDH	piRNAs	Girard et al., 2006
MIWI2	Not investigated	DDH	Not investigated	
MILI	Not investigated	DDH	piRNAs	Aravin et al., 2006

important for embryonic development, cell differentiation, and stem cell maintenance.

The number of Argonaute genes is highly variable between species, ranging from one in *S. pombe* to 27 in *C. elegans*. Both human and mouse express eight Argonaute family members (Sasaki et al., 2003). Based on sequence similarities, the mammalian Argonaute protein family has been separated into the Ago and Piwi subfamilies. In human, the Ago subfamily consists of hsAgo1–4, in mouse of mmAgo1–5 (Table 1). Members of the Piwi subfamily are phylogenetically closer related to PIWI, the founding member in *D. melanogaster* (Carmell et al., 2002). Although the human genome encodes four members of this subfamily, only three are found in the mouse genome (see below). Expression studies revealed that the Ago subfamily is ubiquitously expressed, whereas expression of the Piwi subfamily seems to be restricted to germ cells (Meister et al., 2004; Sasaki et al., 2003). However, a comprehensive expression study analyzing all mammalian tissues has not been performed yet.

Argonaute proteins have a molecular weight of about 100 kDa and are characterized by piwi-argonaute-zwille (PAZ) and PIWI domains (Cerutti et al., 2000). Structural studies on isolated PAZ domains in complex with a ds siRNA revealed that the PAZ domain forms a specific binding module for the characteristic 2 nt 3' overhangs

generated by RNase III-type enzymes such as Dicer (for a comprehensive overview of structural studies on Argonaute proteins, see Parker and Barford [2006] and Song and Joshua-Tor [2006]). X-ray crystallography studies of bacterial Argonaute proteins found a third functionally important domain, which is located between the PAZ and the PIWI domain and therefore referred to as MID domain (Parker et al., 2005; Yuan et al., 2005). The MID domain contains a highly basic pocket, which specifically binds the characteristic 5' phosphate of small RNAs and therefore anchors the small RNA onto Argonaute proteins. Further structural studies indicated that the PIWI domain folds similar to RNase H. Consistently, some Ago proteins are indeed endonucleases and cleave substrate RNAs complementary to the bound small RNA. In analogy to Dicer, such proteins are often referred to as "Slicer." Like RNase H, three residues within the PIWI domain form a catalytic triad. Based on mutation studies, the catalytic triad of human Ago2 has been identified as D(597), D(669), and H(807) (Rivas et al., 2005; Song et al., 2004). In vitro assays using RNA substrates complementary to exogenous siRNAs (Liu et al., 2004) as well as endogenous miRNAs (Meister et al., 2004) identified Ago2 as the only member of the human Ago subfamily with endonuclease activity. Interestingly, human Ago3 is catalytically inactive, even though the catalytic triad DDH is

conserved (Table 1), indicating that additional factors such as posttranslational modification or interaction with specific proteins may modify the activity of Ago proteins.

Members of the mammalian Piwi subfamily have not directly been analyzed for Slicer activity thus far. Interestingly, *Drosophila* PIWI shows Slicer activity in vitro, although the putative catalytic triad is formed by DDK (Saito et al., 2006). Furthermore, it has been shown that highly pure fractions from rat testes containing the Piwi subfamily member RIWI and piRNAs contain Slicer activity as well, suggesting that RIWI might be endonucleolytically active (Lau et al., 2006). The most intriguing question is, however, what natural RNAs are targeted by mammalian Piwi proteins. Answering this question will clearly be a major research focus in the next few years and will provide new interesting insights into RNA-guided gene silencing in general.

Loading of Argonaute Proteins with Small RNAs

Ago proteins most likely recognize the characteristic 2 nt 3' overhangs of ds small RNA duplexes by their PAZ domains. Because the affinity of recombinant bacterial Ago proteins to dsRNA is very low (Yuan et al., 2005), it is likely that the small RNA is unwound while one strand stably associates with Ago as guide strand. The opposing strand, often referred to as passenger strand, is most likely degraded by nucleases. A yet to be identified helicase may contribute to the unwinding process and help to load Ago proteins with small RNAs. Recently, a model for Ago loading involving cleavage-competent Ago proteins has been suggested. *Drosophila* Ago proteins as well as hsAgo2 are capable of cleaving the passenger strand of the siRNA duplex, which will therefore not be incorporated into Ago complexes (Matranga et al., 2005; Miyoshi et al., 2005; Rand et al., 2005). Because of their short length, helicase activity is presumably not required to remove the cleavage fragments. However, such a model does not explain how cleavage-incompetent Ago proteins are loaded. Moreover, miRNA precursors that are unpaired at the cleavage position can also not be loaded as predicted by such a model, indicating that alternative mechanisms for Ago loading exist.

For most miRNAs, only one strand accumulates as mature miRNA. Such asymmetric loading is guided by the relative thermodynamic stability of the 5' ends of the small RNA duplex. The strand whose 5' end is less stably paired is preferentially incorporated into Ago complexes (Khvorova et al., 2003; Schwarz et al., 2003). In *Drosophila*, the dsRNA binding domain (dsRBD) protein R2D2 forms a heterodimer with Dicer2 and binds the more stable end of the siRNA, thereby positioning the duplex in order to allow incorporation of the right strand (Tomari et al., 2004). In human, the dsRBD proteins TRBP and PACT, which are highly homologous to *Drosophila* R2D2, are involved in RNA silencing as well (Chendrimada et al., 2005; Haase et al., 2005; Lee et al., 2006). Both TRBP and PACT reside independently in a complex with hsAgo2 and Dicer. Such a trimeric complex is capable of generating small RNAs

from dsRNA precursors, transferring one strand to Ago2 and cleaving complementary substrate RNAs (Gregory et al., 2005). Moreover, inactivation of TRBP as well as PACT results in a loss of mature miRNAs. Therefore, these proteins may have a similar role in strand selection and/or Ago loading as R2D2 in *Drosophila*, albeit this speculation remains to be experimentally investigated.

Ago-Mediated Posttranscriptional Gene Silencing Pathways

Depending not only on the bound small RNA but also on the specific mRNA that is targeted, Ago protein complexes mediate different posttranscriptional gene silencing mechanisms. Such Ago complexes are often referred to as effector complexes, and their individual functions will be discussed in the following paragraphs.

Ago Proteins and Translational Regulation

Initial studies in *C. elegans* showed that the miRNA lin-4 binds to the 3' untranslated region (UTR) of the lin-14 mRNA. Further expression studies revealed that the mRNA levels of lin-14 are not affected by lin-4 but the lin-14 protein levels dropped dramatically when lin-4 is present, indicating that this miRNA inhibits gene expression at the level of translation (Lee et al., 1993; Olsen and Ambros, 1999; Wightman et al., 1993). However, these initial observations have been challenged recently. Although not perfectly complementary, lin-4 as well as other miRNAs can inhibit target gene expression during *C. elegans* development by altering mRNA levels (Bagga et al., 2005), indicating that inhibition of gene expression on the translational level might not be the predominant function of miRNAs. Nevertheless, it has also been shown in mammals that miRNAs can inhibit protein production without changing mRNA levels (O'Donnell et al., 2005; Poy et al., 2004). Because Ago proteins are the cellular binding partners of miRNAs and miRNAs most likely function as guides to the target RNA, it is reasonable that Ago proteins are the mediators of translational repression. Indeed, tethering of Ago proteins to the 3'UTR of an artificial reporter mRNA inhibited translation of the mRNA (Pillai et al., 2004). However, in this study, Ago loading has not been experimentally addressed. Therefore, it is unclear if Ago proteins can repress translation independently of small RNAs.

The molecular mechanism of how miRNPs inhibit the translation of target mRNAs is highly controversial. Early studies in *C. elegans* and later on in mammals demonstrated that both Ago proteins and miRNAs cosediment with polyribosomes in sucrose gradients (Maroney et al., 2006; Nottrott et al., 2006; Olsen and Ambros, 1999; Petersen et al., 2006; Seggerson et al., 2002). Therefore, it has been proposed that miRNPs regulate translation after initiation. Indeed, several lines of evidence support such a model. First, artificial or natural mammalian miRNA targets comigrate with polyribosomes as well. Second, destruction of polyribosomes by different agents results in a shift of Ago proteins and miRNAs to smaller mRNP complexes, indicating that indeed miRNPs associate with

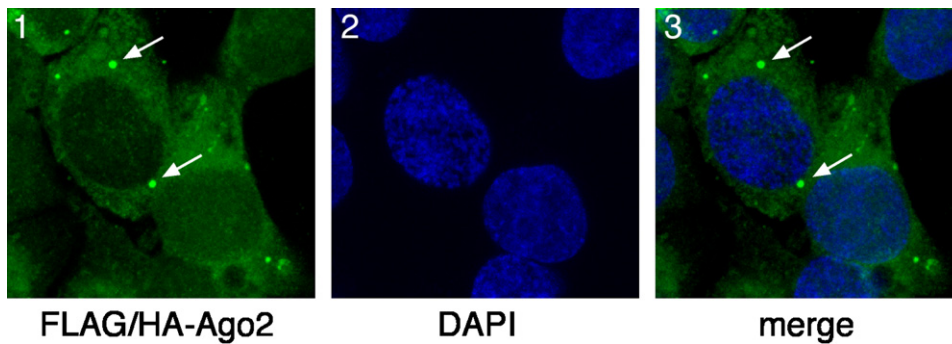


Figure 1. Mammalian Ago Proteins Localize to Cytoplasmic P Bodies

FLAG/HA-tagged human Ago1 was transfected into HEK 293T cells and stained with anti-FLAG antibodies (panel 1). DNA was stained with DAPI (panel 2). The merged image is displayed in panel 3. P bodies are indicated by arrows.

polyribosomes (Maroney et al., 2006; Nottrott et al., 2006; Petersen et al., 2006). Consistently, a “ribosome drop-off” model has been suggested. This model describes the rapid ribosome “drop-off” from mRNAs that are targeted by miRNPs (Petersen et al., 2006). A logical consequence of translational inhibition at the elongation step would be the production of nascent polypeptide chains that have to be removed after inhibition (Figure 2). Moreover, the association of miRNPs with actively translating ribosomes suggests that miRNAs directly influence the destruction of growing polypeptide chains. Indeed, using antibodies against the N terminus of a growing polypeptide that is under the control of a miRNA, Richter and coworkers recently showed that the N terminus is not accessible either, because it is rapidly degraded or it is masked and targeted for destruction by other proteins (Nottrott et al., 2006). Further biochemical studies that aim for the identification of factors that link Ago proteins with the protein degradation machinery such as the proteasome or the ubiquitin-conjugating system will help to elucidate the mode of translational repression mediated by Ago proteins and associated miRNAs.

However, the model described above does not explain two experimental observations. First, Ago proteins and miRNAs as well as artificial and also natural target mRNAs localize to processing bodies (P bodies), cellular sites where ribosomal proteins have not been found thus far (Figure 1, see below). Second, miRNPs do not affect cap-independent translation initiated by internal ribosomal entry sites (IRES) (Humphreys et al., 2005; Pillai et al., 2005). Indeed, it has been shown that efficient repression of miRNA targets requires the 5' cap structure as well as a poly(A) tail, indicating that the translation initiation step rather than the elongation step is affected by miRNPs (Humphreys et al., 2005). Moreover, the CAT-1 mRNA, which is released from miRNP-122-mediated repression upon cellular stress in liver cells, reassociates with polyribosomes, indicating that the initiation step is blocked by miR-122 (Bhattacharyya et al., 2006).

The two models of miRNP function in translation are controversial, and some results are even contradictory.

A simple explanation of this controversy would be that translational inhibition mediated by miRNPs could be specific to cellular conditions or the individual miRNA targets that have been used. Moreover, different experimental systems as well as different miRNA targets and reporter constructs that have been used in different studies might also contribute to controversial data. A more comprehensive study analyzing many different natural miRNA targets in different cell types will be needed to understand the controversial results reported thus far.

RISC and RNA Turnover

Ago proteins affect the stability of target RNAs by different mechanisms. In human RNAi, exogenous siRNAs guide RISC to highly complementary RNA molecules where Ago2 sequence specifically cleaves the target RNA. The cleavage reaction itself requires Mg^{2+} ions, is ATP independent, and leaves 5' phosphate as well as 3' hydroxyl groups (Martinez and Tuschl, 2004; Schwarz et al., 2004). Endogenous miRNAs are capable of guiding the same cleavage reaction and are therefore functionally not distinguishable from siRNAs (Hutvagner and Zamore, 2002). Indeed, the HoxB8 mRNA shows an extensive complementarity to miR-196 in mammals, and it has been experimentally demonstrated that RISC indeed cleaves the HoxB8 message during mouse development (Yekta et al., 2004). However, most cellular target mRNAs are not perfectly complementary to the miRNA, indicating that sequence-specific destruction of mRNAs is not the predominant function of miRNA-loaded Ago complexes. Indeed, it has been demonstrated in *Drosophila*, Zebrafish, and mammals that miRNAs, although not perfectly complementary to the target, can induce its destruction by recruiting deadenylating and decapping enzymes to the message (Behm-Ansmant et al., 2006; Giraldez et al., 2006; Mishima et al., 2006; Wu et al., 2006). Moreover, genome-wide analyses of siRNA effects in human cells have shown that, beside the complementary target RNA, a large portion of other mRNAs are affected by specific siRNAs, although they were not perfectly complementary (Jackson and Linsley, 2004). Consistently, studies on human miRNAs revealed that large portions of mRNAs are

destabilized independently of RISC (Lim et al., 2005). A complementarity of 10–14 nt between the target mRNA and the siRNA is sufficient for mRNA destabilization (Jackson and Linsley, 2004).

Because miRNAs function as guides, it is very likely that Ago proteins interact either directly or through adaptor proteins with specific factors of the deadenylation and decapping machinery. In *Drosophila*, Ago1 directly interacts with GW182, an RNA binding domain containing protein that recruits the CCR4:NOT complex to the mRNA (Behm-Ansmant et al., 2006). The CCR4:NOT complex is one of the two major deadenylase complexes in *Drosophila*, and it has been shown that miRNA target mRNAs are destabilized by deadenylation mediated by the CCR4:NOT complex. GW182 belongs to a conserved family of proteins that has three paralogs in mammals (Behm-Ansmant et al., 2006). The human members of this protein family are termed trinucleotide repeat containing (TNRC) 6A (GW182), 6B, and 6C. Experimental evidence indicates that both TNRC6A (GW182) and TNRC6B interact with members of the Ago subfamily (Table 2) and are functionally involved in miRNA function in mammalian cells (Jakymiw et al., 2005; Liu et al., 2005a; Meister et al., 2005). It is tempting to speculate that TNRC6A and/or B may recruit specific deadenylase complexes to miRNA target mRNAs by interacting with human Ago proteins similarly to *Drosophila*. Furthermore, it will be interesting to analyze if TNRC6C has a function in the miRNA pathway as well.

P Bodies, Stress Granules, and Ago Function

Localization studies using immunofluorescence approaches and tagged Ago proteins revealed that Ago proteins are enriched in distinct cytoplasmic foci (Figure 1). Colocalization studies with antibodies against diverse marker proteins such as Dcp1, LSM4, or GW182 identified Ago proteins as components of cytoplasmic P bodies (Liu et al., 2005b; Sen and Blau, 2005). Remarkably, P bodies are cellular sites where mRNA turnover occurs (for a comprehensive overview, see Eulalio et al. [2007]). mRNA decapping and degradation enzymes localize to P bodies to ensure rapid and efficient mRNA turnover. Therefore, it has been suggested that Ago proteins may identify target mRNAs by sequence complementarity to the bound miRNAs and target those mRNAs to P bodies where cleavage and degradation occur. In support of such a model, it was found that depletion of the P body components TNRC6A (GW182), TNRC6B, MOV-10, and Dcp1/2 inhibited miRNA-guided RISC activity (Jakymiw et al., 2005; Liu et al., 2005a; Meister et al., 2005; Rehwinkel et al., 2005). Consistently, Ago mutants that can no longer bind to miRNAs do not localize to P bodies, suggesting that Ago proteins have to be incorporated into higher-order structures such as mRNA protein complexes (mRNPs) via miRNA-mRNA interactions in order to localize to P bodies (Liu et al., 2005b). Because Ago complexes can stably associate with specific mRNAs without affecting their stability, a model in which Ago proteins target their

translationally repressed mRNA targets to P bodies, thereby separating them spatially from the translation machinery, has been suggested (Figure 2). Such a model is supported by findings in yeast, where a movement of mRNAs between polyribosomes and P bodies as well as localization of nontranslating mRNAs to P bodies has been observed (Bregues et al., 2005; Teixeira et al., 2005). A model of mRNA storage also implies that mRNAs can relocate to the cytoplasm and re-enter polyribosomes for translation. Indeed, the CAT-1 mRNA is repressed by the liver-specific miR-122 and stored in P bodies under normal conditions. Upon cellular stress, the translational block is released and the CAT-1 mRNA is actively translated to produce CAT-1 protein, which is required for the cellular stress response (Bhattacharyya et al., 2006). Therefore, at least for the very specific CAT-1 mRNA, the model of P body storage and release has been experimentally proven. Interestingly, the release of the CAT-1 mRNA from Ago repression involves the RNA binding protein HuR. Under normal conditions, HuR localizes to the nucleus. Upon cellular stress, HuR localizes to the cytoplasm, where it helps to release the CAT-1 mRNA from Ago repression. How such release mechanisms function is still unclear. Most likely, other mRNA binding proteins may contribute not only to Ago-mediated inhibition but also to possible mRNA release mechanisms. Whether such mechanisms apply to other mRNAs than the CAT-1 mRNA, however, remains unclear. At least one recent study revealed that disruption of P bodies by depletion of LSM1 had no effect on miRNA-guided translational inhibition of an artificial reporter construct (Chu and Rana, 2006).

Very recently, a more quantitative analysis has shown that Ago proteins localize not only to P bodies but also to the diffuse cytoplasm and stress granules (SGs) (Leung et al., 2006). EGFP tagging of Ago2 followed by three-dimensional measurements revealed that only about 1.3% of EGFP-Ago2 localizes to P bodies. After inhibition of translational initiation with hippuristanol, EGFP-Ago2 accumulated in SGs. Moreover, using photobleaching, it was demonstrated that the P body pool of Ago proteins seems to be static, whereas a more dynamic behavior has been observed for Ago proteins that localize to SGs. However, SGs form when cells experience different forms of stress such as heat shock or oxidative stress, and a physiological role for SGs under stress-free conditions has not been established yet. A possible explanation of the controversial data on SGs and P bodies could be that, under normal conditions, mRNAs that are required for stress response, like the CAT-1 mRNA, might be repressed by Ago proteins and stored in P bodies. Under stress conditions, however, such mRNAs could be released and translated, whereas many other Ago containing mRNPs accumulate in SGs during stress response (Figure 2). A detailed analysis of the localization and translational repression of other miRNA targets will clearly help to better understand the contribution of P body and SG localization to Ago function.

Table 2. Proteins Associated with Human or Mouse Argonaute Proteins

Associated Protein	Domains/Motifs	Function in Gene Silencing	Cellular Localization	Reference(s)
hsAgo1				
Dicer	DExH box, PAZ, RNase III, dsRBD	Small RNA processing	Cytoplasm	Meister et al., 2005
TNRC6B	RRM, GW repeats	miRNA-guided cleavage	Cytoplasm, P bodies	Meister et al., 2005
DCP1a	–	Not investigated	Cytoplasm, P bodies	Liu et al., 2005b
DCP2	Nudix	Not investigated	Cytoplasm, P bodies	Liu et al., 2005b
MOV10	DExH box	miRNA-guided cleavage	Cytoplasm, P bodies	Meister et al., 2005
PRMT5	Methyl-transferase	Not investigated	Cytoplasm, nucleus	Meister et al., 2005
hsAgo2				
Dicer	DExH box, PAZ, RNase III, dsRBD	Small RNA processing	Cytoplasm	Gregory et al., 2005; Meister et al., 2005
TNRC6A/ GW182	RRM, GW repeats	miRNA-guided cleavage, translational repression	Cytoplasm, P bodies	Jakymiw et al., 2005; Liu et al., 2005a
TNRC6B	RRM, GW repeats	miRNA-guided cleavage	Cytoplasm, P bodies	Meister et al., 2005
DCP1a	–	Not investigated	Cytoplasm, P bodies	Liu et al., 2005b
DCP2	Nudix	Not investigated	Cytoplasm, P bodies	Liu et al., 2005b
TTP	Zn-finger	AU-rich mRNA destabilization	Cytoplasm	Jing et al., 2005
MOV10	DExH box	miRNA-guided cleavage	Cytoplasm, P bodies	Meister et al., 2005
PRMT5	Methyl-transferase	Not investigated	Cytoplasm, nucleus	Meister et al., 2005
eIF4E	–	Not investigated	Nucleus, cytoplasm, P bodies	Chu and Rana, 2006
Rck/p54	DEAD box	Translational repression	Cytoplasm, P bodies	Chu and Rana, 2006
Gemin3	DEAD box	miRNA-guided cleavage	Nucleus, cytoplasm	Mourelatos et al., 2002
Gemin4	–	Not investigated	Nucleus, cytoplasm	Mourelatos et al., 2002
PACT	dsRBD	Small RNA processing, RISC activity	Cytoplasm	Lee et al., 2006
FMRp	KH domain, RGG box	Not investigated	Nucleus, cytoplasm	Jin et al., 2004
FXR1	KH domain, RGG box	Not investigated	Nucleus, cytoplasm	Jin et al., 2004
FXR2	KH domain, RGG box	Not investigated	Nucleus, cytoplasm	Jin et al., 2004
hsAgo3				
Dicer	DExH box, PAZ, RNase III, dsRBD	Small RNA processing	Cytoplasm	Meister et al., 2005
hsAgo4				
Dicer	DExH box, PAZ, RNase III, dsRBD	Small RNA processing	Cytoplasm	Meister et al., 2005
TTP	Zn-finger	AU-rich mRNA destabilization	Cytoplasm	Jing et al., 2005
MIWI				
Dicer	DExH box, PAZ, RNase III, dsRBD	Small RNA processing	Cytoplasm	Kotaja et al., 2006a

Table 2. Continued

Associated Protein	Domains/Motifs	Function in Gene Silencing	Cellular Localization	Reference(s)
KIF17b	Kinesin motor	Not investigated	Cytoplasm, chromatoid body	Kotaja et al., 2006b
MVH	DEAD box	Not investigated	Cytoplasm, chromatoid body	Kuramochi-Miyagawa et al., 2004
MAEL	HMG box	Not investigated	Cytoplasm, chromatoid body, XY-body, nucleus	Costa et al., 2006
MILI				
MAEL	HMG box	Not investigated	Cytoplasm, chromatoid body, XY-body, nucleus	Costa et al., 2006

Mammalian Ago Proteins in the Nucleus—Transcriptional Silencing?

It is well established that the predominant function of the sole *S. pombe* Ago protein is to guide transcriptional gene silencing processes by recruiting methyltransferases to heterochromatic regions of the genome (for a detailed overview, see Lippman and Martienssen [2004] and Matzke and Birchler [2005]). Until now, nuclear functions for Ago proteins have been reported in a variety of different organisms, including plants, fungi, *Drosophila*, and *C. elegans* (reviewed in Matzke and Birchler [2005]). A nuclear function of mammalian Ago proteins in somatic cells, however, is still a matter of debate. Initial biochemical fractionations separating nuclear from cytoplasmic extracts demonstrated that Ago proteins as well as mature miRNAs could be found both in cytoplasmic and nuclear fractions (Meister et al., 2004; Robb et al., 2005). However, it was not excluded that Ago proteins associated with the outer nuclear envelope and therefore contaminated the nuclear fractions. In further studies, it has been shown that siRNAs against the nuclear RNAs 7SK and the U6 snRNA are functional, suggesting that Ago2, the cleavage-competent Ago protein in mammals, is present in the nucleus as well (Robb et al., 2005). More recent approaches showed that siRNAs directed against the promoter of a GFP reporter construct repress GFP expression by transcriptional gene silencing (Kim et al., 2006; Morris et al., 2004). Knockdown of human Ago1 suppressed the observed gene silencing effect, indicating that Ago proteins are involved in this process. Moreover, siRNAs against the transcription start sites of endogenous genes such as huntingtin or the progesterone receptor (PG) inhibited transcription as well (Janowski et al., 2006). In this study, no transcriptional silencing was observed when either human Ago1 or Ago2 was depleted. Additionally, chromatin immunoprecipitations revealed that both Ago proteins associate with the PG promoter, suggesting that Ago1 and Ago2 are involved not only in posttranscriptional gene silencing but also in transcriptional gene silencing.

Although it is becoming more and more apparent that Ago proteins also function in the nucleus, immunofluorescence approaches using antibodies against tagged ver-

sions of Ago proteins show only a cytoplasmic Ago localization. Possible explanations for this discrepancy could be that only a minor portion of Ago proteins localize to the nucleus and are not detected by classical immunofluorescence experiments. Furthermore, the nuclear localization of Ago proteins could be transient or highly dynamic, and under steady-state conditions, most Ago protein is detected in the cytoplasm. It is also reasonable that Ago proteins act on chromatin structures specifically during the cell cycle after nuclear envelope breakdown and could therefore not be detected in the nucleus of interphase cells. Finally, nuclear Ago proteins could be incorporated into large protein complexes and are presumably not accessible for antibodies. Further studies such as the identification of specific nuclear interactors will be required to elucidate the nuclear function of human Ago proteins.

The Piwi Subfamily and piRNAs

The human Piwi subfamily of Argonaute proteins is composed of HIWI, HIWI2 (also termed piwi-like2 or piwil2), HIWI3 (piwil3), and HILI (piwil). In mouse, only MIWI, MIWI2, and MILI exist. The Piwi subfamily was originally named after the *Drosophila* piwi gene and has been implicated in germ cell development, stem cell self-renewal, and retrotransposon silencing (Cox et al., 2000; Kalmykova et al., 2005). Based on primary sequence, different members of the Piwi subfamily have been identified in various organisms. Moreover, many of these proteins are germ cell specific, suggesting a phylogenetically conserved function in the germline. Interestingly, gene inactivation approaches in mouse revealed that MILI as well as MIWI is essential for spermatogenesis (Deng and Lin, 2002; Kuramochi-Miyagawa et al., 2004). Female *mili*^{-/-} mice are fertile with no abnormalities in the ovaries, whereas male *mili*^{-/-} mice are sterile with smaller testes. In MILI null mice, sterility is due to meiosis defects leading to an arrest in spermatogenesis from zygotene to pachytene stages (Figure 3). Similarly to MILI null mice, *miwi*^{-/-} mice are female fertile and male sterile as well. However, in *miwi*^{-/-} mice, defects are manifested at later stages of spermatogenesis, presumably after the formation of

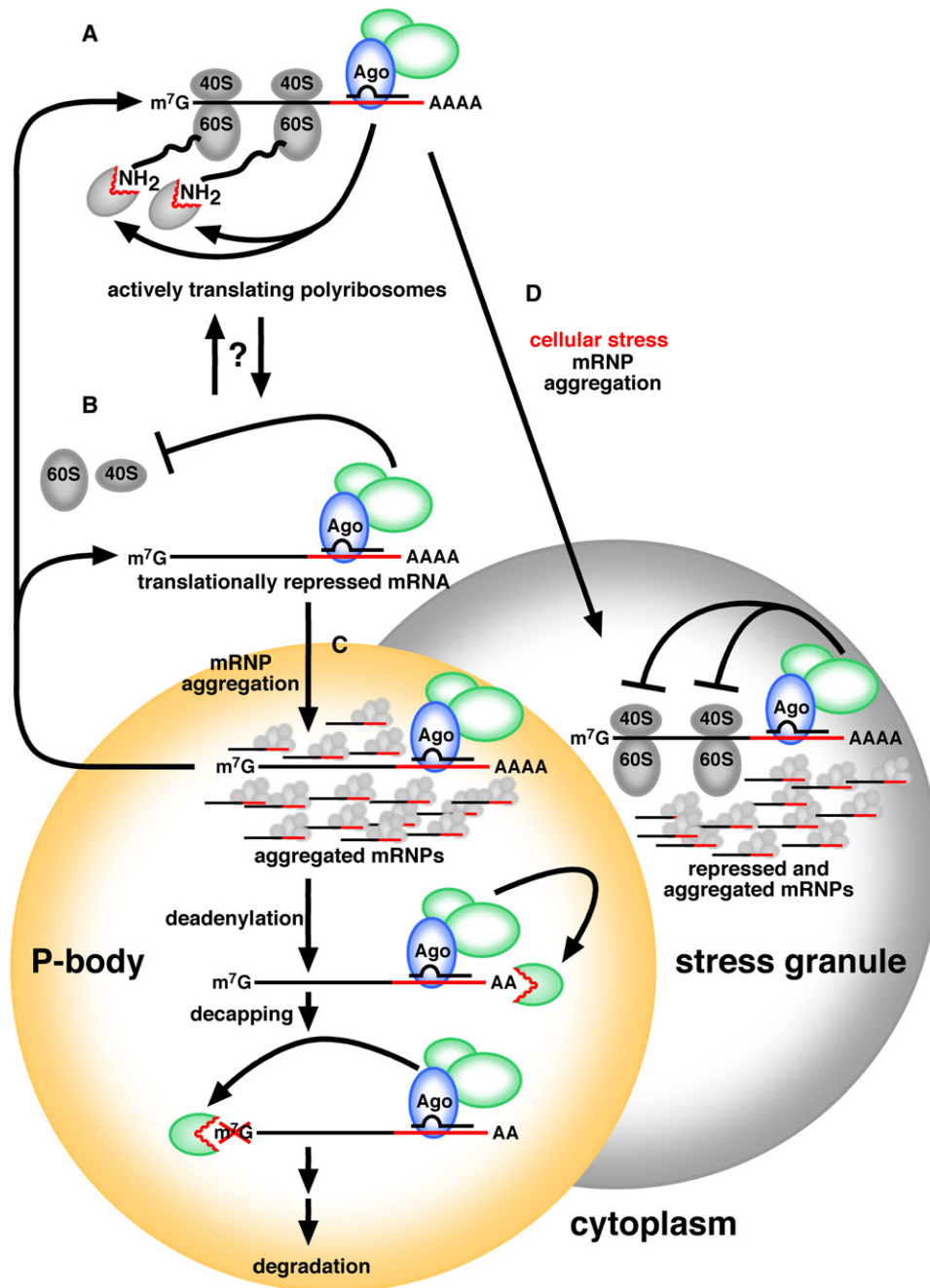


Figure 2. A Model for Ago-Mediated Translational Repression and RNA Turnover

Ago proteins repress translation either on the level of actively translating polyribosomes (A) or initiation of translation (B). Repressed Ago containing mRNPs aggregate to P bodies where repressed mRNAs can either be stored or degraded involving deadenylation and decapping enzymes (C). Upon cellular stress, actively translating polyribosomes aggregate and form stress granules. Ago proteins may repress the translation of mRNAs that are not needed for an efficient stress response (D). For further details, see text. m⁷G, m⁷G-cap; AAA, polyA-tail; NH₂, N terminus of nascent polypeptides; and 40S and 60S, ribosomal subunits.

spermatids (Figure 3) (Deng and Lin, 2002). Not much is known about the function of MIWI2 and HIWI3 so far. Gene targeting approaches as well as biochemical experiments using testes extracts will be needed to find out if MIWI2 and HIWI3 are involved in spermatogenesis as well.

In *Drosophila*, germ cells are characterized by a cytoplasmic structure containing dense material, which is called nuage and contains the Argonaute proteins PIWI and Aubergine (Aub). A similar structure has been identified in mammalian germ cells and termed the chromatoid

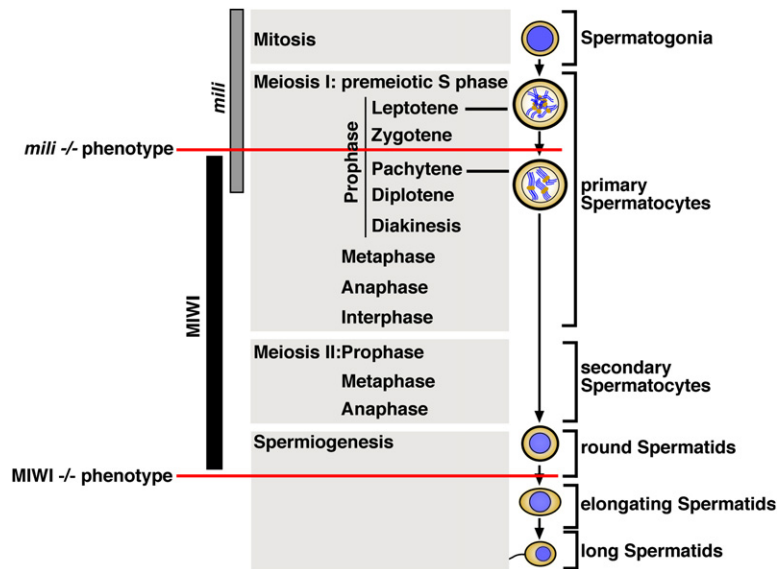


Figure 3. Function of Mammalian Argonaute Proteins in Spermatogenesis

The stages of spermatogenesis and the developmental stages of the corresponding cell types are displayed in the middle and right panels. The expression of MILI and MIWI during spermatogenesis is shown on the left side. MILI associates with 26–28 nt piRNAs and is expressed until the pachytene stage in meiosis I. Correspondingly, *mili*^{-/-} spermatocytes are arrested between the zygotene and pachytene stages in the early prophase of meiosis I. The expression of MIWI, which associates with 29–31 nt piRNAs, is detectable from the pachytene stage in meiosis I until round spermatids are formed in early spermiogenesis. *MIWI*^{-/-} spermatocytes are arrested at the stage of round spermatids, coinciding with the final phase of MIWI expression.

body (reviewed in Kotaja and Sassone-Corsi [2007]). Interestingly, chromatoid bodies contain P body components such as Argonaute proteins both from the Ago and the Piwi subfamily, Dcp1a or GW182, miRNAs, and polyadenylated mRNAs. Therefore, chromatoid bodies might be the male germ cell counterparts of somatic P bodies and may have similar functions in gene silencing (Kotaja et al., 2006a).

Very recently, a novel class of small RNAs has been identified that specifically interacts with members of the Piwi subfamily. Therefore, these small RNAs have been termed piRNAs (Aravin et al., 2006; Girard et al., 2006; Grivna et al., 2006; Watanabe et al., 2006). Immunoprecipitations from mouse testes using antibodies directed against MIWI or MILI identified MIWI-associated piRNAs of 29–31 nt and MILI-associated piRNAs of 26–28 nt in length. Both HILI- and HIWI-associated piRNAs derive from genomic clusters. Although many piRNAs are not conserved from mouse to human on the sequence level, piRNA clusters are embedded into syntenic genomic regions. Consistently with the MILI and MIWI protein function, the MILI-associated piRNAs accumulate at the onset of meiosis in male germ cells, whereas the MIWI-associated piRNAs seem to have functions at later stages of spermatogenesis (Figure 3).

Interestingly, cloning studies from mouse oocytes found a class of 20–24 nt long RNAs, which are derived from retroelements such as LINE, SINE, and LTR retrotransposons (Watanabe et al., 2006). Furthermore, injection of a reporter construct containing a perfectly complementary binding site for such a small RNA into oocytes led to the inactivation of the reporter, suggesting that retroelements are suppressed by an RNAi-like mechanism in mouse oocytes. However, it remains unclear if the mRNA of the reporter construct is cleaved sequence specifically, because neither cleavage products nor an asso-

ciation of the identified small RNAs with Argonaute proteins has been analyzed.

Although the analysis of the mammalian members of the Piwi subfamily is at a very early stage, far more is known about the function of this subfamily in *Drosophila*. PIWI is required both for posttranscriptional and transcriptional gene silencing (TGS) phenomena in flies (Pal-Bhadra et al., 2002). Moreover, it has been shown that PIWI is required for transcriptional silencing of selfish genetic elements such as retrotransposons in the male germline (Aravin et al., 2004; Kalmykova et al., 2005). An interesting hint of how Piwi subfamily proteins function in TGS came from mutant flies that lack functional PIWI or Aub, two Piwi subfamily proteins that are enriched in germ cells. As a consequence of loss-of-function mutations in the *piwi* and *aubergine* genes, H3/K9 methylation, a hallmark of heterochromatin, was strongly reduced. Consistently, the heterochromatin proteins HP1 and HP2 were delocalized from heterochromatic regions and therefore transcriptional silencing was suppressed (Pal-Bhadra et al., 2004). Interestingly, both PIWI and Aub bind to rasiRNAs, which constitute a class of small RNAs that derive from repetitive genetic elements (Aravin et al., 2003; Vagin et al., 2006). The most intriguing finding, however, was that rasiRNAs are most likely not generated by Dicer and therefore constitute a third gene silencing pathway in *Drosophila* (Vagin et al., 2006).

The findings in *Drosophila* may also help to elucidate the function of mammalian Piwi proteins and even piRNAs. It is tempting to speculate that members of the mammalian Piwi subfamily may function similarly to their *Drosophila* homologs and guide the formation of silenced heterochromatin. The analysis of HP1 localization in mammalian cells that lack functional proteins of the Piwi subfamily will clearly help to address this speculation. It is also reasonable that piRNAs or other classes of small RNAs protect

the mammalian germline from mobile genetic elements as shown for some *Drosophila* Piwi subfamily members. However, only a minor portion of mammalian piRNAs is derived from repetitive elements, suggesting that piRNAs may have different, probably mammalian-specific functions as well.

The small RNA content of male and female germ cells is clearly different, leading to the very interesting question of why the two genders need the action of different classes of small RNAs for germ cell development. Further biochemical and genetic analyses such as genetic inactivation of piRNA clusters in the mouse genome are needed to elucidate the detailed molecular functions of piRNAs and associated Argonaute proteins of the Piwi subfamily during spermatogenesis and germ cell development.

Concluding Remarks

Although the mammalian Argonaute protein family was identified only a few years ago, some of their cellular functions, such as the Slicer function of mammalian Ago2, are well understood. Nevertheless, many questions about Argonaute proteins are still not answered and will clearly be subject of extensive research in the future. Why is only human Ago2 a Slicer endonuclease even though the catalytic residues are conserved in other Ago proteins? What is the contribution of posttranslational modifications such as phosphorylation to the activity of Argonaute proteins? What are the cellular interaction partners of Argonaute proteins, and how do they contribute to their function? Other very important questions that still remain mysterious are what mRNAs are regulated by Ago-containing miRNPs and what are the biological consequences of such regulatory events. Although several very promising and conclusive bioinformatics approaches that predict mammalian miRNA targets have been published (Krek et al., 2005; Lewis et al., 2003; Stark et al., 2003), clear biochemical strategies that aim for a detailed characterization of miRNP-mRNA interactions are still lacking. Ago proteins are most likely embedded into large regulatory networks that have to be analyzed systematically. Such networks are most likely unique to each individual mRNA, and other specific mRNA binding proteins may contribute to Ago protein function. Only a detailed and systematic analysis of such networks will provide an understanding of the Ago proteins in particular and posttranscriptional gene silencing in general.

Ago proteins have also been associated with different diseases. It has been shown that Ago proteins as well as miRNAs interact with FMRp, the disease gene product affected in the inherited fragile X syndrome (Jin et al., 2004). Members of the Piwi subfamily have been reported to be misexpressed in some specific forms of cancer, and many other forms have not been analyzed yet (Taubert et al., 2007). Finally, in some forms of autoimmune diseases, autoantibodies against Ago proteins have been found, indicating a possible role of Ago proteins in such diseases (Jakymiw et al., 2006). A detailed investigation of the function of all mammalian Ago proteins will therefore

also provide a better understanding of the molecular basis of many different diseases.

ACKNOWLEDGMENTS

We thank C. Ender and S. Rüdél for critically reading the manuscript and S. Jentsch for support. We apologize to those whose work was not cited due to space constraints. Our research is supported by the Max-Planck-Society, the Deutsche Forschungsgemeinschaft (DFG Me 2064/2-1), the European Union (LSHG-CT-2005-037900), and the Deutsche Krebshilfe. L.P. receives a fellowship from the Boehringer Ingelheim Fonds (BIF).

REFERENCES

- Ambros, V. (2004). The functions of animal microRNAs. *Nature* 431, 350–355.
- Aravin, A.A., Lagos-Quintana, M., Yalcin, A., Zavolan, M., Marks, D., Snyder, B., Gaasterland, T., Meyer, J., and Tuschl, T. (2003). The small RNA profile during *Drosophila melanogaster* development. *Dev. Cell* 5, 337–350.
- Aravin, A.A., Klenov, M.S., Vagin, V.V., Bantignies, F., Cavalli, G., and Gvozdev, V.A. (2004). Dissection of a natural RNA silencing process in the *Drosophila melanogaster* germ line. *Mol. Cell. Biol.* 24, 6742–6750.
- Aravin, A., Gaidatzis, D., Pfeffer, S., Lagos-Quintana, M., Landgraf, P., Iovino, N., Morris, P., Brownstein, M.J., Kuramochi-Miyagawa, S., Nakano, T., et al. (2006). A novel class of small RNAs bind to MILI protein in mouse testes. *Nature* 442, 203–207.
- Bagga, S., Bracht, J., Hunter, S., Massirer, K., Holtz, J., Eachus, R., and Pasquinelli, A.E. (2005). Regulation by let-7 and lin-4 miRNAs results in target mRNA degradation. *Cell* 122, 553–563.
- Behm-Ansmant, I., Rehwinkel, J., Doerks, T., Stark, A., Bork, P., and Izaurralde, E. (2006). mRNA degradation by miRNAs and GW182 requires both CCR4:NOT deadenylase and DCP1:DCP2 decapping complexes. *Genes Dev.* 20, 1885–1898.
- Bhattacharyya, S.N., Habermacher, R., Martine, U., Closs, E.I., and Filipowicz, W. (2006). Relief of microRNA-mediated translational repression in human cells subjected to stress. *Cell* 125, 1111–1124.
- Bohmert, K., Camus, I., Bellini, C., Bouchez, D., Caboche, M., and Benning, C. (1998). AGO1 defines a novel locus of *Arabidopsis* controlling leaf development. *EMBO J.* 17, 170–180.
- Borchert, G.M., Lanier, W., and Davidson, B.L. (2006). RNA polymerase III transcribes human microRNAs. *Nat. Struct. Mol. Biol.* 13, 1097–1101.
- Bregues, M., Teixeira, D., and Parker, R. (2005). Movement of eukaryotic mRNAs between polysomes and cytoplasmic processing bodies. *Science* 310, 486–489.
- Carmell, M.A., Xuan, Z., Zhang, M.Q., and Hannon, G.J. (2002). The Argonaute family: tentacles that reach into RNAi, developmental control, stem cell maintenance, and tumorigenesis. *Genes Dev.* 16, 2733–2742.
- Cerutti, L., Mian, N., and Bateman, A. (2000). Domains in gene silencing and cell differentiation proteins: the novel PAZ domain and redefinition of the piwi domain. *Trends Biochem. Sci.* 25, 481–482.
- Chendrimada, T.P., Gregory, R.I., Kumaraswamy, E., Norman, J., Cooch, N., Nishikura, K., and Shiekhattar, R. (2005). TRBP recruits the Dicer complex to Ago2 for microRNA processing and gene silencing. *Nature* 436, 740–744.
- Chu, C.Y., and Rana, T.M. (2006). Translation repression in human cells by microRNA-induced gene silencing requires RCK/p54. *PLoS Biol.* 4, e210. 10.1371/journal.pbio.0040210.
- Costa, Y., Speed, R.M., Gautier, P., Semple, C.A., Maratou, K., Turner, J.M., and Cooke, H.J. (2006). Mouse MAELSTROM: the link between

meiotic silencing of unsynapsed chromatin and microRNA pathway? *Hum. Mol. Genet.* 15, 2324–2334.

Cox, D.N., Chao, A., and Lin, H. (2000). *piwi* encodes a nucleoplasmic factor whose activity modulates the number and division rate of germline stem cells. *Development* 127, 503–514.

Deng, W., and Lin, H. (2002). *miwi*, a murine homolog of *piwi*, encodes a cytoplasmic protein essential for spermatogenesis. *Dev. Cell* 2, 819–830.

Eulalio, A., Behm-Ansmant, I., and Izaurralde, E. (2007). P bodies: at the crossroads of post-transcriptional pathways. *Nat. Rev. Mol. Cell Biol.* 8, 9–22.

Giraldez, A.J., Mishima, Y., Rihel, J., Grocock, R.J., Van Dongen, S., Inoue, K., Enright, A.J., and Schier, A.F. (2006). Zebrafish MiR-430 promotes deadenylation and clearance of maternal mRNAs. *Science* 312, 75–79.

Girard, A., Sachidanandam, R., Hannon, G.J., and Carmell, M.A. (2006). A germline-specific class of small RNAs binds mammalian Piwi proteins. *Nature* 442, 199–202.

Gregory, R.I., Chendrimada, T.P., Cooch, N., and Shiekhattar, R. (2005). Human RISC couples microRNA biogenesis and posttranscriptional gene silencing. *Cell* 123, 631–640.

Grivna, S.T., Beyret, E., Wang, Z., and Lin, H. (2006). A novel class of small RNAs in mouse spermatogenic cells. *Genes Dev.* 20, 1709–1714.

Haase, A.D., Jaskiewicz, L., Zhang, H., Laine, S., Sack, R., Gatignol, A., and Filipowicz, W. (2005). TRBP, a regulator of cellular PKR and HIV-1 virus expression, interacts with Dicer and functions in RNA silencing. *EMBO Rep.* 6, 961–967.

Hammond, S.M., Bernstein, E., Beach, D., and Hannon, G.J. (2000). An RNA-directed nuclease mediates post-transcriptional gene silencing in *Drosophila* cells. *Nature* 404, 293–296.

Humphreys, D.T., Westman, B.J., Martin, D.I., and Preiss, T. (2005). MicroRNAs control translation initiation by inhibiting eukaryotic initiation factor 4E/cap and poly(A) tail function. *Proc. Natl. Acad. Sci. USA* 102, 16961–16966.

Hutvagner, G., and Zamore, P.D. (2002). A microRNA in a multiprotein turnover RNAi enzyme complex. *Science* 297, 2056–2060.

Jackson, A.L., and Linsley, P.S. (2004). Noise amidst the silence: off-target effects of siRNAs? *Trends Genet.* 20, 521–524.

Jakymiw, A., Lian, S., Eystathiou, T., Li, S., Satoh, M., Hamel, J.C., Fritzier, M.J., and Chan, E.K. (2005). Disruption of GW bodies impairs mammalian RNA interference. *Nat. Cell Biol.* 7, 1267–1274.

Jakymiw, A., Ikeda, K., Fritzier, M.J., Reeves, W.H., Satoh, M., and Chan, E.K. (2006). Autoimmune targeting of key components of RNA interference. *Arthritis Res. Ther.* 8, R87.

Janowski, B.A., Huffman, K.E., Schwartz, J.C., Ram, R., Nordsell, R., Shames, D.S., Minna, J.D., and Corey, D.R. (2006). Involvement of AGO1 and AGO2 in mammalian transcriptional silencing. *Nat. Struct. Mol. Biol.* 13, 787–792.

Jin, P., Zarnescu, D.C., Ceman, S., Nakamoto, M., Mowrey, J., Jongens, T.A., Nelson, D.L., Moses, K., and Warren, S.T. (2004). Biochemical and genetic interaction between the fragile X mental retardation protein and the microRNA pathway. *Nat. Neurosci.* 7, 113–117.

Jing, Q., Huang, S., Guth, S., Zarubin, T., Motoyama, A., Chen, J., Di Padova, F., Lin, S.C., Gram, H., and Han, J. (2005). Involvement of microRNA in AU-rich element-mediated mRNA instability. *Cell* 120, 623–634.

Kalmykova, A.I., Klenov, M.S., and Gvozdev, V.A. (2005). Argonaute protein PIWI controls mobilization of retrotransposons in the *Drosophila* male germline. *Nucleic Acids Res.* 33, 2052–2059.

Khvorova, A., Reynolds, A., and Jayasena, S.D. (2003). Functional siRNAs and miRNAs exhibit strand bias. *Cell* 115, 209–216.

Kim, D.H., Villeneuve, L.M., Morris, K.V., and Rossi, J.J. (2006). Argonaute-1 directs siRNA-mediated transcriptional gene silencing in human cells. *Nat. Struct. Mol. Biol.* 13, 793–797.

Kotaja, N., and Sassone-Corsi, P. (2007). The chromatoid body: a germ-cell-specific RNA-processing centre. *Nat. Rev. Mol. Cell Biol.* 8, 85–90.

Kotaja, N., Bhattacharyya, S.N., Jaskiewicz, L., Kimmins, S., Parvinen, M., Filipowicz, W., and Sassone-Corsi, P. (2006a). The chromatoid body of male germ cells: similarity with processing bodies and presence of Dicer and microRNA pathway components. *Proc. Natl. Acad. Sci. USA* 103, 2647–2652.

Kotaja, N., Lin, H., Parvinen, M., and Sassone-Corsi, P. (2006b). Interplay of PIWI/Argonaute protein MIWI and kinesin KIF17b in chromatoid bodies of male germ cells. *J. Cell Sci.* 119, 2819–2825.

Krek, A., Grun, D., Poy, M.N., Wolf, R., Rosenberg, L., Epstein, E.J., MacMenamin, P., da Piedade, I., Gunsalus, K.C., Stoffel, M., and Rajewsky, N. (2005). Combinatorial microRNA target predictions. *Nat. Genet.* 37, 495–500.

Kuramochi-Miyagawa, S., Kimura, T., Ijiri, T.W., Isobe, T., Asada, N., Fujita, Y., Ikawa, M., Iwai, N., Okabe, M., Deng, W., et al. (2004). Mili, a mammalian member of piwi family gene, is essential for spermatogenesis. *Development* 131, 839–849.

Lau, N.C., Seto, A.G., Kim, J., Kuramochi-Miyagawa, S., Nakano, T., Bartel, D.P., and Kingston, R.E. (2006). Characterization of the piRNA complex from rat testes. *Science* 313, 363–367.

Lee, R.C., Feinbaum, R.L., and Ambros, V. (1993). The *C. elegans* heterochronic gene *lin-4* encodes small RNAs with antisense complementarity to *lin-14*. *Cell* 75, 843–854.

Lee, Y., Kim, M., Han, J., Yeom, K.H., Lee, S., Baek, S.H., and Kim, V.N. (2004). MicroRNA genes are transcribed by RNA polymerase II. *EMBO J.* 23, 4051–4060.

Lee, Y., Hur, I., Park, S.Y., Kim, Y.K., Suh, M.R., and Kim, V.N. (2006). The role of PACT in the RNA silencing pathway. *EMBO J.* 25, 522–532.

Leung, A.K., Calabrese, J.M., and Sharp, P.A. (2006). Quantitative analysis of Argonaute protein reveals microRNA-dependent localization to stress granules. *Proc. Natl. Acad. Sci. USA* 103, 18125–18130.

Lewis, B.P., Shih, I., Jones-Rhoades, M.W., Bartel, D.P., and Burge, C.B. (2003). Prediction of mammalian microRNA targets. *Cell* 115, 787–798.

Lim, L.P., Lau, N.C., Garrett-Engele, P., Grimson, A., Schelter, J.M., Castle, J., Bartel, D.P., Linsley, P.S., and Johnson, J.M. (2005). Microarray analysis shows that some microRNAs downregulate large numbers of target mRNAs. *Nature* 433, 769–773.

Lippman, Z., and Martienssen, R. (2004). The role of RNA interference in heterochromatic silencing. *Nature* 431, 364–370.

Liu, J., Carmell, M.A., Rivas, F.V., Marsden, C.G., Thomson, J.M., Song, J.J., Hammond, S.M., Joshua-Tor, L., and Hannon, G.J. (2004). Argonaute2 is the catalytic engine of mammalian RNAi. *Science* 305, 1437–1441.

Liu, J., Rivas, F.V., Wohlschlegel, J., Yates, J.R., 3rd, Parker, R., and Hannon, G.J. (2005a). A role for the P-body component GW182 in microRNA function. *Nat. Cell Biol.* 7, 1161–1166.

Liu, J., Valencia-Sanchez, M.A., Hannon, G.J., and Parker, R. (2005b). MicroRNA-dependent localization of targeted mRNAs to mammalian P-bodies. *Nat. Cell Biol.* 7, 719–723.

Maroney, P.A., Yu, Y., Fisher, J., and Nilsen, T.W. (2006). Evidence that microRNAs are associated with translating messenger RNAs in human cells. *Nat. Struct. Mol. Biol.* 13, 1102–1107.

Martinez, J., and Tuschl, T. (2004). RISC is a 5' phosphomonoester-producing RNA endonuclease. *Genes Dev.* 18, 975–980.

- Martinez, J., Patkaniowska, A., Urlaub, H., Lührmann, R., and Tuschl, T. (2002). Single-stranded antisense siRNAs guide target RNA cleavage in RNAi. *Cell* **110**, 563–574.
- Matranga, C., Tomari, Y., Shin, C., Bartel, D.P., and Zamore, P.D. (2005). Passenger-strand cleavage facilitates assembly of siRNA into Ago2-containing RNAi enzyme complexes. *Cell* **123**, 607–620.
- Matzke, M.A., and Birchler, J.A. (2005). RNAi-mediated pathways in the nucleus. *Nat. Rev. Genet.* **6**, 24–35.
- Meister, G., and Tuschl, T. (2004). Mechanisms of gene silencing by double-stranded RNA. *Nature* **431**, 343–349.
- Meister, G., Landthaler, M., Patkaniowska, A., Dorsett, Y., Teng, G., and Tuschl, T. (2004). Human Argonaute2 mediates RNA cleavage targeted by miRNAs and siRNAs. *Mol. Cell* **15**, 185–197.
- Meister, G., Landthaler, M., Peters, L., Chen, P.Y., Urlaub, H., Lührmann, R., and Tuschl, T. (2005). Identification of novel argonaute-associated proteins. *Curr. Biol.* **15**, 2149–2155.
- Mishima, Y., Giraldez, A.J., Takeda, Y., Fujiwara, T., Sakamoto, H., Schier, A.F., and Inoue, K. (2006). Differential regulation of germline mRNAs in soma and germ cells by zebrafish miR-430. *Curr. Biol.* **16**, 2135–2142.
- Miyoshi, K., Tsukumo, H., Nagami, T., Siomi, H., and Siomi, M.C. (2005). Slicer function of *Drosophila* Argonautes and its involvement in RISC formation. *Genes Dev.* **19**, 2837–2848.
- Morris, K.V., Chan, S.W., Jacobsen, S.E., and Looney, D.J. (2004). Small interfering RNA-induced transcriptional gene silencing in human cells. *Science* **305**, 1289–1292.
- Mourelatos, Z., Dostie, J., Paushkin, S., Sharma, A., Charroux, B., Abel, L., Rappsilber, J., Mann, M., and Dreyfuss, G. (2002). miRNPs: a novel class of ribonucleoproteins containing numerous microRNAs. *Genes Dev.* **16**, 720–728.
- Nottrott, S., Simard, M.J., and Richter, J.D. (2006). Human let-7a miRNA blocks protein production on actively translating polyribosomes. *Nat. Struct. Mol. Biol.* **13**, 1108–1114.
- O'Donnell, K.A., Wentzel, E.A., Zeller, K.I., Dang, C.V., and Mendell, J.T. (2005). c-Myc-regulated microRNAs modulate E2F1 expression. *Nature* **435**, 839–843.
- Olsen, P.H., and Ambros, V. (1999). The lin-4 regulatory RNA controls developmental timing in *Caenorhabditis elegans* by blocking LIN-14 protein synthesis after the initiation of translation. *Dev. Biol.* **216**, 671–680.
- Pal-Bhadra, M., Bhadra, U., and Birchler, J.A. (2002). RNAi related mechanism affect both transcriptional and posttranscriptional transgene silencing in *Drosophila*. *Mol. Cell* **9**, 315–327.
- Pal-Bhadra, M., Leibovitch, B.A., Gandhi, S.G., Rao, M., Bhadra, U., Birchler, J.A., and Elgin, S.C. (2004). Heterochromatic silencing and HP1 localization in *Drosophila* are dependent on the RNAi machinery. *Science* **303**, 669–672.
- Parker, J.S., and Barford, D. (2006). Argonaute: a scaffold for the function of short regulatory RNAs. *Trends Biochem. Sci.* **31**, 622–630.
- Parker, J.S., Roe, S.M., and Barford, D. (2005). Structural insights into mRNA recognition from a PIWI domain-siRNA guide complex. *Nature* **434**, 663–666.
- Petersen, C.P., Bordeleau, M.E., Pelletier, J., and Sharp, P.A. (2006). Short RNAs repress translation after initiation in mammalian cells. *Mol. Cell* **21**, 533–542.
- Pillai, R.S., Artus, C.G., and Filipowicz, W. (2004). Tethering of human Ago proteins to mRNA mimics the miRNA-mediated repression of protein synthesis. *RNA* **10**, 1518–1525.
- Pillai, R.S., Bhattacharyya, S.N., Artus, C.G., Zoller, T., Cougot, N., Basyuk, E., Bertrand, E., and Filipowicz, W. (2005). Inhibition of translational initiation by Let-7 MicroRNA in human cells. *Science* **309**, 1573–1576.
- Poy, M.N., Eliasson, L., Krutzfeldt, J., Kuwajima, S., Ma, X., Macdonald, P.E., Pfeffer, S., Tuschl, T., Rajewsky, N., Rorsman, P., and Stoffel, M. (2004). A pancreatic islet-specific microRNA regulates insulin secretion. *Nature* **432**, 226–230.
- Rand, T.A., Petersen, S., Du, F., and Wang, X. (2005). Argonaute2 cleaves the anti-guide strand of siRNA during RISC activation. *Cell* **123**, 621–629.
- Rehwinkel, J., Behm-Ansmant, I., Gatfield, D., and Izaurralde, E. (2005). A crucial role for GW182 and the DCP1:DCP2 decapping complex in miRNA-mediated gene silencing. *RNA* **11**, 1640–1647.
- Rivas, F.V., Tolia, N.H., Song, J.J., Aragon, J.P., Liu, J., Hannon, G.J., and Joshua-Tor, L. (2005). Purified Argonaute2 and an siRNA form recombinant human RISC. *Nat. Struct. Mol. Biol.* **12**, 340–349.
- Robb, G.B., Brown, K.M., Khurana, J., and Rana, T.M. (2005). Specific and potent RNAi in the nucleus of human cells. *Nat. Struct. Mol. Biol.* **12**, 133–137.
- Saito, K., Nishida, K.M., Mori, T., Kawamura, Y., Miyoshi, K., Nagami, T., Siomi, H., and Siomi, M.C. (2006). Specific association of Piwi with rasiRNAs derived from retrotransposon and heterochromatic regions in the *Drosophila* genome. *Genes Dev.* **20**, 2214–2222.
- Sasaki, T., Shiohama, A., Minoshima, S., and Shimizu, N. (2003). Identification of eight members of the Argonaute family in the human genome. *Genomics* **82**, 323–330.
- Schwarz, D.S., Hutvagner, G., Du, T., Xu, Z., Aronin, N., and Zamore, P.D. (2003). Asymmetry in the assembly of the RNAi enzyme complex. *Cell* **115**, 199–208.
- Schwarz, D.S., Tomari, Y., and Zamore, P.D. (2004). The RNA-induced silencing complex is a Mg(2+)-dependent endonuclease. *Curr. Biol.* **14**, 787–791.
- Seggerson, K., Tang, L., and Moss, E.G. (2002). Two genetic circuits repress the *Caenorhabditis elegans* heterochronic gene *lin-28* after translation initiation. *Dev. Biol.* **243**, 215–225.
- Sen, G.L., and Blau, H.M. (2005). Argonaute 2/RISC resides in sites of mammalian mRNA decay known as cytoplasmic bodies. *Nat. Cell Biol.* **7**, 633–636.
- Sijen, T., and Plasterk, R.H. (2003). Transposon silencing in the *Caenorhabditis elegans* germ line by natural RNAi. *Nature* **426**, 310–314.
- Song, J.J., and Joshua-Tor, L. (2006). Argonaute and RNA-getting into the groove. *Curr. Opin. Struct. Biol.* **16**, 5–11.
- Song, J.J., Smith, S.K., Hannon, G.J., and Joshua-Tor, L. (2004). Crystal structure of Argonaute and its implications for RISC slicer activity. *Science* **305**, 1434–1437.
- Stark, A., Brennecke, J., Russell, R.B., and Cohen, S.M. (2003). Identification of *Drosophila* microRNA targets. *PLoS Biol.* **1**, 397–409.
- Taubert, H., Greither, T., Kaushal, D., Wurl, P., Bache, M., Bartel, F., Kehlen, A., Lautenschlager, C., Harris, L., Kraemer, K., et al. (2007). Expression of the stem cell self-renewal gene *Hiwi* and risk of tumour-related death in patients with soft-tissue sarcoma. *Oncogene* **26**, 1098–1100.
- Teixeira, D., Sheth, U., Valencia-Sanchez, M.A., Brengues, M., and Parker, R. (2005). Processing bodies require RNA for assembly and contain nontranslating mRNAs. *RNA* **11**, 371–382.
- Tomari, Y., Matranga, C., Haley, B., Martinez, N., and Zamore, P.D. (2004). A protein sensor for siRNA asymmetry. *Science* **306**, 1377–1380.
- Vagin, V.V., Sigova, A., Li, C., Seitz, H., Gvozdev, V., and Zamore, P.D. (2006). A distinct small RNA pathway silences selfish genetic elements in the germline. *Science* **313**, 320–324.
- Watanabe, T., Takeda, A., Tsukiyama, T., Mise, K., Okuno, T., Sasaki, H., Minami, N., and Imai, H. (2006). Identification and characterization

of two novel classes of small RNAs in the mouse germline: retrotransposon-derived siRNAs in oocytes and germline small RNAs in testes. *Genes Dev.* *20*, 1732–1743.

Wightman, B., Ha, I., and Ruvkun, G. (1993). Posttranscriptional regulation of the heterochronic gene *lin-14* by *lin-4* mediates temporal pattern formation in *C. elegans*. *Cell* *75*, 855–862.

Wu, L., Fan, J., and Belasco, J.G. (2006). MicroRNAs direct rapid deadenylation of mRNA. *Proc. Natl. Acad. Sci. USA* *103*, 4034–4039.

Yang, N., and Kazazian, H.H., Jr. (2006). L1 retrotransposition is suppressed by endogenously encoded small interfering RNAs in human cultured cells. *Nat. Struct. Mol. Biol.* *13*, 763–771.

Yekta, S., Shih, I.H., and Bartel, D.P. (2004). MicroRNA-directed cleavage of HOXB8 mRNA. *Science* *304*, 594–596.

Yuan, Y.R., Pei, Y., Ma, J.B., Kuryavyi, V., Zhadina, M., Meister, G., Chen, H.Y., Dauter, Z., Tuschl, T., and Patel, D.J. (2005). Crystal structure of *A. aeolicus* Argonaute, a site-specific DNA-guided endoribonuclease, provides insights into RISC-mediated mRNA cleavage. *Mol. Cell* *19*, 405–419.

Zhang, H., Kolb, F.A., Brondani, V., Billy, E., and Filipowicz, W. (2002). Human Dicer preferentially cleaves dsRNAs at their termini without a requirement for ATP. *EMBO J.* *21*, 5875–5885.

Zhang, H., Kolb, F.A., Jaskiewicz, L., Westhof, E., and Filipowicz, W. (2004). Single processing center models for human Dicer and bacterial RNase III. *Cell* *118*, 57–68.